Monoclonal Antibody Therapy: The Development of a Liquid Chromatography Tandem Mass Spectrometry Method to Measure Rituximab Concentrations in Human Plasma

Ana Kuhar | KHRANA001

SUBMITTED TO THE UNIVERSITY OF CAPE TOWN

In fulfilment of the requirements for the degree Master of Science in Clinical Pharmacology

Supervisors

Prof. Lubbe Wiesner, Dr Jill Combrinck, Dr Sandra Castel and Mr Anton Joubert

November 2023

FACULTY OF HEALTH SCIENCES

Division of Clinical Pharmacology

PLAGIARISM DECLARATION

I know that plagiarism is wrong. Plagiarism is to use another's work and pretend that it is one's own.

I have used the Vancouver Convention for citation and referencing. Each contribution to, and quotation in, this thesis from the work(s) of other people has been attributed and has been cited and referenced.

This thesis is my own work.

I have not allowed and will not allow anyone to copy my work with the intention of passing it off as his or her own work.

Signed by candidate

Date: 01 November 2023

ACKNOWLEDGEMENTS

There is no question that taking on a project this big takes an entire community. I would like to thank the following people for standing with me throughout this work and for playing a crucial role in the success of this thesis.

First and foremost, I would like to thank Dr Jill Combrinck. She has played an integral role in my life since my Honours year, and without her completing this thesis would have been impossible. Thank you for standing by my side since the very beginning. I owe this degree to you. Your infectious smile and grace kept me going through some of the tougher times in this project. You have taught me so much about being a woman in science: I admire you and look up to you.

I would like to acknowledge and give my deepest appreciation to Dr Marthinus van der Merwe. His guidance and advice carried me through all the stages of writing my project. Thank you for believing in not only this project but also in me. The knowledge I have gained from you is irreplaceable. I am grateful to have been able to 'pick your mind' and to work under your leadership. Thank you for always making yourself available to me – your passion is contagious.

I would also like to extend my sincere gratitude to my supervisor, Professor Lubbe Wiesner. Thank you for the privilege of being one of your students. The skills I have learned under your supervision are invaluable. You are a great leader, and I will forever be grateful for all of the opportunities you have provided me with.

Thank you, Anton Joubert and Dr Sandra Castel. I appreciate your time and contribution. With this magnitude of work, every one of your contributions affected this project. Thank you for your patience and for being available for me in your busy schedules.

To my parents and sister, thank you for your unconditional love and unwavering support. Everything I am is because of you. Thank you for motivating me through all of life's big and small moments. I love you all.

Thank you to my friends for your love, support and words of encouragement during this process. Without them, this journey would have been impossible. A special thank you to Yashara Ryan for being my pillar of strength and guidance after I had the privilege of getting to know you in my Honours year. You will forever be one of the greatest blessings in my life.

Lastly, thank you to my peers and the PK team. Every contribution, big or small, has helped move me to where I am today. I am extremely appreciative.

I would like to thank the following sponsors: Pharmacology departmental funding, and National Research Foundation and UCT postgraduate funding. Thank you for making the past few years of research possible. All this would have been impossible without your help.

Grammarly was used as an editing tool.

ABSTRACT

Escalating global cancer incidence has emphasised the urgent need for innovative therapeutic strategies. Monoclonal antibodies (mAbs) have emerged as promising candidates for cancer treatment and driving the pursuit of tumour-targeted therapies. Rituximab (RTX) is one such mAb which has been of substantial interest in recent years as a therapy. The aim of this research project was to develop and optimise the extraction and quantification of RTX in human plasma using appropriate sample preparation techniques and liquid chromatography tandem mass spectrometry (LC-MS/MS) as the detection method. This was achieved by employing a bottom-up approach, culminating in the identification of a target peptide that serves as a representative of RTX.

Sample preparation started with affinity binding purification using protein A bound to agarose beads. Based on the highly specific binding of protein A to the Fc region of immunoglobulins (IgG), this purification allowed for the specific extraction of IgG from plasma, including RTX, while all non-specific plasma proteins were excluded. The affinity binding process was optimised by investigating the addition of different volumes of protein A to purify the RTX from the matrix so that the available binding sites were not completely occupied by plasma IgG. The optimal volume of the protein A slurry used during the affinity binding purification procedure was found to be 200 µL.

The extracted RTX molecules were subsequently digested while still bound to the protein A beads, by incubation with trypsin, a protease that cleaves proteins by breaking the peptide bonds at the C-terminal side of the basic amino acids arginine and lysine. The optimal conditions for tryptic digestion were found to be in 25 mM Tris-HCl buffer at pH 8, including 10% acetonitrile and an enzyme-to-substrate ratio of 1:20 (trypsin: RTX). Overnight incubation at room temperature was followed by a second addition of trypsin and a further 3 hours of incubation.

Trypsin digestion of the bound proteins produced a large number of peptides, including the specific signature peptide (s-Pep) chosen to represent RTX. The sequence of this peptide is GLEWIGAIYPGNGDTSYNQK. The final process applied to extract the s-Pep from the total tryptic digest was solid phase extraction (SPE) using Strata-X 33 µm polymeric reverse phase 30 mg/1 mL SPE extraction cartridges, with elution using 70% acetonitrile containing 10% formic acid.

Most of the method development was performed using a Sciex API-3200 triple quadrupole mass spectrometer for detection, coupled to an Agilent 1200 high performance liquid chromatography (HPLC) system used for chromatographic separation. The sensitivity of the Sciex API-3200 was however not adequate to analyse the s-Pep at the expected concentration range. Therefore, the project was concluded by transferring the analytical method to a Shimadzu Nexera X3 8050 LC-MS/MS system. Using chromatographic separation on an Agilent Poroshell C18 column (2.1 mm x 50 mm 2.7-Micron) by applying a gradient mobile phase resulted in the successful quantification of RTX at the required lower level of quantification of 12.5 µg/mL, and linearity throughout the analytical range of 12.5–300 µg/mL RTX in plasma.

The analytical method was used to determine which internal standard (ISTD) would be the best for use during a quantitative method for RTX. There are several steps during the bottom-up sample preparation

that can lead to increased variability, and the implementation of an ISTD may therefore greatly enhance the robustness and performance of a bioanalytical method used to quantify mAbs in a biological matrix. Three ISTDs were investigated for analyte compensation based on repeatability and accuracy. These included stable isotope-labelled (SIL) RTX (SIL-protein), stable isotope-labelled signal peptide (SIL-peptide), and purified horse IgG. Definite limitations were observed when horse IgG was used, mostly because of its different affinity for binding to protein A compared to RTX. The SIL-protein, following the whole sample preparation procedure, showed much promise but did not compensate completely. This was ascribed mainly to the fact that the representative signal peptide of the SIL-protein was different from that of RTX, and was therefore not totally representative in all aspects. The most successful ISTD was the SIL-peptide, and although only introduced during the last step in sample preparation, the SIL-peptide is regarded to be the better ISTD to use.

In conclusion, this project investigated the development of a platform that could serve as a much-needed bridging technology linking development-intensive biomarker research to clinical application. The field of drug development encounters distinct hurdles when handling macromolecules, particularly in the development of analytical methods. Nevertheless, these obstacles open avenues for innovative bioanalytical methodologies and instruments capable of precisely measuring drug molecules. These strides could result in regulatory revisions offering more defined guidelines for drug development and the approval of novel drugs.

TABLE OF CONTENTS

LIST OF ABBREVIATIONS AND ACRONYMS

~	Approximately
°	Degrees
µg	Microgram
µL	Microlitre
µm	Micrometre
%	Percentage
ADA	Anti-drug antibody
ADCC	Antibody-dependent cellular cytotoxicity
API	Atmospheric pressure ionisation
ART	Antiretrovirals
BCA	Bicinchoninic acid
C18	Carbon 18
C	Celsius
CAD	Collision gas
CDC	Complement-dependent cytotoxicity
CDR	Complementarity-determining region
CE	Collision energy
CEM	Detector parameter
CEP	Collision cell entrance potential
CID	Collision cell
Cu	Copper
CUR	Curtain gas
CV	Coefficient variation
CXP	Collision exit potential
Da	Daltons
DDI	Drug–drug interactions
dL	Decilitre

DMSO	Dimethyl sulfoxide
DP	De-clustering potential
ELISA	Enzyme-linked immunosorbent assay
EMA	European Medicines Agency
EP	Entrance potential
ESI	Electrospray ionisation
eV	Electronvolt
FA	Formic acid
Fab	Fragment antigen-binding
Fc	Fragment crystallisable
FDA	Food and Drug Administration
GS1	Ion source gas 1
GS2	Ion source gas 2
h	Hour
HCl	Hydrogen chloride
HIV	Human immunodeficiency virus
HPLC	High-Performance Liquid Chromatography
IE1	Ion energy 1
IE3	Ion energy 3
Ig	Immunoglobulin
INN	International non-proprietary names
IS	Ion spray voltage
ISTD	Internal standard
kPa	Kilopascal
L	Litre
LC-MS	Liquid Chromatography Mass Spectrometry
LC-MS/MS	Liquid Chromatography Tandem Mass Spectrometry
LLOQ	Lower limit of quantification

mAb	Monoclonal antibody
mg	Milligram
MHC	Major histocompatibility complex
min	Minutes
mL	Millilitre
mm	Millimetre
mM	Millimolar
MRM	Multiple reaction monitoring
msec	Millisecond
MS	Mass Spectrometry
MS/MS	Tandem Mass Spectrometry
MW	Molecular weight
m/z	Mass-to-charge
NaN_3	Sodium azide
nm	Nanometre
nM	Nanomolar
OTG	Octyl β-D-1-thioglucopyranoside
pAb	Polyclonal antibody
PBS	Phosphate buffered saline
pmol	Picomol
p-QVQ	QVQQPGAELVK($^{13}C_6{}^{15}N_2$)PGASVK($^{13}C_6{}^{15}N_2$)
p-VNN	VNNQALPQPIER
Q	Quadrupole
QC	Quality control
QCH	Quality control high
QCL	Quality control low
QCLLOQ	Quality control lower limit of quantification
QCM	Quality control medium

refWS	Reference working solution
RTX	Rituximab
SD	Standard deviation
SIL	Stable isotope-labelled
SIL-mAb	Stable isotope-labelled monoclonal antibody
SIL-RTX	Stable isotope-labelled rituximab
SIL-s-Pep	Stable isotope-labelled rituximab signature peptide
SPE	Solid phase extraction
s-Pep	Rituximab signal peptide
S	Standard calibration
SS	Stock solution
SYS	System suitability sample
testWS	Test working solution
TB	Tuberculosis
TDM	Therapeutic drug monitoring
TEM	Temperature
ULOQ	Upper limit of quantification
V	Volt
WHO	World Health Organization
WR	Working reagent
WS	Working solution
Z	Test statistic

LIST OF FIGURES

LIST OF TABLES

CHAPTER 1

INTRODUCTION

1.1 BACKGROUND

Cancer is a significant global health challenge. Demographic trends on a global scale suggest a rising incidence of cancer in the next decades, with projections indicating that there could be more than 20 million new cancer cases reported each year by 2025 (1). The goal of oncology has long been focused on finding a treatment that specifically targets the tumour cell while sparing the host (2). Early diagnosis, universal access to healthcare, and the constant development of current and new therapies have significantly improved cancer survival (3). Immunotherapy is a type of medical treatment that harnesses and enhances the body's immune system to fight diseases (4). This therapy has shown significant promise in revolutionising cancer treatment by offering the potential for more targeted and effective therapies with fewer side effects compared to traditional treatments like chemotherapy and radiation (5–7). Antibodies play a crucial role in immunotherapy as they are the primary agents to target specific molecules or cells in the immune system (4,8,9). Immunotherapy involving antibodies is known as antibody-based immunotherapy or monoclonal antibody therapy. Monoclonal antibodies (mAbs) mono-specifically bind to certain cells or proteins in order to remove them from the body (10). Therefore, the development of mAbs as immunotherapy provided hope that tumour-target therapy would someday play a principal role in cancer treatment (2,11). Rituximab (RTX) is one such mAb that has remained of substantial interest as a therapy in recent years.

This research project aimed to explore the development of a reliable and sensitive liquid chromatography tandem mass spectrometry (LC-MS/MS) method for measuring RTX in human plasma. This powerful and highly sensitive analytical technique combines the separation capabilities of high performance liquid chromatography (HPLC) with the precise and selective detection of mass spectrometry (MS). As technology continues to evolve, LC-MS/MS is expected to become the gold standard for drug quantification of therapeutic drugs in biological samples (12–14). Liquid chromatography tandem mass spectrometry methods have been applied to various clinical scenarios, including pharmacokinetic studies and therapeutic drug monitoring (TDM) (15,16). These applications may provide valuable insights into the optimal dosing regimens and patient-specific treatment strategies (15). Continued method refinement and validation efforts will further strengthen its clinical utility and broader adoption in research and clinical practice.

1.2 IMMUNOTHERAPY

The immune system serves as a safeguard for the body against foreign invaders. It uses proteins and cells that circulate throughout the body to detect and eliminate foreign cells, viruses, and macromolecules (4,17). Its primary function is to distinguish between self (the body's own cells and tissues) and non-self (invading pathogens or foreign substances) and mount appropriate responses to protect against infections, so ultimately playing a crucial role in disease prevention and overall health maintenance (17). The immune system has two major lines of defence. Innate immunity is the first line of defence and includes physical barriers like the skin and mucous membranes involving non-specific

immune responses (17,18). The aim of innate immunity is to provide immediate protection. Adaptive immunity is the second line of defence and involves a more sophisticated specific immune response that develops over time (17,18). Part of the second line of defence involves B lymphocytes (B cells) that produce antibodies. Antibodies are proteins that target specific foreign molecules or pathogens, known as antigens (non-self molecules), and neutralise or mark them for destruction by other immune cells (17–19).

Immunogenicity is the ability of a molecule to solicit an immune response (4,8,9). This is relevant in therapeutic applications, such as the development and use of biological drugs, including mAbs. Monoclonal antibodies are a specific type of immunotherapy that can be designed to have varying degrees of immunogenicity (20,21). Immunogenicity in the context of mAbs refers to the potential of these therapeutic antibodies to provoke an immune response in patients receiving them (20–22). Understanding and managing immunogenicity have improved the safety and efficacy of mAb-based therapies (19,20).

1.3 ANTIBODIES

Antibodies, or immunoglobulins, are host proteins produced by the immune system in response to foreign molecules entering the body (23,24). These foreign molecules or antigens and their molecular recognition by the immune system result in the selective production of antibodies that are able to bind the specific antigen (25,26). Antibodies are made by B cells and circulate throughout the blood and lymph where they bind to their specific antigen, enabling them to be cleared from circulation (25).

1.3.1 Antibody structure

Antibody molecules are Y-shaped glycoproteins composed of four polypeptide chains comprising two identical heavy chains and two identical light chains (Figure 1.1)(25,27). These chains are linked together to form the basic structure of the antibody. Heavy and light chains are held together by a combination of non-covalent interactions and covalent interchain disulfide bonds, forming a bilaterally symmetrical structure (28). Each heavy chain has about twice the number of amino acids as each light chain, resulting in a total immunoglobulin molecular weight (MW) of approximately 150 000 Da (27). The tips of the Y-shaped antibody, the fragment antigen-binding (Fab) regions, are the variable regions of the antibody (28,29). These regions are highly diverse and contain specific binding sites that recognise and attach to specific antigens (30). The complementarity-determining region (CDR), positioned in the variable Fab region's portion, defines the antibody's specificity, and therefore plays a major role in antigen binding (27,30,31). The fragment crystallisable (Fc) region is the constant region of the antibody and interacts with various immune cells and molecules, mediating different immune response functions (28). The constant region is identical in all antibodies of the same isotype (28).

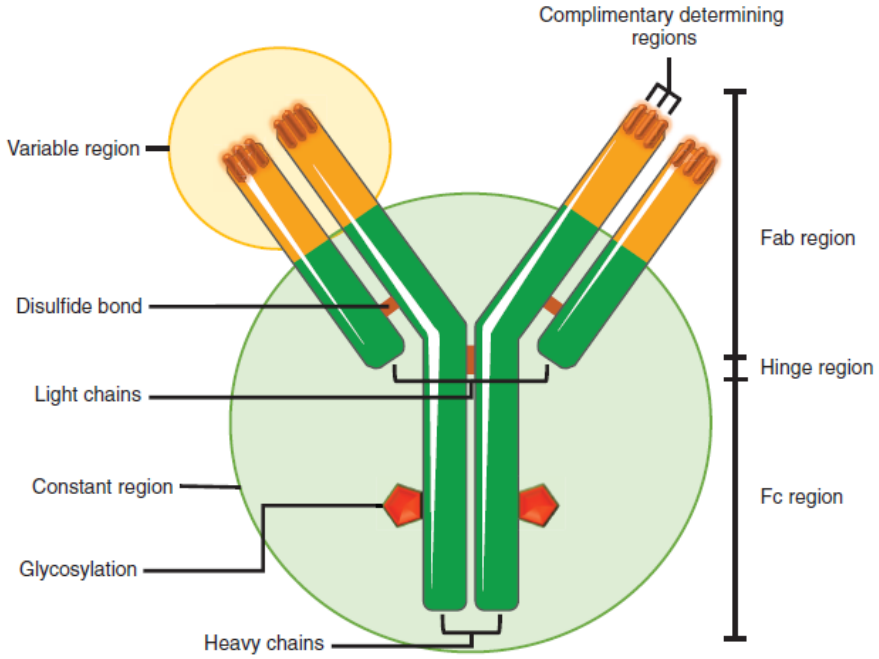

Figure 2.1. The structure of an antibody. *These large biological molecules are comprised of four subunits containing two heavy and two light chains making up the basis of the antibody structure. A flexible hinge region connects the rigid Fc region to the variable Fab region. The complementary determining region (CDR), positioned in the portion of the variable Fab region, defines the specificity of the antibody, and plays a major role in antigen binding* (27).

Immunoglobulins are classified into different isotypes (IgA, IgD, IgE, IgG, and IgM) based on the type of heavy chain they contain (21,25). Each isotype has distinct roles in the immune response (23,25,27). Immunoglobulin G is the most abundant immunoglobulin in the blood and provides long-term immunity (25).

1.3.2 Antibody production

For the purpose of this project, a brief background in immunology is important in order to later clarify the mechanisms of action of mAbs. The two most important factors to consider are the functions of the B cells and the antibodies.

B cells perform an important part of the specific immune system because of their ability to produce antibodies and they are therefore central contributors to the pathogenesis of immune-related diseases (32). Each B cell has antibodies located on the cell membrane specific to a single antigen (29,33). Once a B cell encounters an antigen that matches its antibody, it becomes activated and undergoes differentiation to become either a plasma cell or a memory B cell (Figure 1.2) (25,32). Plasma cells rapidly produce large amounts of their specific antibody whereas B cells remain present for years as part of the immune memory and can be quickly activated (32). Antibodies selectively identify specific antigens that are part of a harmful process and largely contribute to the elimination and/or termination of such processes (34).

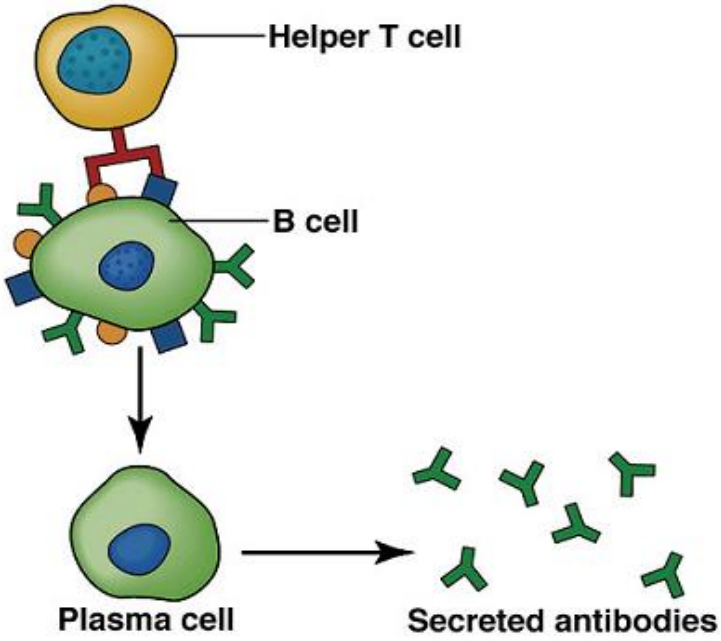

Figure 1.2. The basis of how B cells produce antibodies. *When a naïve B cell comes into contact with an antigen that fits its receptors, it binds to it and this leads to the formation of an antigen major histocompatibility complex (MHC) that T cells can recognise. When the T cell binds to the antigen–MHC complex, it releases cytokines that activate the B cell. Activation of the B cell allows for the division of the cell to form one of two types of daughter cells, namely inactive memory cells or activated plasma cells that secrete antibodies* (32).

1.3.3 Monoclonal and polyclonal antibodies

Both mAbs and polyclonal antibodies (pAbs) are important tools used in research, diagnostics, and therapeutic applications (34). They are derived from different sources and have distinct characteristics. The production of a mAb involves the fusion of a specific B cell with a myeloma cell, resulting in a hybridoma that secretes a single type of antibody with identical antigen specificity (26,32). In contrast, a pAb is generated from a mixture of different B cells, each producing a specific antibody against the same antigen (26,32). They are obtained by immunising an animal with the target antigen, and the resulting antibody response is a diverse mixture of antibodies with varying specificities (26,32). Monoclonal antibodies are highly specific and bind only to a single epitope on the target antigen, whereas pAbs recognise multiple epitopes on the target antigen, leading to broader binding capabilities (24,26). The high degree of specificity and selectivity of mAb make it the ideal tool in therapeutic applications (26).

1.4 MONOCLONAL ANTIBODIES

Initially developed in the 1970s, mAbs have become a versatile tool for treating various diseases (27). The pioneering work of Köhler and Milstein, who developed the hybridoma technology in 1975, resulted in the production of mAbs (5,35). The first therapeutic mAb, muromonab-CD3, was approved by the Federal Drug Association (FDA) in 1986 for preventing organ rejection in transplant patients (36). This

work led to the evolution of mAb development and the milestones that have shaped the field. Therapeutic monoclonal antibodies are mAbs that are designed for clinical use to treat various diseases, including cancer, autoimmune disorders, infectious diseases, and inflammatory conditions (5,37). These mAbs are engineered to have specific properties, such as enhanced affinity, a longer half-life, or reduced immunogenicity, to optimise their therapeutic efficacy (4,38).

1.4.1 Types of monoclonal antibodies

International non-proprietary names (INNs) have been assigned to mAbs since 1991 and use *-mab* as a stem and specific substems to cover their source (39,40). These substems include *-omab* for murine, *-ximab* for chimeric, *-zumab* for humanised, and *-umab* for human antibodies (Figure 1.3) (40). Monoclonal antibodies work by blocking targeted molecule functions, inducing apoptosis of cells that express the target, or modulating signalling pathways (41,42).

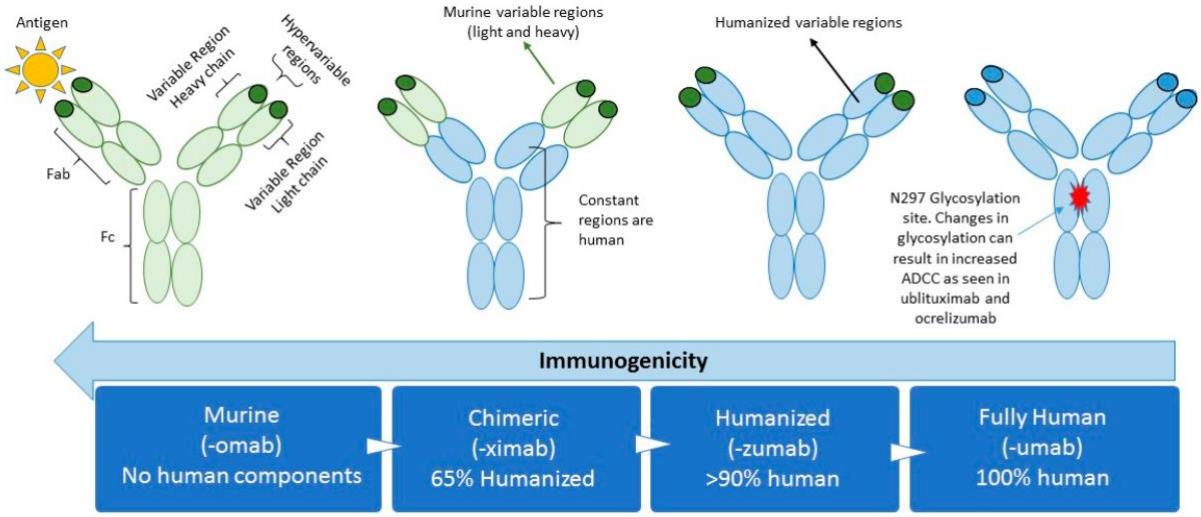

Figure 1.3. The different types of monoclonal antibodies. *Fully murine mAbs contain no human components. The chimeric and humanised mAbs contain humanised components in their Fab and hypervariable CDR regions, respectively. Fully human mAbs are entirely derived from human sources* (40).

1.4.1.1 Human versus non-human mAbs

The earliest mAbs developed were typically derived from non-human sources, such as mice (40,43,44). These non-human mAbs were more likely to induce an immune response when administered to human patients, as the immune system recognised them as foreign proteins (40). This could lead to the formation of an anti-drug antibody (ADA) response, which could reduce the effectiveness of the mAb or, in some cases, cause adverse effects (22,40).

1.4.1.2 Chimeric and humanised mAbs

To reduce immunogenicity and increase the compatibility of mAbs with the human immune system, researchers developed chimeric and humanised mAbs (Figure 1.3) (40). Chimeric mAbs combine portions of the non-human and human antibodies, while humanised mAbs have been engineered to be

predominantly human, with only a small part derived from non-human sources (27,40,43). Therefore, the variable region of chimeric mAbs is from a non-human source, usually murine, and is linked by disulfide bonds to a human immunoglobulin (40). In humanised mAbs, only the hypervariable CDR regions are non-human and are therefore 'grafted' onto human variable regions (40,44). These modifications help to minimise the immune response against the therapeutic mAb (40).

1.4.1.3 Fully human mAbs

Some newer mAbs are fully human, meaning they are entirely derived from human sources. Fully human mAbs have the lowest risk of inducing an immune response and ADAs in patients, as they are less likely to be recognised as foreign by the immune system (40).

1.4.2 Clinical applications

Monoclonal antibodies have numerous clinical applications and are widely used in various fields of medicine (45). Their specificity, effectiveness, and safety make them valuable therapeutic agents (46). Some of the key clinical applications of mAbs include cancer treatment, autoimmune diseases, and infectious diseases (45). Monoclonal antibodies have revolutionised cancer treatment – specifically, combination therapies involving mAbs have shown significant success in improving patient outcomes (7,11). In autoimmune diseases such as rheumatoid arthritis and multiple sclerosis, mAbs targeting specific inflammatory mediators have effectively reduced disease activity and slowed progression (40,47). Monoclonal antibodies have emerged as a promising treatment option for infectious diseases, including viral infections such as human immunodeficiency virus (HIV) (48,49). These antibodies are designed to target specific components of the virus or host cells to either neutralise the virus or modulate the immune response (50). The use of mAbs for HIV treatment and prevention is an ongoing area of research and development (51).

1.5 RITUXIMAB

Rituximab is a genetically engineered chimeric murine-human mAb that directly targets the B cell surface membrane protein CD20 (52,53). Treatment with this anti-B cell drug results in the rapid elimination of B cells from circulation and is therefore used to treat diseases characterised by overexpressed B cells (31,52). The CD20 antigen is proposed to contribute to signal transduction as well as B cell proliferation, differentiation and activation (54). Since its discovery, the CD20 phosphoprotein has been an attractive target for mAbs (55). CD20 expresses itself on 95% of normal and malignant B cells with no natural ligand identified to date (55,56). In addition, CD20 is absent on normal B stem cells, precursor B cells, and most plasmocytes (54,56). The special properties of RTX provide strong possibilities regarding the possible application of this drug in various antibody-associated disorders (52).

Murine anti-CD20 molecules have been available for some time (55). However, RTX's short half-life of normally less than 20 hours was a major limitation (55). This prompted the development of chimeric antibodies by replacing the murine constant domain with a human domain (55). This engineered

chimeric murine-human mAb now has an extended half-life of up to a few days with the potential to interact with human effector cells with less immunogenicity (53,55,56).

1.5.1 Pharmacodynamic properties

Monoclonal antibodies are becoming increasingly popular as a therapy entity with the potential to revolutionise the treatment of some of the worst conditions. Understanding the mechanism of action of mAbs may lead to a maximised opportunity for drug response by allowing treatment at the optimal time in the clinical course and subsequently augmenting the antitumour effect (8,57,58). Furthermore, this knowledge proves useful when considering that some patients are unresponsive to RTX, with only 40% to 50% of responsive patients being receptive to a repeat treatment course (2). Pharmacodynamics refers to how a drug affects the body and its biological mechanisms (2,8,59). There are at least four proposed mechanistic pathways responsible for the elimination of CD20 cells by RTX, namely: antibody-dependent cellular cytotoxicity (ADCC), antibody-dependent cellular phagocytosis, complement-dependent cytotoxicity (CDC), and direct apoptosis (Figure 1.4) (42,54,60). While these events are not completely understood, is it likely that RTX functions as a sum of multiple mechanisms.

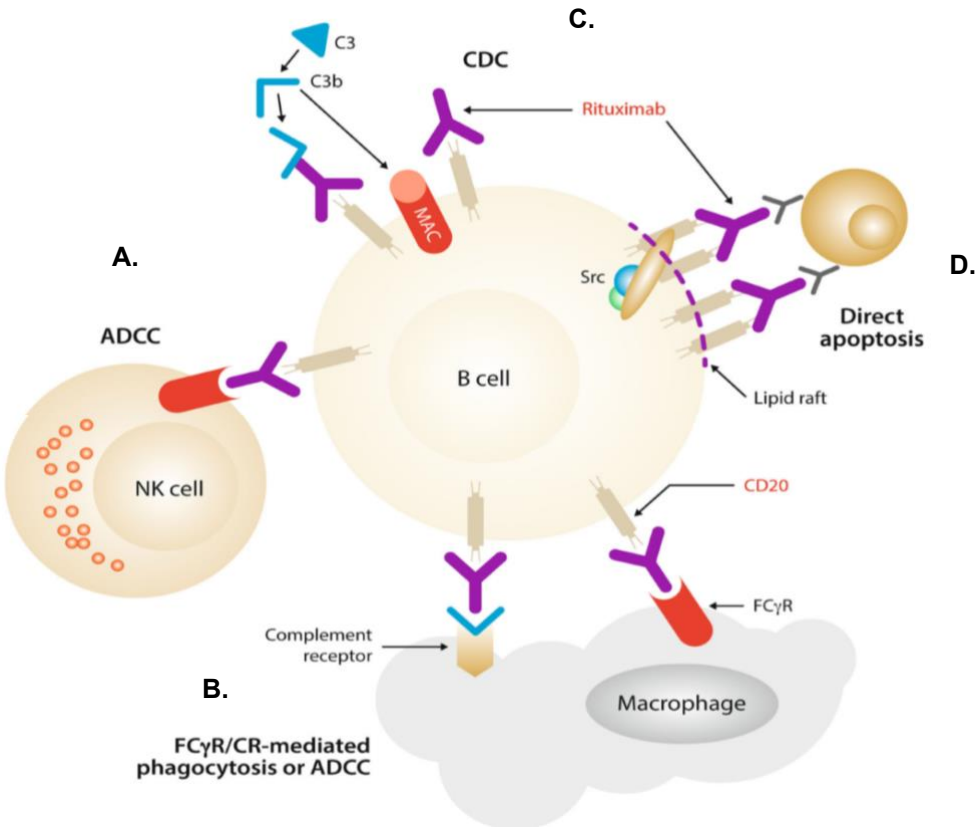

Figure 1.4. The four proposed mechanistic pathways of RTX. *A. antibody-dependent cellular cytotoxicity (ADCC), B. antibody-dependent cellular phagocytosis, C. complement-dependent cytotoxicity (CDC), and D. direct apoptosis* (42).

The binding of RTX mAbs to CD20 antigens results in the depletion of B cells by these four proposed mechanisms (54). Antibody-dependent cellular cytotoxicity (Figure 1.4, part A) occurs as a result of the interaction between the Fc region of RTX and the Fcγ receptor on the surface of natural killer cells, granulocytes and macrophages (54,61,62). Rituximab-bound B cells are then destroyed by phagocytosis or by the release of cytokines, chemokines and mediators from immune effector cells (Figure 1.4, part B) (54). Complement-dependent cytotoxicity (Figure 1.4, part C) is triggered by the binding of the antigen binding region to the tumour cell (54,61). This binding results in the reorganisation of the CD20 molecule triggering the activation and initiation of the complement cascade (61,62). The formation of the membrane attack complex leads to CDC, including tumour cell lysis and the augmentation of phagocytosis (54,61). The CDC mechanistic pathway is believed to be the most dominant *in vivo* (63). It is the Fc region of antibodies that is particularly important for mediating tumour cell lysis through ADCC and CDC (60). Rituximab binding may also induce non-classical apoptosis (Figure 1.4, part D), a controlled and orderly process of programmed cell death (54,61). The fact that RTX demonstrates mediation of human effector functions in an antigen-specific manner and induces apoptosis is a rationale for combining RTX with chemotherapy (53).

1.5.2 Pharmacokinetic properties

Pharmacokinetics is the study of how the body interacts with a drug after administration (64). It involves the process of absorption, distribution, metabolism, and excretion of a drug in the body (65,66). Understanding pharmacokinetics is essential for determining the drug's fate in the body, its concentration at different sites, and how it is eliminated from the body over time (64). This is crucial for determining the appropriate dosing regimen for a drug in order to achieve the desired therapeutic effect while minimising adverse effects (66).

Rituximab is administered intravenously, and its pharmacokinetics follow a typical two-compartment model. A two-compartment pharmacokinetic model is a representation used to describe the distribution and elimination of drugs in the body (35,65,66). It assumes that the body can be divided into two main compartments: the central compartment (usually the bloodstream), and the peripheral compartment (tissues and organs). After infusion, it rapidly distributes into the central compartment, primarily the vascular space. From there, it is distributed into the peripheral compartment, which includes the lymphoid tissues where B cells are targeted and eliminated (64).

The pharmacokinetic profile of RTX is characterised by a biphasic elimination pattern (Figure 1.5)(66). This phenomenon describes the process of drug elimination from the body using two distinct elimination phases. The initial phase is characterised by a fast clearance, and the second phase, which exhibits a slower elimination rate, extends the half-life of the drug (42,65,66). In this pattern, the drug concentration in the body decreases in a biphasic manner over time. The terminal half-life of RTX is approximately 20–30 days, accounting for its potential for extended therapeutic effects and allowing for less frequent dosing (67). Several factors may influence RTX pharmacokinetics, including body weight, age, gender, and concurrent therapies (65,66). However, these factors have shown limited clinical

significance in most cases, and RTX dosing adjustments are typically not required based on these individual characteristics (67).

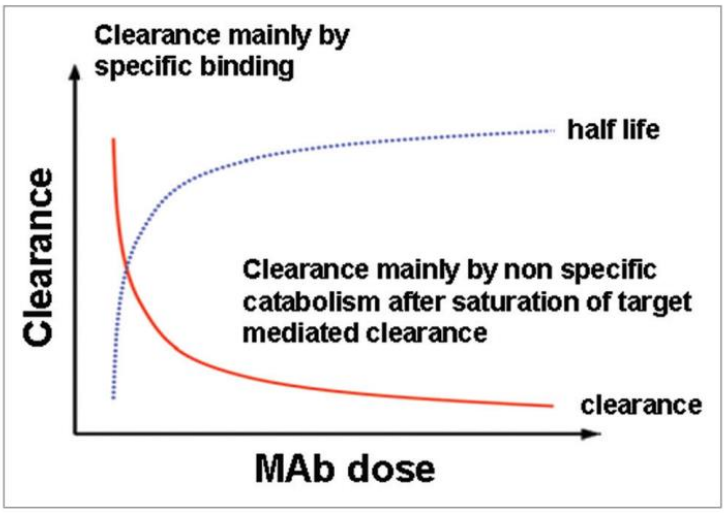

Figure 1.5. Biphasic pharmacokinetics of RTX. *This model shows high clearance by specific binding to CD20 which, after saturation, leads to low clearance through non-specific binding via FcyR* (66).

Tumour mass and the number of CD20 molecules per cell effect pharmacokinetics because of variable absorption of circulating RTX (65,67,68). This may explain why a greater concentration of RTX may be required in cases of large tumour burdens (67). Rituximab concentration is inversely related to tumour burden and antigen load (54). Tumour burden determines the number of target antigens and can therefore influence serum RTX concentrations (69). According to Golay *et* al., an increase in tumour burden is associated with low RTX serum levels. Rituximab is degraded by non-specific catabolism in the liver and other organs (54,70). Therefore, mAbs have a complex pharmacology that is currently only partially understood (70). Very little is known about the metabolism and elimination of RTX (69,70).

According to Golay *et al*., in the context of B cell malignancies, the maintenance of a minimum level of drug (>25 µg/mL) (Figure 1.6) for prolonged periods (up to two years for maintenance therapy) seems to be of greater importance than rapid achievement of a very high dose (200–300 µg/mL) for a shorter period (66). The two-compartment model describing RTX clearance involves a nonspecific and specific pathway mediated by IgG1 and CD20, respectively (54,65). The non-specific pathway remains unchanged during therapy, and the specific pathway is reduced to a first-order decay rate following the first infusion (54). According to Müller *et al*., clearance is inversely correlated to the half-life of RTX (67). They also found that the drug had a shorter half-life in men (24.7 days) compared to women (30.7 days) and that women had a 32% lower clearance compared to men (66,67). A steady-state condition (the condition in which, during each dosing interval, the intake of a drug is equal to the amount eliminated from the body) is achieved after approximately 3–5 half-lives. Immunoglobulins in general take longer to reach steady-state compared to small molecules and have a longer elimination half-life [64]. Small molecules (e.g., chemotherapy) have an elimination half-life in the magnitude of hours and rapidly achieve steady-state following administration (hours-days), while macromolecules (e.g., mAbs) have a very long elimination half-life (in the magnitude of weeks) and may take up to 12 weeks to achieve

steady-state (27,67,71,72). According to Pestronk *et al*., the serum half-life of RTX was found to be one week immediately after infusion and five weeks thereafter (73). After the infusion of RTX, the initial half-life of one week suggests that the drug's concentration in the bloodstream decreases by half in this timeframe. This immediate post-infusion half-life is relatively short compared to the subsequent half-life. The serum half-life of RTX increases to five weeks after the initial one-week period. This means that the rate of drug elimination from the body slows down, and the drug's concentration in the bloodstream decreases more gradually over this extended timeframe. These findings agree with half-life values described in previous studies (73). Treatment with RTX results in a substantial depletion of B cells, which may persist for up to six months post-treatment before a gradual recovery (53,65).

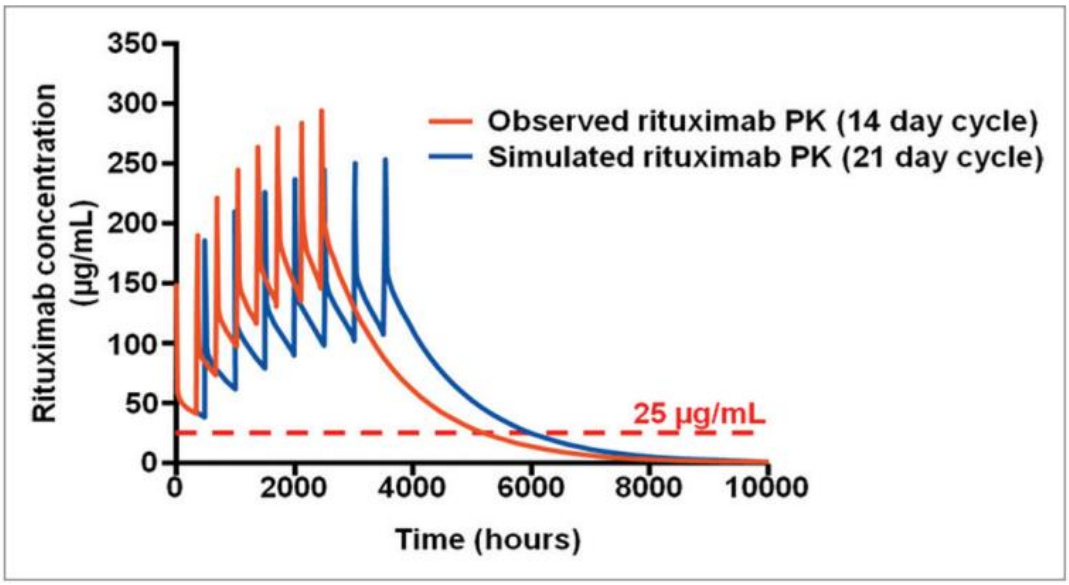

Figure 1.6. Model of RTX pharmacokinetics with 21 vs 14 day cycles. *This model shows that RTX levels >25 µg/mL are maintained for a longer period of time when RTX is administered every 21 days (red) rather than every 14 days (blue)* (66).

In summary, the interaction between pharmacodynamics and pharmacokinetics plays a crucial role in determining the optimal dosing regimen, maintaining therapeutic drug levels, and achieving the desired therapeutic effects of RTX. Optimising the dosing schedule and monitoring both these parameters are imperative for maximum efficacy and minimising adverse effects in patients receiving RTX treatment. According to Golay *et al*., the polymorphism of FCγRIIIA expressed on natural killer cells and monocytes may describe the response of patients to RTX as a monotherapy. Increasing the RTX dose *in vivo* may overcome the effect of this FCγRIIIA polymorphism (66).

1.5.3 Tolerance and efficacy

Many studies have shown RTX to be a well-tolerated, comparatively safe and efficacious treatment (73,74). This mAb effectively eliminates virtually all circulating B cells within one week of initial treatment (73). A study by Pestronk *et al*. found that after a single course of four treatments, B cell levels remained undetectable in all patients after one month (73). Rituximab is generally well tolerated with only minimal

infusion-related symptoms (35,54,75). Some occasional symptoms associated with the initial infusion include episodes of light-headedness, chills and hypotension which are easily treated by slowing the rate of infusion (73,75). According to Boye *et al*., 95% of adverse reactions associated with RTX are mild to moderate and are resolved immediately after infusion (35).

Rituximab's pharmacokinetic and pharmacodynamic properties have significantly improved the treatment landscape for B cell malignancies and autoimmune diseases (76,77). Its targeted approach to B cell depletion through CD20 binding demonstrated remarkable efficacy and safety in numerous clinical trials and real-world settings (65). As research continues, further insights into the RTX mechanism of action and potential applications may lead to even more effective and personalised therapies for patients with these conditions (1).

1.5.4 Rituximab on immune response

In some cases, immune effectors can be defective for patients heavily treated with chemotherapeutics or for advanced stage diseases, therefore decreasing the efficacy of RTX (66,74). These immune effectors include a number of immune cells that play a crucial role in the body's immune response by directly eliminating or neutralising infections, pathogens, and abnormal cells (74,78). An increase in infection rate has been found in a subset of patients with lymphoma and HIV infection (48–50). The route of metabolism of RTX is independent of CYP3A4 oxidation and therefore, according to Pham and Flexner, drug-drug interactions (DDIs) are unlikely between antiretrovirals (ARTs) and RTX (79). The standard dose is therefore still recommended for HIV-infected patients (70). Patients with rheumatoid arthritis treated with RTX have been noted to develop tuberculosis (TB) following the breakdown of the granulomatous response (79). The probability of these DDIs is not well understood, specifically in a population in which TB is highly prevalent, such as the South African population.

1.5.5 Clinical applications

Rituximab is a mAb medication that has been used in various clinical applications primarily targeting B cell malignancies and autoimmune diseases. In 1997, the FDA granted regulatory approval to intravenously administered RTX (42,80). The standard dosage regime involves a 375 mg/m^2 intravenous infusion weekly for four weeks (58,65). A new class of anticancer drugs was thus recognised when RTX became the first therapeutic mAb to be used in the field of oncology (42).

Currently, RTX is often used as an effective therapy for the treatment of non-Hodgkin's B cell lymphoma (35,73,80). Lymphomas are solid tumours of the immune system, and non-Hodgkin's lymphoma accounts for about 90% of all lymphomas (81–83). The wide range of histological appearances and clinical features at presentations can make this cancer particularly difficult to diagnose (84). Lymphomas are not rare and therefore timely diagnosis is important because effective, and often curative, therapies are available for many subtypes (84).

The potential regulation of normal B cell function through CD20 targeting led to the testing of RTX for a variety of antibody-mediated autoimmune diseases, such as rheumatoid arthritis (58,80). Rituximab is an approved treatment for patients that do not respond adequately to disease-modifying antirheumatic

drugs (70,85). Rheumatoid arthritis is a multifactorial autoimmune disease of unknown etiology, primarily affecting the joints, from which extra-articular manifestations can occur (85,86). Given its complexity, which is based on an incomplete elucidated pathophysiological mechanism, good management of rheumatoid arthritis requires a multidisciplinary approach (86). The clinical status of rheumatoid arthritis patients has improved in recent years due to medical advances in diagnosis and treatment that have made it possible to reduce disease activity and prevent systemic complications (58,70,80).

While RTX is not a curative therapy, it may lead to prolonged survival as a consolidation or maintenance therapy (53). The precise mechanism of action of RTX remains unknown, and thus a better understanding would prove beneficial when guiding its use for combination therapy alongside cytotoxics and possibly other immunotherapies (8,54,58).

1.6 BIOANALYSIS

There has been an ongoing increase in the development of various new mAbs, with currently more than 30 different therapeutic mAbs approved for the treatment of a number of oncological disorders (65). The development of reliable bioanalytical methods that allow for the reproducible quantification of mAbs must therefore keep pace with this revolution in medical therapies (87,88).

For decades, the most common method for the quantification of therapeutic mAbs in biological fluids included immunoassays such as the enzyme-linked immunosorbent assay (ELISA) (75,80,89). However, while immunoassays have been used in various industrial and clinical settings for years, they also have known flaws (75). Because of lower specificity compared to direct analysis, such as with LC-MS/MS, immunological-based assays are not the most versatile or reliable method for many human plasma and serum samples (80,89). In these instances, mass spectrometry-based methodologies exhibit superior sensitivity and selectivity for mAb quantification (80). In recent years, liquid chromatography coupled to tandem mass spectrometry (LC-MS/MS) has been applied to mAbs analysis as the method of choice and substitution method to ELISA for the bioanalysis of patient samples (80,90). LC-MS/MS has also been employed for the accurate and sensitive quantification of RTX concentrations in plasma (80).

Quantification by LC-MS/MS is a method used to determine the concentration of specific analytes (such as proteins, peptides, metabolites, drugs, or small molecules) in a sample based on their mass spectrometric signals. This technique involves comparing the signals from the analytes of interest to those from known standards of known concentrations. Quantification by LC-MS/MS can be achieved through various strategies, and the choice of method depends on the specific analytical goals and the characteristics of the analytes being studied.

Such a method is usually based on known protein quantification procedures involving sample preparation techniques such as protein precipitation, affinity binding purification, enzymatic digestion and further purification of a target peptide by extraction methods such as solid phase extraction (SPE) (91).

1.6.1 Liquid chromatography mass spectrometry

Liquid chromatography tandem mass spectrometry (LC-MS/MS) represents the integration of two robust analytical methods: the efficient molecule separation capability of high-performance liquid chromatography (HPLC) and the precise identification and quantification powers of mass spectrometry (MS). The implementation of tandem mass spectrometry (MS/MS), involving fragmentation analysis, elevates the sensitivity and specificity of the analytical workflow to an unparalleled degree of analytical potency.

High performance liquid chromatography is a separation technique that segregates compounds based on their chemical and physical properties, such as size, polarity, and affinity for the chromatographic stationary phase (92,93). During HPLC, a sample containing the compounds to be separated is introduced in a liquid solvent, referred to as the mobile phase, and is subsequently passed through a chromatographic column housing the stationary phase (92). As the sample moves through the column, different compounds interact in varied manners with the stationary phase, causing them to separate and elute at different times (92,93). The retention time, or time taken to elute each compound from the column, is characteristic and can be used for identification (92).

Mass spectrometry is an analytical technique that measures the mass-to-charge (m/z) ratio of ions (charged molecules) (87,94,95). During tandem mass spectrometry, a specific ion (precursor ion) can be selected by a mass analyser and directed into a higher energy compartment in the mass spectrometer (the collision cell) where the ion is fragmented by collision-induced dissociation with the introduction of an inert collision gas (96). The fragment ions, also known as product ions, can then be analysed in a second mass analyser, providing a further dimension of mass analysis by which structural information about the precursor ion can be deduced (87,96). Applied to proteins and peptides as precursor ions, such fragmentation analysis can also provide information about the amino acid sequences, thereby identifying and characterising such macromolecules.

Liquid chromatography is coupled to mass spectrometry through the ionisation source which is an interface where molecules eluting from the chromatographic column are ionised before introduction into the mass spectrometer. The most widely used ionisation technique applied for biologically relevant molecules is electrospray ionisation, in which desolvation and ionisation takes place at atmospheric pressure by the application of a high voltage and high temperature in the ion source (87,88,92,95,97). One of the most widely used mass spectrometers used in LC-MS/MS systems is the triple quadrupole mass spectrometer, and a schematic presentation of such a LC-MS/MS system is depicted in Figure 1.7 (below).

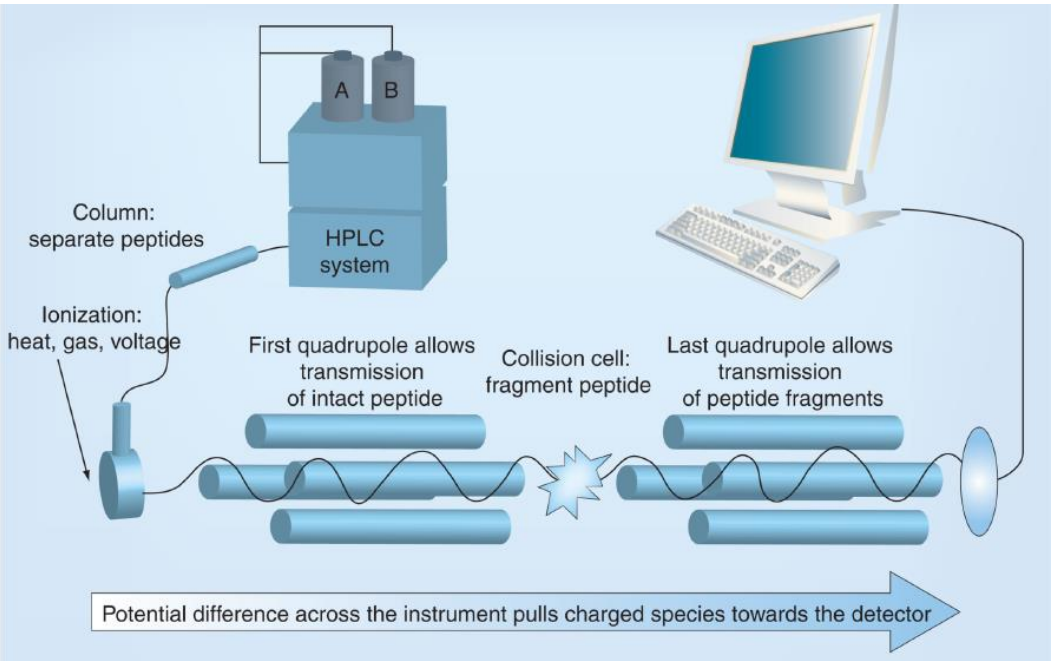

Figure 1.7. Summary of the LC-MS/MS system. *In the HPLC, the sample is separated into components based on their properties in a chromatography column. The eluted components are then introduced into the MS. In MS/MS, molecules are ionised and sorted based on their m/z and MRM is used to selectively monitor specific precursor–product ion pairs for precise quantification of targeted analytes* (89).

For the purpose of quantification, the abundance of mass-separated ions can be recorded by the ion detector and represented as a chromatographic peak in a chromatogram. The area of the chromatographic peak is therefore a direct indication of the relative abundance of the ion, which can be directly related to the concentration of the compound exiting the chromatographic column.

Most quantitative methods employing LC-MS/MS are based on the measurement of a specific product ion produced by collision-induced dissociation of one selected precursor ion. This highly sensitive measurement technique is termed multiple reaction monitoring (MRM) and can be used to quantitatively analyse complex biological samples (87,98). In MRM, the mass spectrometer is set up to monitor the specific transition of a given analyte ion: the precursor ion (parent ion) to a unique product ion (daughter ion) (87,88). The precursor ion is the molecule of interest that is selected based on its m/z value, and the product ion is a specific fragment produced from the precursor ion. By selecting a precursor–product ion pair specific to the analyte of interest, MRM provides high selectivity and sensitivity. The mass spectrometer transfers, detects and quantifies the transitions that match the predefined precursor–product ion pairs, thereby eliminating potential interferences from other compounds in the sample. This makes MRM particularly useful for accurately quantifying low-abundance compounds in complex mixtures (87,99). The MRM technique is depicted in Figure 1.8 (below).

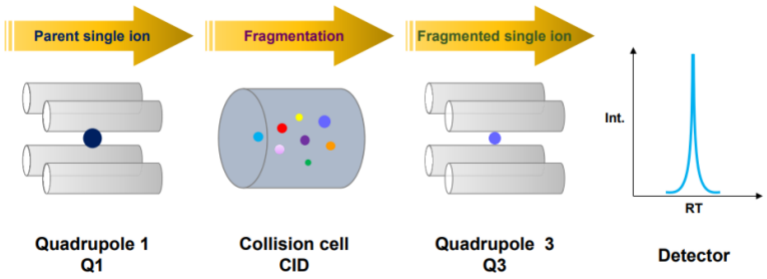

Figure 1.8. The highly sensitive and specific monitoring system, MRM. *Only the selected parent ion passes through the first quadrupole (Q1), and then enters the collision cell and undergoes fragmentation by collision-induced dissociation (CID). Quadrupole 3 (Q3) selectively passes a fragment ion of selected mass derived from the parent ion, allowing the target molecule-specific ion to be detected by the ion detector* (99).

1.6.2 Sample preparation

Monoclonal antibodies are large and complex molecules; therefore, sample preparation plays an important role in ensuring sensitive and reproducible analytical methods. When working with proteins and peptides, it is generally recommended to use labware that is specifically designed for these kinds of molecules (87,100). Given the amphiphilic nature of proteins and peptides, they are easily non-specifically absorbed into most metals, glasses, and plastics (101,102). It is a challenge to dissociate proteins that have been absorbed by these surfaces during non-specific binding. Proteins may lose their original structure as they often change orientation upon surface binding. These factors may ultimately affect the recovery, reproducibility, and sensitivity of an assay and therefore it is important to consciously choose specific tubes and vials when developing an LC-MS/MS method for the quantification of proteins and peptides (101).

Sample preparation refers to the process of cleaning up or purifying a sample (90). A robust and stable sample preparation method must be implemented to acquire reliable bioanalytical results (27,90). The ultimate role of sample preparation is to eliminate possible interferences from sample matrices and thereby optimise the analytical system performance (90,103). Some sample preparation procedures include protein precipitation, affinity binding purification and solid phase extraction (SPE). A combination of techniques may need to be used to obtain the best results. If no sample preparation procedures are performed only the micromolar level may be analysed, whereas affinity binding purification, for example, allows for picomolar levels to be analysed (104).

There are three main LC-MS/MS approaches for the quantification of proteins such as mAb in biological matrices, often referred to as the top-down, middle-down, and bottom-up approaches (101). Top-down analysis involves the quantification of the intact mAb. This approach results in low sensitivity due to complex mass spectra (27,105,106). In middle-down analysis, the formation of subunits during mAb sample preparation is used for quantification in biomatrices (27,107,108). The bottom-up analysis involves the enzymatic digestion of mAbs to form representative signature peptides, sometimes referred to as surrogate peptides (27,105–107). In order to obtain these peptides, comprehensive sample

preparation is essential (105–107). The bottom-up approach is still the gold standard for the LC-MS/MS quantification of mAbs in biological matrices due to its increased sensitivity and specificity when compared to the top-down and middle-down approaches (27).

Proteins are large and complex molecules, making their direct analysis by LC-MS/MS challenging (104,109,110). Peptides are smaller and more soluble in the HPLC mobile phase, allowing for efficient separation and analysis (28). In addition, MS/MS provides fragmentation data that are specific to peptide sequences (111).

Analysing peptides rather than intact proteins allows for more accurate identification and quantification using MS/MS data (105). Peptides are easier to ionise than intact proteins, leading to better sensitivity and detection in the mass spectrometer (105,106). Complex biological samples often contain numerous proteins with varying concentrations. Digesting proteins into peptides simplifies the sample complexity, reducing interference and enhancing the sensitivity of the analysis (28). Therefore, breaking up proteins into peptides before LC-MS/MS analysis is a fundamental step in proteomic research. Enzymatic digestion of proteins yields a mixture of peptides that can be separated and analysed efficiently using LC-MS/MS, thereby enabling comprehensive and high-throughput protein identification and quantification in complex biological samples (109).

LC-MS/MS after tryptic digestion of proteins is potentially an attractive solution for further increased sensitivity (75,89). In contrast to immunoassays, this technique is not subject to interference by endogenous immunoglobulins since those antibodies are destroyed by tryptic digestion. Tryptic digestion is, however, variable and typically does not result in the complete digestion of all proteins in the sample (75). Various enrichment methods may be beneficial for further increased sensitivity, especially when quantifying low-abundance proteins (75,89).

The superior separation power of HPLC combined with the specificity and selectivity of the MRM process, as described in Figure 1.8, can therefore be applied to the final detection and quantification of peptides.

1.6.2.1 Pre-digestion purification

During the quantification of proteins in a biological matrix it is often necessary to introduce a pre-digestion purification step due to the high number of interfering components in the matrix.

1.6.2.1.1 Protein precipitation

The most straightforward pre-digestion purification strategy is protein precipitation. With this, either the analyte or interfering matrix components are precipitated out of the solution by the addition of an organic solvent (15). The most common and also the most frequently used solvent for protein precipitation is methanol (27). Once methanol is added to a biological matrix, the precipitate will contain the proteins and denatured mAbs while the supernatant will contain the phospholipids, salts and sugars. Precipitating with acetonitrile was also found to result in a similar recovery when compared to precipitation using methanol (27). Organic solvents added to the matrix will alter the three-dimensional structure of proteins, disrupting their solvation potential, and thus rendering the proteins insoluble in the

adjusted matrix (15,100,104,112). Large intact proteins will therefore precipitate out of a biological fluid, while smaller molecules including peptides will remain soluble (104). With protein precipitation, the target protein can thus be separated from the biological matrix, but the process is very non-specific since most matrix proteins, such as albumins and globulins, will co-precipitate when preparing plasma for analysis (113). The speed and simplicity of this approach are, however, a major advantage when aiming to extract precipitated proteins and to dispose of other unwanted matrix components (113).

1.6.2.1.2 Affinity binding purification

Affinity binding purification selectively binds and retains the target protein while removing other sample matrix proteins and other components (104). This sample preparation procedure is the most specific and often leads to the cleanest sample by removing interferences such as albumin and other endogenous proteins found in human plasma (80). The mechanism of affinity binding purification is illustrated in Figure 1.9 (below).

Both protein A and protein G are often used to immobilise mAbs in a biological matrix prior to enzymatic digestion (87,114). Protein A and protein G are naturally produced by *Staphylococcus aureus* and *G. streptococci*, respectively, and have a specific binding site for the FC region of antibodies (114). They both have similar molecular structures but differ with regards to their subclasses and their binding affinities for human antibodies (115).

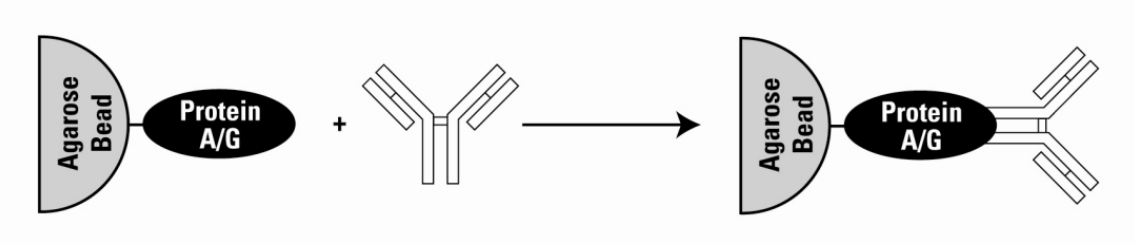

Figure 1.9. The basis of affinity binding purification using protein A or G bound to agarose beads. *The protein A or G bind specific antibodies allowing non-bound sample components to be washed away. The bound antibody can then be eluted with a buffer that disrupts binding interactions in preparation for tryptic digestion, or digestion can occur while the antibody remains bound to the agarose/protein complex* (115).

Protein A and protein G are often used as an affinity binding complex by binding it to agarose beads, thereby creating an immobilisation medium. The binding of the immobilised protein A or G to the antibody allows for the immobilisation of the antibody and separates it from other proteins in the serum or sample (114). In addition, binding changes the orientation of the antibody into a specific configuration whereby the Fab region of the antibody becomes exposed, thereby increasing the efficacy of trypsin digestion – which is described in the following section.

1.6.2.2 Digestion

The LC-MS/MS analysis of high molecular weight proteins, such as antibodies, is performed after the cleavage of the protein into smaller peptides using a protease, such as trypsin (109). This process often results in the generation of the signature peptide, which is unique to a specific antibody, depending on its immunogenic specificity embedded in the amino acid sequence of its Fab region. Selective proteolysis can improve the reproducibility and robustness of the analytical system while maintaining antibody specificity (116). The goal of sample preparation is to optimise a method that allows for reproducible quantification of the peptide target (104).

The most frequently used proteolytic enzyme is trypsin, which cleaves the protein backbone at the C-terminal residues of the basic amino acids arginine and lysine (105,106,117). Prior to digestion, a buffer is used to dilute the proteolytic enzyme to maintain an optimal pH. In order for trypsin to remain at its desirable activity, a pH of 7–9 is optimal and can be maintained by the addition of Tris buffer (118). Other external factors can be monitored in order to further facilitate trypsin activity, including incubation time and temperature conditions (119). There are also several grades of trypsin available for purchase which vary greatly in price and activity. For the bottom-up approach of mAb quantification, MS-grade trypsin is favoured (27). Trypsin activity may also be enhanced by adding low concentrations of organic solvents (101,120). The addition of 10–20% acetonitrile concentrations may increase the activity of trypsin up to three-fold (101). However, higher concentrations may hinder trypsin activity (101). Manufacturers commonly recommend a trypsin/protein ratio of anywhere between 1:100 and 1:20 (101,110,120) The optimal trypsin/protein ratio depends on the amount of total protein present in a sample prior to digestion (101). Plasma, as a biological matrix, contains a large number of proteins. There may also be large variations in plasma protein contents between patients. In this case, prior affinity binding purification is essential to improve and optimise the tryptic digestion phase of a bioanalytical method. Performing the proteolytic digestion on the mAb while it is still bound to the agarose-protein-A/G ensures that the trypsin can only digest at the Fab regions of the immunoglobulins and that it does not have access to the Fc region. This ultimately leads to cleaner digestion, resulting in higher sensitivity and increased reproducibility and accuracy (15,87,98).

1.6.2.3 Post-digestion purification

In some cases, the implementation of a post-digestion purification step to specifically isolate the target peptide following digestion may further improve the robustness of a bioanalytical method. Similar to pre-digestion purification, this step also aims to remove interfering compounds from a biological matrix and, in this case, also removes non-specific products following proteolytic digestion. Solid phase extraction (SPE) is an example of a post-digestion purification strategy that is usually used for this purpose.

1.6.2.3.1 Solid phase extraction

With regard to mAbs, SPE does not constitute a pre-digestion purification strategy as intact mAbs are typically too large to undergo SPE. Therefore, this step is readily used as a post-digestion purification step to purify the target peptide (87,100). Developing an SPE method can often be time-consuming and

requires careful optimisation due to the low concentration levels of mAbs when compared to the endogenous proteins in human plasma (100,121).

Solid phase extraction semi-selectively isolates the target of interest while removing a subset of other sample matrix components (104). This extraction method is illustrated below in Figure 1.11. It involves the use of solvents of different polarities to elute a compound from a sample following the compound's interaction with an immobilised extraction medium (sorbent). Depending on its interaction with the sorbent, the compound will elute in a more polar or more non-polar solvent. For example, if the sorbent is non-polar and the solvent is polar, polar compounds will elute with the polar solvent while non-polar compounds will remain on the sorbent (122). In Figure 1.10 (below), a sample is passed through a sorbent packed in a column or cartridge, and the sorbent selectively retains specific components based on their interactions with the sorbent's surface chemistry, and unwanted compounds are washed away while the target compound of interest is retained on the sorbent. The target compound is then eluted from the sorbent by using a solvent that cancels the interactions between the sorbent and the compound (99,122).

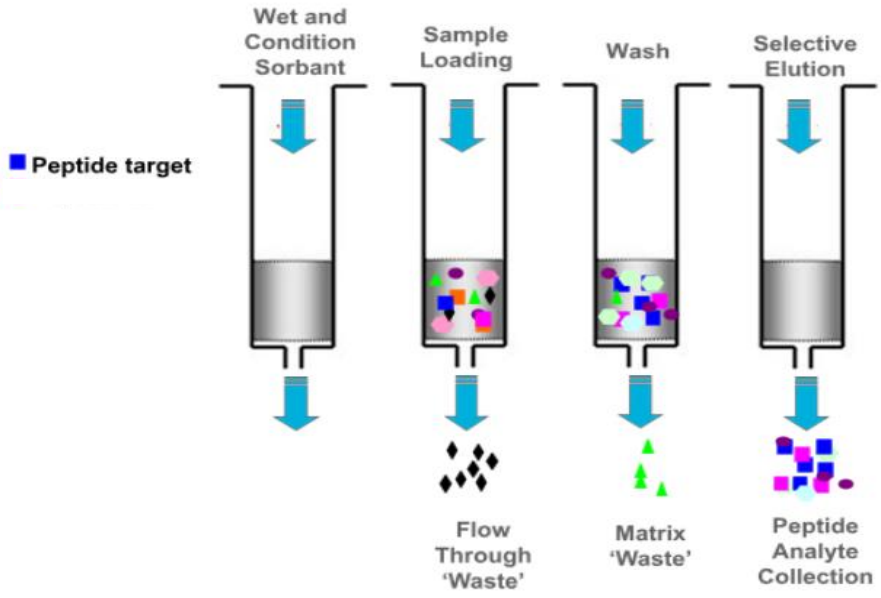

Figure 1.10. SPE sample preparation method. *Unwanted matrix components are washed through the SPE cartridge, leaving the peptide analyte retained. The analyte may then be eluted with an appropriate solvent and collected* (99).

1.6.3 Signature peptide selection

Trypsinization is used to cut the target protein into tryptic peptides and unique signature peptides. A resulting signature peptide is a unique tryptic peptide used to represent and determine the concentration of the intact target protein (110,123). There are a number of software tools available to predict the production of these signature peptides as a result of proteolysis. Because the sequence of chimeric mAbs differs from human peptide sequences, there are several possible signature peptides produced by a single mAb during proteolysis (27,111,124). It can become overwhelming when deciding which

signature peptide to use for the quantification of the intact mAb in a bioanalytical method. Therefore, several different factors can be considered. Peptide sequences that contain amino acids such as cystine, methionine, tryptophan and histidine are prone to oxidation while asparagine or glutamine may undergo deamination, ultimately influencing peptide stability (27,124). Peptide sequences that contain the amino acid proline are preferred because product ions with prolines at the N-terminal of the peptide are favourably formed by collision-induced ion dissociation during the final mass spectrometric (MS) assessment of the target peptide (27). This leads to higher sensitivity as product ion variability is eliminated. Lastly, it is important to differentiate between a signature peptide being theoretically and practically favourable. Peptide sequences that are theoretically suitable may result in low ionisation efficiency or low yield after tryptic digestion, resulting in low MS signals and poor reproducibility (27,111,124). Therefore, the most important factors to consider when selecting a signature or surrogate peptide are practical considerations such as chromatographic properties, MS response and the stability of the peptide in the biological matrix (27,123). Literature research is essential to facilitate and substantiate the selection of a signature peptide to represent an intact mAb in a bioanalytical method.

1.6.4 Internal standard selection

To account for variability during sample preparation and LC-MS/MS detection, the addition of an internal standard (ISTD) is generally included in a bioanalytical method, although it is not an absolute requirement by the EMA and FDA guidelines for bioanalytical methods (27,123,124). There are many points during the bottom-up approach where variability can be introduced during sample preparation, affinity binding, enzymatic digestion and general sample clean-up. The implementation of an ISTD may therefore greatly affect the robustness and performance of a bioanalytical method used to quantify mAb in a biological matrix (27,125). An additional challenge in method development is introduced when deciding on the optimal ISTD for a particular assay.

1.6.4.1 Stable isotope labelled peptides

Stable isotope-labelled (SIL) peptides are commonly used as ISTDs in quantitative MS-based proteomics and peptide analysis (27,123). An SIL-peptide is a synthetic peptide that is chemically identical to its endogenous counterpart but contains a stable isotope incorporated into certain amino acids (often a heavy isotope like 13C or 15N) (27,123,124). This results in a distinct mass shift compared to the naturally occurring peptide (123).

There is some uncertainty about when, during the bioanalytical method, the peptide internal standard should be added. Some papers report the addition of the peptide ISTD before sample preparation while others report the addition of the peptide ISTD after enzymatic digestion. One may think that the most appropriate time to add the ISTD is at the beginning of the bioanalytical assay, before sample preparation, so that the ISTD is subject to all the same conditions and processes as the signature peptide. However, during the bottom-up approach, the signature peptide is still incorporated in the intact mAb before enzymatic digestion during sample preparation. Therefore, both the chemical and physical properties differ between the *in situ* signature peptide and the peptide ISTD. The peptide ISTD is therefore not able to correct for variation in the sample preparation steps before digestion. It is thus

important to understand that no matter when in the bioanalytical assay the peptide ISTD is added, it cannot fully correct for all variations originating during sample preparation (27,124). Peptide ISTDs are mostly commercially available and much more affordable compared to a stable isotope labelled monoclonal antibody (SIL-mAb), as they are easier to produce with no post-translational modifications necessary (27).

1.6.4.2 Stable isotope labelled proteins

To eliminate some of the negative aspects of using peptide internal standards, a SIL-mAb may frequently be used as an ISTD for mAb quantification (27,111,123). The SIL-mAb should have the same sequence as the analyte mAb or signature peptide, but contain stable isotopes. This form of ISTD can be added right at the beginning of a bioanalytical method to track the entire process as SIL-mAb are intact proteins, and the ISTD will have identical properties to the analyte mAb (27,124,125). This is particularly useful during the steps in the bioanalytical method that have low reproducibility, such as the pre-digestion purification steps and the enzymatic digestion steps. The SIL-mAb can correct for variation through pre-digestion purification, enzymatic digestion, post-digestion purification, and LC-MS/MS analysis. SIL-mAbs are genetically modified mammalian, bacterial or yeast cell lines grown in a medium containing one or more SIL-amino acids (27,124). These cells will then produce mAbs by incorporating SIL-amino acids. Given the extensive and complex techniques used for the production of SIL-mAbs, their use as ISTDs is limited by their low availability and high cost (27,124).

1.6.4.3 Alternative internal standards

Some papers have reported the use of purified horse immunoglobulins or analogue mAbs as ISTDs (27,28,124). However, when considering the addition of these alternative internal standards it is important to remember that they may not work for a particular assay. A bioanalytical method should not be altered to accommodate an ISTD, especially if the assay is sensitive and reproducible without the addition of one.

1.6.5 Summary

Considering sample preparation for the quantification of macromolecules such as proteins, the process is significantly different and more complex than sample preparation for the quantification of small molecules. Not only are there more preparatory steps, but the primary protein being quantified cannot be analysed directly, and is ultimately measured by the analysis of a representative moiety produced from the protein by enzymatic cleavage (126). It is therefore essential to develop a robust sample preparation method to assure accuracy, precision and repeatability of the quantification method. The necessary steps are summarised by the schematic representation in Figure 1.11 (below).

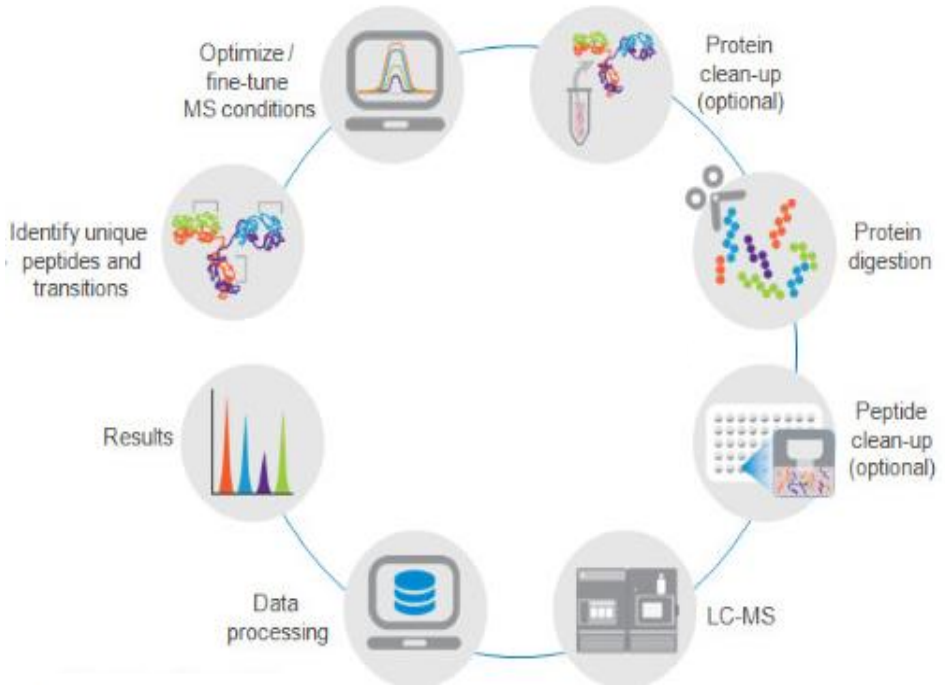

Figure 1.11. Summary of the bioanalytical workflow for quantifying digested proteins using LC-MS/MS. *This basic workflow includes the identification and selection of unique peptides and transitions, the optimisation and fine-tuning of MS conditions, and sample preparation techniques in the form of protein level clean-up, protein digestion, and peptide level clean-up. The resultant peptide may then be analysed by LC-MS in the form of a chromatographic peak* (103).

CHAPTER 2

PROJECT OUTLINE

2.1 RATIONALE

As a class of drugs, monoclonal antibodies (mAbs) are widely used in onco-haematology and are currently in development for the treatment of several autoimmune diseases. The ability of mAbs to target specific antigens in the body has led to the understanding that rituximab (RTX) may exhibit improved efficacy along with fewer side effects compared to other drugs. Up to this point, various pharmacokinetic studies have shown variability in RTX exposure, and thus variability in clinical response or efficacy. RTX exposure has been shown to be affected by several factors, including tumour burden, CD20 expression, genetic polymorphisms, and gender.

Although the drug is already widely used, there is a paucity of literature describing the use of RTX in the South African context. Part of South Africa's quadruple burden of disease is the ongoing battle with the high prevalence of tuberculosis (TB) and HIV, along with the co-treatment of these diseases. However, there is a lack of data on drug–drug interactions (DDIs) between antiretroviral therapy and TB treatment on RTX exposure. The probability of these DDIs is not well understood, and therefore knowledge of the possible interactions will inform dosing regimens for a large cohort of the South African population. Some papers suggest that RTX affects immunocompetency in patients with autoimmune diseases (70). The standard doses of RTX are suggested for patients co-infected with HIV and TB. Therefore, understanding the different RTX levels in human plasma amongst South African patients may guide further research and treatments for patients with co-infections. This project aims to develop a bioanalytical method to quantify RTX to assist with the clinical application in this specific setting.

This aim will be achieved by developing and optimising a sensitive and reproducible method for RTX using LC-MS/MS. Bioanalytical methods that provide therapeutic drug monitoring (TDM) of mAb concentrations may prove beneficial when trying to understand the relationship between exposure and clinical efficacy. Analyses such as this may prove the necessity of increased individualised therapies. Clinical treatments that are more patient-focused will allow for optimal dose-adjusting regimens and clinical efficacy in specific cases. In some instances, lower doses of RTX for a prolonged period may potentially be considered more important than a rapid high-dosage regime for a shorter period.

In this rapidly growing field, the knowledge acquired from RTX studies can be appropriately applied to optimise treatments with new-generation anti-CD20 therapies and other anti-tumour mAbs. Focusing on investigational and developmental experimental work is critical when considering the clinical application of these bioanalytical quantification methods. One of the major factors that make this approach appealing is that once an LC-MS/MS method is validated for a particular mAb it can readily be adapted to other mAbs across various biological matrices. This is particularly crucial when considering where most biotherapies are heading, as therapeutic mAbs have become one of the primary focuses for the pharmaceutical industry worldwide.

2.2 AIM

The aim of this research project was to develop and optimise the extraction and quantification of RTX in human plasma using appropriate sample preparation techniques and LC-MS/MS as the detection method.

2.3 OBJECTIVES

The objectives of this research project were to:

1. Develop an LC-MS/MS method for the detection and quantification of the RTX signature peptide.
2. Isolate RTX from human plasma
    a. by total protein extraction from the plasma employing precipitation.
    b. by affinity binding purification using protein A bound to agarose beads.
3. Produce the signature peptide from the RTX antibody by on-bead trypsin digestion.
4. Isolate the RTX signal peptide by solid phase extraction.
5. Investigate the suitability of two analytical instruments for the quantitative analysis of the RTX signal peptide at the required concentrations.
6. Explore the potential of different macromolecules to serve as an internal standard.

CHAPTER 3

MATERIALS

The different reagents, chemicals, consumables and equipment required to develop and optimise the bioanalytical method are outlined in this chapter. The necessary information on these materials is summarised in Tables 3.1–3.3. In addition, the preparation of buffers and solutions used for the development of the bioanalytical method are described in Section 3.4.

3.1 REAGENTS AND CHEMICALS

Table 3.2. *Reagents and chemicals*

Reagent	Catalogue No.	Grade	Supplier
Protein A Agarose	20334	N/A	ThermoFisher Scientific
Methanol	LC230-2.5	LC-MS	Sigma-Aldrich
Acetonitrile	015-4	LC-MS	Honeywell
Formic acid	1.00253.100	LC-MS	Merck
Phosphate buffered saline tablets	SLBS4223	Reagent Grade	Sigma-Aldrich
Dimethyl sulfoxide	1.02950.0500	For Spectroscopy	Merck
Water	In house Millipore	LC-MS	Millipore
Octyl β-D-1-thioglucopyranoside	SLBL4678V	Reagent Grade	Sigma-Aldrich
Trypsin protease	90057	LC-MS	ThermoFisher Scientific
1M Tris-HCl buffer, pH 8.0	15567027	Reagent Grade	ThermoFisher Scientific
Acetic acid	984303	LC-MS	ThermoFisher Scientific
Rituximab	10129440	N/A	Roche Products (Pty) Ltd (donated by Groote Schuur Hospital)
Rituximab signature peptide	PUJ-040	N/A	PEPSCAN
BCA Reagent A	23222	N/A	ThermoFisher Scientific
BCA Reagent B	23224	N/A	ThermoFisher Scientific

3.2 NECESSARY CONSUMABLES

Table 3.3. *Necessary consumables*

Description	Catalogue No.	Supplier
96 well plates	5042-1385	Agilent Technologies
Sealing mats	AM-2ML-RD	Lasec SA
Pipette tips (200 µL low bind)	Z719579	Merck
Pipette tips (1000 µL low bind)	Z719668	Merck
5 mL borosilicate tubes	ITEM 1505 (12 x 75)	Lasec SA
50 mL centrifuge tubes	P1TUB012B-000050SR	Lasec SA
15 mL centrifuge tubes	P1TUB013B-000015STR	Lasec SA
1.5 mL microcentrifuge tubes (low bind)	EP0030108116	Merck
Strata-X 33 µm polymeric reverse phase 30 mg / 1 mL SPE cartridges	S180004403	Phenomenex
InfinityLab Poroshell 120 EC-C18, 2.1 mm x 50 mm 2.7-Micron	699775-902	Agilent Technologies
InfinityLab Poroshell 120 EC-C18, 4.6 mm x 50 mm 2.7-Micron	699975-902	Agilent Technologies

3.3 EQUIPMENT REQUIRED

Table 3.4. *Equipment required*

Name	Model	Manufacturer
Pipette	0.5–10 µL	Various
Pipette	20–200 µL	Various
Pipette	200–1000 µL	Various
Vortex	G560E	Scientific Industries
Tube revolver rotator	88881001	ThermoFisher Scientific
Centrifuge	5424 and 5415D	Heraeus
Evaporator with heating block (incubator)	SBH 130D/3	Stuart
Synergy S Kit Millipore water purification system	SYNS00000	Millipore
SPE positive pressure manifold	Biotage Pressure+48 PPM48	Anatech

3.4 BUFFERS AND SOLUTIONS

Mobile Phase A: 0.1% formic acid in water with 2% dimethyl sulfoxide (DMSO) (water: formic acid: DMSO, 97.9:0.1:2, v/v/v): Add 500 µL of formic acid and 10 mL DMSO to 250 mL water. Dilute to 500 mL with water. No pH adjustment is made. De-gas with helium. The solution is stored at room temperature in normal light for a period of 2 weeks before being replaced.

Mobile Phase B: 0.1% formic acid in acetonitrile with 2% DMSO (acetonitrile: formic acid: DMSO, 97.9:0.1:2, v/v/v): Add 500 µL of formic acid and 10 mL DMSO to 250 mL acetonitrile. Dilute to 500 mL with acetonitrile. No pH adjustment is made. De-gas with helium. The solution is stored at room temperature in normal light for a period of 2 weeks before being replaced.

Autosampler needle rinse: 80% acetonitrile in water (acetonitrile: water, 80:20, v/v): Add 400 mL acetonitrile. Dilute to 500 mL with water. No pH adjustment is made. De-gas with helium. The solution is stored at room temperature in normal light for a period of 4 weeks before being replaced.

25 mM Tris-HCl buffer: A 25 mM tris-buffer dilution is made by adding 25 mL of the commercially obtained 1 M Tris-HCl buffer and diluted to 1 L with water. The pH was adjusted to pH and the buffer stored at ~2°C.

25 mM acetic acid solution: A 25 mM acetic acid dilution is made by adding 287 µL of 100% acetic acid to 200 mL of water.

Injection solvent: 0.1% formic acid in 50% acetonitrile (water: acetonitrile: formic acid, 50:50:0.1, v/v/v): Add 10 µL of 0.1% formic acid to 5 mL of acetonitrile. Dilute to 10 mL in water. The solution is made fresh on the day of extraction.

Phosphate buffered saline (PBS): Add one tablet of PBS (see Table 3.1) to 200 mL of water. The solution is stored at room temperature in normal light for a period of 2 weeks before being replaced.

Reconstituted trypsin solution: 100 µL of 25 mM acetic acid is added to reconstitute 100 µg of lyophilised trypsin. The 1 µg/µL solution is stored at ~20°C.

Trypsin working solution A: A 7 µg/mL solution is made by adding 140 µL of the reconstituted trypsin solution to 20 mL of 25 mM Tris-HCl buffer. The solution is made fresh on the day of extraction.

Trypsin working solution B: A 14 µg/mL solution is made by adding 280 µL of the reconstituted trypsin solution to 20 mL of 25 mM Tris-HCl buffer. The solution is made fresh on the day of extraction.

0.1% Octyl β-D-1-thioglucopyranoside (OTG) solution: (PBS: OTG, 99.9:0.1, v/v): 75 mg of OTG is weighed out and diluted in 75 mL of PBS. The solution is made fresh on the day of extraction.

10% formic acid in water: (water: formic acid, 90:10, v/v): 200 µL of formic acid is added to 1800 µL of water. The solution is made fresh on the day of extraction.

0.1% formic acid in water: (water: formic acid, 99.9:0.1, v/v): 70 µL of formic acid is added to 70 mL of water. The solution is made fresh on the day of extraction.

10% acetonitrile in water: (water: acetonitrile, 90:10, v/v): 500 µL of acetonitrile is added to 4500 µL of water. The solution is made fresh on the day of extraction.

70% acetonitrile in water with 1% formic acid: (water: acetonitrile: formic acid, 30:70:0.1, v/v/v): 100 µL of formic acid is added to 7 mL of acetonitrile and is diluted to 10 mL using water. The solution is made fresh on the day of extraction.

BCA working reagent: (BCA reagent A: BCA reagent B, 50:1, v/v): 100 µL of BCA reagent B is added to 50 mL of BCA reagent A. The solution is stored at room temperature in normal light for a period of 2 weeks before being replaced.

CHAPTER 4

DEVELOPING AN ANALYTICAL METHOD ON THE SCIEX API-3200 LC-MS/MS SYSTEM

The primary objective of this research project was to quantify RTX concentrations. This was achieved through a bottom-up approach, culminating in the identification of a target peptide that serves as a representative of RTX. To effectively analyse this target peptide, an analytical method was developed. This method hinges on liquid chromatography tandem mass spectrometry (LC-MS/MS) chromatographic separation, ensuring accurate detection and quantification. Notably, the Sciex API-3200 system was employed for initial development, in particular because of the generally elevated concentrations of RTX in human plasma. This system provided essential insights as the project progressed.

4.1 SELECTING THE SIGNAL PEPTIDE

A known signal peptide was selected based on the sequence of the heavy chain of RTX and information acquired from the literature (80). The full RTX sequence is indicated in Figure 4.1 with the signal peptide highlighted in bold. Being an IgG molecule, RTX consists of two heavy and two light chain subunits and the molecular weights of the subunits and the total protein are indicated in Table 4.1.

4.1.1 Rituximab protein

Heavy Chain

VQLQQPGAELVKPGASVKMSCKASGYTFTSYNMHWVKQTPGR**GLEWIGAIYPGNGDTSYNQK**FKG
KATLTADKSSSTAYMQLSSLTSEDSAVYYCARSTYYGGDWYFNVWGAGTTVTVSAASTKGPSVFPLA
PSSKSTSGGTAALGCLVKDYFPEPVTVSWNSGALTSGVHTFPAVLQSSGLYSLSSVVTVPSSSLGTQT
YICNVNHKPSNTKVDKKAEPKSCDKTHTCPPCPAPELLGGPSVFLFPPKPKDTLMISRTPEVTCVVVD
VSHEDPEVKFNWYVDGVEVHNAKTKPREEQYNSTYRVVSVLTVLHQDWLNGKEYKCKVSNKALPAPI
EKTISKAKGQPREPQVYTLPPSRDELTKNQVSLTCLVKGFYPSDIAVEWESNGQPENNYKTTPPVLDS
DGSFFLYSKLTVDKSRWQQGNVFSCSVMHEALHNHYTQKSLSLSPGK

Light Chain

QIVLSQSPAILSASPGEKVTMTCRASSSVSYIHWFQQKPGSSPKPWIYATSNLASGVPVRFSGSGSGT
SYSLTISRVEAEDAATYYCQQWTSNPPTFGGGTKLEIKRTVAAPSVFIFPPSDEQLKSGTASVVCLLNN
FYPREAKVQWKVDNALQSGNSQESVTEQDSKDSTYSLSSTLTLSKADYEKHKVYACEVTHQGLSSP
VTKSFNRGEC

Figure 4.1. Full amino acid sequence of RTX. *This figure summarises the amino acid sequence of one of the two heavy and light subunits that constitute the RTX protein. The selected signal peptide amino acid sequence is highlighted in bold, GLEWIGAIYPGNGDTSYNQK.*

Table 4.1. *Total molecular weight of RTX*

	Heavy chain	Light chain
Sequence length	451	213
Molecular weight	49215 Da	23057 Da
Total molecular weight*	**144544 Da**	

*Total molecular weight: 98430 (2x heavy chain 49215) + 46114 (2x light chain 23057) = 144544 Da

4.1.2 Rituximab signal peptide

The amino acid sequence of the RTX signal peptide (s-Pep) is schematically depicted in Figure 4.2. The molecular weight and monoisotopic mass of s-Pep are indicated in Table 4.2. Since the s-Pep originates from the heavy chain and has two subunits of the heavy chain in each RTX molecule, the s-Pep constitutes 3% of the molecule (See Tables 4.1 and 4.2).

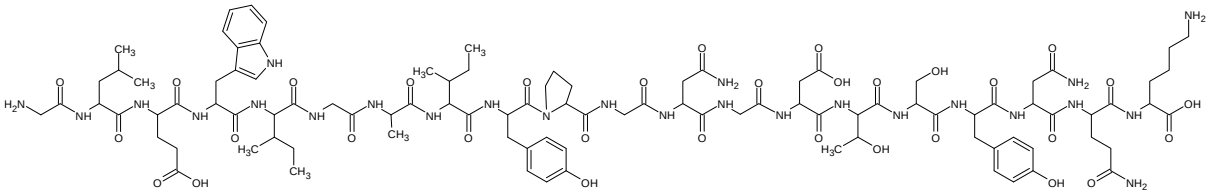

Figure 4.2. *Schematic depiction of the amino acid sequence for s-Pep.*

Table 4.2. *Molecular weight and monoisotopic mass for s-Pep*

	s-Pep
Amino acid sequence	GLEWIGAIYPGNGDTSYNQK
Molecular weight	**2183 Da***
Monoisotopic mass	2182 Da

*two s-Pep per one RTX molecule (2183 x 2 = **4366 Da**)

4.2 THE ANALYTICAL METHOD

The development of the analytical method involved the identification of the analytes' precursor ion and producing an ion fragment spectrum by collision-induced dissociation. The most abundant fragment ions were investigated to select the transition for use during multiple reaction monitoring to indicate the presence of the analyte. This was on the basis of the mass spectrometric detection method which was employed to develop chromatographic separation of the analyte. The chromatographic separation will result in a chromatographic peak, the area of which is a measure of analyte concentration.

During this process, ionisation and mass spectrometer settings were optimised to obtain the most sensitive detection parameters. Optimisation of chromatography involved the choice of an appropriate analytical column as well as the mobile phase composition.

4.3 INFUSIONS

The s-Pep stock solution was diluted in 20% acetonitrile in water with 0.1% formic acid to a concentration of 10 µg/mL. Infusion of the solution containing the s-Pep into the ionisation source of the Sciex API-3200 triple quadrupole mass spectrometer, applying positive mode electrospray ionisation and using Q1 scanning, resulted in the mass spectrum of the precursor ion depicted in Figure 4.3. The base peak in the mass spectrum represents the expected doubly protonated ion ($[M+2H]^{2+}$) of s-Pep at m/z = 1092. Minor peaks representing proposed adduct ions of the s-Pep with sodium ions and water ($[M+Na+H]^{2+}$, $[M+Na+H_2O+H]^{2+}$ and $[M+Na+2H_2O+H]^{2+}$) originating from the solvent, are also indicated in the mass spectrum.

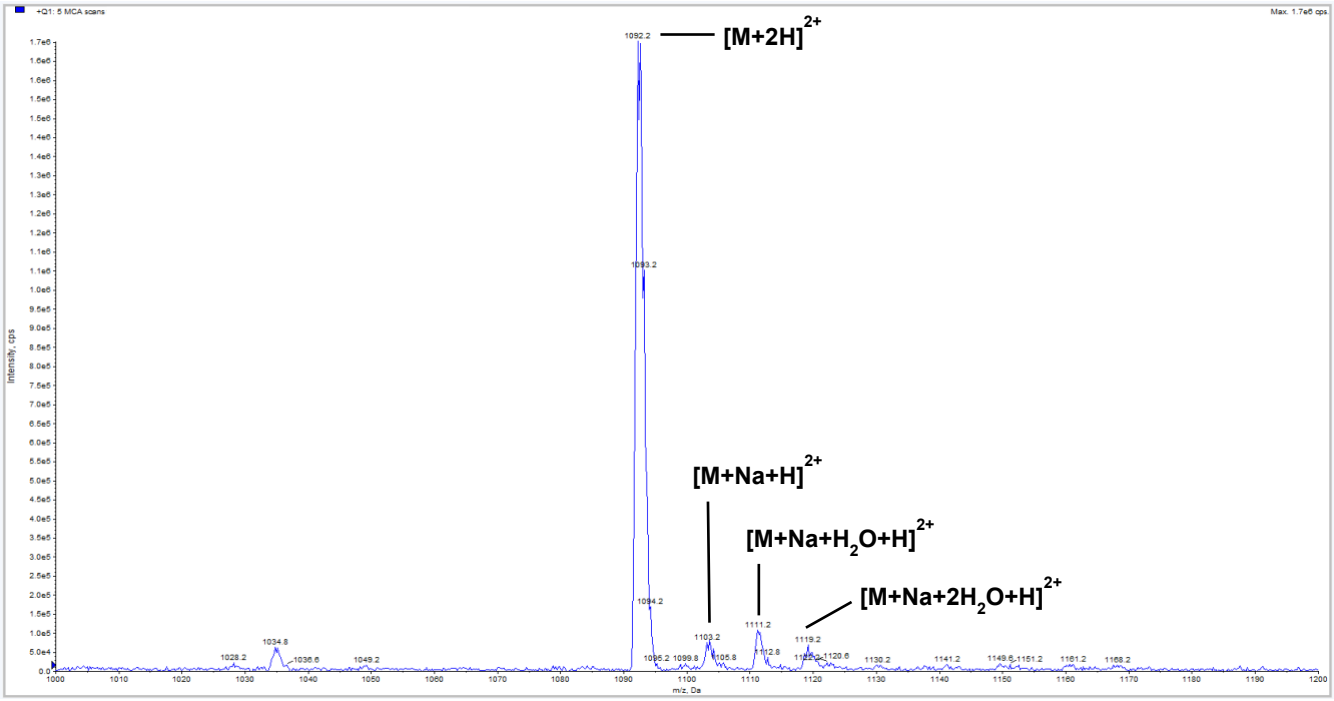

Figure 4.3. Precursor ion mass spectrum of s-Pep. *Electrospray ionisation in the positive mode was used, with Q1 scanning on a Sciex API-3200 triple quadrupole mass spectrometer. Ion peaks are indicated by the doubly protonated precursor ion and doubly charged sodium and water adduct ions.*

Fragmentation of the precursor ion by collision-induced dissociation resulted in a product ion mass spectrum, which is used to select the most abundant product ion for quantification of the analyte by multiple reaction monitoring (MRM). Using the Sciex API-3200 LC-MS/MS system, the ion with an intensity that could successfully be employed for this purpose was that at m/z = 82.2, as indicated in the product ion mass spectrum depicted in Figure 4.4 (quantifier transition). A second ion at m/z = 159.2 was selected as a qualifier ion to assure the identity of the analyte (qualifier transition). The production of these two ions was optimised by using relatively high collision energies (127 V and 119 V respectively; see Table 4.3). The two product ions are therefore secondary fragment ions, the proposed structures of which are indicated in Figure 4.4. Under these circumstances, expected fragments of the s-Pep precursor ion could be identified in the spectrum according to the expected fragmentation mechanisms of peptides when applied to the amino acid sequence s-Pep (see amino acid sequence indicated in

Figure 4.2). Apart from these two most abundant ions, b- and y-series fragment ions formed by the breaking of the peptide bonds were also identified, as well as less numerous a- and z-series ions. The evidence gleaned from this product ion mass spectrum therefore also positively identified s-Pep as the target ion.

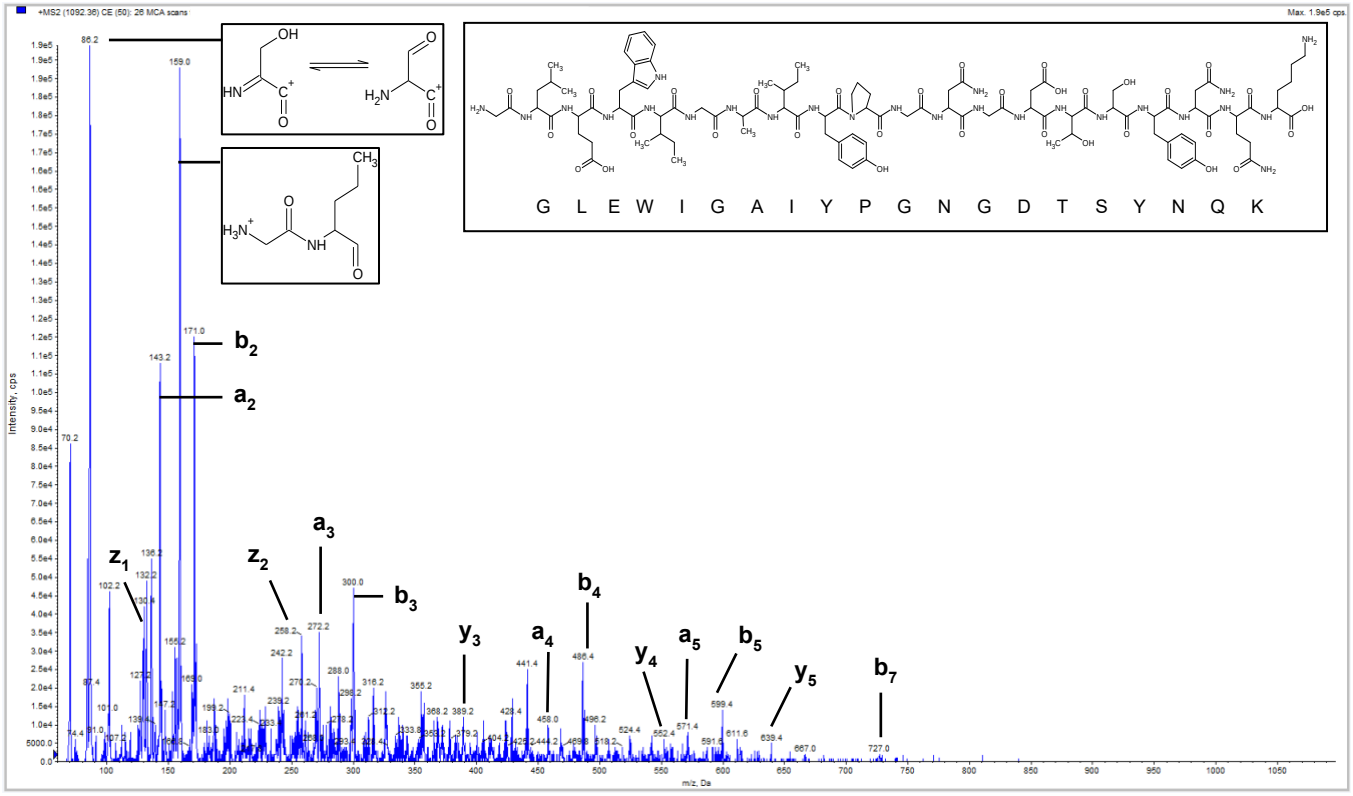

Figure 4.4. Product ion mass spectrum of s-Pep precursor ion at m/z = 1092.2. *The structure and amino acid sequence of s-Pep is indicated as well as the proposed structures of the quantifier product ion (m/z = 82.2) and qualifier product ion (m/z = 159.2). Peptide fragment ions of the a-, b-, y- and z-series, identified according to the expected fragmentation mechanisms for peptides, are also indicated for representative peaks.*

During the optimisation process, the parameters for optimum detection were automatically adjusted. Table 4.3 summarises the optimal parameters for the quantifier and qualifier transitions. Since optimisation was done during infusion at a very low flow rate (10 µL per minute) the final settings used for detection under LC-MS/MS conditions, where the flow rate is much higher (100–500 µL/min) included an adapted source temperature and gas settings as indicated in Table 4.3.

Although the optimisation was performed automatically, the resultant spectra can also be used to identify the fragments and thereby confirm the identity of the precursor ion and in this case some sequence information of s-Pep.

Table 4.3. *Sciex API-3200 instrument settings*

		Quantifier (1092.2/86.2)	**Qualifier (1092.2/159.2)**
ESI source settings	Curtain Gas (CUR), psi	30	30
	Ion Spray Voltage (IS), V	5500	5000
	Temperature (TEM), °C	600	600
	Ion Source Gas 1 (GS1), psi	55	55
	Ion Source Gas 2 (GS2), psi	65	65
	Declustering Potential (DP), V	156	156
Collision cell settings / Q2 settings	Collision Gas (CAD), psi	5	5
	Entrance Potential (EP), V	12	12
	Collision Energy (CE), V	127	119
	Collision Cell Entrance Potential (CEP), V	36	36
	Collision Cell Exit Potential (CXP), V	2	4
Detector settings	Ion Energy 1 (IE1), V	0.7	0.7
	Ion Energy 3 (IE3), V	1.7	1.7
	Detector Voltage (CEM), V	2800	2800

4.4 CHROMATOGRAPHY

The target peptide can be chromatographically separated using C18 columns and it is always preferable to use a gradient elution. Therefore, the initial choice of analytical column was an Agilent Poroshell C18 column (4.6 x 50 mm 2.7-Micron). The mobile phase consisted of the solvents and flow program, as indicated in Table 4.4. The resultant chromatograms are depicted in Figure 4.5.

Table 4.4. *Summary of the analytical column, mobile phase solvents, and flow program*

<table>
<tr><td>Analytical column</td><td>Agilent Poroshell 120 C18, 4.6 x 50 mm 2.7-Micron</td></tr>
<tr><td>Column temperature</td><td>~60ºC</td></tr>
<tr><td>Mobile phase and gradient elution</td><td>Mobile phase A: water: formic acid (99.9:0.1, v/v)
Mobile phase B: acetonitrile: formic acid (99.9:0.1, v/v)
<table>
<tr><th>Time (min)</th><th>Mobile phase A (%)</th><th>Mobile phase B (%)</th><th>Flow rate (µL/min)</th></tr>
<tr><td>0.01</td><td>95</td><td>5</td><td>500</td></tr>
<tr><td>0.2</td><td>95</td><td>5</td><td>500</td></tr>
<tr><td>1.2</td><td>20</td><td>80</td><td>500</td></tr>
<tr><td>3.1</td><td>20</td><td>80</td><td>500</td></tr>
<tr><td>3.5</td><td>95</td><td>5</td><td>500</td></tr>
<tr><td>5.9</td><td>95</td><td>5</td><td>500</td></tr>
<tr><td>6</td><td>95</td><td>5</td><td>500</td></tr>
</table>
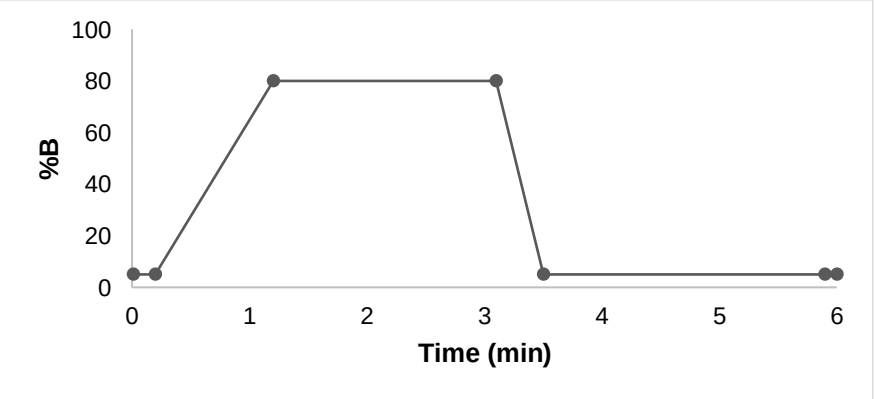
</td></tr>
</table>

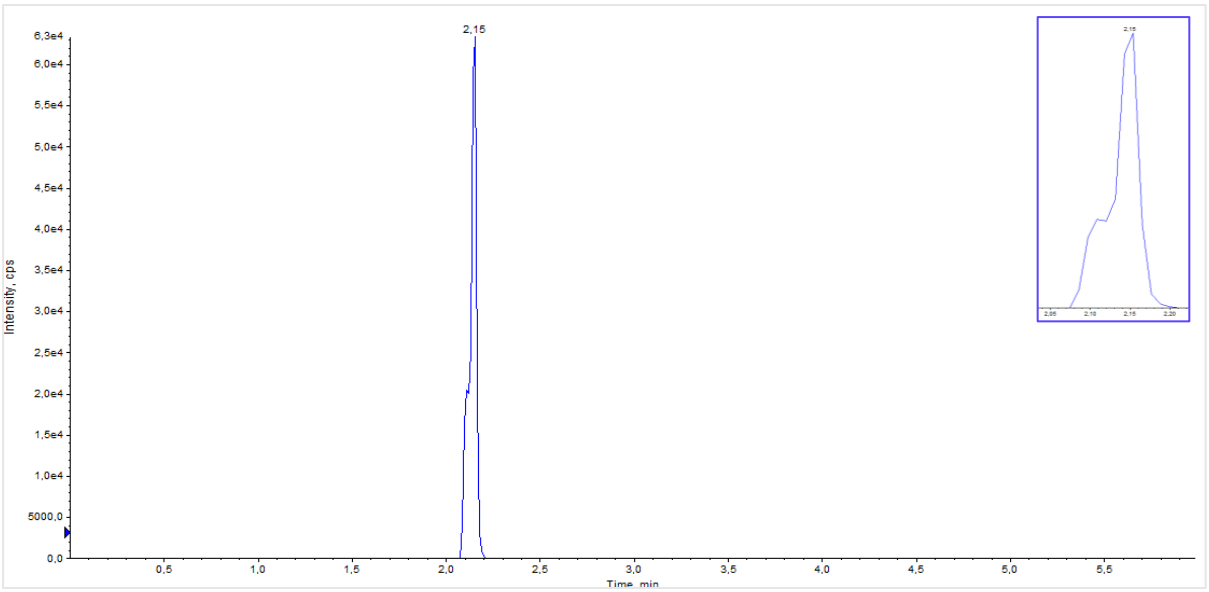

Figure 4.5. Chromatographic peak of s-Pep. *The peak shape of the analyte in the mass chromatogram when a 10 µg/mL s-Pep stock solution was injected into the Sciex API-3200 system.*

The chromatographic peak representing s-Pep shows a pronounced leading shoulder, making the peak shape not ideal for quantification. In addition, the retention time of the peak is 2.2 min, which is near to the void volume of the column (1.1 min). The void volume of the column is calculated in Scheme 4.1. These two factors are probably due to a combination of the inner diameter of the column, the flow rate used, and the slope of the gradient.

Scheme 4.1

Vm = dead volume

$Vm = 0.5 \times L \times d^2 / 1000$

$Vm = 0.5 \times 50 \times (4.6)^2 / 1000$

= 0.529 mL

T0 = column dead time

T0 = Vm / Flow

= 0.529 / 0.5

= 1.1 min

Where L (mm) is the length of the column, d (mm) is the diameter of the column, and flow is the flow rate in mL/min (see Table 4.4).

It was therefore decided to use an analytical column with a smaller inner diameter and also to adjust the mobile phase and gradient. The details of these changes are shown in Table 4.5. For acceptable chromatography of peptides, it is known that low concentrations of DMSO may be added to the mobile

phase to increase sensitivity but also to improve chromatography by producing better peak shapes (127). Therefore, the mobile phases were adjusted by the addition of 2% DMSO and a less steep gradient was applied (Table 4.5). Table 4.5 also indicates a lower column temperature than was used before. Although relatively high column temperatures are applied for the chromatography of peptides (128), this adjustment was considered necessary to preserve the analytical column and also to investigate this lower temperature for adequate chromatography. Applying all these changed parameters, the resultant chromatogram is depicted in Figure 4.6.

Table 4.5. *Summary of the adjusted analytical column, mobile phase solvents, and flow program*

<table>
<tr><td>Analytical column</td><td>Agilent Poroshell 120 C18, 2.1 x 50 mm 2.7-Micron</td></tr>
<tr><td>Column temperature</td><td>~50ºC</td></tr>
<tr><td>Mobile phase and gradient elution</td><td>Mobile phase A: water: formic acid: DMSO (97.9:0.1:2, v/v/v)
Mobile phase B: acetonitrile: formic acid: DMSO (97.9:0.1:2, v/v/v)
<table>
<tr><th>Time (min)</th><th>Mobile phase A (%)</th><th>Mobile phase B (%)</th><th>Flow rate (µL/min)</th></tr>
<tr><td>0.01</td><td>85</td><td>15</td><td>300</td></tr>
<tr><td>0.2</td><td>85</td><td>15</td><td>300</td></tr>
<tr><td>2.3</td><td>15</td><td>85</td><td>300</td></tr>
<tr><td>3.1</td><td>15</td><td>85</td><td>300</td></tr>
<tr><td>3.5</td><td>85</td><td>15</td><td>300</td></tr>
<tr><td>5.9</td><td>85</td><td>15</td><td>300</td></tr>
<tr><td>6</td><td>85</td><td>15</td><td>300</td></tr>
</table>
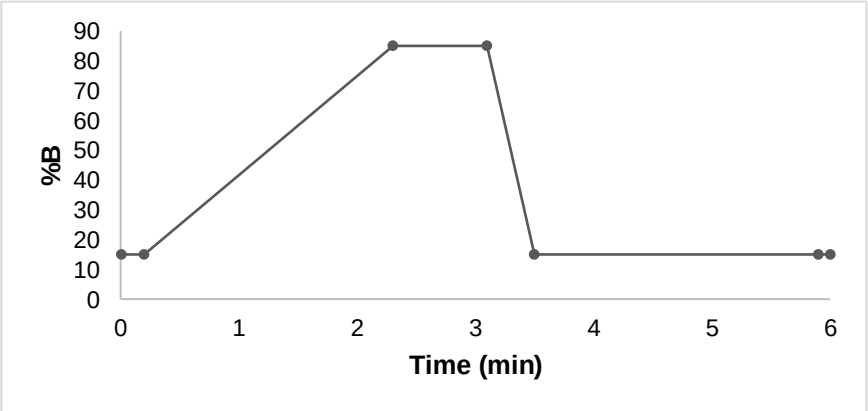
</td></tr>
</table>

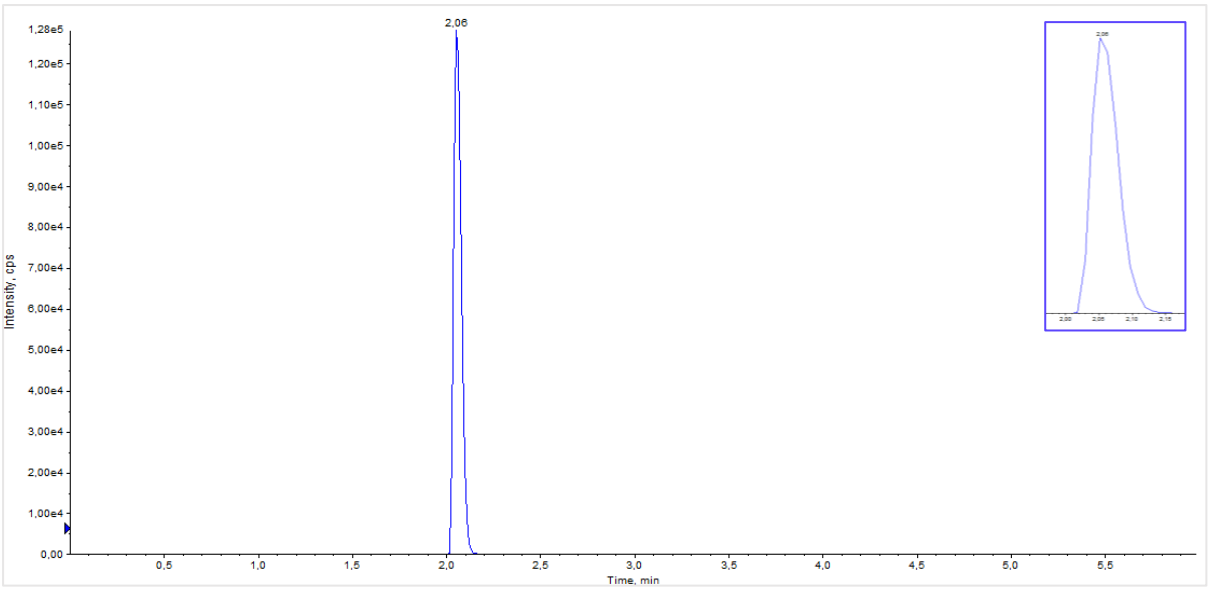

Figure 4.6. Chromatographic peak of s-Pep. *The peak shape of the analyte in the mass chromatogram when a 10 µg/mL s-Pep stock solution was injected into the Sciex API-3200 system using the adjusted parameters.*

The analyte peak shape was now greatly improved with a symmetrical shape which will be totally acceptable for quantification. It was also calculated that the void volume of this column is 0.4 min, which means that the analytical peak is better separated from the solvent front compared to the previous chromatographic conditions. The void volume is calculated in Scheme 4.2

Scheme 4.2

Vm = dead volume

$$Vm = 0.5 \times L \times d^2 / 1000$$

$$Vm = 0.5 \times 50 \times (2.1)^2 / 1000$$

$$= 0.11 \text{ mL}$$

T0 = column dead time

$$T0 = Vm / Flow$$

$$= 0.11 / 0.3$$

= 0.4 min

Where L (mm) is the length of the column, d (mm) is the diameter of the column, and flow is the flow rate in mL/min (see Table 4.5).

The peak intensity ratio of the quantifier and qualifier transitions is graphically demonstrated in Figure 4.7.

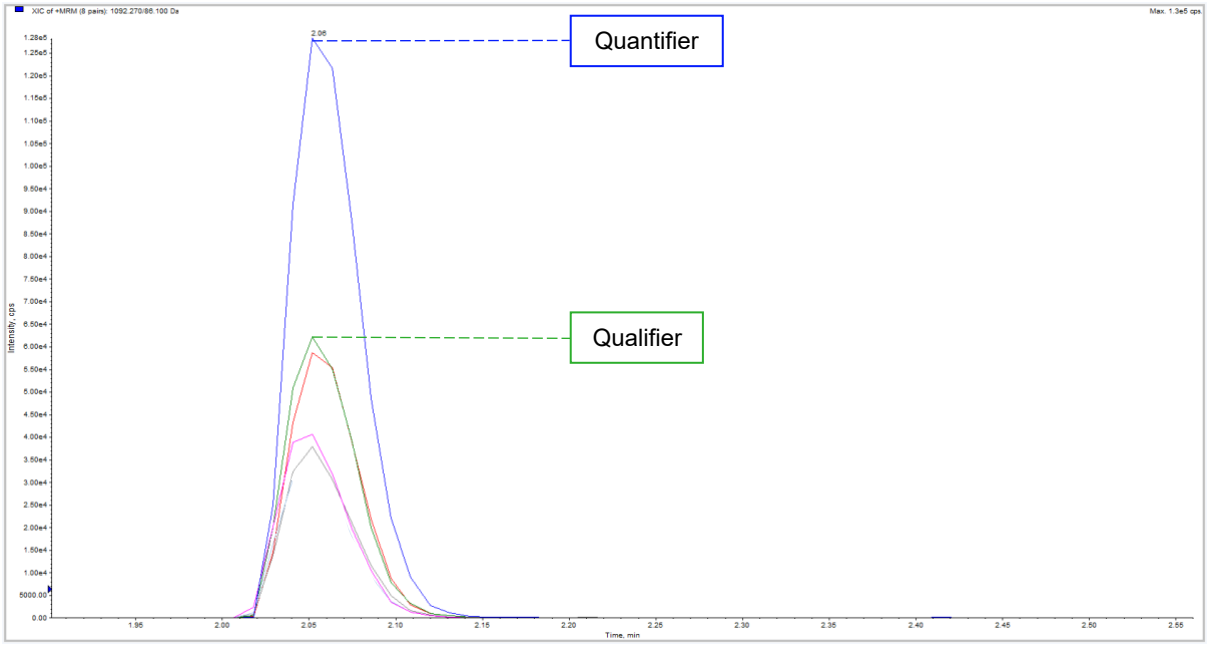

Figure 4.7. Quantifier and qualifier intensities. *Quantifier fragment illustrated in blue (1092.2/86.2) as well as the qualifier fragment illustrated in green (1092.2/159.2); minor fragments are also illustrated.*

To prove that this analytical method can be used for quantitative purposes, a concentration range of the s-Pep was prepared in injection solution (see Section 3.4) at the following concentrations: 0.25, 0.5, 1, 2, 4, 6, 8 and 10 µg/mL. These were analysed as a batch which contained a blank sample injected after the highest standard. The chromatograms of the samples with s-Pep at the highest and lowest concentrations are indicated in Figure 4.8 (Panels A and B). The signal-to-noise ratio (S/N) of the peak area of the lowest concentration of s-Pep was 49 (≥ 5), which is an acceptable S/N value. The blank chromatogram following that of the highest concentration indicated that there was no apparent carryover of the analyte (Panel C).

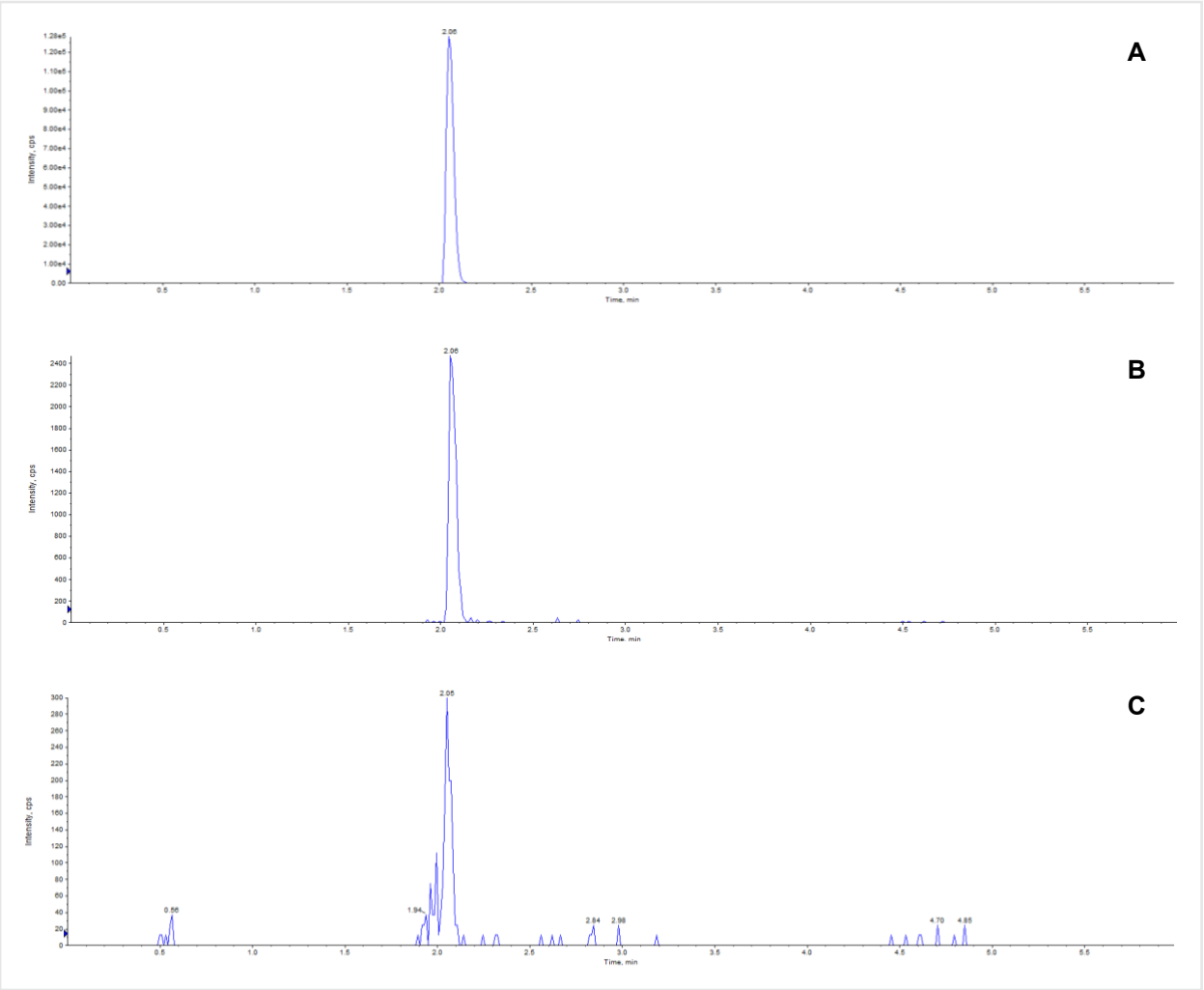

Figure 4.8. Representative chromatograms for s-Pep. Panel A: *10 µg/mL s-Pep in injection solution,* ***Panel B:*** *0.25 µg/mL s-Pep in injection solution,* ***Panel C:*** *blank sample containing only injection solution and no s-Pep (negligible carryover observed in the blank, <15% of Panel B).*

Integration of the chromatographic peaks of the s-Pep standards indicated the peak areas and if these are plotted against the analyte concentration, a curve, as depicted in Figure 4.9, is observed. The curve follows a linear function f(x) = mx + c, with R^2 = 0.998.

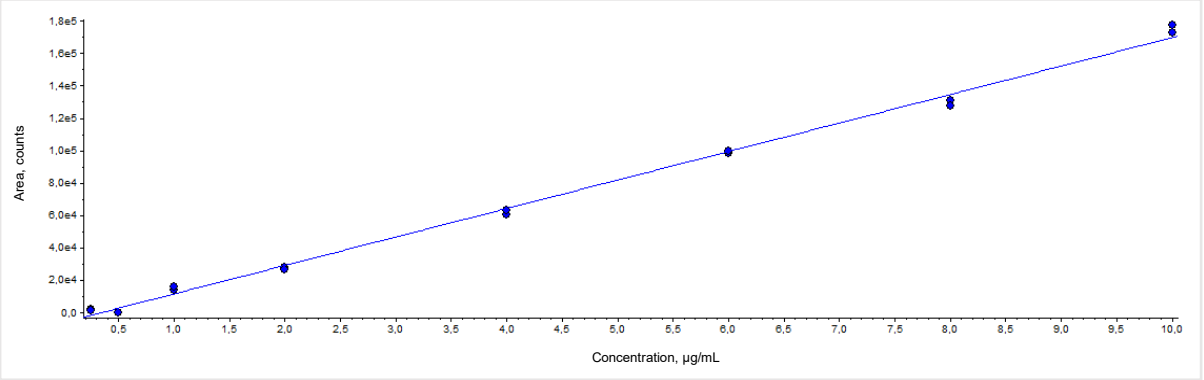

Figure 4.9. Representative calibration curve for s-Pep. *Concentration of s-Pep (0.25–10 µg/mL) plotted against analyte peak area, R^2 = 0.998.*

Even though this does not represent the concentration range of the final reconstituted and extracted analyte that will be assessed once a complete method has been developed, the calibration curve demonstrates that the analytical method accurately identifies the analyte. Consequently, this chapter's findings can be successfully applied to develop a comprehensive procedure for quantifying RTX in human plasma.

CHAPTER 5

BIOANALYTICAL METHOD DEVELOPMENT

5.1 ISOLATING THE SIGNATURE PEPTIDE: PROTEIN DIGESTION USING TRYPSIN

To quantify mAbs in plasma using mass spectrometry, the mAb of interest must first be differentiated from the very similar polyclonal background of over 1 g/dL of endogenous human immunoglobulins in blood (28). Historically, proteins have been quantified by LC-MS/MS using specific tryptic fragments referred to as proteotypic peptides (proteolytically derived peptides) (27,28,101). For chimeric mAbs, such as RTX, the entire variable region (>250 amino acids) is of animal origin. Therefore, trypsin digestion of that region increases the likelihood of finding unique signature peptides specific to that mAb. This process is briefly illustrated in Figure 5.1.

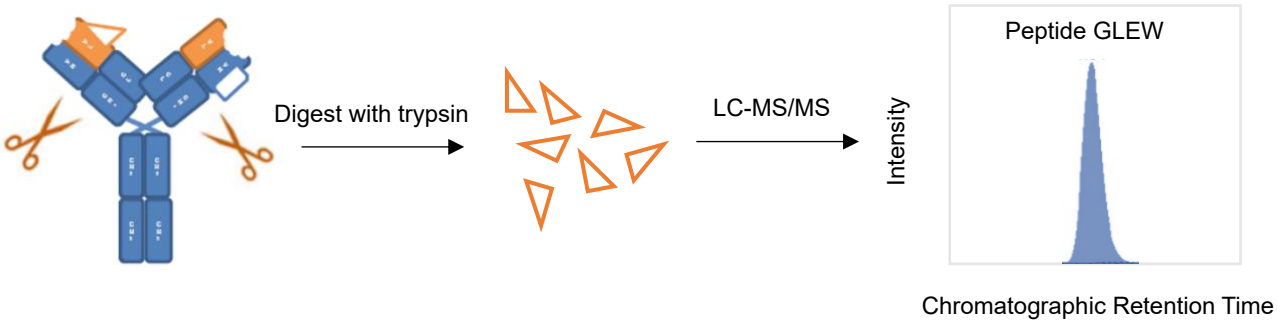

Figure 5.1. Trypsinization procedure. *Illustration of protein digestion using trypsin to produce unique and quantifiable signature peptides for LC-MS/MS quantification* (28).

Digestion by trypsin cleaves the intact immunoglobulin into smaller peptides which are separated by liquid chromatography before analysis by MS/MS. Peptides specific to the variable region of the mAb, either on the light or heavy chain, and which do not cross-react with human sequences, are used for quantification. The unique RTX signature peptide (s-Pep) is produced during this process, and will be measured as a representative marker for RTX. Successful production of this signature peptide is essential since it will be the measuring moiety employed during most of the method development process.

The efficiency of trypsin digestion directly influences quantification accuracy and analytical precision. Therefore, optimisation of trypsin digestion is essential for developing a successful analytical method. This chapter delineates this optimisation in terms of the trypsin / RTX ratio and incubation conditions. Since the complete method will also include the specific extraction of the RTX molecules from the biological matrix before trypsinization, the experiments in this section are performed in a physiological buffer and not in plasma. According to the literature on RTX quantification in plasma, trypsinization of RTX in plasma without prior affinity binding purification will not result in efficient sensitivity for successful quantification (27,105). Therefore, the experimental samples represent a plasma-free sample to as closely as possible mimic the purification that will occur during the affinity binding procedure, which is explored later in the method development section.

5.1.1 Experiment 1: Enzyme-to-substrate ratio and incubation time

Introduction

Trypsin digestion is conventionally performed by incubation at 37°C for at least 4 to 16 hours, typically at a final protease-to-protein ratio of between 1:100 and 1:20 (w/w). If necessary, fresh trypsin can also be added during the incubation period (101,120).

For a protein sample to be enzymatically digested, the enzyme must access the cleavage sites (the protein must be solubilised), and the solution must be at an appropriate pH for enzyme activity. Optimal trypsin activity occurs at pH 8 (118,119). Therefore, lyophilised trypsin is prepared in 25 mM Tris buffer at pH 8 (Chapter 3, Section 4).

Selecting an appropriate incubation time depends on a compromise between various factors. Generally, the incubation time should be long enough to permit a moderate amount of product to be formed, and the error in timing is insignificant but not beyond the plateau of the concentration of the signal peptide production. Overnight incubation for trypsinization is therefore performed conventionally (119).

Methodology

The first investigation involved two experimental groups (Groups A and B) in which the same concentration of RTX was incubated with two different enzyme concentrations for five different periods. The incubations were performed in appropriate glass vials.

The 1 µg/µL lyophilised trypsin was reconstituted with 100 µL of acetic acid and diluted with 25 mM Tris-HCl buffer at pH 8 to a final concentration of 7 µg/mL (Group A trypsin working solution) and 14 µg/mL (Group B trypsin working solution).

For Group A, 500 µL of a 7 µg/mL trypsin working solution was added to 7 µL of the 10 mg/mL RTX stock solution (RTX in water) to achieve a final protease (trypsin) to protein (RTX) ratio of 1:20 (w/w), and thus 3.5 µg of trypsin was added for every 70 µg of RTX.

For Group B, 500 µL of a 14 µg/mL trypsin working solution was added to the same volume and concentration of RTX used for Group A to achieve a final protease (trypsin) to protein (RTX) ratio of 1:10 (w/w), and thus 7 µg of trypsin was added for every 70 µg of RTX.

All 10 experimental samples of Group A and Group B were then incubated at approximately 37°C for five different time intervals (T=1h, T=3h, T=5h, T=19h and T=24h). At each time interval, the digestion was terminated by adding 25 µL of 10% formic acid to result in 0.5% formic acid in the mixture and lowering the pH to 2 (previously determined with pH strips). At this pH, the trypsin activity is totally quenched (119).

The final volume, post digestion, was 525 µL. All experimental samples were directly analysed on the Shimadzu liquid chromatography system coupled to a Sciex API-3200 Q-Trap mass spectrometer using the LC-MS/MS settings outlined in Chapter 4. This experiment is briefly outlined in the flow diagram depicted in Figure 5.2.

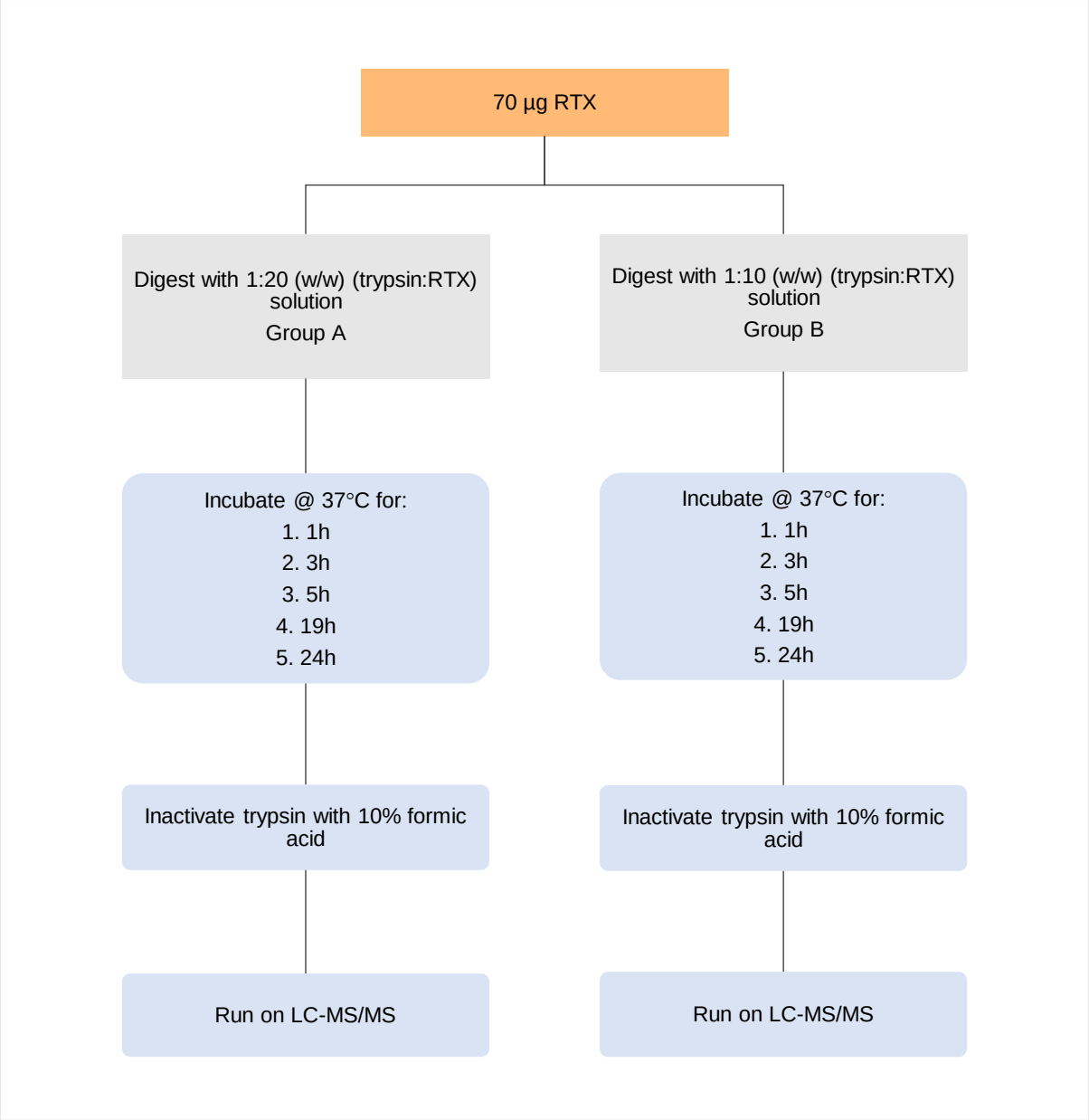

Figure 5.2. Experimental workflow. *Flow diagram illustrating the efficiency of protein digestion for two different proteases: protein concentrations for five different incubation periods.*

For quantification, a set of s-Pep calibration standards was prepared by diluting the 2 mg/mL stock solution of s-Pep and analysed with the experimental samples. The final concentrations of the standards were 0.25; 0.5; 1; 2; 4; 6; 8; 10 µg/mL. The dilutions were performed using an injection solution (see Section 3.4). The peak areas of the calibration peptide standards were plotted against their concentration using linear regression. The resultant standard curve, depicted in Figure 5.3, was used to determine the s-Pep concentrations of the experimental samples.

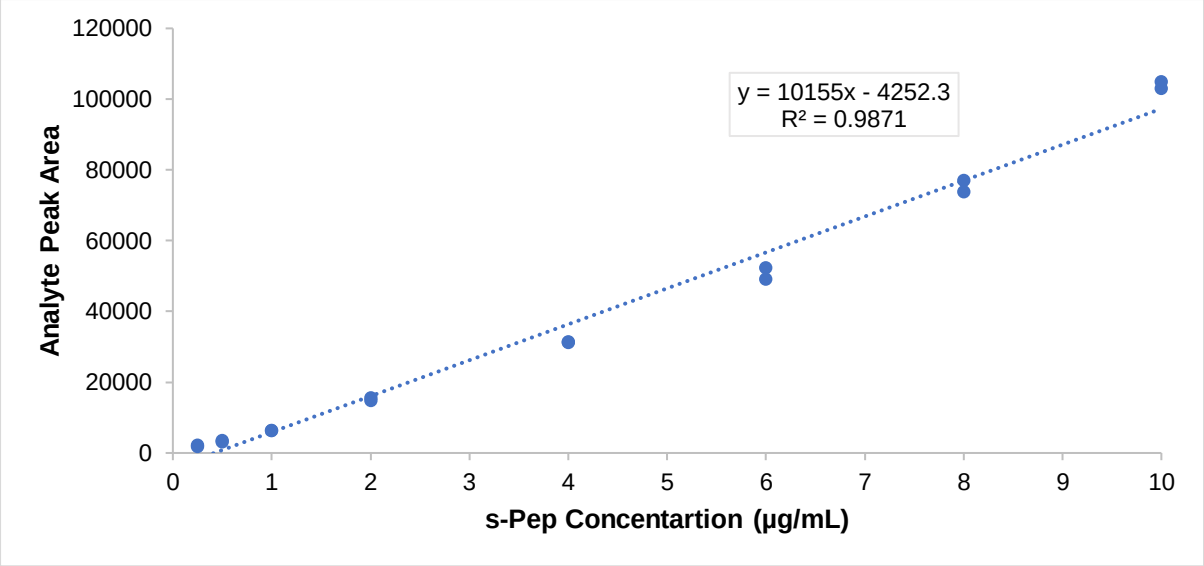

Figure 5.3. Representative calibration curve for s-Pep. *Line graph illustrating peptide concentration in µg/mL versus analyte peak area response for the s-Pep calibration standards used to calculate the s-Pep concentration of the experimental samples. Equation y = 10155x – 4252.3, R² = 0.987.*

Results

The s-Pep concentrations of the experimental samples produced from the tryptic digestion under various conditions are indicated graphically in Figure 5.4. Based on the peptide calibration curve, actual s-Pep concentrations were calculated for the experimental samples, using the below calculation (Scheme 5.1) for the fifth sample of Group B (the sample incubated for 24h with the 1:10 ratio). The same calculation was applied to all the other digested samples (A1-5 and B1-5).

Scheme 5.1

Example calculation for sample B5 based on the equation from Figure 5.3

$$y = 10155 (x) – 4252$$

where y is = 3406 (peak area for 1:10 24h sample)

$$3535= 10155 (x) – 4252$$

$$x = 0.767 \text{ µg/mL}$$

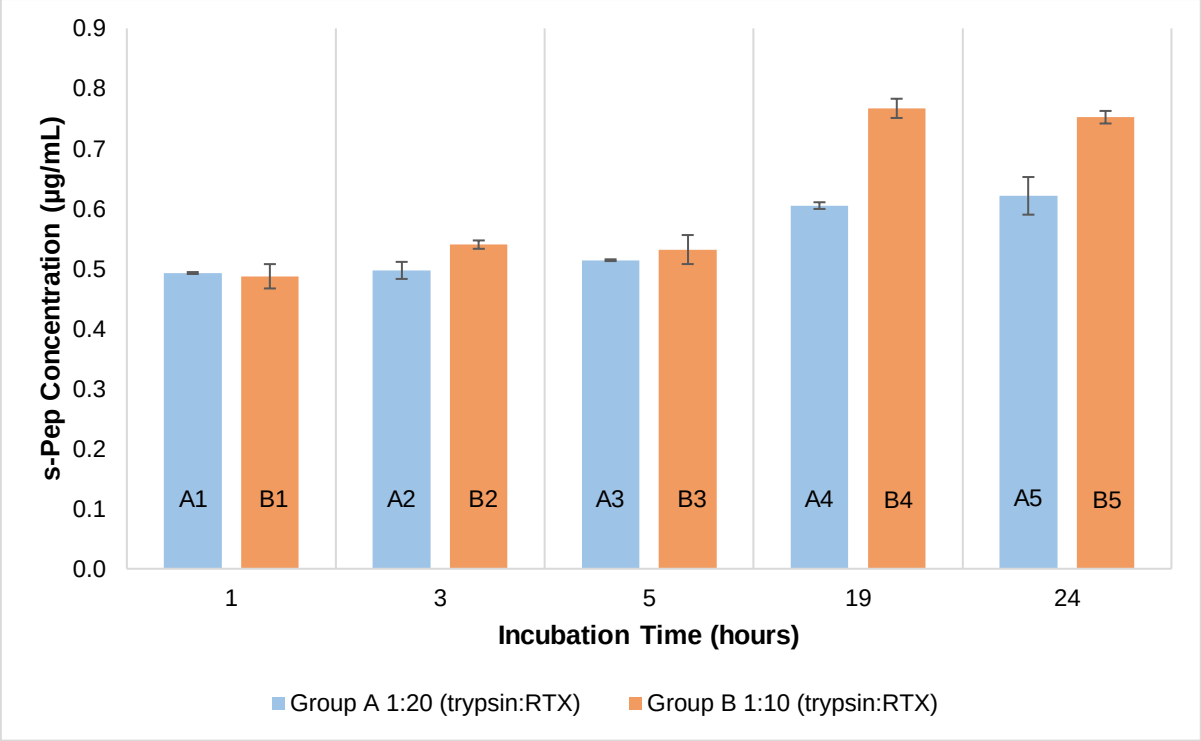

Figure 5.4. s-Pep concentration over time. *Bar graph illustrating the s-Pep concentration (µg/mL) over 24 hours when a 1:20 and 1:10 protease: protein ratio was explored. Five separate collection points at T=1h, T=3h, T=5h, T=19h and T=24h. Each experimental sample (A1–5, B1–5) was injected in duplicate, and error bars represent standard deviation, N=2.*

Figure 5.4 depicts a gradual increase in s-Pep concentration for the samples left in the incubator for 1, 3 and 5 hours for both Group A and Group B (A1–3, B1–3). For Group A, the overall increase in peptide concentration from A1 to A3 was 0.0214 µg/mL. For Group B, the overall increase in peptide concentration from B1–B3 was 0.0445 µg/mL. The increase over the first 5 hours for Group B was twice that of the increase over the first 5 hours for Group A.

The increase in s-Pep concentration was significantly more when the incubation time was extended to 19 hours. For Group A, the overall increase in peptide concentration from A3 to A4 was 0.0909 µg/mL. For Group B, the overall increase in peptide concentration from B3 to B4 was 0.235 µg/mL, which is 2.6 times that of Group A.

The difference between the samples left for 19 hours versus 24 hours was minimal. For Group A, the s-Pep concentration between A4 and A5 increased by 0.0163 µg/mL (less than the increase in the first 5 hours, A1–A3). For Group B, the s-Pep concentration between B4 and B5 decreased by 0.0148 µg/mL (significantly less than the change observed in the first 5 hours, B1–B5). The overall difference between A4–A5 and B4–B5 was similar (0.0163 vs 0.0148 µg/mL), therefore indicating a plateau between 19 and 24 hours.

Lastly, when comparing Group A and B for all time intervals, the s-Pep concentrations for Group B are consistently higher than Group A. Over the first three-time intervals (A1–3 and B1–3), Group A averages

an s-Pep concentration of 0.501 µg/mL, and Group B averages an s-Pep concentration of 0.520 µg/mL. The overall s-Pep concentration in the first 5 hours is similar in both Groups between 19 and 24 hours. Group A averages an s-Pep concentration of 0.613 µg/mL, and Group B averages an s-Pep concentration of 0.759 µg/mL. Therefore, the biggest and most significant difference between Group A and B is observed at 19 and 24 hours.

Discussion

The concentration of s-Pep increases with time during the incubation of RTX with trypsin, reaching a plateau between 19 and 24 hours. An incubation time of 19 hours is sufficient for optimal peptide production and it can thus be selected as the optimal incubation time.

Using a trypsin/RTX ratio of 1:10, higher s-Pep concentrations were observed. When the 1:20 ratio was used, s-Pep concentration improved even after 19 hours, compared to the 1:10 ratio. This points to the possibility that the 1:20 digestion was not fully complete, and adding extra trypsin later in the incubation period may further increase the yield of s-Pep, as confirmed in the literature (101,120).

Later in the extraction procedure, when affinity binding enrichment employing protein A beads was introduced, tryptic digestion was performed while tumbling the tubes at room temperature and not at 37°C. This is an additional incentive to investigate the addition of extra trypsin after an initial incubation period to yield optimal s-Pep concentration and increase digestion efficacy.

5.1.2 Experiment 2: Final optimisation

Introduction

The amount of trypsin needed will vary depending on the amount of protein sample present and the desired tempo of digestion. Typically, a 1:20 (w/w) ratio is sufficient for complete digestion (28). In some cases, if protein concentration is high or the accessibility of trypsin to the cleavage site is hampered (because of insolubility), adding an additional aliquot of fresh trypsin may be helpful.

It is well documented that trypsin activity is enhanced in the presence of acetonitrile (10% to 50% v/v) (101,106). This may because of the enhancement of the accessibility of the target sequence of the protein to the active site of the proteolytic enzyme given a low level of unfolding and denaturing of the target protein. It is known that trypsin and some other proteases are resistant to unfolding in organic solvents, retaining activity under conditions that denature other proteins. Acetonitrile may also aid in the continual solubilisation of the substrate proteins during the incubation (106). It was therefore decided to investigate the further enhancement of the process by adding acetonitrile to the incubation mixture.

Methodology

Experiment 2 was carried out similarly to Experiment 1, using the optimised incubation time of 19 hours, but with now adding a third group of experimental samples (Group C) to investigate the addition of more trypsin later during a second incubation period. A volume of 50 µL of acetonitrile was added to all experimental samples before incubation (approximately 10% acetonitrile, v/v) to bring the final volume of the incubation mixture to 557 µL.

Groups A, B and C were incubated for 19 hours at approximately 37°C. Similar to Experiment 1, the experimental samples from only Group A and B were quenched with the addition of 25 µL 10% formic acid.

At this time, an additional volume of 4 µL of the 1 µg/µL trypsin stock solution was added to the samples of Group C to maintain the 1:20 protease: protein ratio as closely as possible. Group C was then incubated for a further 3 hours before terminating the enzyme reaction with 25 µL 10% formic acid. The final volumes for Groups A and B were 582 µL, and the final volume for Group C was 586 µL.

All samples were then analysed by LC-MS/MS to quantify the target peptide in each, as described for the samples of Experiment 1 using the calibration curve in Figure 5.5 to calculate the s-Pep concentrations.

This experiment is briefly outlined in the flow diagram depicted in Figure 5.6.

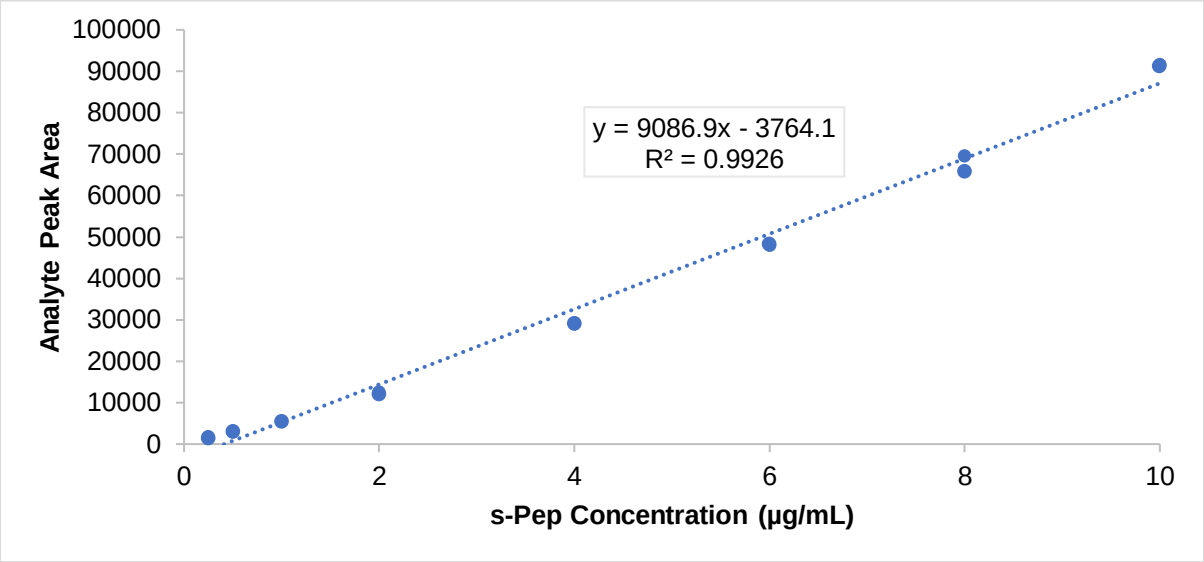

Figure 5.5. Representative calibration curve for s-Pep. *Line graph illustrating peptide concentration in µg/mL versus analyte peak area response for the calibration standards used to calculate the s-Pep concentration of the experimental samples. Equation y = 9086.9x – 3764.1, R² = 0.993.*

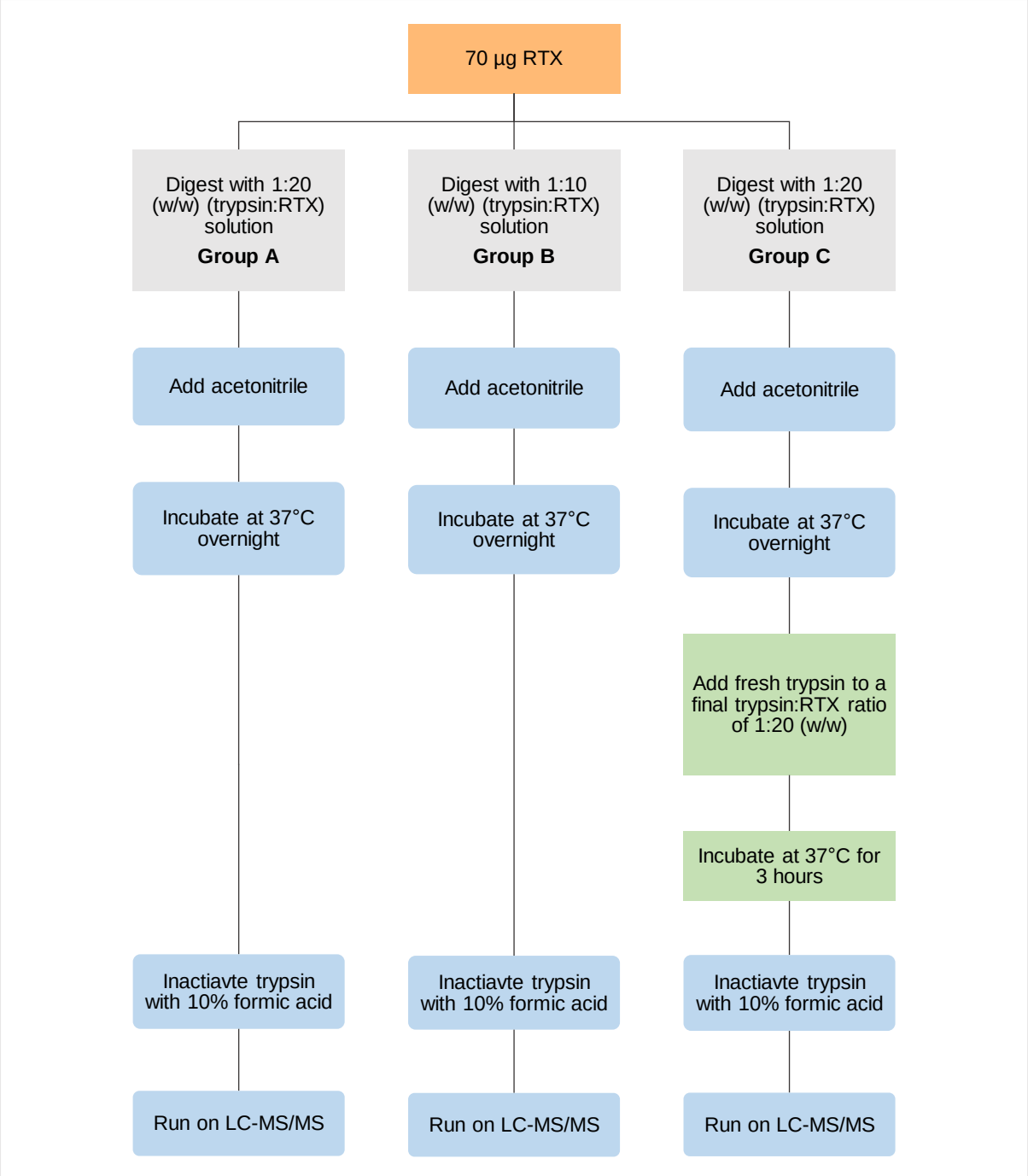

Figure 5.6. Experimental workflow. *Flow diagram illustrating the efficiency of protein digestion for three different proteases: protein concentrations.*

Results

The s-Pep concentrations of the experimental samples produced from the tryptic digestion under various conditions are indicated graphically in Figure 5.7. Based on the peptide calibration curve, actual s-Pep concentrations were calculated for the experimental samples.

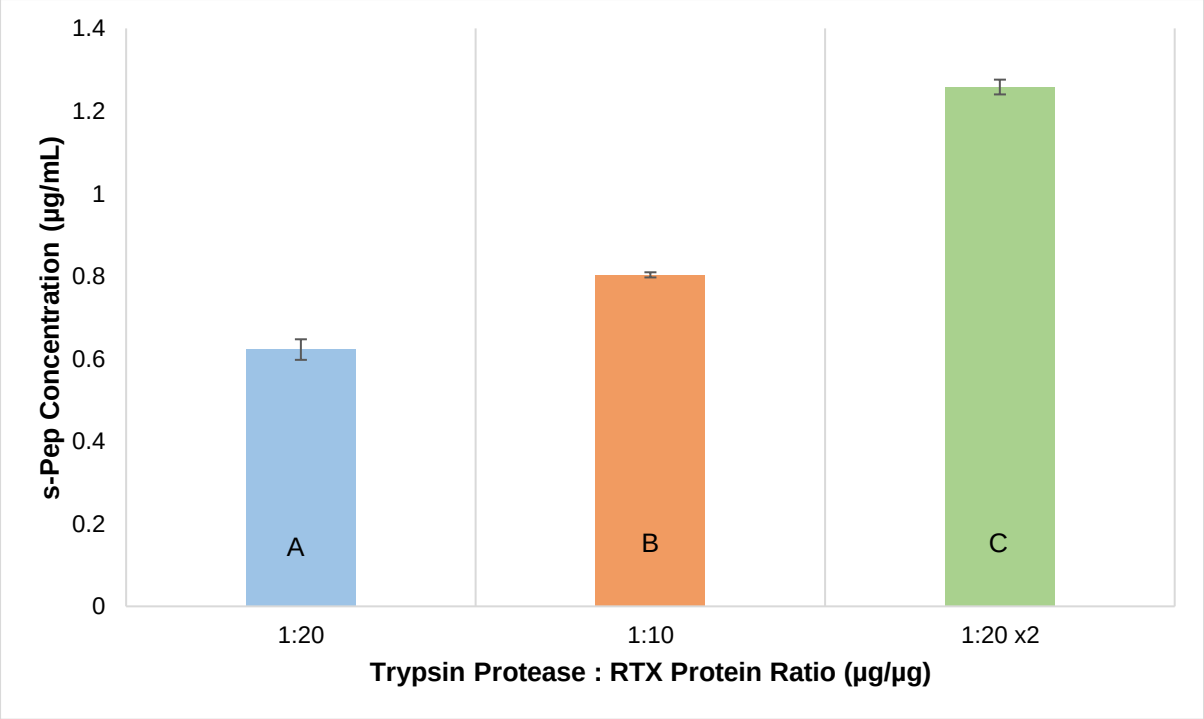

Figure 5.7. Amount of s-Pep generated from trypsinization. *Bar graph illustrating the s-Pep concentrations generated by digesting RTX with three different ratios. Group A: 1:20 once for 19 h, Group B: 1:10 once for 19 h, Group C: 1:20 for 19 h followed by 1:20 for a further 3 h. Error bars represent standard deviation, N=2.*

The incubation applied to the samples of Group C resulted in the highest yield of s-Pep. When 3.5 µg of trypsin was added once at the beginning to digest 70 µg of RTX (Group A, 1:20), an s-Pep concentration of 0.622 µg/mL was generated. When 7 µg of trypsin was added once at the beginning to digest 70 µg of RTX (Group B, 1:10), an s-Pep concentration of 0.803 µg/mL was generated. But, when approximately 7 µg of trypsin was added over two incubation periods to digest 70 µg of RTX (Group C, 1:20 x2), an s-Pep concentration of 1.26 µg/mL was generated. Group B yielded 1.3 times the s-Pep yielded in Group A, but for Group C, using the same total amount of trypsin as Group B but applying it over two incubation periods, the yield was 1.6 times higher.

Discussion

Even though the same amount of total trypsin was added to Groups B and C, there is a 1.6 times improvement in overall s-Pep generated when the additional fresh enzyme is added after overnight incubation. The initial digestion will allow the target protein to unfold partly, and more cleavage sites will become available for the second dose of trypsin to act. This will result in optimal peptide recovery.

Experiment 1 indicated that more s-Pep is produced using a protein/trypsin ratio of 1:10 than a 1:20 ratio. However, the increase in yield is less than the increase in trypsin usage and, therefore, it is not worth the cost of using so much trypsin. Furthermore, using the 1:20 ratio with the final addition after 19 hours yielded a sufficient s-Pep concentration to be detected (as will become more evident from further method development experiments) – especially considering that for the final method, a more

sensitive instrument was used, as will become apparent later. This ratio is also confirmed and is widely reported as optimal in the literature (28,101,106,119).

Summary

The optimal digestion procedure uses an enzyme-to-substrate ratio of 1:20 (trypsin: RTX) in 25 mM Tris-HCl buffer at pH 8. The incubation period was overnight (approximately 19 hours) in the presence of approximately 10% acetonitrile. A second addition of trypsin was implemented to a final ratio of 1:20 (trypsin: RTX) and left to incubate for a further 3 hours and finally quenched with 10% formic acid. The implemented digestion procedure was later performed on the bench at room temperature and not at 37°C.

5.2 EXTRACTION OF THE SIGNAL PEPTIDE BY SOLID PHASE EXTRACTION

Following the affinity binding purification of RTX from plasma and its on-bead trypsinization, the signal peptide (s-Pep) is present in the resultant reaction mixture from which it must be extracted. The most efficient extraction procedure to accomplish this is solid phase extraction (SPE) (122).

While SPE is most often used to remove interfering compounds from a sample, it can also be used to concentrate analytes of interest (87). This is particularly important with regard to the signal peptide selected for analysis, as it makes up a small percentage of the RTX total protein (see Section 4.1). Solid phase extraction can therefore improve analytical results by reducing the complexity of a sample, reducing baseline interferences, and/or increasing detection sensitivity (87,100,129). Because of the multi-step sample preparation before the SPE procedure, the sample has already been exposed to various buffers, salts, and solutions from the affinity binding purification and digestion steps. Reducing such interfering components improves the subsequent analytical procedures during LC-MS/MS detection (87). As an efficient extraction procedure, SPE can also prevent the buildup of highly hydrophobic compounds on the analytical column, which could potentially reduce chromatographic efficiency and column lifetime (130).

Optimisation of the SPE procedure is an important aspect of method development. The major steps of the SPE extraction, including the loading, washing and eluting procedures, were experimentally optimised using the signal peptide (s-Pep). The efficiency of the extraction was also investigated by calculating the percentage recovery of the s-Pep by SPE.

5.2.1 Investigation 1: Optimising the retention and elution of the analyte during solid phase extraction

Introduction

The retention of an analyte on an SPE column depends on the preparation of the extraction column and the solution/buffer in which the analyte is dissolved. For this project, Strata-X 33 µm polymeric reverse phase extraction columns were used. Therefore, the extraction depended on a hydrophobic interaction between the analyte (s-Pep) and the extraction medium. The analyte was hence dissolved in an aqueous solution and applied to the extraction column. In the sample preparation sequence for

this project, SPE occurs directly after trypsinization; therefore, the s-Pep was prepared in the Tris-HCl buffer in which trypsinization occurred.

After applying and binding the analyte to the extraction column, salts and polar compounds are washed off the column with water. Increasing the organic content of subsequent washing solutions may eliminate relatively more hydrophobic compounds while still allowing the analyte to be retained. Then the analyte can be eluted with a solution with sufficient organic content that would ideally allow more hydrophobic compounds than the analyte to remain on the column. All of these washing and eluting conditions are experimentally determined during the optimising experiments here described.

Methodology

For the development of the SPE extraction of s-Pep, an aliquot of the stock solution (2 mg/mL) was diluted with 25 mM Tris, pH 8, to produce a working solution with a concentration of 1 µg/mL.

Duplicate Strata-X 33 µm polymeric reverse phase 30 mg/mL extraction columns were each conditioned with 1 mL methanol, passed through at maximum flow, and then equilibrated with 1 mL water followed by 1 mL 0.1% formic acid in water.

Three hundred µL of the working solution of the s-Pep was then loaded onto the column together with 300 µL 0.1% formic acid in water. This was allowed to flow through the column by applying positive pressure.

The cartridge was then sequentially washed with 100 µL of solvents with increasing acetonitrile content. Starting with pure water, the acetonitrile content was increased by 10% for each wash. The flow-through of each wash was separately collected and the solvent dried at 37°C under a flow of nitrogen gas. Each residue was then reconstituted in 200 µL 20% acetonitrile with 0.1% formic acid (injection solution – see Section 3.4) and analysed for the presence of the s-Pep by LC-MS/MS on a Sciex API-3200 as described in Chapter 4. The presence of s-Pep was indicated by a chromatographic peak at the expected retention time, and relative concentrations expressed as peak areas, where higher peak areas represented higher concentrations of s-Pep in the fractions analysed.

Results and Discussion

Figure 5.8 demonstrates the stepwise elution of s-Pep from a Strata-X polymeric reversed phase SPE column, using increasing acetonitrile content in the wash solutions.

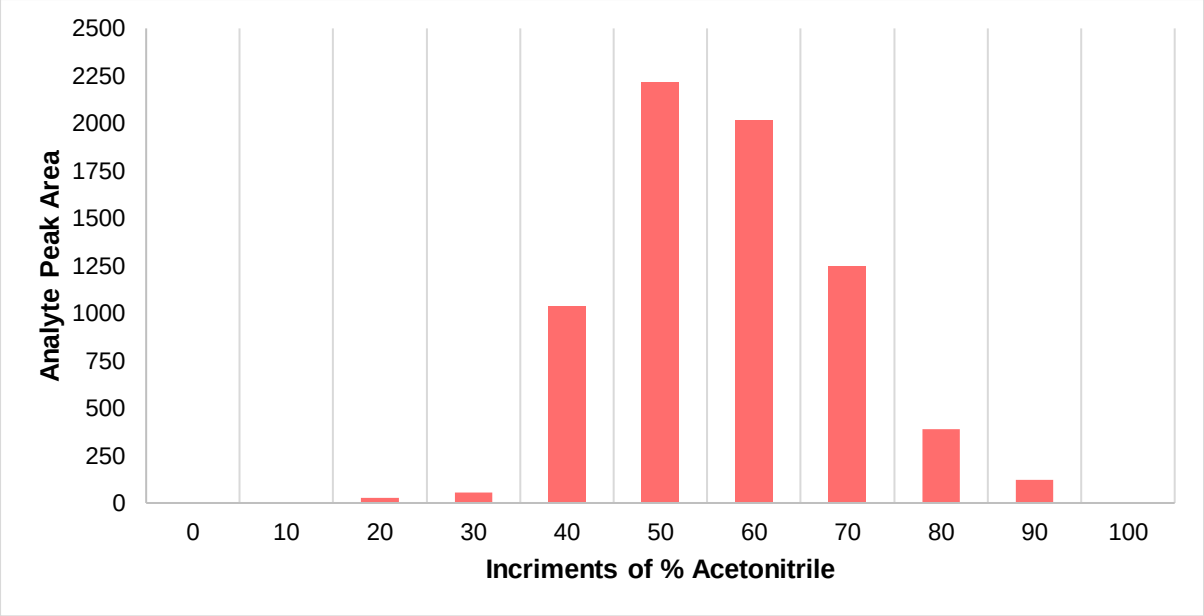

Figure 5.8. Analyte peak area response of elution fractions. *Significant peak areas were observed between the 40% and 70% acetonitrile fractions.*

No s-Pep eluted from the SPE column when washed with solvents containing less than 20% acetonitrile, with only very low concentrations observed in the washes containing 20–30% acetonitrile. The bulk of the s-Pep could be washed off the column between 40% and 70% acetonitrile, with only low concentrations observed in the 80–90% acetonitrile washes. No further s-Pep could be recovered when washing with 100% acetonitrile.

The results indicated that the optimal washing conditions for the SPE of s-Pep using Strata-X polymeric reversed phase SPE columns are an aqueous solution containing <20% acetonitrile. While significant elution can already be observed when using 40% acetonitrile, the elution peaks at 50% and is still at a relatively high rate when using 70% acetonitrile. The profile in Figure 5.8 indicates that most of the s-Pep can be eluted with 70% acetonitrile. No benefit was observed from adding an organic solution of >70% acetonitrile as insignificant peak areas were observed with the 80–100% organic fractions. In addition, peptides will lose solubility in highly organic solutions (131). Limiting the acetonitrile content to less than 75% organic will thus result in most of the s-Pep being eluted and any interfering material with higher hydrophobicity will retain on the column and thus be removed from the sample.

By keeping the organic content of the elution solvent as low as possible, the solubility of the s-Pep is improved. It has also been reported that solubility can be further promoted by the inclusion of organic modifiers in such solvents (132). For that reason, in the next investigation where the efficiency of the SPE procedure was assessed, the elution solvent was 70% acetonitrile containing 1% formic acid as a modifier.

5.2.2 Investigation 2: Assessing the efficiency of solid phase extraction

Introduction

The recovery of an analyte, when subjected to an analytical procedure, can be used as an accurate indication of the efficiency of such a procedure. The recovery of s-Pep during SPE can be measured because the pure reference standard of s-Pep is available, and the presence of s-Pep is not dependent on either of the two major sample preparation steps preceding SPE: affinity binding purification and trypsinization of RTX. Comparing the concentration of s-Pep (as represented by chromatographic peak area) in the final eluate from the SPE column with the expected concentration spiked directly into the injection solution can provide a direct indication of the percentage recovery during SPE.

Methodology

A reference working solution (refWS) of 1 µg/mL s-Pep was prepared by diluting 10 µL of the 2 mg/mL stock solution to 20 mL with injection solution (see Section 3.4). The refWS served as a reference for comparison with extracted samples.

A working solution (testWS) of 1 µg/mL s-Pep was prepared by dilution of 10 µL of the stock solution to 20 mL with 25 mM Tris, pH 8. Duplicates of the testWS were extracted on conditioned Strata-X SPE columns as described above, and are briefly summarised as follows:

- Three hundred µL of testWS and 300 µL of 0.1% formic acid were loaded onto the column and left to flow through.
- The columns were washed twice with 1 mL water.
- The columns were then washed with 100 µL 10% acetonitrile in water and the flow through was collected.
- The s-Pep was eluted three times with 100 µL 70% acetonitrile in water containing 1% formic acid, and the eluates were separately collected.
- The 10% acetonitrile wash and the three separate eluates were dried at 37°C under a gentle stream of nitrogen gas and then reconstituted in 200 µL injection solvent.

All the SPE fractions and duplicates of the refWS were analysed for the presence of the s-Pep by LC-MS/MS on a Sciex API-3200 as described in Chapter 4. The presence of s-Pep was indicated by a chromatographic peak at the expected retention time, and relative concentrations were expressed as peak areas, where higher peak areas represented higher concentrations of s-Pep in the SPE fractions.

Results and Discussion

The s-Pep content measured as peak areas in the refWS and the SPE fractions of the testWS are compared in Figure 5.9.

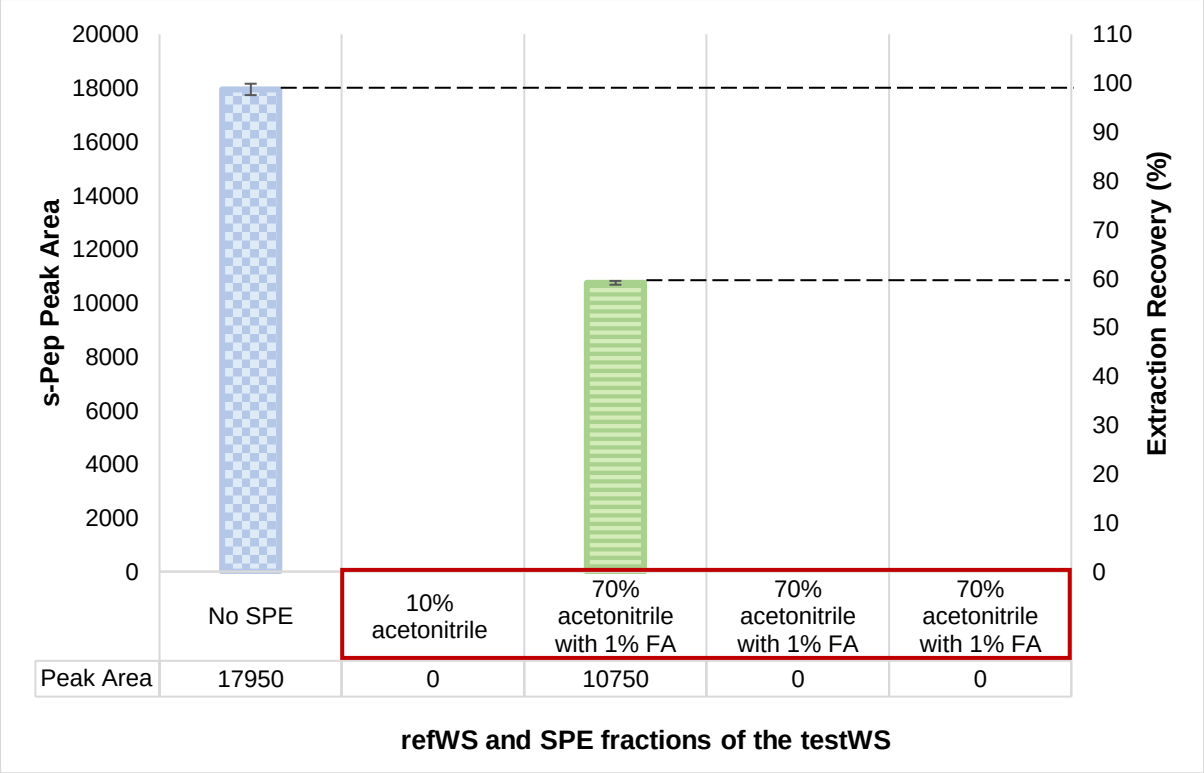

Figure 5.9. Bar graph illustrating the percentage extraction recovery in relation to analyte peak area for the peptide samples that underwent SPE vs a peptide sample that did not (blue bar, representing 100% theoretical recovery). *The SPE fractions (testWS) are indicated in the red rectangle, including the organic wash (10% acetonitrile) and the three consecutive elutions with 70% acetonitrile containing 1% formic acid (FA). The green bar graph illustrates the actual extraction recovery (%). The error bars show the standard deviation, N=2.*

The efficiency of the SPE process is proven by indicating a 60% recovery. No s-Pep was observed in the 10% acetonitrile wash, and all the eluted s-Pep was present in the first 70% acetonitrile/1% formic acid elution. Neither a second and/nor a third elution with 70% acetonitrile/1% formic acid contained any s-Pep, therefore proving that elution is complete with one 100 µL elution step.

The water wash followed by the 10% acetonitrile wash – while s-Pep is still retained on the extraction column – will ensure that most buffer salts and other interfering compounds will be washed from the column. This is important for minimising deleterious influences during the analytical process, such as matrix effects that may cause signal suppression or enhancement.

A relatively high extraction recovery, along with the elution of s-Pep in 100 µL of 70% acetonitrile/1% formic acid, is advantageous since interfering compounds that are more non-polar than s-Pep will be retained on the extraction column. Such non-polar compounds may influence chromatography and detection by later elution in successive injections, and also causing unwanted matrix effects. This could significantly improve the overall robustness of the method, resulting in better chromatography and prolonging the functional lifetime of the analytical column.

The effect of including a modifier (1% formic acid) in the elution solvent can be calculated by comparing the results depicted in both Figures 5.8 and 5.9. In both investigations, the same volume and concentration of s-Pep was applied to the extraction column, and the solvent in the fractions analysed was evaporated to dryness and reconstituted with 200 µL injection solvent. Representative concentrations measured in the different fractions in the two investigations can thus be directly compared. For elution without a modifier (Investigation 1), where eluted s-Pep could already be observed with a wash of 20% acetonitrile, all the peak areas of subsequent washes with increasing acetonitrile content were summed and are indicated in Table 5.1 as “Elution without modifier”. If this value is compared to the peak area of the s-Pep eluted with 70% acetonitrile containing 1% formic acid as a modifier (Investigation 2), a 34% enhancement is observed in the presence of the modifier, therefore confirming published results to this effect (133,134). The 34% enhancement observed is regarded to be a result of enhanced recovery from the SPE process rather than an enhancement of ionisation when the reconstituted sample was analysed. Solid phase extraction is conducted on a mixed mode medium and therefore interactions between the analyte and the extraction medium do not only depend only on hydrophobic interaction but also on ionic interactions. Such ionic interactions can be reversed with the addition of a higher concentration of formic acid, resulting in enhanced recovery. Because the elution solvent is completely evaporated following the elution step, the formic acid will also be evaporated and therefore should not have an enhancement effect on ionisation.

Table 5.1. *Comparison of s-Pep eluted, in terms of peak area, with and without the addition of an organic modifier*

	Elution solvent	**Combined peak area (relative s-Pep concentration)**	**Enhancement due to modifier**
Elution without modifier	70% acetonitrile	7104	–
Elution with modifier	70% acetonitrile with 1% formic acid	10750	34%

Summary

The RTX signal peptide (s-Pep) could successfully be extracted successfully from the buffer in which trypsinization was conducted by performing SPE using Strata-X polymeric reversed phase columns. After binding the s-Pep to the column, more polar compounds could be eliminated by washing with water and solvents with low organic content such as 10% acetonitrile. The s-Pep could be successfully eluted in 100 µL 70% acetonitrile containing 1% formic acid, with a relatively high extraction recovery. This process ensures a sensitive and specific extraction of the s-Pep, following its formation by on-bead trypsinization.

5.3 SAMPLE PREPARATION PROTEIN LEVEL CLEAN-UP: PROTEIN PRECIPITATION VERSUS AFFINITY BINDING PURIFICATION

Depending on the required specificity and sensitivity of the analytical method, protein precipitation or affinity binding purification can be used as a sample preparation procedure for the bioanalysis of therapeutic proteins. Figure 5.10 schematically compares the two strategies. Although affinity binding purification will naturally result in much higher analytical specificity, it was decided to explore protein precipitation since the therapeutic concentrations of RTX are relatively high, and protein precipitation is a less expensive and specialised procedure than immunocapture.

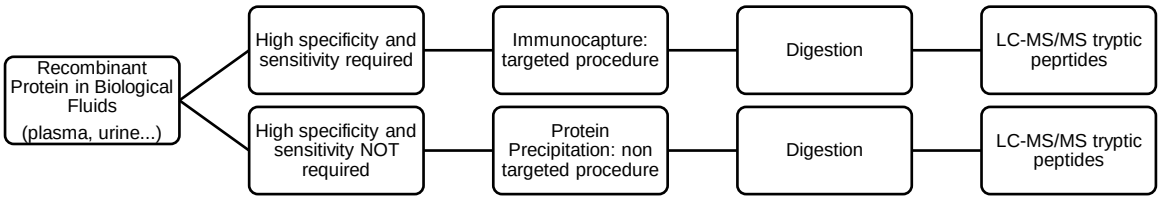

Figure 5.10. Possible protein level sample preparation techniques. *This schematic illustrates the comparison of two sample preparation procedures involving clean-up at the protein level, namely protein precipitation and affinity binding purification.*

5.3.1 Protein precipitation

Introduction

During the protein precipitation strategy, recombinant proteins in biological fluids undergo protein precipitation followed by digestion and SPE to produce tryptic peptides, which are then analysed using LC-MS/MS (100). This experiment aims to precipitate the larger proteins, leaving the smaller endogenous plasma proteins in solution. Following centrifugation, the soluble matrix components will be discarded with the supernatant, while the proteins, including all immunoglobulins, will be harvested as a pellet to undergo digestion.

To explore protein precipitation as a sample preparation option, a series of samples were precipitated using acetonitrile and then digested using trypsin before performing peptide-level purification by SPE. A set of control samples containing the target protein and 25 mM Tris buffer instead of trypsin were also analysed. Precipitation experiments were performed with RTX in PBS and normal plasma for comparison.

Methodology

The precipitation procedure is depicted in summary in Figure 5.11, and the following steps were executed:

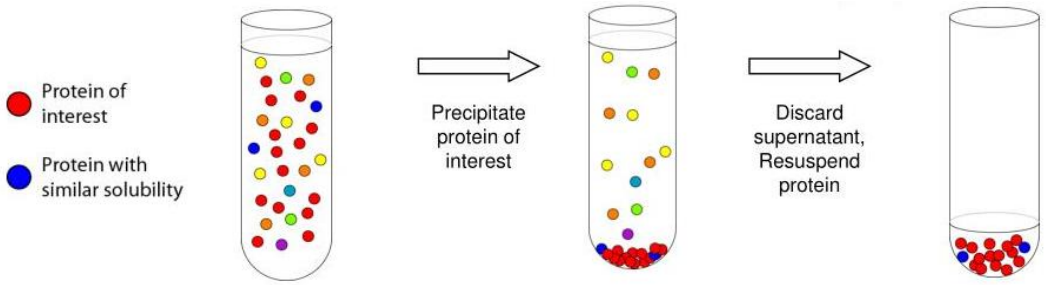

Figure 5.11. Protein precipitation. *The precipitate (pellet) contains proteins precipitated out of the matrix, including RTX. The supernatant contains soluble matrix components to be discarded* (148).

A working solution containing 300 µg/mL of RTX was prepared by diluting 300 µL of the 10 mg/mL stock solution with 970 µL of PBS or plasma. Two identical sets of experimental samples were prepared by transferring 100 µL of the working solution to low-bind 1.5 microcentrifuge tubes, as shown in Tables 5.2 and 5.3. Blank samples containing only PBS or plasma were included as negative controls. All samples were prepared, as shown in Table 5.2.

Table 5.2. *The negative controls and RTX samples*

Experimental samples	Contents
Negative controls	
A	100 µL of blank PBS
B	100 µL of blank plasma
Rituximab samples	
C	100 µL of 300 µg/mL RTX in PBS
D	100 µL of 300 µg/mL RTX in plasma

A hundred µL of ice-cold acetonitrile was added to all samples following brief vortex-mixing. The samples were left on the bench at room temperature for approximately 20 minutes. The precipitated proteins were collected by centrifugation of the sample tubes at approximately 10 000 g for 10 minutes. The supernatant from each sample was discarded.

Protein digestion was performed on the precipitated pellet using a previously developed and optimised method described in Section 5.1. The first set of experimental samples (A1–D1) were prepared for comparison, and therefore 25 mM Tris buffer was added instead of trypsin solution during the digestion step. The second set of experimental samples (A2–D2) was digested with trypsin. The pellets were resuspended for the digestion procedure by brief vortex-mixing. The volumes of all mixtures added to

the pellets during the digestion procedure (previously described in Section 5.1) are summarised in Table 5.3.

Table 5.3. *The two experimental sets*

Set 1	Set 2
215 µL of Tris buffer	215 µL of 7 µg/mL trypsin working solution (see Section 3.4)
22 µL of 100% acetonitrile	22 µL of 100% acetonitrile
1.5 µL of Tris buffer	1.5 µL of 1 µg/µL trypsin
Quench using 12 µL of 10% formic acid	Quench using 12 µL of 10% formic acid
Final volume = 250.5 µL	Final volume = 250.5 µL

Following trypsin digestion, the target peptide in each sample was extracted by SPE according to the developed and optimised procedure described in Section 5.2. The experimental samples were centrifuged at approximately 10 000 g for 1 minute to reform the pellet. For each experimental sample in each set, 80% of the digested supernatant volume was extracted by SPE. The presence and relative concentration of the signal peptide (s-Pep) produced during trypsin digestion were determined in the extracts by LC-MS/MS on the Sciex API-3200 Q-Trap – as described in Chapter 4. The relative concentrations of the s-Pep in the samples were expressed as the areas of the chromatographic peaks representing the peptide.

Results

The effectiveness of protein precipitation as sample preparation for the analysis of RTX is demonstrated by the results depicted in Figure 5.12.

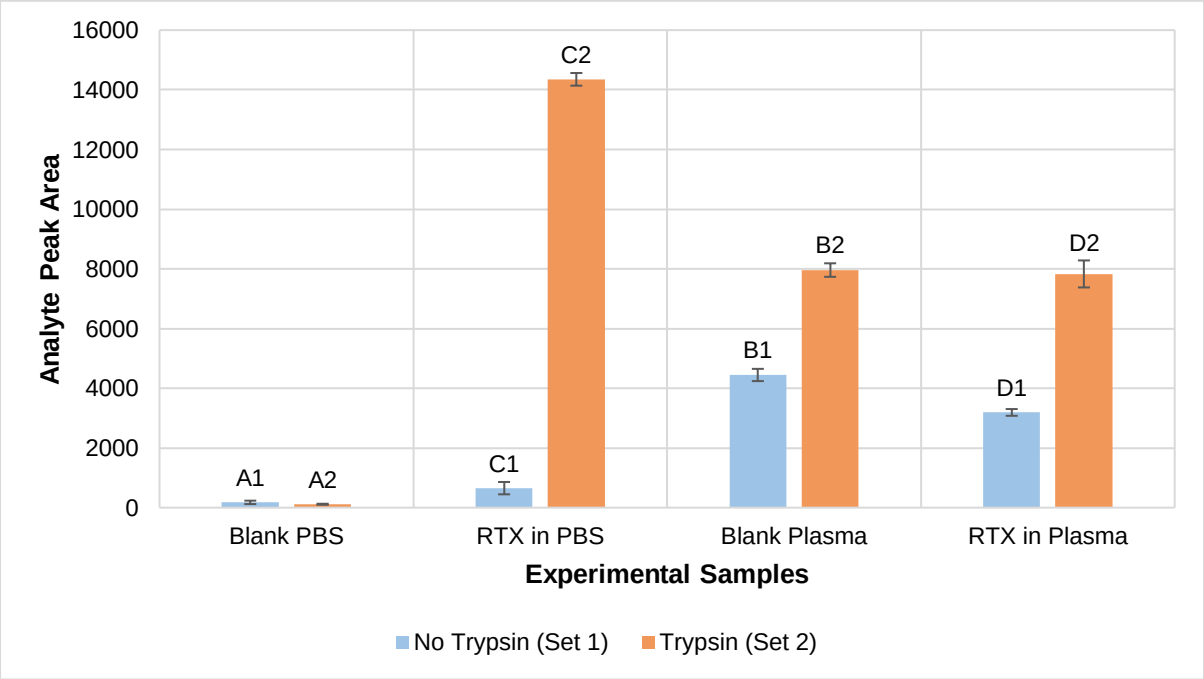

Figure 5.12. Bar graph illustrating the amount of s-Pep recovered using the protein precipitation sample preparation technique. *RTX in PBS and plasma was explored with and without the addition of trypsin.*

In Figure 5.12, the first group of bars, representing the extracted blank samples in PBS (A1 and A2), indicates that no significant peak area was observed regardless of whether trypsin was added or not.

The second group of bars (C1 and C2) represents the samples with RTX in PBS. This indicates that the samples in which trypsin was added (C2) displayed a significantly larger peak area than the samples containing RTX without trypsin (C1). Without trypsin added to the RTX in PBS, the peak area is slightly higher than that observed in the first group, in which no RTX was added (compare C1 to A1 and A2).

The third bar graph group represents the extracted blank samples in plasma (B1 and B2). The blank digested with trypsin (B2) generated a higher peak area than the blank without trypsin (B1). Because no RTX was present in these samples, the relatively high peak areas represent non-specific background interference from plasma.

The values in the last group of bars, representing the extracted RTX samples in plasma (D2), are closely similar to the values observed in the blank plasma samples to which no RTX was added (B2).

The peak areas of the experimental samples digested with trypsin (A2–D2) are summarised in Table 5.4.

Table 5.4. *A summary of the experimental samples of Set 2*

Experimental sample	Peak area	Summary
A2: Blank PBS	113	Blank PBS < 1% of RTX in PBS
C2: RTX in PBS	14350	
B2: Blank plasma	7960	Blank plasma > RTX in plasma
D2: RTX in plasma	7830	

The most significant increase due to RTX was observed in the sample in which trypsinization was performed in PBS (C2). This is indicated in Table 5.4. The blank PBS (A2) is <1% of sample RTX in PBS (C2). The RTX in PBS (C2) exhibited a peak area of 1.8 times that of the RTX in plasma (D2).

Discussion

The experiments involving sample preparation by protein precipitation proved that the plasma matrix significantly contributed to non-specific background interference. Even without trypsin, the interference due to plasma components contributes to about 50% of the peak area observed when trypsin is added. Adding RTX to the plasma did not increase the peak area of the s-Pep, proving that the overwhelming presence of plasma proteins negatively influenced the trypsinization of RTX. The increase in peak area in the presence of trypsin indicates that tryptic digestion did occur, but the non-specificity of the detection of the formed peptides is too high. Using protein precipitation as sample preparation is thus only sensitive or selective enough to solely detect the s-Pep if other plasma proteins are removed through another sample preparation process.

The extracted RTX sample in PBS digested with trypsin would be equivalent to a sample undergoing affinity binding enrichment of the target protein before trypsinization since there are no interfering plasma proteins.

Therefore, protein precipitation was not explored further for this research project as a possible sample preparation procedure. An affinity binding procedure in which immunoglobulins are selectively isolated from all the other plasma proteins in the sample was therefore explored. This should significantly increase the specificity of detection of the s-Pep and will also contribute to using optimal amounts of trypsin for digestion.

5.3.2 Affinity binding purification

Peptide quantification requires sensitive and reproducible methods. In many cases, protein precipitation will not result in the sufficient sample purification necessary to analyse peptides in complex matrices such as plasma. Specificity is gained by using a sample preparation method that uses orthogonal clean-up approaches to selectively capture the peptide target while eliminating unwanted matrix interferences. Therapeutic proteins represent less than 0.01% of the total plasma protein content (126). To avoid masking effects during quantitative analysis, the majority of proteins should be depleted using the appropriate sample preparation technique (100,126). Affinity binding purification coupled with LC-

MS/MS methods is readily applicable to the analysis of therapeutic antibodies. It is now considered an essential clean-up procedure during peptide analysis (98). The affinity binding purification process may increase the sensitivity of an analytical method by as much as 250-fold (126).

Protein A is a cell wall protein naturally produced by several strains of *Staphylococcus aureus* (114,135,136). Each protein contains four high-affinity binding sites capable of interacting with the Fc region of IgG-class antibodies from selected mammalian species (136). This high binding capacity of IgG by protein A can effectively be used to isolate IgG molecules from a complex protein-rich matrix such as plasma. The immobilisation of protein A by binding it to agarose beads is a highly efficient mechanism for the immobilisation of IgG in biological matrices.

ThermoScientific Pierce protein A Agarose is a preparation of protein A coupled covalently to agarose beads. It is presented as a slurry and reported to be used in various antibody affinity purification methods (12,27,80,99). The protein A Agarose beads are specifically produced to result in a high-capacity resin, incorporating specialised linking groups to eliminate steric hindrance during ligand binding, and eliminating undesired non-specific binding. The protein A Agarose gel slurry provides a binding capacity of about 16 mg human IgG per 1 mL of resin (137). It was therefore selected for the development and optimisation of this assay and including this technology during sample preparation introduced a protein-level clean-up step, more specific than protein precipitation, before enzymatic digestion. The affinity binding purification procedure is summarised in Figure 5.13.

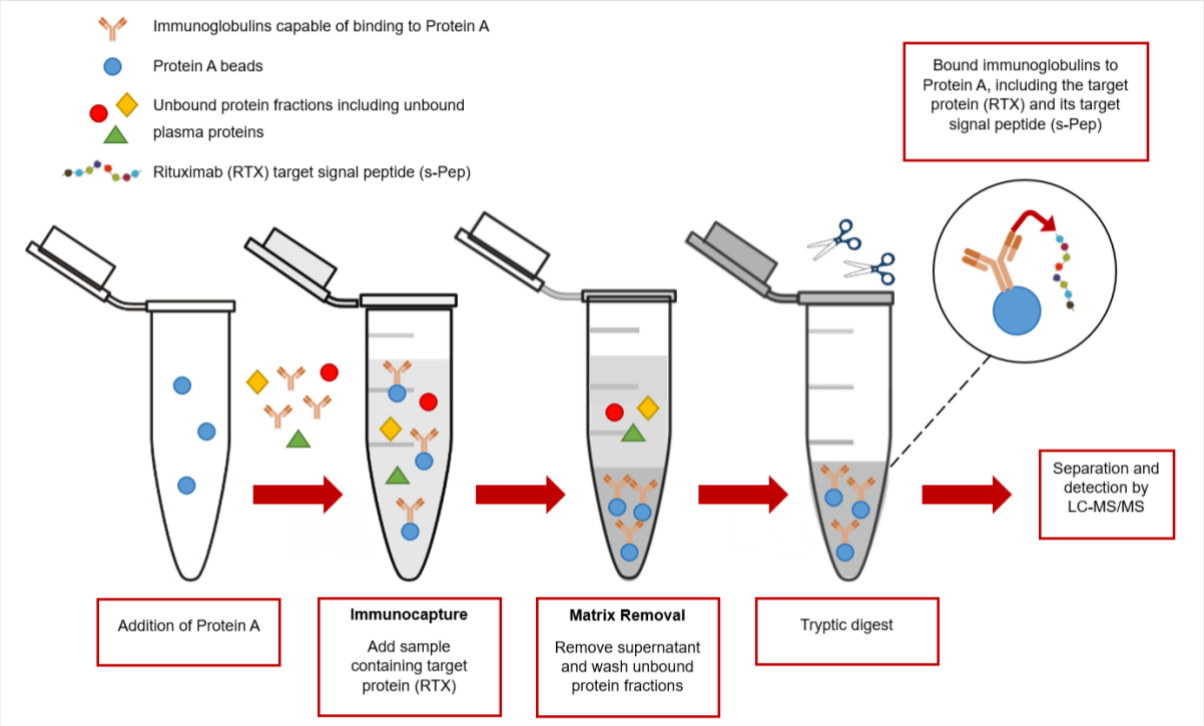

Figure 5.13. Diagram summarising the affinity binding purification procedure. *Protein A coupled to agarose beads binds IgG's, including the target protein (RTX). The RTX-Protein A bound pellet is then washed to remove unbound protein fractions prior to tryptic digestion.*

As indicated in Figure 5.13, protein A acts as the binding component to capture antibodies. Unlike immunoaffinity binding purification methods, an antibody is not used to purify the analyte of interest, as the analyte of interest (RTX) is an IgG antibody.

Introduction

This section describes the optimisation of the affinity binding process. For this purpose, the bound IgG molecules will be eluted from the beads to determine optimal binding conditions.

Once affinity binding is completed, there are two options for tryptic digestion. First, protein digestion can occur while bound to the protein A beads or after elution from the beads (26,101,120). The generation of tryptic peptides is protein-dependent and influenced by protein folding and accessibility of trypsin both on-bead and in the eluate (26).

Part 1: Optimising the volume of protein A slurry

This experiment aimed to establish the protein A Agarose slurry volume to be added to purify the RTX from the matrix optimally. A constant concentration of RTX was used for all test samples, and this concentration represents a value above the expected maximum concentration of RTX in plasma to compensate for other IgGs in plasma competing for binding sites. All samples were prepared in PBS, and protein concentration was measured using the bicinchoninic acid (BCA) protein assay (138). Optimisation of the binding affinity process was established by adding the RTX to different volumes of protein A slurry, performing a series of washes, and measuring the amount of protein in the washes. If no protein is detected, the total binding will have been accomplished, indicating the optimal ratio of RTX to protein A slurry. For this reason, the RTX was not prepared in plasma since that would interfere with the BCA protein assay. Protein A binds all human IgG; therefore, the RTX protein and plasma IgG will compete for binding sites. The relatively high protein A volume used in this experiment ensures that enough protein A is used to compensate for this background affinity when actual plasma samples are prepared.

Methodology

Materials and solutions

The materials and solutions for this procedure were the same as those described in Chapter 3.

Preparation of rituximab working solution

A 1 mg/mL working solution of RTX was prepared from the 10 mg/mL stock solution by diluting 100 µL of the stock solution with 900 µL of PBS.

Preparation of the protein A beads

The protein A gel slurry was briefly mixed on a vortex mixer. Different volumes of the slurry were transferred to 1.5 mL microcentrifuge tubes and centrifuged for 1 minute at approximately 10 000 g. The supernatant was then discarded, and the pellet was resuspended with 1 mL of PBS and washed by brief vortex mixing. Centrifugation and resuspension in PBS were repeated once more, and the final

pellet was resuspended in a specific volume as required for the experimental conditions described in Table 5.5. In addition, 400 µL of 0.1% octylthioglucoside (OTG) detergent was added to prevent nonspecific binding (139).

Table 5.5. *Summary of the amount of buffer needed to resuspend the washed protein A pellet*

Initial volume of protein A slurry added	Equivalent volume of PBS added to resuspend the washed protein A pellet	Final volume of protein A resuspension
100 µL	50 µL	100 µL
150 µL	75 µL	150 µL
200 µL	100 µL	200 µL

Determination of binding capacity in buffer

A schematic representation of the experimental procedure used to determine the binding of RTX to the protein A beads is represented in Figure 5.14.

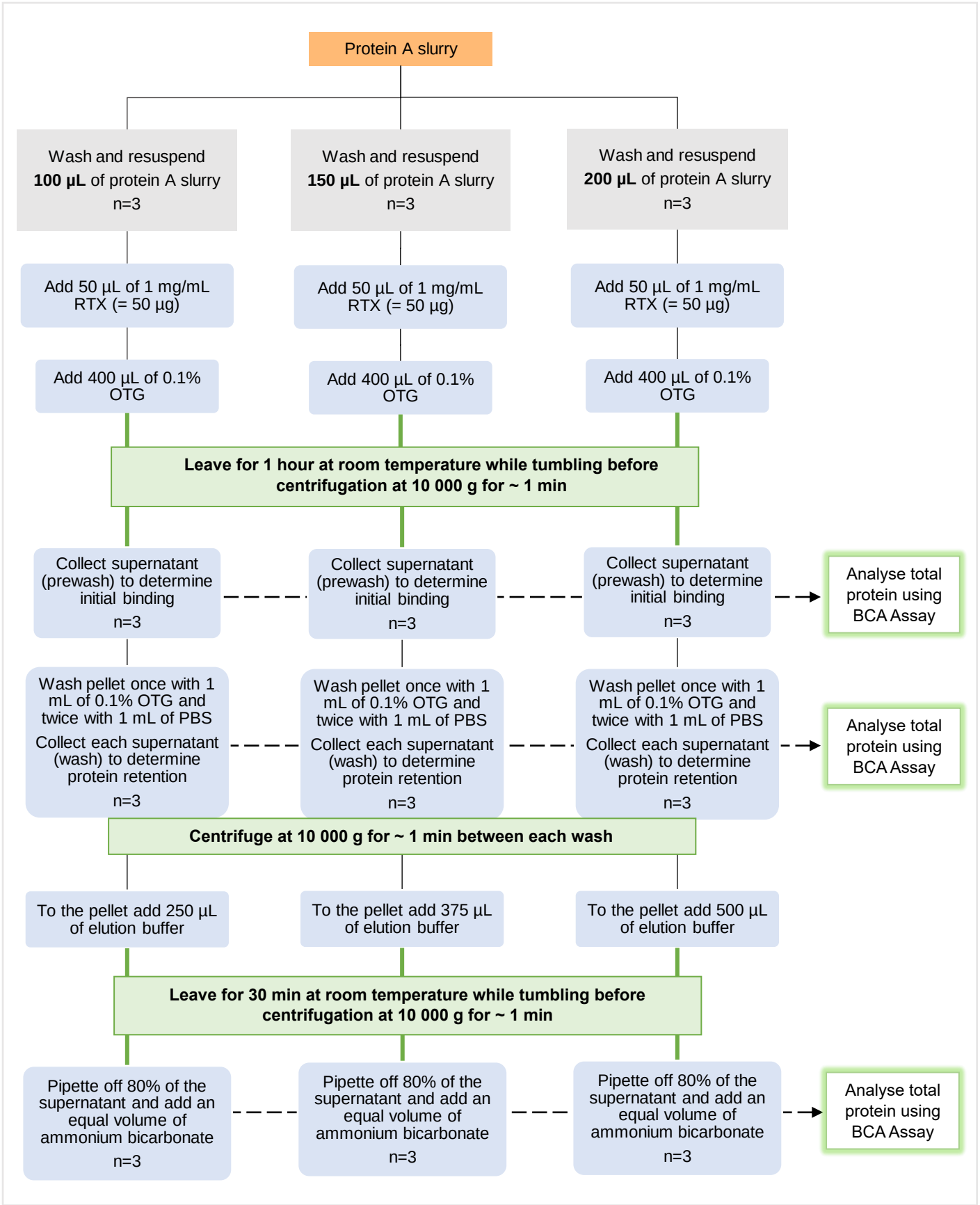

Figure 5.14. Flow diagram summarising the methodology for the experimental samples.

In summary, the execution of the experiment started by adding 50 µL of 1 mg/mL RTX (50 µg of RTX) to the 100 µL, 150 µL and 200 µL of resuspended protein A beads. In this experiment, 50 µL of blank PBS was added to an additional 100 µL and 200 µL of resuspended protein A beads to act as a control. Each experimental sample was prepared in triplicate. The samples were mixed using a vortex at maximum speed for approximately 10 seconds and were left for 1 hour at room temperature while tumbling on a tube revolver rotator. The samples were subsequently centrifuged at 10 000 g for 1 minute, and the supernatants, referred to as pre-wash samples, were transferred to clearly labelled 1.5 mL microcentrifuge tubes to determine the protein concentration in each, thereby establishing the initial binding of RTX to protein A in each sample. The protein A pellet was then washed using 1 mL of 0.1% OTG, followed by two washes with 1 mL PBS. Between each wash, the pellets were resuspended by vortex mixing at maximum speed for approximately 10 seconds and centrifuged at 10 000 g for 1 minute. The supernatants of the three washes were also collected in separate clearly labelled 1.5 mL microcentrifuge tubes for protein determination and are referred to as washes. The washes indicated to what extent RTX was bound to the protein A before elution.

Part 2: Elution

IgG elution buffer was added to the pellets to elute the IgG from the protein A beads. The volume of elution buffer used was adjusted to the initial volume of protein A beads used so that it was 2.5 times more than the protein A slurry. Therefore, 250 µL of elution buffer was added to the sample containing the initial protein A suspension volume of 100 µL, 375 µL to the sample containing 150 µL protein A suspension and 500 µL to the sample containing 200 µL protein A suspension. For the respective blanks, 250 µL and 500 µL of IgG elution buffer were added. The samples were mixed using a vortex at maximum speed for about 10 seconds before being left on a bench for approximately 30 minutes at room temperature while tumbling on a tube revolver rotator before centrifugation for about 1 minute at approximately 10 000 g. Eighty percent of the supernatant was then transferred to new, clearly labelled, clean 1.5 mL microcentrifuge tubes, and the remaining pellet was discarded. An equal volume of 0.2 M ammonium bicarbonate was added to each eluate. The ammonium bicarbonate neutralises the sample's pH to prevent denaturation of the enzyme used for digestion in a subsequent step (101). Table 5.6 indicates the detail of the contents of all samples.

Table 5.6. *Summary of the experimental samples*

Description	Pellet		Supernatant		
	50 µL of 1 mg/mL RTX added / 50 µL PBS	**Volume of protein A Agarose suspension used (µL)**	**Volume of IgG elution buffer added (µL)***	**Volume of ammonium bicarbonate added (µL)**	**Final volume of supernatant (µL)**
Experimental sample 1	50 µL RTX	100	200	200	400
Experimental sample 2	50 µL RTX	150	300	300	600
Experimental sample 3	50 µL RTX	200	400	400	800
Blank 1	50 µL PBS	100	200	200	400
Blank 2	50 µL PBS	200	400	400	800

*80% of eluate

The total IgG eluted from the beads was determined by applying the BCA protein assay.

Determination of protein concentration by the BCA protein assay

The BCA assay is a copper-based colourimetric assay for total protein quantification. This assay involves the formation of a copper-protein complex, followed by the reduction of Cu^{2+} to Cu^{+} (138). This formation is illustrated in Figure 5.15. Quantities of Cu^{2+} reduced are proportional to the protein concentration in solution. The colour change from green to purple is achieved when two molecules of BCA chelate to each Cu^{+}ion. This purple by-product has a strong absorbance at 562 nm, which is measurable by spectrophotometry.

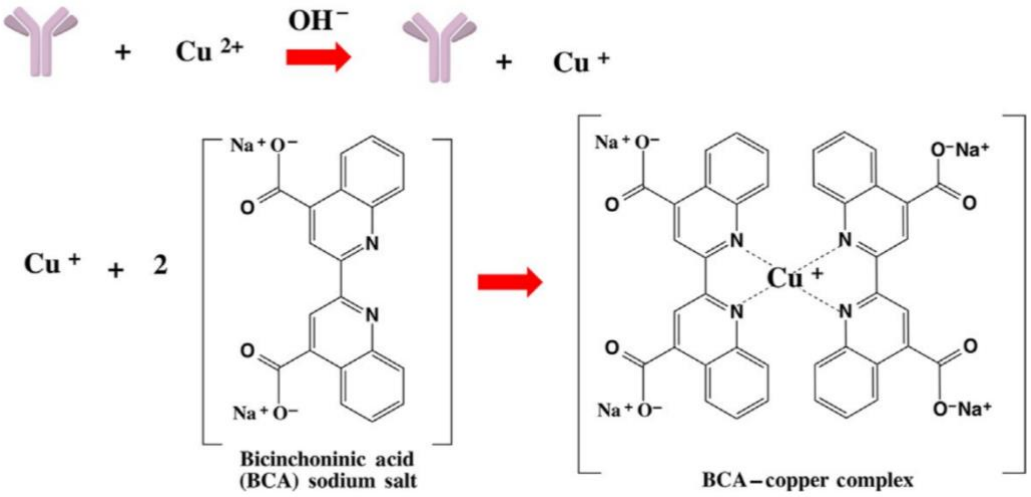

Figure 5.15. Schematic of the BCA colour reaction. *The formation of the bicinchoninic acid (BCA) – copper complex for the BCA total protein assay. The assay proceeds in two steps: first the reduction of* Cu^{2+} *by antibodies in a basic environment, and second the reduced* Cu^{+} *chelating with two molecules of bicinchoninic acid* (138).

The BCA–copper complex formation depends on the number of peptide bonds and the presence of the side chains on the amino acids cysteine, cystine, tyrosine, and tryptophan (138). This complex is best formed at higher temperatures. Therefore, to increase sensitivity, the BCA assay was performed at 37°C.

Since the only protein being quantified in these experiments is RTX, calibration standards were prepared by serially diluting 125 µg/mL RTX to a final concentration of 7.81 µg/mL. After that, a BCA Working Reagent (WR) was prepared by mixing 50 parts of BCA Reagent A with 1 part of BCA Reagent B (50:1, Reagent A: B). This WR was then added to the antibody calibration standards and the unknown samples before incubation at 37°C for 30 minutes. Samples were cooled to room temperature in a dark cupboard before measuring the absorbance at 562 nm within 10 minutes. The unknown protein concentrations were determined by applying blank correction from the calibration plot of antibody standards obtained from the BCA assay. A blank correction was performed by subtracting the absorbance produced by the reagents in the total absence of protein. Therefore, reagent blanks were included in the quantification.

The average 562 nm absorbance measurements of the experimental blank samples (containing only PBS, see Table 5.6) replicates were subtracted from the 562 nm absorbance measurements of all the other individual standards and unknown sample replicates. Absorbance values were measured for each blank and sample in triplicate (prewash absorbance, wash absorbance, and elution absorbance). The standard curve (Figure 5.16) was then used to determine the protein concentration of each unknown sample.

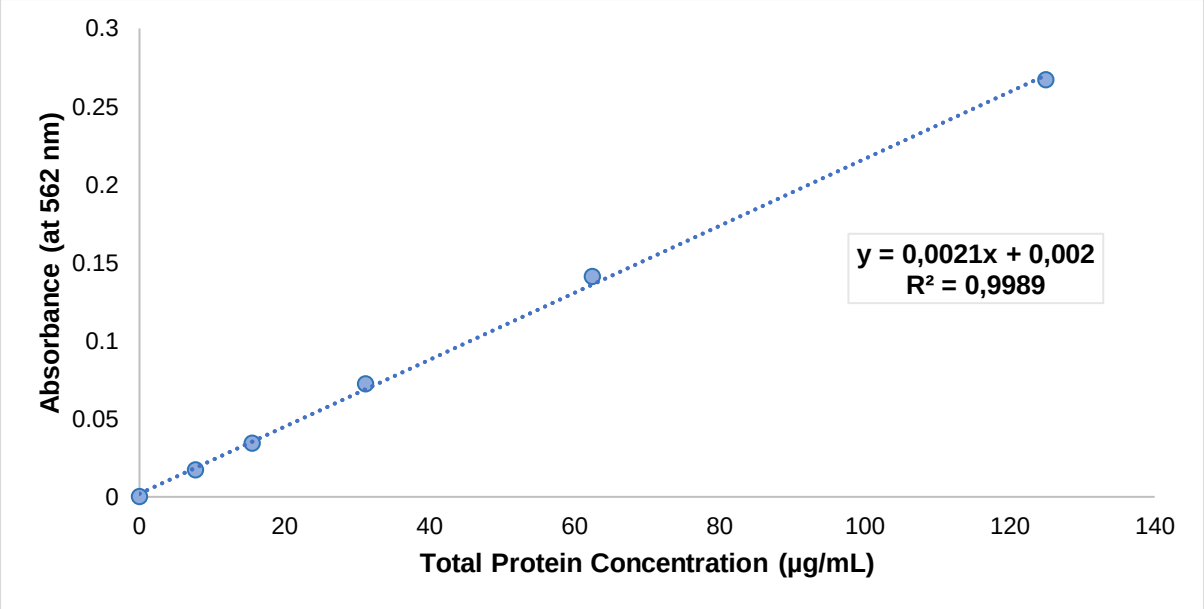

Figure 5.16. Calibration curve for protein determination. *Linear regression showing total protein concentration (µg/mL) in relation to absorbance at 562 nm. With the equation y = 0.0021x + 0.002, R^2 = 0.999.*

Results and Discussion

Part 1: Optimising the volume of protein A slurry

The total protein concentration in the pre-wash and washes following binding of the same concentration of RTX to different volumes of protein A beads are depicted as a bar graph in Figure 5.17.

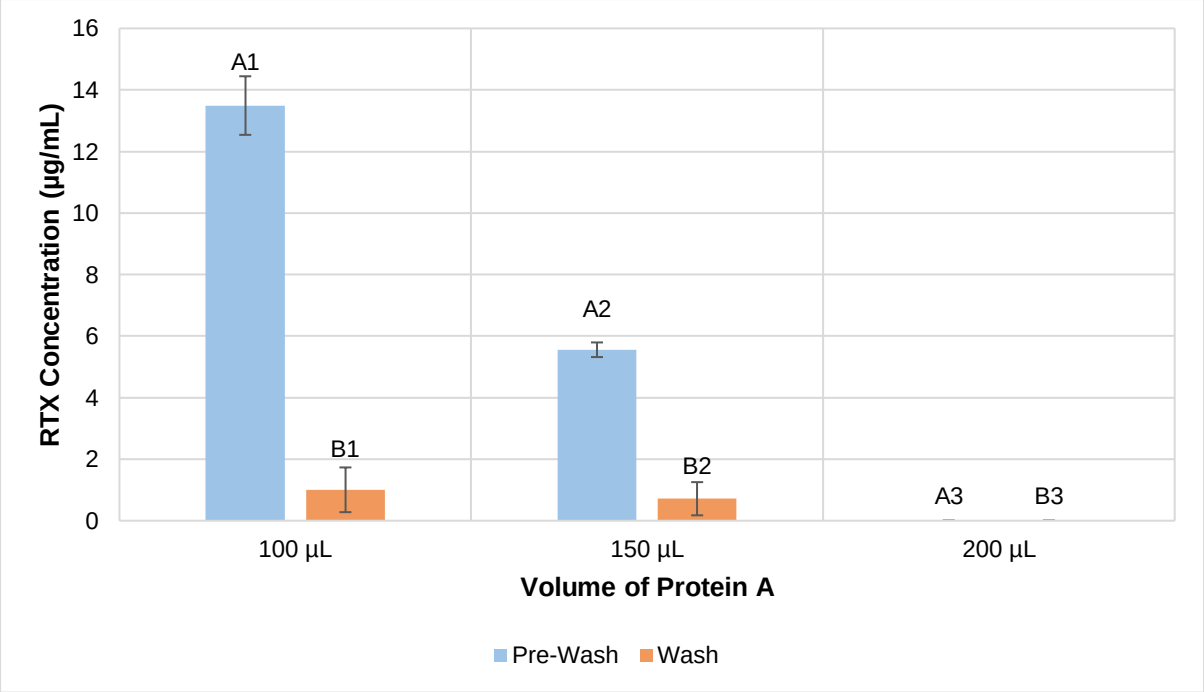

Figure 5.17. RTX protein concentration in relation to volume of protein A. *Bar graph illustrating protein concentration in the pre-wash (blue bars) and washes (orange bars) for different volumes of protein A. Error bars represent standard deviation; pre-wash N=3 and wash N=9.*

The RTX concentrations indicated by the blue bars (A1–3) in Figure 5.17 represent the RTX not bound by incubation with different volumes of protein A. About 13.5 µg/mL was still unbound and remained in solution when 50 µg RTX was incubated with 100 µL of the protein A beads. The unbound RTX was reduced significantly when 150 µL of protein A was used, with about 5.50 µg/mL still unbound. However, all the RTX added (50 µg) was bound to the protein A beads when 200 µL of the beads was used for affinity binding. The greater the volume of protein A added, the more binding sites were available. Therefore, as the protein A volume increased, the protein concentration in the pre-wash supernatant decreased. This indicates an inverse relationship between RTX concentration in the pre-wash / wash and the volume of protein A.

Following affinity binding, the pellets containing bound RTX were washed, and the washes were also analysed for total protein content. The second set of supernatants collected, the washes (B1–3), indicated the ability of the protein to remain bound to the protein A beads throughout the exposure of various washes. This can further be described as protein retention before elution. Regardless of the volume of protein A added, the protein level in the washes remained relatively low. Protein concentration in all samples was ≤1.40 µg/mL. There was, however, a slight decrease as the protein A volume increased (B1–3). No protein could be measured in B3, which indicates the highest binding in this sample to protein A. Overall, no significant amounts of protein eluted in the washes, indicating irreversible binding of IgG to the protein A beads. This can also be interpreted as indicating very low non-specific binding under experimental conditions.

It should however be noted that Figure 5.17 is not a quantitative representation of the results. The binding trends are indicated by considering actual absorbance values and the representative RTX concentration without considering the different volumes across experimental samples, as summarised in Table 5.6. The quantitative results are, however, represented in Table 5.7.

Table 5.7. *Summary of the calculations for the experimental samples*

Volume of protein A slurry (µL)	**100 µL**	**150 µL**	**200 µL**
Description	roughly 50 µL of beads resuspended in 50 µL of PBS	roughly 75 µL of beads resuspended in 75 µL of PBS	roughly 100 µL of beads resuspended in 100 µL of PBS
Amount of RTX added to protein A (µg)	50 µg	50 µg	50 µg
Volume of pre-wash supernatant (µL)	50 µL of PBS to resuspend beads 50 µL of 1 mg/mL RTX working solution 400 µL of 0.1% OTG V_f = 500 µL	75 µL of PBS to resuspend beads 50 µL of 1 mg/mL RTX working solution 400 µL of 0.1% OTG V_f = 525 µL	100 µL of PBS to resuspend beads 50 µL of 1 mg/mL RTX working solution 400 µL of 0.1% OTG V_f = 550 µL
Concentration of RTX in pre-wash supernatant (µg/mL) *	13.5 µg/mL	5.56 µg/mL	0 µg/mL
Amount of RTX in pre-wash supernatant (µg)	6.75 µg (because the pre-wash volume is 500 µL)	2.92 µg (because the pre-wash volume is 525 µL)	0 µg
Amount of RTX bound to protein A (µg)	50 – 6.75 = 43.3 µg	50 – 2.92 = 47.1 µg	50 – 0 = 50 µg
Concentration of RTX in wash supernatant (µg/mL) *	1.32 µg/mL	1.16 µg/mL	0 µg/mL
Amount of RTX in wash supernatant (µg)	1.32 µg (because wash volume is 1 mL)	1.16 µg (because wash volume is 1 mL)	0 µg
Amount of RTX bound to protein A (µg)	43.3 (amount bound after pre-wash) – 1.32 = 41.9 µg	47.1 (amount bound after pre-wash) – 1.16 = 45.9 µg	50 (amount bound after pre-wash) – 0 = 50 µg

*Concentration calculated from the regression equation

The amount of RTX bound to the protein A beads, pre-wash and post-wash, is represented in Table 5.7. Fifty micrograms of RTX were added to all three volumes of protein A beads. When 100 µL of protein A was used, 6.75 µg of RTX was lost in the pre-wash, leaving 43.3 µg bound to the protein A beads. When

150 µL of protein A was used, 2.92 µg of RTX was lost in the pre-wash, leaving 47.1 µg bound to the protein A beads. Lastly, when the largest volume of 200 µL of protein A was used, no RTX was lost in the pre-wash, leaving all 50 µg of RTX added bound to the protein A beads (100% bound).

When 100 µL of protein A was used, a further 1.32 µg of RTX was lost during the washes, leaving 41.9 µg of RTX bound to the protein A beads. When 150 µL of protein A was used, a further 1.16 µg of RTX was lost during the washes, leaving 45.9 µg of RTX bound to the protein A beads. Lastly, when the largest volume of 200 µL of protein A was used, no RTX was lost during the washes, leaving all 50 µg of RTX added bound to the protein A beads (100% still bound).

As seen in Table 5.7, as the volume of protein A slurry increases, the amount of RTX bound increases. This indicates a directly proportional relationship between the amount of RTX bound to protein A and the volume of protein A used. This relationship is further illustrated in Figure 5.18.

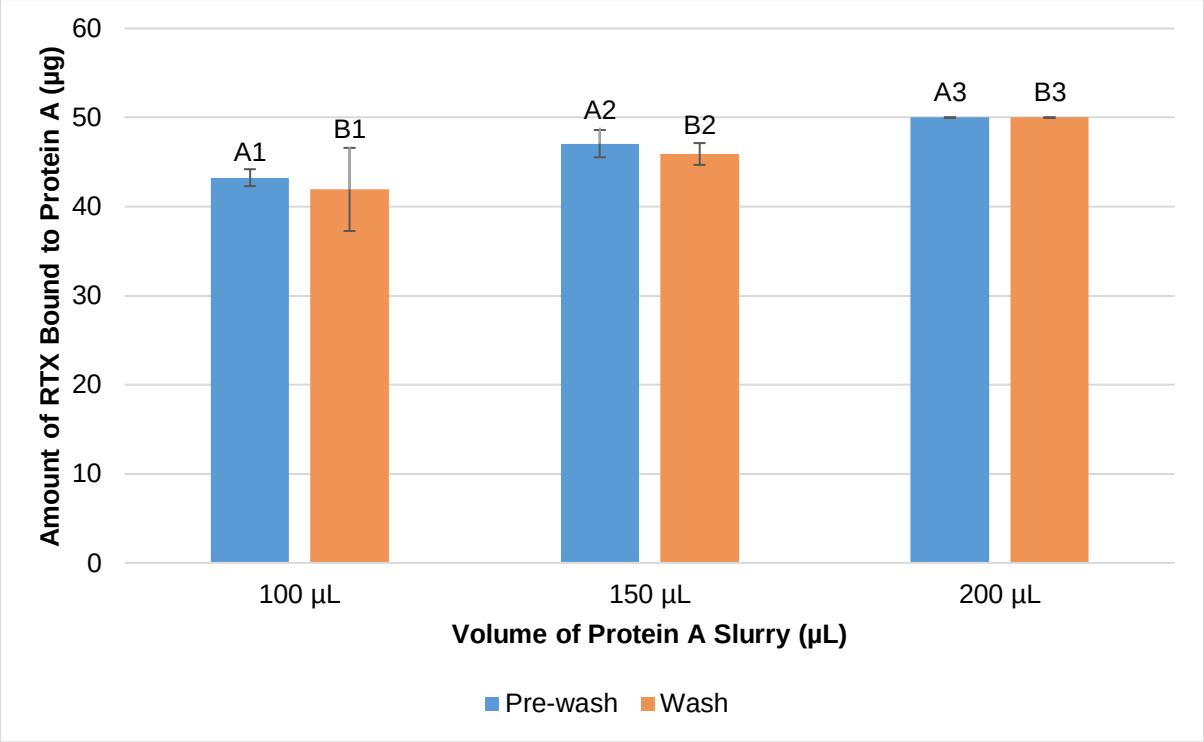

Figure 5.18. Relationship between the amount of RTX bound and the volume of protein A. *Bar graph illustrating the amount of RTX in the pre-wash (blue bars) and washes (orange bars) for different volumes of protein A. Error bars represent standard deviation; pre-wash N=3 and wash N=9.*

As seen in Figure 5.18, the most significant difference in the amount of RTX bound to protein A was observed between A1 and B1 (loss of 1.32 µg – see Table 5.7). A smaller difference was observed between A2 and B2 (1.16 µg – see Table 5.7). Finally, no difference was found in the amount of RTX bound to protein A between A3 and B3. This indicates that when using 200 µL of the protein A slurry, all the RTX is bound to the beads and remains bound during the washes.

Considering the quantitative representation in Figure 5.18, no big difference was observed between the different volumes of protein A added (A1–A3, B1–B3). This indicates that the method was near optimisation regardless of whether 100, 150 or 200 µL of protein A was added.

Part 2: Elution

While the analysis of the pre-wash and wash solutes indicated an indirect manner of measuring the amount of RTX bound to the protein A beads, the analysis of the eluates following application of the elution buffer will indicate the amount of RTX that can be eluted from the beads. This is summarised in Table 5.8.

Table 5.8. *Summary of the amount of total protein in the eluate (supernatant after elution) and the percentage of protein bound versus unbound (the amount of protein lost during the pre-wash and wash collections was considered when calculating theoretical RTX concentration)*

Volume of protein A slurry	**100 µL**	**150 µL**	**200 µL**
Absorbance at 562 nm (n=3) in eluate	0.0920 (± 0.00794)	0.0714 (± 0.00153)	0.0514 (± 0.00231)
Actual RTX concentration in eluate (µg/mL) *	42.9 µg/mL	33.0 µg/mL	23.5 µg/mL
Final volume in eluate (µL)	400 µL	600 µL	800 µL
Amount of RTX in eluate (µg)	17.1 µg	19.8 µg	18.8 µg
Theoretical amount of RTX in eluate (µg) (80% expected in eluate – see methodology, Table 5.6 and Figure 5.14)	40.0 µg	40.0 µg	40.0 µg
Amount of RTX lost in pre-wash (µg)	6.75 µg	2.92 µg	0 µg
Amount of RTX lost in wash (µg)	1.32 µg	1.16 µg	0 µg
Amount of RTX in eluate (µg)	40.0 – 6.75 – 1.32 = 31.9 µg	40.0 – 2.92 – 1.16 = 35.9 µg	40.0 µg
Percentage RTX unbound / percentage RTX in eluate (%)	53.7%	55.1%	47.0%
Average percentage RTX eluted from protein A beads (%)	**51.9%**		
Percentage RTX bound to protein A (%)	46.3%	44.9%	53.0%
Average percentage RTX still bound to protein A beads (%)	**48.1%**		

* Concentration calculated from the regression equation

A percentage recovery can be calculated when the actual protein concentration is divided by the theoretical protein concentration. This percentage recovery is representative of the success of the affinity binding purification and how much of the protein concentration is in the supernatant to be digested by the trypsin. When considering the percentage recovery of all three protein A volumes, it is evident that roughly half the amount of protein remains on the beads for all three cases. This shows that the elution still needs to be completed with the current elution conditions. Even though the elution was incomplete, the quantitative yield of RTX eluted was reproducible. Therefore, because a relatively high percentage of the RTX is still bound to the protein A beads following elution, it was decided to perform the digestion on the protein A beads rather than performing the digestion on the eluted supernatant. It is known that protein A immobilises and holds the IgGs in a configuration that still allows sufficient cleavage of the IgG to detect the signal peptide (114). Using on-bead trypsinization also results in a shorter and more concise extraction procedure.

Both the elution method and the on-bead trypsinization have inherent disadvantages. Levernæs *et al*. found that the elution of proteins bound to the beads may be incomplete (140). However, on-bead trypsin digestion may also be non-specific. Peptides generated by on-bead digestion may also bind non-specifically to the beads, reducing the signal intensity. The authors included an elution step following on-bead digestion and found that the non-specific binding of such peptides may be reduced. The possibility of combining both methods to improve the signal peptide's quantitative and qualitative yield was proposed. Considering this, no clear answer could be formulated on whether or not the protein should be eluted before digestion (140). On-bead digestion is less time-consuming since elution has to be preceded by neutralisation of the eluate before digestion, and hence more steps are introduced to the sample preparation procedure. However, these additional steps may give less chromatographic background and increase the overall method's sensitivity and specificity. In this project, the digestion was performed on-bead to avoid the potential loss of RTX in the eluate, thereby eliminating further loss in sensitivity.

Summary

Protein precipitation was not selective or specific enough, but affinity binding purification proved to be the optimal protein-level cleanup procedure before tryptic digestion. The optimal volume of the protein A slurry used during the affinity binding purification procedure was 200 µL. It was also decided to perform tryptic digestion on-bead instead of digestion of the protein in the eluate since the results confirmed published reports of non-optimal elution of the IgG from protein A beads.

CHAPTER 6

METHOD EXECUTION: INTRODUCING THE PLASMA MATRIX, PERCENTAGE RECOVERY AND SENSITIVITY

Complete execution of the sample preparation method was performed in phosphate-buffered saline (PBS) and plasma using the optimised affinity binding purification, digestion, and solid phase extraction (SPE) procedures. The analysis was performed by LC-MS/MS as described in Chapter 4. Overall method efficiency was expressed as percentage recovery and found to be similar in PBS and plasma. Once that was established, the percentage recovery was assessed over a range of RTX concentrations in plasma.

6.1 INVESTIGATION 1: RITUXIMAB IN PBS

Introduction

In the first investigation, a single RTX concentration in PBS was extracted to test method efficiency.

Methodology

The materials and solutions used for this methodology were the same as those used in sections that separately describe the development of the different procedures.

A working solution of 300 µg/mL RTX was prepared in PBS by diluting 30 µL of the 10 mg/mL RTX stock solution in 970 µL of PBS.

Affinity binding purification was performed using the procedure previously optimised as described in Section 5.3.2. Aliquots of 100 µL of the 300 µg/mL RTX working solution (30 µg of RTX) in PBS were added to 200 µL of protein A suspension, in duplicate, with 400 µL of 0.1% octylthioglucoside (OTG) detergent, before being left at room temperature while tumbling for 3 hours. As described in Section 5.3.2, the pellet was washed by centrifugation and resuspension, first with 1 mL 0.1% OTG, followed by 1 mL PBS and, lastly, with 1 mL 25 mM Tris buffer pH 8 to condition the pellet for tryptic digestion. The final pellet contained RTX bound to the protein A beads following affinity binding purification.

On-bead tryptic digestion was then performed using the procedure optimised as described in Section 5.1. To digest 30 µg of RTX, 1.5 µg trypsin is required since the optimal ratio was established in Section 5.1 to be 1:20 (protease/protein). Therefore, the 1 µg/µL trypsin stock solution was diluted to 7 µg/mL in 25 mM Tris buffer, pH 8 (see Section 3.4). A volume of 215 µL of this trypsin preparation was used to suspend the pellet and 21 µL of 100% acetonitrile was added. The samples were left overnight at room temperature while tumbling and were then spiked with an additional 1.5 µL of the 1 µg/µL trypsin stock solution. Following a further 3 hours at room temperature while tumbling, the digestion was quenched with 12 µL of 10% formic acid and centrifuged, and the pellet was discarded. The supernatant (final volume 249.5 µL) contains tryptic peptides, including the s-Pep for RTX.

The supernatant from the digestion procedure was then extracted using SPE, as described in Section 5.2. The SPE cartridges were conditioned with 1 mL of methanol, followed by 1 mL 0.1% formic acid

and 1 mL water. Thereafter, 200 µL of the supernatant from the digestion step was loaded onto the cartridge together with 200 µL 0.1% formic acid. The columns were washed twice with 1 mL of water and once with 100 µL of 10% acetonitrile. The s-Pep was eluted with 200 µL of 70% acetonitrile containing 1% formic acid. The eluate was dried down under a steady stream of nitrogen gas at 37°C, resuspended with 100 µL of injection solution, and analysed on the Sciex API-3200 LC-MS/MS system. The optimised chromatographic conditions and instrument settings, as described in Chapter 4, were used for the analysis of the s-Pep in the samples.

For quantification, a set of s-Pep calibration standards was prepared by dilution of the 2 mg/mL stock solution into an injection solution consisting of 20% acetonitrile and 0.1% formic acid. The final concentrations of the calibration standards covered the s-Pep range of 0.25–10 µg/mL and these were analysed together with the experimental samples. The peak areas of the calibration peptide standards were plotted against their respective concentration using linear regression. The resultant standard curve depicted in Figure 6.1 was used to determine the s-Pep concentrations of the experimental samples.

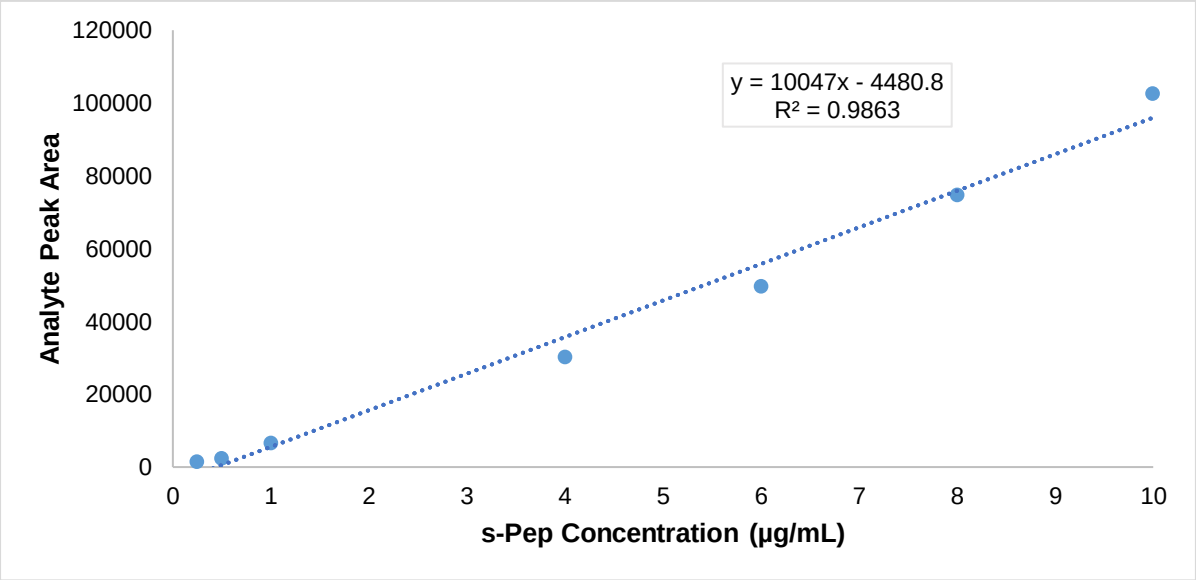

Figure 6.1. Representative calibration curve for s-Pep. *Peptide concentration in µg/mL versus analyte peak area response for the signature peptide calibration standards used to calculate the s-Pep concentrations of the experimental samples. Equation y = 10047x – 4480.8, R^2 = 0.986.*

Results and Discussion

The chromatogram shown in Figure 6.2 is that of the experimental sample, and depicts the peak shape, retention time and peak intensity obtained.

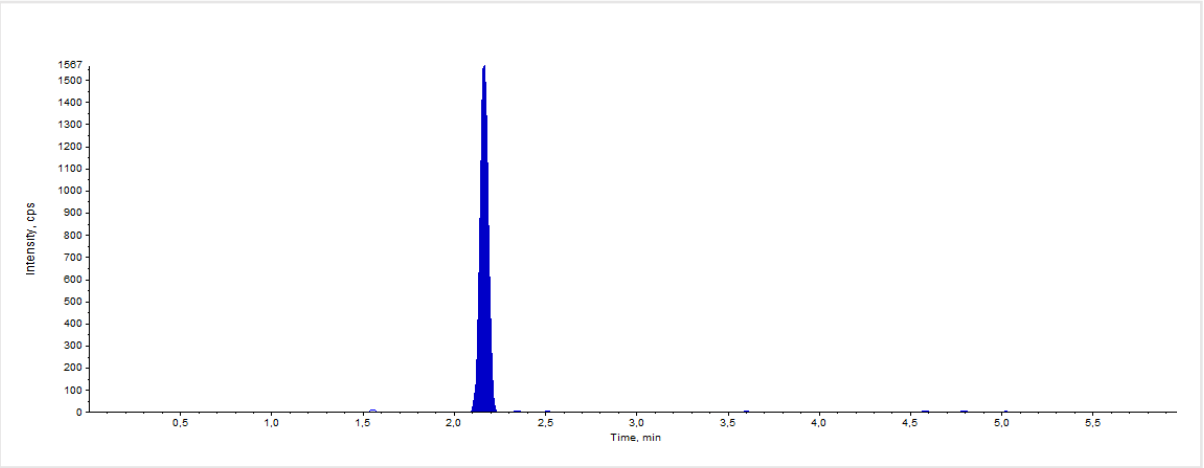

Figure 6.2. Representative chromatogram for s-Pep. *Chromatogram for the experimental sample depicting the peak shape, retention time and peak intensity obtained (s-Pep concentration of 7.21 µg/mL).*

The s-Pep concentrations of the experimental samples were calculated using the regression equation in Figure 6.1 and are summarised in Table 6.1. As previously described and as calculated using the sequence information of RTX (Section 4.1.2), the mass-to-mass ratio of s-Pep to RTX is 3%. This was accounted for when calculating the expected / theoretical s-Pep concentration in the experimental samples, as indicated in Scheme 6.1:

Scheme 6.1 Theoretical s-Pep Concentration

3% of 30 µg = 0.9 µg

0.9 µg / 249.5 µL x 200 µL = 0.721 µg

0.721 µg / 100 µL x 1000 = **7.21 µg/mL**

(where 249.5 µL is the volume after digestion, 200 µL is the volume of supernatant loaded onto the SPE cartridge, and 100 µL is the reconstitution volume)

Table 6.1. *Summary of the actual s-Pep concentrations of the experimental samples compared to the theoretical s-Pep concentration in order to calculate method efficiency through percentage recovery (the actual s-Pep concentration of the experimental samples was calculated using the equation y = 10047x – 4480.8 from the regression produced by the s-Pep calibration standards)*

RTX (µg)	Actual peak area	Actual s-Pep concentration (µg/mL)	Theoretical s-Pep concentration (µg/mL)	Percentage recovery
30.0	4950	0.939	7.21	13.0%
30.0	4650	0.909	7.21	12.6%
			Average percentage recovery	**12.8%**
			Standard deviation	**0.3%**

The percentage recovery of s-Pep from extracted RTX in PBS was 12.8% (±0.3%).

6.2 INVESTIGATION 2: COMPARISON OF RITUXIMAB IN PBS AND PLASMA

Introduction

In the second set of experiments, the full extraction method was performed in PBS and plasma for comparison. In addition, during the SPE procedure, the elution step was repeated three times, and each eluate was analysed separately to ensure that the optimised SPE procedure was still effective when plasma was introduced.

Methodology

In the previous investigation (Investigation 1: RTX in PBS, Section 6.1), the final amount of RTX applied to sample preparation was 30 µg. In this investigation, where sample preparation in plasma was compared to that in PBS, the final RTX concentration was adjusted to compensate for the endogenous IgGs in plasma that are expected to bind to the protein A. Therefore, the amount of RTX applied to sample preparation in this investigation was 50 µg of RTX.

The materials and solutions used for this methodology were the same as those used in sections that separately describe the development of the different procedures. The same overall steps were followed as described above in Investigation 1 (Section 6.1).

A working solution of 1 mg/mL RTX was prepared in PBS and plasma by diluting 100 µL of the 10 mg/mL RTX stock solution in 900 µL of PBS and plasma, respectively.

Affinity binding purification was performed using the procedure previously optimised as described in Section 5.3.2 and implemented in Investigation 1. However, in duplicate, aliquots of 50 µL of the 1 mg/mL RTX working solution (50 µg of RTX) in PBS and plasma were added to 200 µL of protein A suspension. The rest of the affinity binding purification procedure followed that of Investigation 1.

On-bead tryptic digestion was then performed, similar to Investigation 1, using the procedure optimised as described in Section 5.1. In order to digest 50 µg of RTX, 2.5 µg of trypsin was required, since the optimal ratio was established in Section 5.1 as 1:20 (protease/protein). A volume of 357 µL of trypsin in Tris buffer (7 µg/mL) was therefore added with the addition of 35 µL of 100% acetonitrile. The samples were left overnight at room temperature while tumbling, and then spiked with an additional 2.5 µL of 1 µg/µL trypsin stock solution. Following a further 3 hours at room temperature while tumbling, the digestion was quenched with 20 µL of 10% formic acid and centrifuged to form a pellet. The final volume after digestion was 414.5 µL.

The supernatant from the digestion procedure was extracted using SPE, similar to Investigation 1, and as optimised and described in Section 5.2. The loading volume onto the SPE cartridges was 300 µL of the supernatant from the digestion step, with the addition of 300 µL 0.1% formic acid. To elute the analyte, 200 µL of 70% acetonitrile with 1% formic acid was added three times. Each elution was collected separately to assess whether all of the analyte was still only eluting with the addition of the first 200 µL of acetonitrile, especially those samples derived from the plasma matrix. The samples were

then dried under a steady stream of nitrogen gas at 37°C and resuspended with 200 µL of injection solution. As with Investigation 1, the samples were analysed on the Sciex API-3200 LC-MS/MS system. The optimised chromatographic conditions and instrument settings described in Chapter 4 were used for this analysis. The presence of the s-Pep in the samples was assessed by comparing relevant peak areas and concentrations.

For quantification, a set of s-Pep calibration standards was prepared by dilution of the 2 mg/mL stock solution into an injection solution consisting of 20% acetonitrile and 0.1% formic acid. The final concentrations of the calibration standards covered the s-Pep range of 0.25–8 µg/mL and were analysed together with the experimental samples. The peak areas of the calibration peptide standards were plotted against their respective concentration using linear regression. The resultant standard curve depicted in Figure 6.3 was used to determine the s-Pep concentrations of the experimental samples.

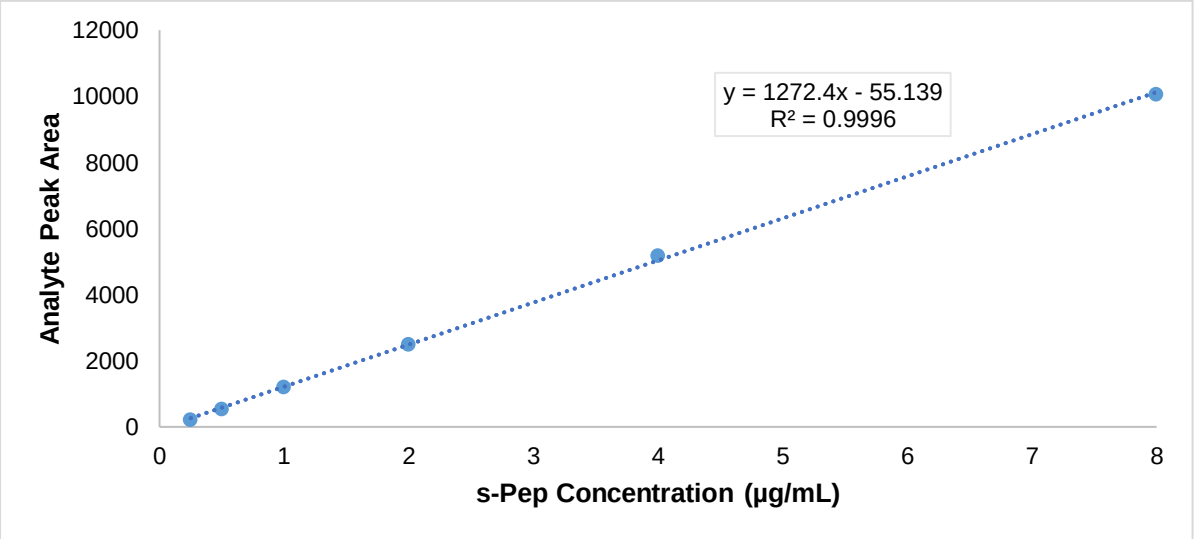

Figure 6.3. Representative calibration curve for s-Pep. *Line graph illustrating peptide concentration in µg/mL versus analyte peak area response for the signature peptide calibration standards used to calculate s-Pep concentration of the experimental samples. Equation y = 1272.4x – 55.1, R^2 = 1.*

Results and Discussion

The two chromatograms shown in Figure 6.4 are those of two of the test samples, and depict the peak shapes, retention times, and peak intensities obtained.

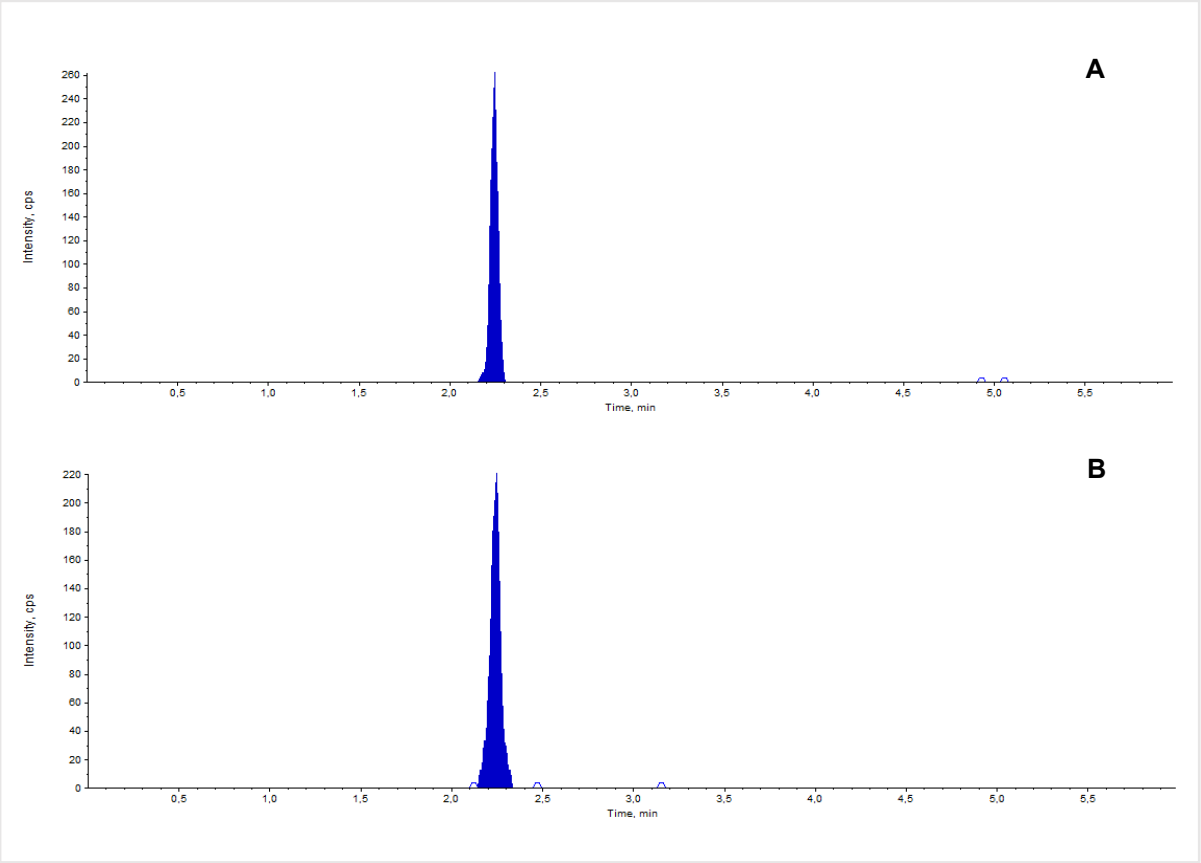

Figure 6.4. Representative chromatograms for RTX. *Chromatograms for RTX in PBS (A), RT 2.2 min, and RTX in Plasma (B), RT 2.2 min. Representative s-Pep concentration of 5.43 µg/mL.*

A comparison of the purified s-Pep prepared from RTX added to PBS and plasma is depicted in Figure 6.5.

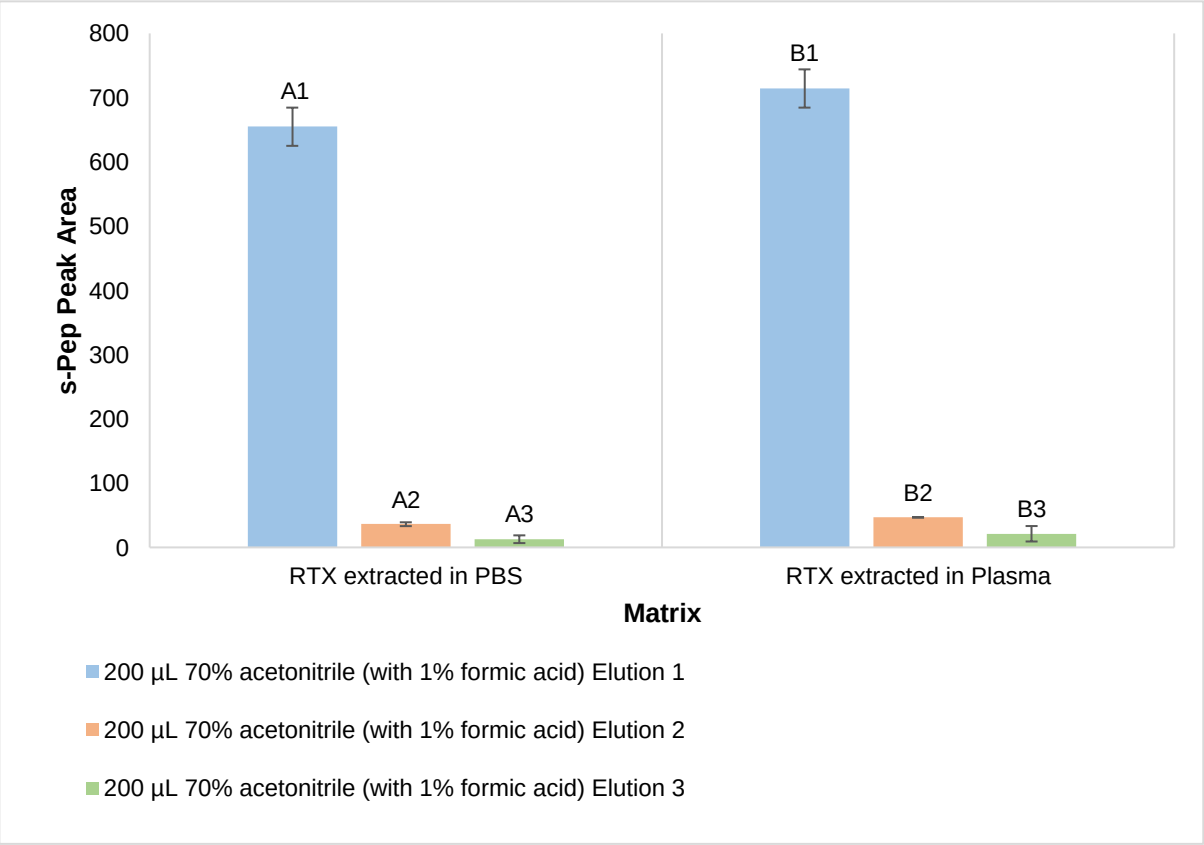

Figure 6.5. Amount of s-Pep recovered from different matrices. *Bar graph illustrating the peak areas of the s-Pep in PBS and plasma when three separate consecutive elutions were collected from the SPE extraction procedure, following the optimised sample preparation. The error bars show the standard deviation, N=2.*

The blue (A1 and B1), orange (A2 and B2) and green (A3 and B3) bars in Figure 6.5 represent the s-Pep measured in the first, second and third elutions of the SPE purification, following affinity binding purification and tryptic digestion in the samples prepared in both PBS (A) and plasma (B). In both matrices, the blue bar (A1 and B2) is significantly greater than the orange bar (A2 and B2) and green bar (A3 and B3). This illustrated that almost all the analyte was eluted with the addition of the first 200 µL of 70% acetonitrile (with 1% formic acid) – regardless of whether the sample was prepared in PBS or plasma.

In addition, at the RTX concentration used in this experiment, it can be concluded that the sample preparation procedures, including affinity binding purification, digestion and SPE, resulted in the same amount of s-Pep being purified, whether the RTX was in PBS or in plasma. Since endogenous immunoglobulins will compete with the RTX during the affinity binding process to the on-bead protein A, these results prove that the ratio of protein A to RTX at this concentration is sufficient to ensure no inhibition of RTX binding because of the endogenous immunoglobulins in plasma. In addition, it proves that the trypsinization step to produce s-Pep is optimised, even with extraction from plasma.

To calculate the percentage recovery, the s-Pep concentrations in the experimental samples were determined using the regression equation in Figure 6.3 and summarised in Table 6.2. The same calculation as previously described in Investigation 1 applies. Therefore, the theoretical s-Pep concentration is expressed by the calculation indicated in Scheme 6.2:

Scheme 6.2 Theoretical s-Pep Concentration

3% of 50 µg = 1.5 µg

1.5 µg / 414.5 µL x 300 µL = 1.086 µg

1.086 µg / 200 µL x 1000 = **5.43 µg/mL**

(where 414.5 µL is the volume after digestion, 300 µL is the volume of supernatant loaded onto the SPE cartridge, and 200 µL is the reconstitution volume)

Table 6.2. *Summary of the actual s-Pep concentrations of the experimental samples compared to the theoretical s-Pep concentration to calculate method efficiency through percentage recovery in both PBS and plasma (actual s-Pep concentration of the experimental samples was calculated using the equation y = 1272.4x – 55.1 from the regression generated from the s-Pep calibration standards)*

Experimental sample	RTX (µg)	Actual peak area	Actual s-Pep concentration (µg/mL)	Theoretical s-Pep concentration (µg/mL)	Percentage recovery
RTX in PBS	50.0	748	0.631	5.43	11.6%
RTX in Plasma	50.0	897	0.748	5.43	13.8%
				Average percentage recovery	**12.7%**
				Standard deviation	**1.5%**

The average percentage recovery of s-Pep from extracted RTX in PBS and plasma was 12.7% (±1.5%).

When compared to Investigation 1, the same percentage recovery was observed (see Tables 6.1 and 6.2). The peak intensities observed, however, were about 4.5 times lower for an equivalent concentration. Therefore, the chromatograms from Investigations 1 and 2 were investigated for the unknown samples (see Figures 6.2 and 6.4) and those of the calibration standards. The peak shapes and retention times for both chromatograms of Investigation 2 were the same as those of Investigation 1. The only difference observed was the peak intensities at similar concentrations. The aim of the two investigations was to assess the efficiency of the extraction procedure and the results acquired were the same notwithstanding the difference in peak intensities. Since the two investigations were performed on different days, this discrepancy was ascribed to instrument performance and the robustness of the results was accepted.

The recovery was assessed over a range of RTX concentrations to round off the investigations into the efficiency of the extraction procedure.

6.3 INVESTIGATION 3: PERCENTAGE RECOVERY AT DIFFERENT RTX CONCENTRATIONS

Introduction

An investigation was conducted into the recovery of the s-Pep from a range of different RTX concentration samples extracted when the complete developed sample preparation method was performed, employing the Sciex API-3200 LC-MS/MS system for detection.

The percentage recovery pertains to the extraction efficiency of the total analytical process within the limits of variability. In this investigation, percentage recovery was determined by comparing the analytical response of the intact RTX in blank plasma with the response of the blank plasma first extracted and then spiked with the s-Pep (as representative of RTX). The peak area response obtained with the post-extracted spiked samples (reference samples) represented 100% recovery.

Methodology

The extracted RTX in plasma samples was compared with reference samples which were prepared by spiking blank plasma extracts with s-Pep. The sample preparation procedure followed for blank plasma and experimental samples was described in Chapter 5 and summarised in Table 6.3. The extraction procedure is also schematically summarised in Figure 6.6.

Experimental samples: Various concentrations of RTX were spiked into blank plasma and extracted as per the analytical method.

Reference samples: Blank plasma was extracted as per the analytical method and the extracts were spiked with various concentrations of s-Pep.

Table 6.3. *Summary of the sample preparation procedure followed for both the experimental samples and the reference samples*

Experimental samples	Reference samples
Add **100 µL** of RTX to 200 µL of protein A beads	Add **100 µL** of blank plasma to 200 µL of protein A beads
Digest with 358 µL of trypsin/Tris solution	Digest with 358 µL of trypsin/Tris solution
Final volume after digestion = **418 µL**	Final volume after digestion = **418 µL**
Load **380 µL** onto the SPE cartridge	Load **380 µL** onto the SPE cartridge
Elute with 200 µL of 70% acetonitrile (1% formic acid)	Elute with 200 µL of 70% acetonitrile (1% formic acid)
Reconstitute with **165 µL** of injection solution	Reconstitute with **140 µL** of injection solution
–	Spike **25 µL** of peptide spiking solution
V_f = **165 µL**	V_f = **165 µL**
Transfer 100 µL into a 96-well plate	Transfer 100 µL into a 96-well plate

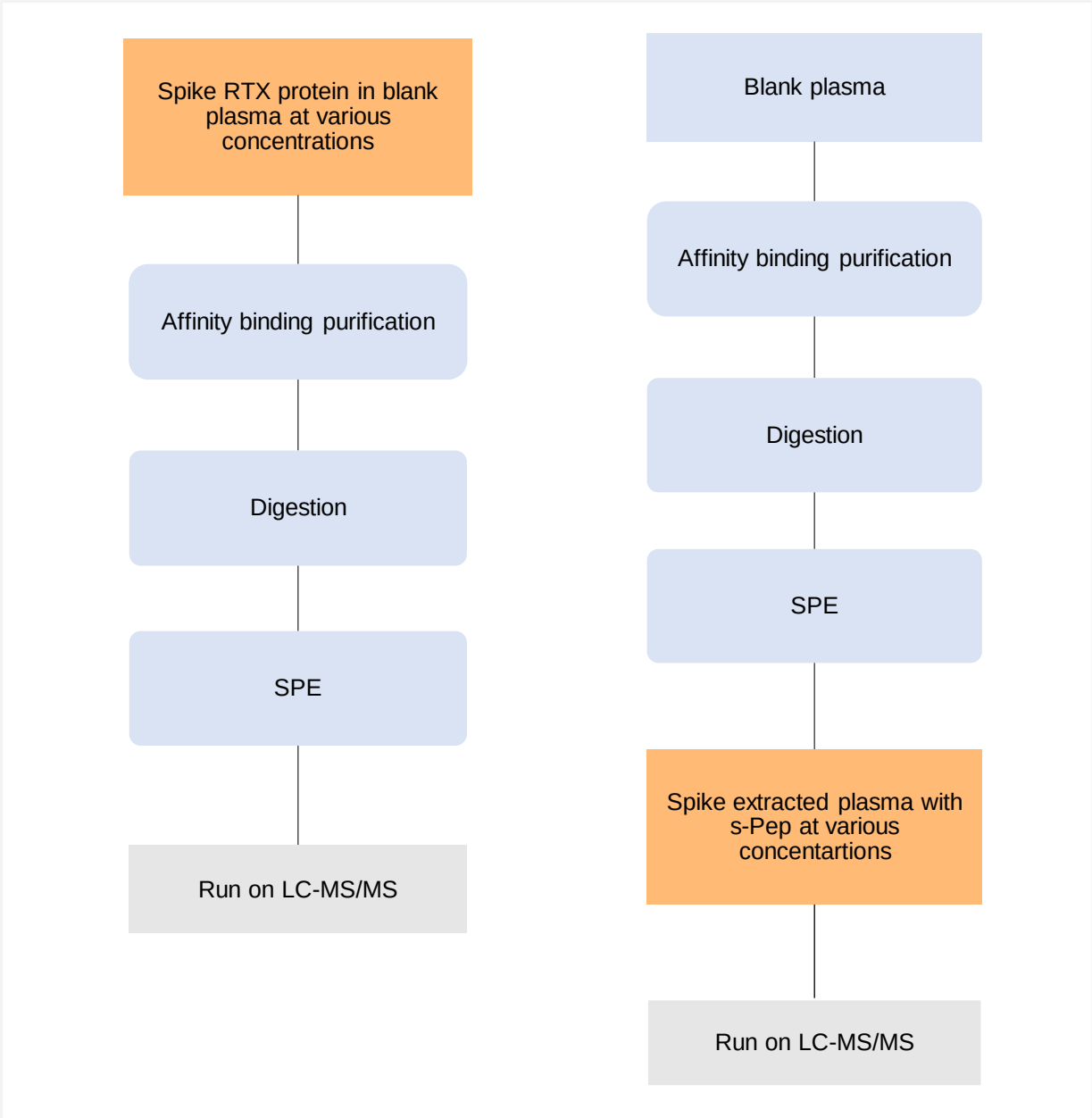

Figure 6.6. Method overview. *Flow diagram summarising the sample preparation procedure followed for the experimental samples and reference samples.*

Preparation of the test samples

As already indicated in Section 4.1.2, the mass of s-Pep expected to result from RTX is 3% of the mass of the RTX subjected to trypsinization. The expected analytical range of RTX in plasma of subjects under treatment is 12.5–300 µg/mL (66). Therefore, the equivalent concentration range of the s-Pep should be 0.375–9 µg/mL. If this range of s-Pep is spiked into the injection solution, the full range can be observed using the Sciex API-3200 LC-MS/MS. However, extracting the full range of RTX mentioned above by using the developed sample preparation technique resulted in s-Pep concentrations that cannot be observed for the full range by the Sciex API-3200. The interpretation was that the recovery

of the s-Pep during sample preparation and analysis was rather low, and to determine what the recovery is expected to be across a range of concentrations, a higher than expected range of RTX in plasma was used and compared to theoretical concentrations of s-Pep (reference samples) that would represent that range of RTX. The results from Investigations 1 and 2 (Sections 6.1 and 6.2) were therefore taken into consideration when setting up this experiment.

To prepare these test samples, the sample volumes as necessitated by the methodology are considered to calculate the concentrations of s-Pep that represent the range of RTX concentrations investigated. These are indicated in Tables 6.4–6.6.

Table 6.4 indicates the actual RTX concentrations in the experimental samples that will be used in the investigation. It also indicates the theoretical / expected s-Pep concentrations for the RTX experimental samples. Considering the 12.8% recovery as determined during Investigations 1 and 2, the range of s-Pep to be prepared, as described in Tables 6.5 and 6.6, is derived from the final theoretical s-Pep concentrations post-extraction in Table 6.4.

Table 6.5 depicts the preparation of s-Pep spiking solutions that will be used to prepare the s-Pep concentration range of the reference samples as indicated in Table 6.6.

Table 6.4. *Theoretical final s-Pep concentrations from RTX extracted samples (experimental samples)*

Initial RTX concentration pre-extraction (µg/mL)	µg of RTX added to the protein A beads	Equivalent µg of s-Pep added to protein A beads*	µg of s-Pep after SPE	Final s-Pep concentration post-extraction (µg/mL)**
800	80.0	2.40	2.18	13.2
600	60.0	1.80	1.64	9.92
500	50.0	1.50	1.36	8.26
400	40.0	1.20	1.09	6.61
300	30.0	0.900	0.818	4.96
150	15.0	0.500	0.409	2.48

*3% of the mass of RTX

**These values were calculated using Schemes 6.1 and 6.2

Table 6.5. *Preparation of s-Pep spiking solutions*

Stock Solution Concentration: 2 mg/mL

s-Pep spiking solution	Water (µL)	Volume stock solution spiked (µL)	Dilution source	Dilution source volume (µL)	Total volume of dilution (µL)	s-Pep spiking solution (µg/mL)
SS1	4940	60.0			5000	24.0
SS2	500		SS1	500	1000	12.0
SS3	500		SS2	500	1000	6.00
SS4	500		SS3	500	1000	3.00
SS5	500		SS4	500	1000	1.50

Table 6.6. *s-Pep reference samples to be used as calibration standards for the determination of RTX in the experimental samples*

s-Pep reference samples	s-Pep spiking solution	Spiking volume (µL)	Volume of injection solution (µ)L	Total volume (µL)	s-Pep concentration (µg/mL)
S1	SS1	25.0	140	165	3.64
S2	SS2	25.0	140	165	1.82
S3	SS3	25.0	140	165	0.909
S4	SS4	25.0	140	165	0.455
S5	SS5	25.0	140	165	0.227

Analysis of these standards from Table 6.6 (S1-S5) resulted in a linear regression as depicted in Figure 6.7.

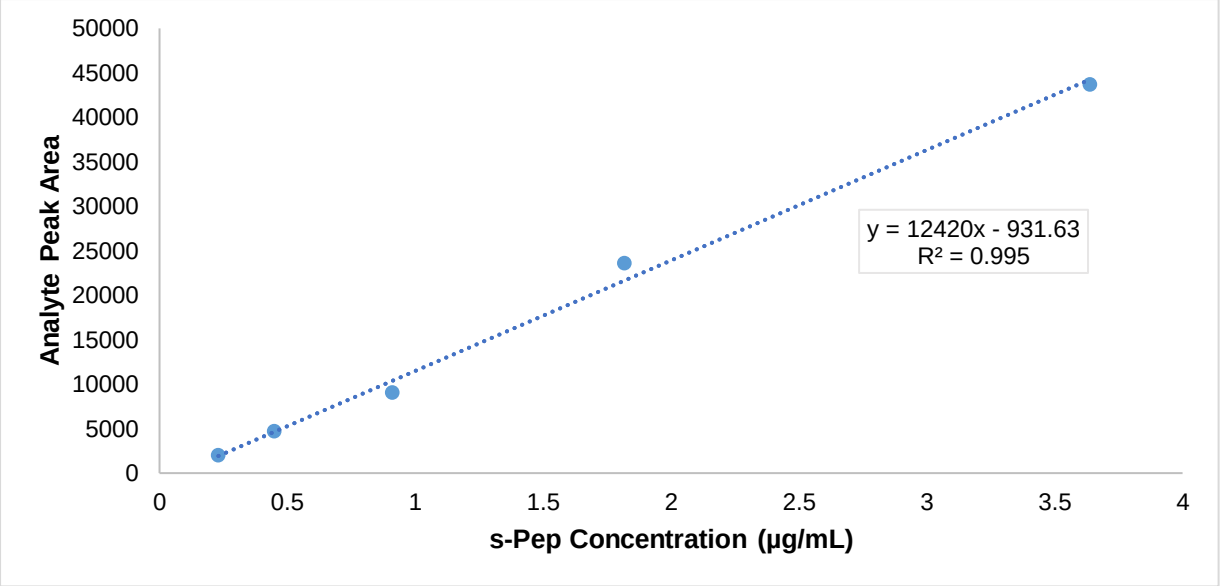

Figure 6.7. Representative calibration curve for s-Pep. *Equation y = 12420x – 931.6, R^2 = 0.995. Reference samples represent 100% recovery.*

Results and Discussion

The analyte peak area found after extraction compared to the theoretical peak area is expressed as a percentage recovery. The equation for the calibration curve in Figure 6.7 was used to calculate actual s-Pep concentrations. The recovery results are presented in Table 6.7.

Table 6.7. *Summary of the percentage recovery of the extracted samples by comparing the actual peak areas to the theoretical peak areas calculated from the equation from the calibration curve setup from post-extracted samples, N=2 (theoretical peak areas were calculated using the calculated theoretical peptide concentrations and the equation y = 12420x – 931.6)*

Experimental samples: Extracted RTX			
Actual peak area	**Actual s-Pep concentration (µg/mL)**	**Theoretical s-Pep concentration (µg/mL)**	**Percentage recovery (%)**
19600	1.65	13.2	12.5
14400	1.23	9.92	12.4
13300	1.15	8.26	13.9
9270	0.821	6.61	12.4
6465	0.596	4.96	12.0
3325	0.343	2.48	13.8
		Average	**12.8**
		Standard deviation	**0.8**

The mean recovery of RTX in plasma over the calibration range was 12.8% (±0.8%), with a CV(%) of 6.3% across the range. The observation of Investigation 2 that no significant difference was found between analyses in PBS and plasma at a single concentration is also true over a range of RTX concentrations. The range used in Investigation 3 is not necessarily that which is expected under therapeutic conditions. However, the conditions used far exceeded the expected load. Therefore, the consistent recovery found across the range confirms that sufficient binding capacity and digestion potential are available for the affinity binding and trypsinization procedures, respectively.

Summary

A consistent percentage recovery for the extraction method was found in PBS and plasma. This was also the case if percentage recovery was determined across a range of RTX concentrations.

6.4 SENSITIVITY ON THE SCIEX API-3200 LC-MS/MS SYSTEM

The recovery as determined in the previous sections (Investigations 1-3) is regarded as a function of the sample preparation procedure and is not necessarily dependent on the sensitivity of the analytical instrument. Therefore, in the recovery experiments, the lowest concentration used was that at which the signal-to-noise ratio (S/N) detected with the Sciex API-3200 LC-MS/MS was above the normal acceptance criterion (S/N ≥ 5). This concentration is 150 µg/mL, which is about the expected mid-range of published therapeutic concentrations. The implication is that the sensitivity of the Sciex API-3200 Q-Trap was considered insufficient to analyse clinically relevant samples.

To confirm this, test samples containing only blank plasma and 150 µg/mL RTX in plasma were prepared. These were processed as described in the sample preparation procedure and analysed on the Sciex API-3200 LC-MS/MS system. The results, as summarised in Table 6.8, confirm that this instrument is not sensitive enough and will not be able to detect RTX in plasma at the expected and published lower concentration (12.5 µg/mL) (66).

Table 6.8. *Summary of the peak areas for a blank plasma sample versus the theoretical LLOQ on the Sciex API-3200 LC-MS/MS system of 150 µg/mL RTX in plasma*

Sample	Peak area
Blank plasma	534 (N=4)
Test sample: RTX in plasma (150 µg/mL)	3325 (N=2)

The two chromatograms shown in Figure 6.8 compare the plasma blank with the test sample (150 µg/mL in plasma), depicting the chromatographic peaks, retention times and the S/N at 150 µg/mL RTX.

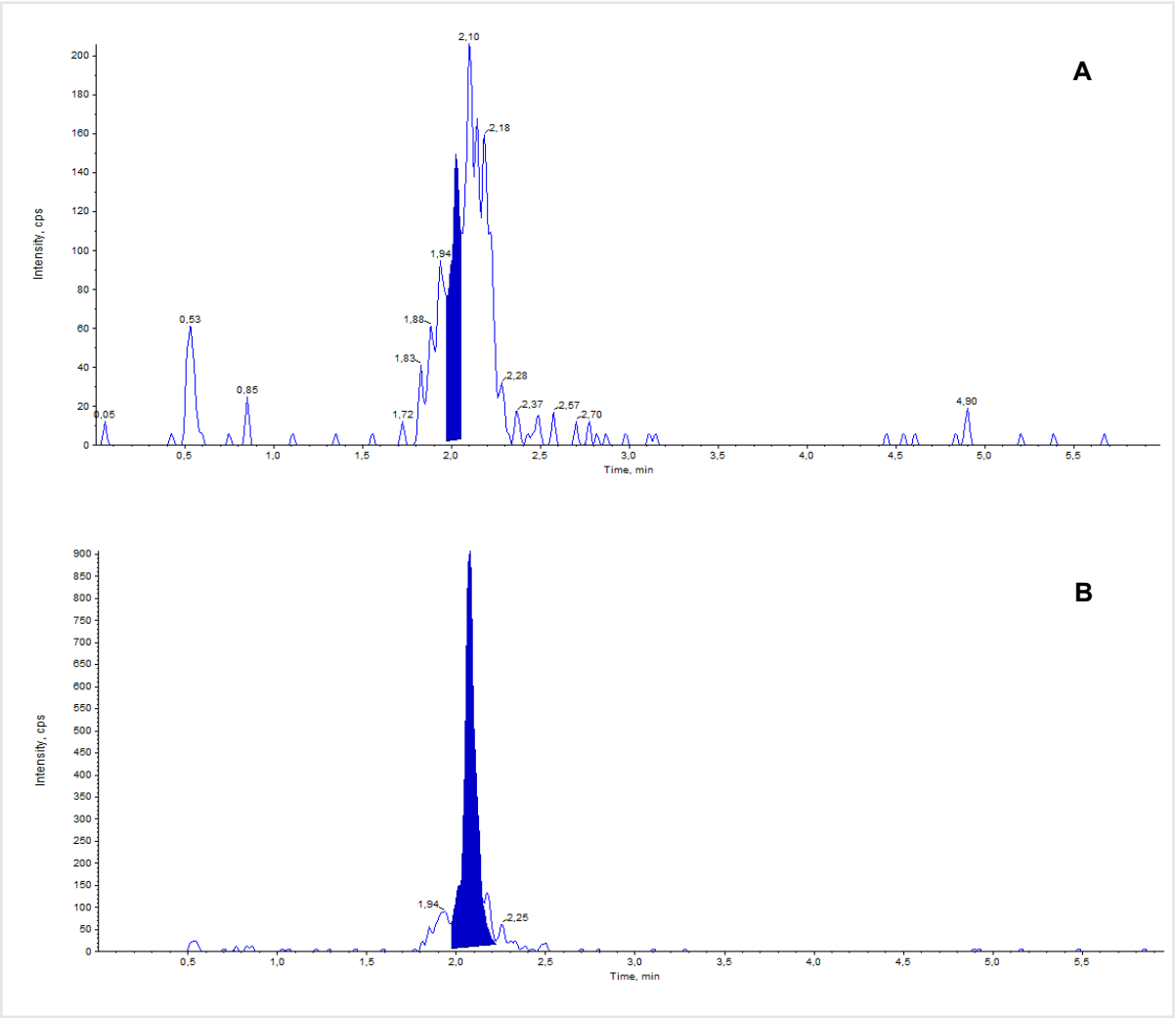

Figure 6.8. Representative chromatograms for s-Pep. *Plasma blank (A) and 150 µg/mL RTX in plasma (B), RT 2.1, S/N=8.*

This confirmed experimentally that, based on the S/N of a mid-range sample, the Sciex API-3200 was not sensitive enough to be used as an analytical instrument to investigate the clinically relevant analytical range. A more sensitive instrument was available in the laboratory in the form of a Shimadzu 8050 LC-MS/MS system. Because of the reproducibility of the extraction method, it was decided to continue with further investigations into the final development of this method on the more sensitive analytical system.

CHAPTER 7

DEVELOPING AN ANALYTICAL METHOD ON THE SHIMADZU 8050 LC-MS/MS SYSTEM

The Shimadzu Nexera X3 8050 LC-MS/MS system was proven to be an instrument of choice to quantify RTX in human plasma (80). Since such a system was available in our laboratory and since the Sciex API-3200 was found to be not sensitive enough for this purpose, it was decided to use the Shimadzu Nexera X3 8050 LC-MS/MS system.

7.1 INITIAL OPTIMISATION OF THE DETECTION METHOD

The optimisation of an analytical detection method on this system does not follow the same protocol as that of the Sciex API-3200 LC-MS/MS system. It is much more automated, and after entering the monoisotopic mass of the RTX signal peptide (s-Pep), a reference in 20% acetonitrile in water with 0.1% formic acid was injected through the chromatographic system and the most abundant product ion was selected as a quantifying transition. This information is summarised in Table 7.1 and entered as such into the detection method.

A final product ion mass spectrum was also provided (Figure 7.1), and from this it can be deduced that the most abundant product ion was that at m/z = 1180.6, representing the y11 fragment ion of s-Pep as also confirmed in the literature (80). In addition, as indicated in Figure 7.1, other product ions could be recognised and used to confirm the sequence of the s-Pep.

Table 7.1. *Parameter settings on the Shimadzu 8050 for the optimised detection method*

Interface settings	**Nebulizing Gas Flow (L/min)**	3
	Drying Gas Flow (L/min)	10
	Heating Gas Flow (L/min)	10
	Interface Temperature (°C)	300
	Desolvation Temperature (°C)	526
	DL Temperature (°C)	250
	Heat Block Temperature (°C)	400
	Drying Gas Flow (L/min)	10
	CID Gas (kPa)	17
MS/MS settings	**Protonated molecular ion mass (m/z) $[M+2H]^{2+}$**	1092.8
	Product ion mass monitored (m/z) $[M+H]^{+}$	1180.6
	Retention time (min)	2.23
	Dwell time (msec)	7
	Q1 Pre Bias (V)	-32
	Collision energy (eV)	-35
	Q3 Pre Bias (V)	-44

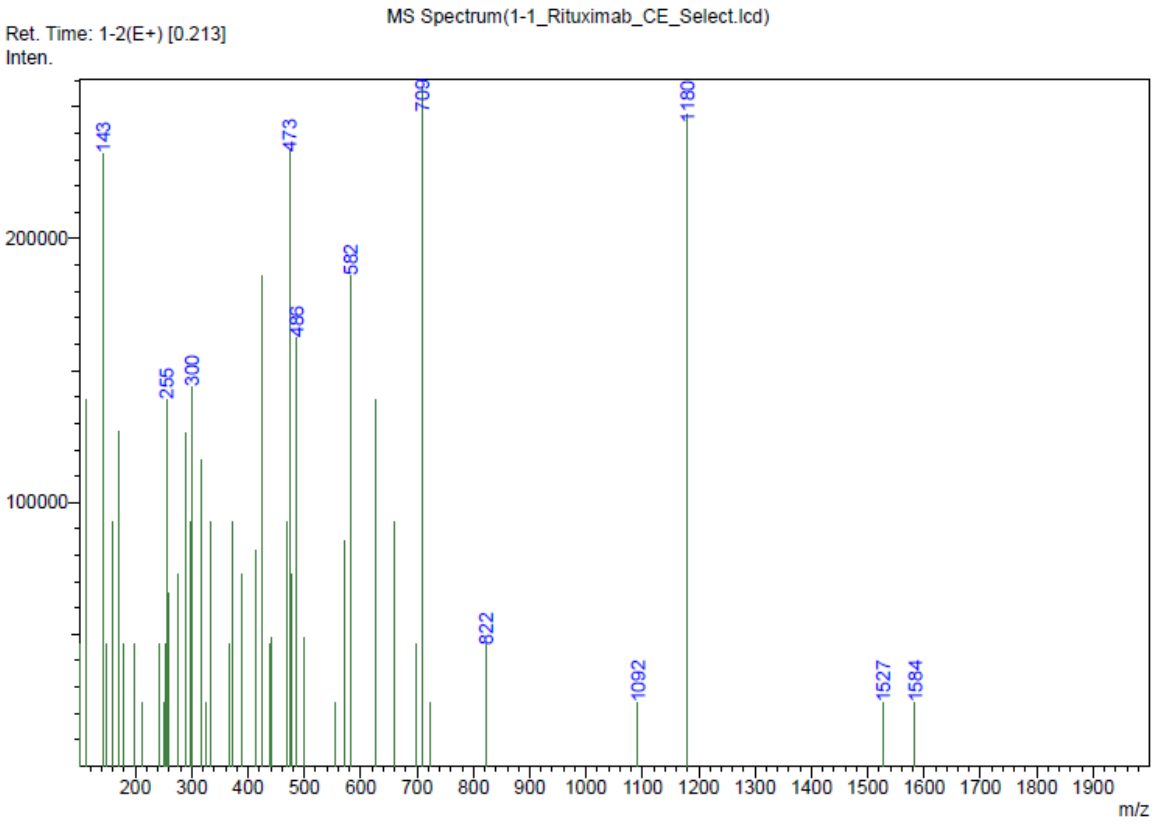

Figure 7.1. Representative product ion scan. *The following is a mass spectrum (product ion scan) of the RTX target peptide, showing the singly charged product ion at m/z = 1180.*

7.2 CHROMATOGRAPHY

The chromatography for the analysis of RTX in plasma has already been optimised using the Sciex API-3200 LC-MS/MS system, as described in Chapter 4. Therefore, the same chromatographic parameters were used for analysis using the Nexera X3 Shimadzu 8050 LC-MS/MS system. These are summarised in Table 7.2. Chromatograms of analysis of the s-Pep on this system are indicated in Figure 7.2.

Table 7.2. *Instrument and chromatographic conditions for the determination of RTX*

<table>
<tr><td>Analytical column</td><td>Agilent Poroshell 120 C18, 2.1 x 50 mm 2.7-Micron</td></tr>
<tr><td>Column temperature</td><td>~50ºC</td></tr>
<tr><td>Mobile phase and gradient elution</td><td>Mobile phase A: water: formic acid: DMSO (97.9:0.1:2, v/v/v)
Mobile phase B: acetonitrile: formic acid: DMSO (97.9:0.1:2, v/v/v)
<table>
<tr><th>Time (min)</th><th>Mobile phase A (%)</th><th>Mobile phase B (%)</th><th>Flow rate (µL/min)</th></tr>
<tr><td>0.01</td><td>95</td><td>5</td><td>300</td></tr>
<tr><td>0.75</td><td>95</td><td>5</td><td>300</td></tr>
<tr><td>2.50</td><td>5</td><td>95</td><td>300</td></tr>
<tr><td>3.50</td><td>5</td><td>95</td><td>300</td></tr>
<tr><td>4.00</td><td>95</td><td>5</td><td>300</td></tr>
<tr><td>5.90</td><td>95</td><td>5</td><td>300</td></tr>
<tr><td>6.00</td><td>95</td><td>5</td><td>300</td></tr>
</table>
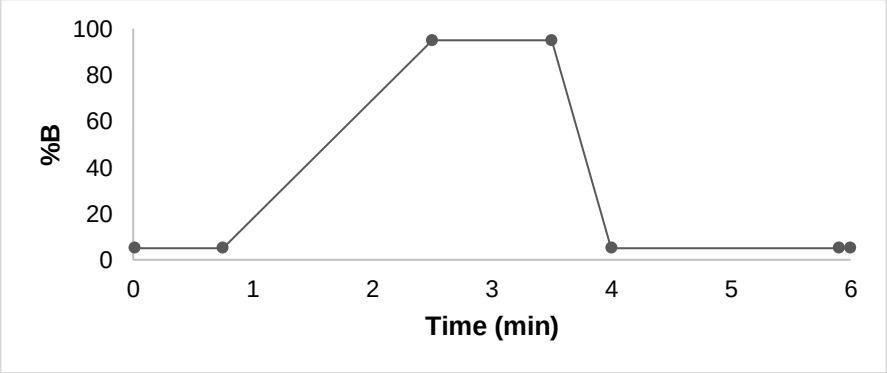
</td></tr>
</table>

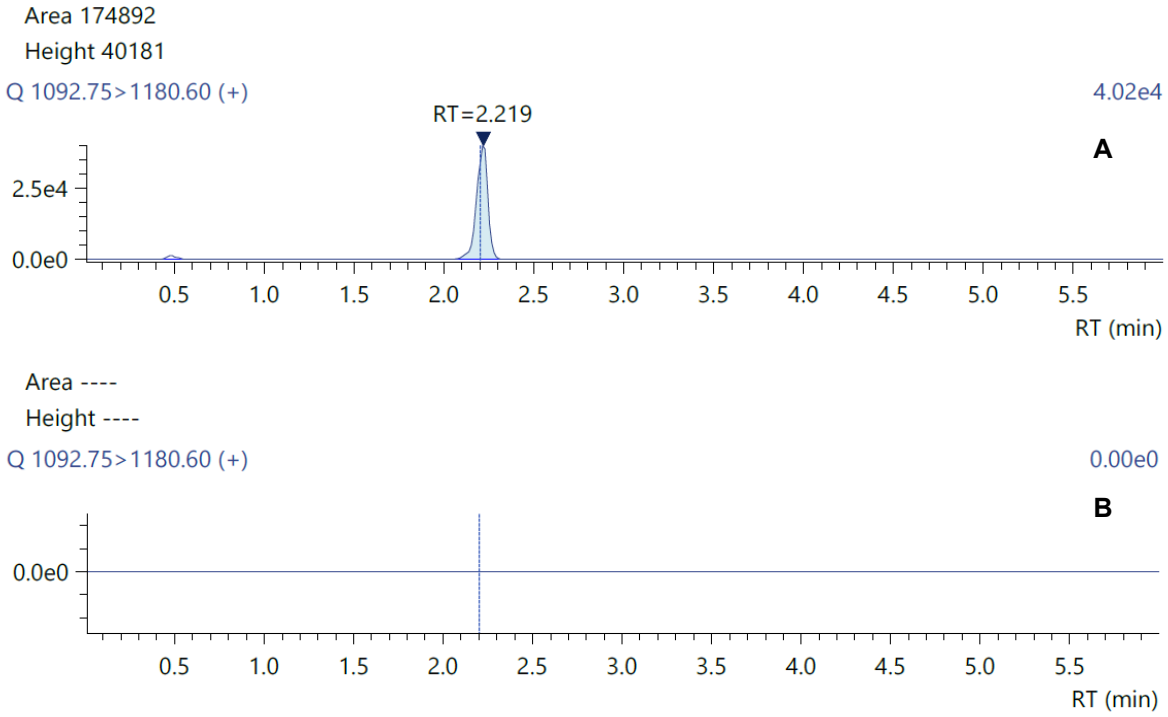

Figure 7.2. Representative chromatogram for RTX. Panel A: *extracted RTX in plasma,* ***Panel B****: blank plasma. 1092.8/1180.6, RT 2.2 min.*

7.3 APPLYING THE SHIMADZU AS AN ANALYTICAL INSTRUMENT

The initial optimisation of the analytical method was performed using the s-Pep on the Sciex API-3200, and with this optimised detection method affinity binding purification, digestion and SPE were fully developed. The application of the Shimadzu 8050 was therefore investigated using the fully developed method with RTX IgG as the reference material and not the s-Pep as was done for initial optimisation.

Calibration standards were prepared by dilution of the RTX stock solution in plasma, resulting in a concentration range of 12.5–300 µg/mL. The developed sample preparation procedure was applied, and the final s-Pep extracts were analysed in duplicate on the Shimadzu 8050. The resultant calibration curve is depicted in Figure 7.3 – indicating linearity throughout the measured range.

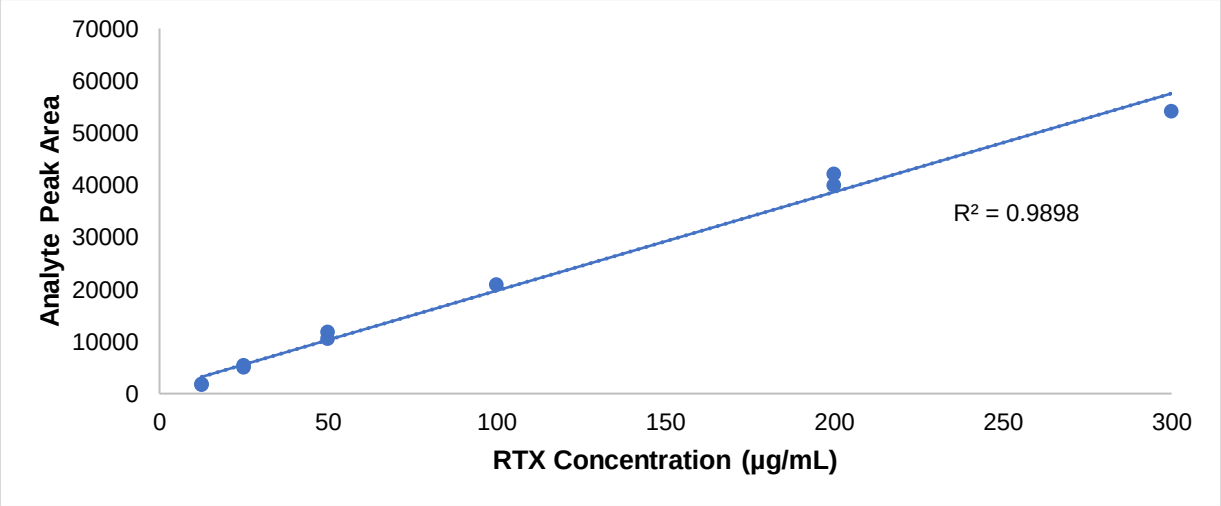

Figure 7.3. Representative calibration curve for RTX. *Linear regression for RTX concentration (µg/mL) plotted against analyte peak area, $R^2 = 0.990$.*

The lowest concentration measurable using the Sciex API-3200 was 150 µg/mL RTX in plasma. The RTX concentration range depicted in Figure 7.3 represents the intended analytical range for this project, confirming that the Shimadzu 8050 is sensitive enough. In addition, this instrument can now be used for a final investigation in which the lowest RTX concentration may be included.

An investigation into the volume of RTX in plasma to be added during the affinity binding purification (sample loading volume) was considered to be important because the volume of plasma may influence the binding of the RTX to the available protein A binding sites on the beads. The more plasma that is added, the more endogenous IgG there is present to potentially compete with the RTX. This investigation was therefore performed using the Shimadzu 8050 LC-MS/MS system.

7.3.1 Investigating the sample loading volume

Introduction

To investigate the sample loading volume, low (12.5 µg/mL) and mid-range (100 µg/mL) concentrations of RTX in plasma were used. For both concentrations, 50 µL and 100 µL volumes were added to the

protein A beads during the affinity binding purification procedure. This was followed by the subsequent sample preparation procedures including trypsin digestion and SPE as described in Chapter 5.

Methodology

The RTX stock solution (10 mg/mL) was diluted to 100 µg/mL and 12.5 µg/mL with plasma. Duplicate volumes of 50 µL and 100 µL of each concentration were added to the same volume of protein A (200 µL slurry). Duplicates of the same volumes of blank plasma were also added, representing blank controls.

The complete sample preparation procedure was followed for these samples and the final extracts analysed on the Shimadzu 8050, as summarised in the schematic representation in Figure 7.4.

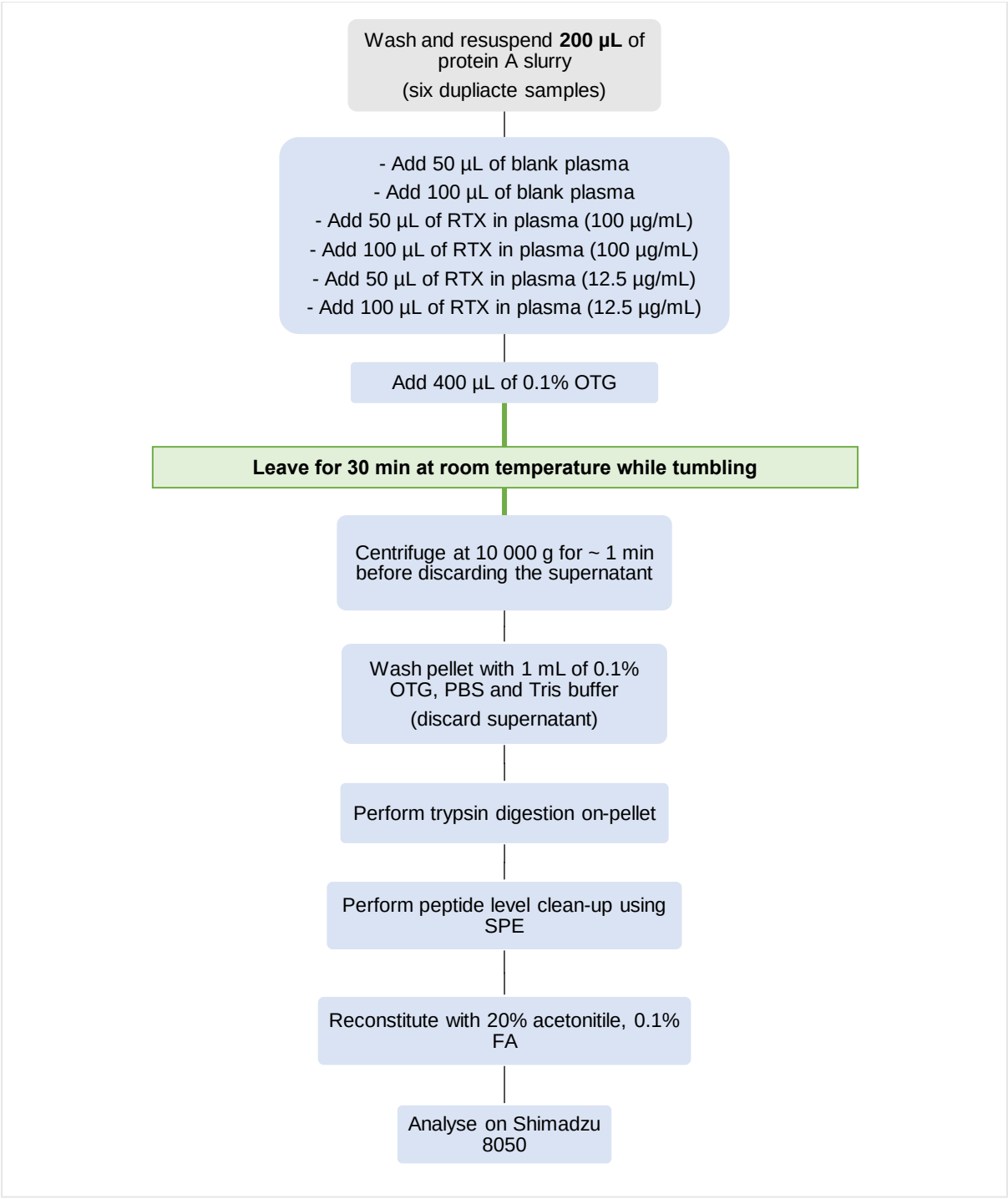

Figure 7.4. Method description. *Basic flow diagram illustrating how the sample loading volume was explored.*

Results and Discussion

The analytical results in terms of analyte peak areas are represented in Figure 7.5.

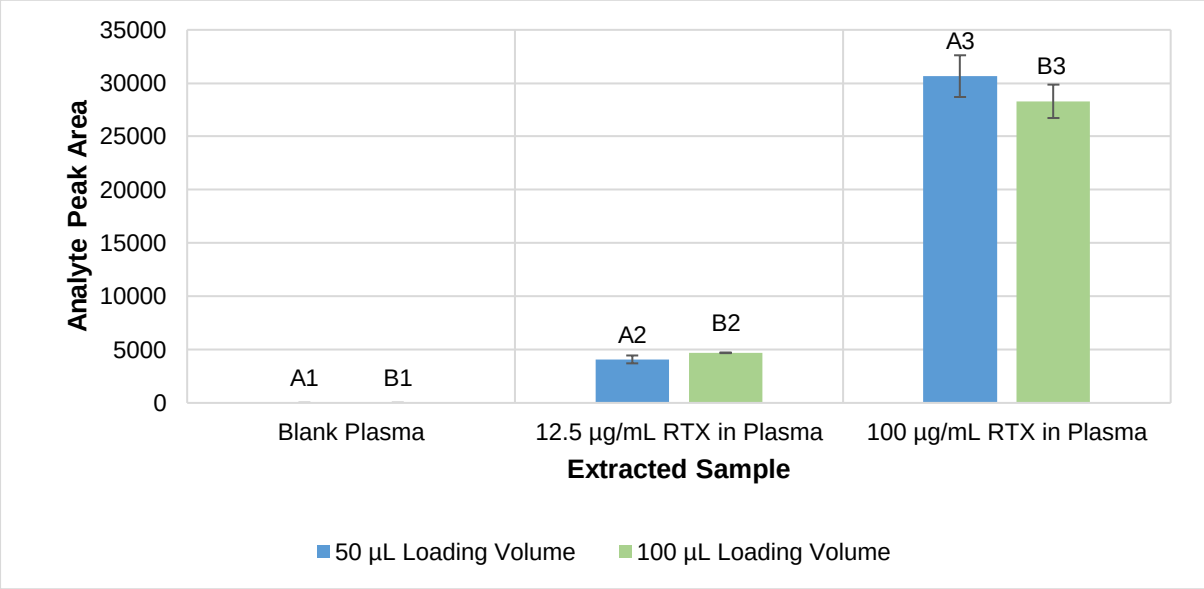

Figure 7.5. Amount of s-Pep recovered from different sample loading volumes. *A mid-range and low-level concentration of RTX was explored by adding 50 or 100 µL to the sample preparation procedure. Error bars represent standard deviation, N=2.*

As seen in Figure 7.5, when 50 (A1–3) or 100 µL (B1–3) of sample was loaded onto the protein A beads, no significant difference was observed at the low-level and mid-range RTX concentration extracted in plasma. When 12.5 µg/mL of RTX was extracted in plasma, a resultant peak area of 4082 and 4702 was observed for the 50 µL (A2) and 100 µL (B2) loading volumes, respectively. For the 100 µg/mL RTX sample, a peak area of 30659 and 28296 was observed for the 50 µL (A3) and 100 µL (B3) loading volumes, respectively. As shown by A1 and B1, no analyte was observed when blank plasma was extracted.

Increasing the volume of plasma present during the affinity binding purification procedure from 50 µL to 100 µL did not make any significant difference to the capacity of protein A for binding RTX. This was proven at the lowest concentration of RTX intended for this project. Considering that this method is developed to measure RTX in subject samples, the fact that 50 µL can be applied to sample preparation resulting in the same sensitivity as 100 µL is a significant advantage. The scarcity of plasma when performing clinical studies can be a limiting factor when higher volumes are needed for analytical purposes.

7.4 FINAL METHOD

The final LC-MS/MS assay is presented in this section.

An LC-MS/MS method for the quantification of RTX in human plasma has been developed. The extraction process involves affinity binding purification using protein A Agarose beads, followed by on-

bead tryptic digestion and peptide-level clean-up using SPE. The affinity binding purification step allows for selectively binding and retaining the protein target while removing other matrix components. Trypsin protease is then used to digest the protein into smaller quantifiable peptides. This process generates a large number of peptides, including the signature peptide target (s-Pep). Solid phase extraction allows for selective sample clean-up and also acts as a concentration step as the signature peptide makes up only a small portion of the total RTX protein.

7.4.1 Affinity binding purification

- Briefly vortex the protein A suspension at maximum speed for ~10 seconds.
- Transfer 200 µL of protein A suspension to individual low-bind 1.5 mL microcentrifuge tubes.
- Centrifuge the low-bind 1.5 mL microcentrifuge tubes at ~10 000 g for ~1 minute in order for the protein A beads to form a pellet.
- Discard the supernatant.
- Wash the protein A beads with 1 mL of PBS.
- Briefly vortex at maximum speed for ~10 seconds.
- Centrifuge the low-bind tubes at ~10 000 g for ~1 minute in order for the protein A beads to form a pellet.
- Discard the supernatant.
- Wash the protein A beads again with 1 mL of PBS.
- Briefly vortex at maximum speed for ~10 seconds.
- Centrifuge the low-bind tubes at ~10 000 g for ~1 minute in order for the protein A beads to form a pellet.
- Discard the supernatant.
- Add 100 µL of PBS to reconstitute the protein A beads.
- Add 400 µL of 0.1% OTG solution (see Section 3.4) – prevents non-specific binding.
- Add 50 µL of the sample to be analysed.
- Briefly vortex at maximum speed for ~10 seconds.
- Leave the samples for ~1 hour at room temperature while tumbling on the Tube Revolver Rotator.
- Centrifuge the low-bind tubes at ~10 000 g for ~1 minute in order for the protein A beads to form a pellet.
- Discard the supernatant.
- Wash the protein A beads with 1 mL of 0.1% OTG solution.
- Briefly vortex at maximum speed for ~10 seconds.
- Centrifuge the low-bind tubes at ~10 000 g for ~1 minute in order for the protein A beads to form a pellet.
- Discard the supernatant.
- Wash the protein A beads with 1 mL PBS.
- Briefly vortex at maximum speed for ~10 seconds.

- Centrifuge the low-bind tubes at ~10 000 g for ~1 minute in order for the protein A beads to form a pellet.
- Discard the supernatant.
- Wash the protein A beads with 1 mL of 25 mM Tris-HCl buffer (see Section 3.4).
- Briefly vortex at maximum speed for ~10 seconds.
- Centrifuge the low-bind tubes at ~10 000 g for ~1 minute in order for the protein A beads to form a pellet.
- Discard the supernatant.

7.4.2 Trypsin digestion

- Add 358 µL of the 7 µg/mL trypsin working solution (see Section 3.4) to each sample.
- Add 35 µL of 100% acetonitrile.
- Briefly vortex at maximum speed for ~10 seconds.
- Leave the samples overnight (at least 16 hours) at room temperature while tumbling.
- Centrifuge the low-bind tubes at ~10 000 g for ~1 minute in order for the protein A beads to form a pellet.
- Add 5 µL of the 1 µg/µL reconstituted trypsin solution (see Section 3.4).
- Briefly vortex at maximum speed for ~10 seconds.
- Leave the samples at room temperature for a further ~ 3 hours while tumbling.
- Centrifuge the low-bind tubes at ~10 000 g for ~1 minute in order for the protein A beads to form a pellet.
- Quench the digestion reaction by the addition of 20 µL of 10% formic acid.
- Briefly vortex at maximum speed for ~10 seconds.
- Centrifuge the low-bind tubes at ~10 000 g for ~1 minute in order for the protein A beads to form a pellet.

7.4.3 Solid phase extraction

- Condition the Strata-X SPE columns three times with 1 mL of methanol.
- Equilibrate with 1 mL of water.
- Equilibrate further with 1 mL of 0.1% formic acid in water.
- Add 380 µL of the supernatant from each sample (the protein A pellet is discarded).
- Add 380 µL of 0.1% formic acid in water.
- Wash twice with 1 mL of water.
- Wash with 100 µL of 10% acetonitrile in water.
- Elute with 200 µL of 70% acetonitrile in water with 1% formic acid into 5 mL borosilicate glass tubes.
- Dry down under a steady flow of nitrogen gas at ~37°C for ~30 minutes.
- Reconstitute in 120 µL injection solvent and vortex for ~30 seconds.
- Transfer 100 µL to a clean 96-well plate for LC-MS/MS analysis.
- Inject 10 µL onto the column.

7.4.4 Special precautions

7.4.4.1 Materials

The extraction is to be performed on-bench at room temperature with low-bind bind plastics (low-bind microcentrifuge tubes and low-bind pipette tips).

7.4.4.2 Stability of analyte in matrix

There were no major concerns with regards to the stability of the analyte in matrix and thus stability was not tested for this project. Iwamoto *et al*., reported short-term stability of the analyte in plasma for 4 hours at room temperature and long-term stability in plasma for 20 days at -20°C (80). It was also reported that the analyte was stable for five freeze-thaw cycles at -20°C and -80°C with at least 24 hours of frozen time (80).

7.4.4.3 Sample preparation considerations

The whole blood is centrifuged at room temperature within 2 hours of collection at 1500–2000 g for 10 minutes to obtain plasma. Immediately after centrifugation, plasma is removed from cells and transferred to a screw-cap cryovial. The samples are frozen at approximately -80°C in a laboratory freezer within 2 hours of collection.

CHAPTER 8

INTERNAL STANDARD INVESTIGATION

8.1 INVESTIGATION 1: EXPLORING THE SUITABILITY OF DIFFERENT INTERNAL STANDARDS BASED ON REPEATABILITY

In this investigation, three different internal standards (ISTDs) were assessed by adding them to different concentrations of RTX standards at different points during the sample preparation procedure. These ISTDs included purified horse immunoglobulin G (horse IgG), stable-isotope labelled RTX monoclonal antibody (SIL-RTX), and stable-isotope labelled RTX signature peptide (SIL-s-Pep). The three ISTDs were investigated separately and compared for efficacy to compensate for any variation in the measurement of s-Pep throughout sample preparation and detection.

A schematic representation of the protein, and peptide ISTDs and at which step in the sequence of sample preparation they are introduced, is depicted in Figure 8.1.

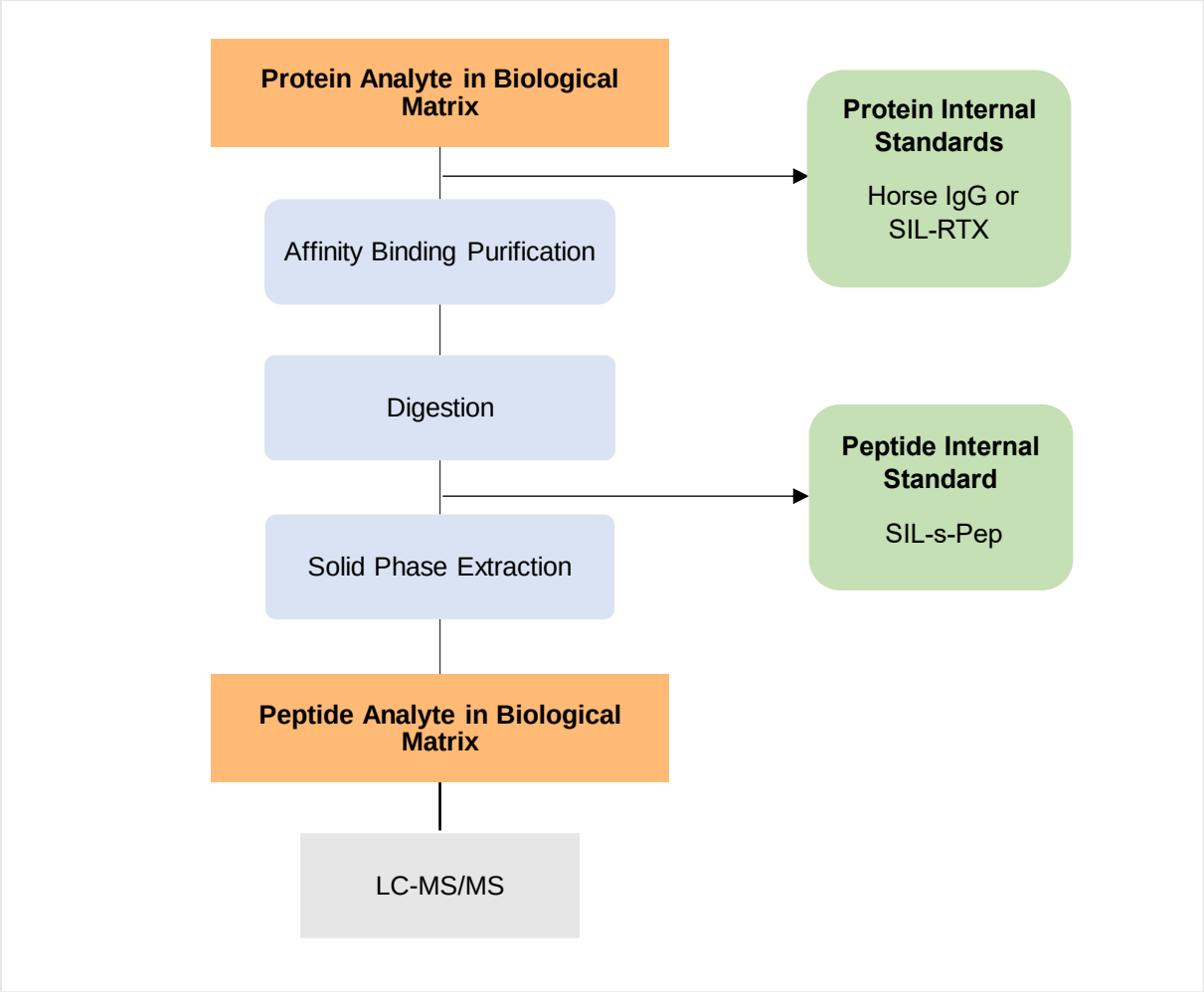

***Figure 8.1. The addition of ISTDs during sample preparation**. Schematic representation of the different workflows and internal standardisation possibilities, and where in the sample preparation procedure they are introduced. Protein ISTDs are introduced prior to affinity binding purification, with the analyte to be detected. Peptide ISTDs are introduced after digestion, prior to solid phase extraction.*

Three RTX standards were prepared by dilution in plasma to concentrations of 300 µg/mL, 100 µg/mL, and 12.5 µg/mL, covering the expected analytical range under normal therapeutic conditions (66). Each standard was prepared in six-fold.

The analytical method used for sample preparation and quantification of RTX was described in Chapter 7. In addition to the parameters used to determine and quantify the signal peptide representing RTX (s-Pep), instrument parameters were introduced to detect and measure the intensities of the different ISTDs tested.

Testing Method Principle: Outlier Test

The efficacy of each ISTD was assessed by testing its ability to compensate for variability during the extraction process. Although three different molecules were assessed, the principle applied to all was the same and was based on a statistical repeatability evaluation.

The LC-MS/MS signal intensities of the standards at different concentrations were expressed in terms of the ratios of the chromatographic peak areas of the standards and the ISTDs used (analyte/ISTD).

The peak area ratios of the six repeats of each concentration were used to assess repeatability by testing for significant outliers using the GraphPad outlier calculator (141). This calculator performs a Grubbs test to determine whether the most extreme value in the data set is a significant outlier from the rest. It is based on a normal distribution and a test statistic (Z) calculated from the most extreme data point. The test statistic corresponds to a p-value representing the likelihood of detecting an outlier assuming the underlying data is Gaussian or of normal distribution.

$$z = \frac{|\ \text{mean} - \text{value}\ |}{\text{SD}}$$

The significance level (alpha), where an outlier will be detected, was selected as p=0.05. The P value is interpreted as in normality testing: If the P value corresponding to Z is less than the alpha value chosen (0.05), it is considered a significant outlier. If the P value is greater than alpha, the test concludes there is no evidence of an outlier in the dataset. The entire dataset is used to calculate the mean and standard deviation for the test.

If an outlier was identified in the dataset, it was excluded. An average peak area ratio was calculated for the six repeats and the variation was expressed as a percentage coefficient of variation (%CV). The threshold for acceptance of imprecision was 20%. If the CV(%) was found to be higher than 20% it was decided that the ISTD was an inadequate internal measure to compensate for the variation of the extraction procedure.

8.1.1 Experiment 1: Surrogate ISTD (Horse IgG)

Introduction

Purified horse IgG was used as a surrogate ISTD because of its similar tertiary structure, species-specific peptides, and relatively low cost compared to synthetically derived proteins. The species-specific and unique signature peptide, – VNNQALPQPIER (p-VNN), the structure of which is depicted in Figure 8.2, was selected to represent total horse IgG.

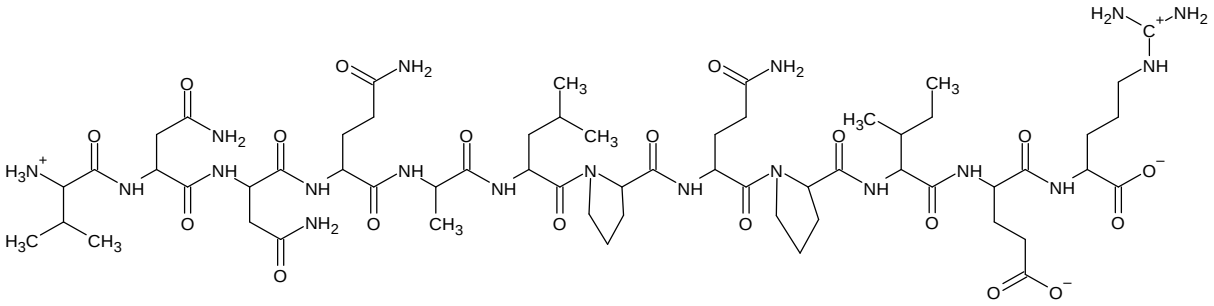

Figure 8.2. Structure of the signature peptide for horse IgG (p-VNN). *Monoisotopic mass: 1377.734 Da.*

Methodology

Once the signature peptide (p-VNN) was selected, a proteomics toolkit was used to predict the possible fragment ions as indicated in Figure 8.3 (refer back to Figure 4.4 as an indication of the expected fragmentation mechanisms of peptides) (142).

	Mass	
	Mono	Avg
(M)	1377.73650	1378.55101
$(M+2H)^{2+}$	689.87555	690.28280

Seq	#	B	Y	# (+1)
V	1	100.07574	1378.74378	12
N	2	214.11866	1279.67537	11
N	3	328.16159	1165.63244	10
Q	4	456.22017	1051.58951	9
A	5	527.25728	923.53093	8
L	6	640.34134	852.49382	7
P	7	737.39411	739.40976	6 ←
Q	8	865.45268	642.35699	5
P	9	962.50545	514.29842	4 ←
I	10	1075.58951	417.24565	3
E	11	1204.63210	304.16159	2
R	12	1360.73322	175.11900	1

Figure 8.3. Fragment ion calculator results for horse IgG. *Sequence: VNNQALPQPIER. Fragment ion table (monoisotopic) and mass/charge table directly copied directly from the Fragment Ion Calculator* (142).

According to Willrich *et al*., the fragments of the doubly charged precursor ion at m/z $(M+2H)^{2+}$ = 689.9, indicated by the arrows in Figure 8.3, were used for detection (28). Using the Shimadzu 8050 LC-MS/MS system, the transition 689.9/739.4 was detected and the signal was optimised in terms of gas settings, capillary voltage, declustering potential, and collision energy.

The s-Pep representing RTX was analysed using the same detection method and parameters that were described in Chapter 7.

The horse IgG stock solution is provided in PBS containing 0.09% sodium azide (NaN_3). The approximate IgG concentration is 1 mg/mL. On the day of extraction, the stock solution was diluted to 100 µg/mL with PBS.

To investigate this ISTD, a volume of 100 µL of 100 µg/mL horse IgG was added at the same time as the analyte during affinity binding purification, prior to digestion, as outlined in Section 7.4 and as indicated in Figure 8.1.

Results and Discussion

A chromatogram indicating the analyte and the ISTD is depicted in Figure 8.4. The RTX s-Pep and the representative peptide from the horse IgG ISTD elute at 2.2 and 2.1 minutes respectively. Therefore, although not coeluting, the respective retention times are considered close enough such that the ISTD should compensate for the s-Pep.

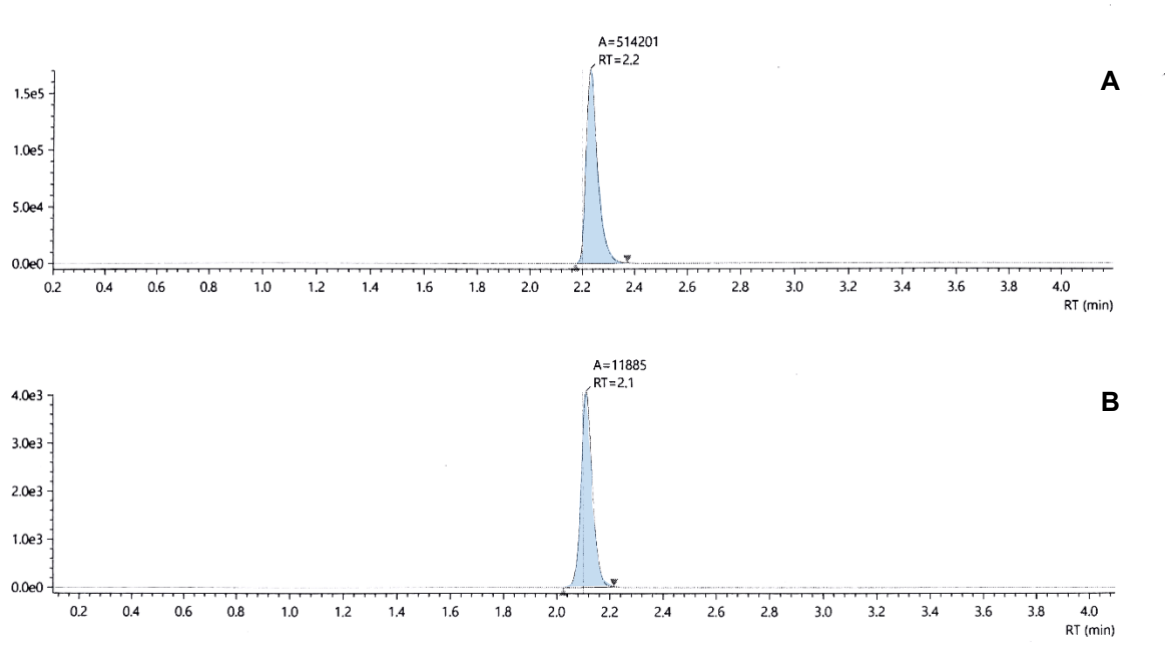

***Figure 8.4. Chromatogram of the RTX standard sample (300 µg/mL) with ISTD**. **A:** analyte channel 1092.75/1180.6, RT 2.2 min, Area 514201. **B:** ISTD channel 689.9/739.4, RT 2.1 min, Area 11885.*

The analytical results, expressed as peak area ratios, are summarised in Figure 8.5. The arrows indicate definite outliers in both the high and low RTX concentration samples. In Table 8.1, the CV(%) are expressed including and excluding the outliers for comparison.

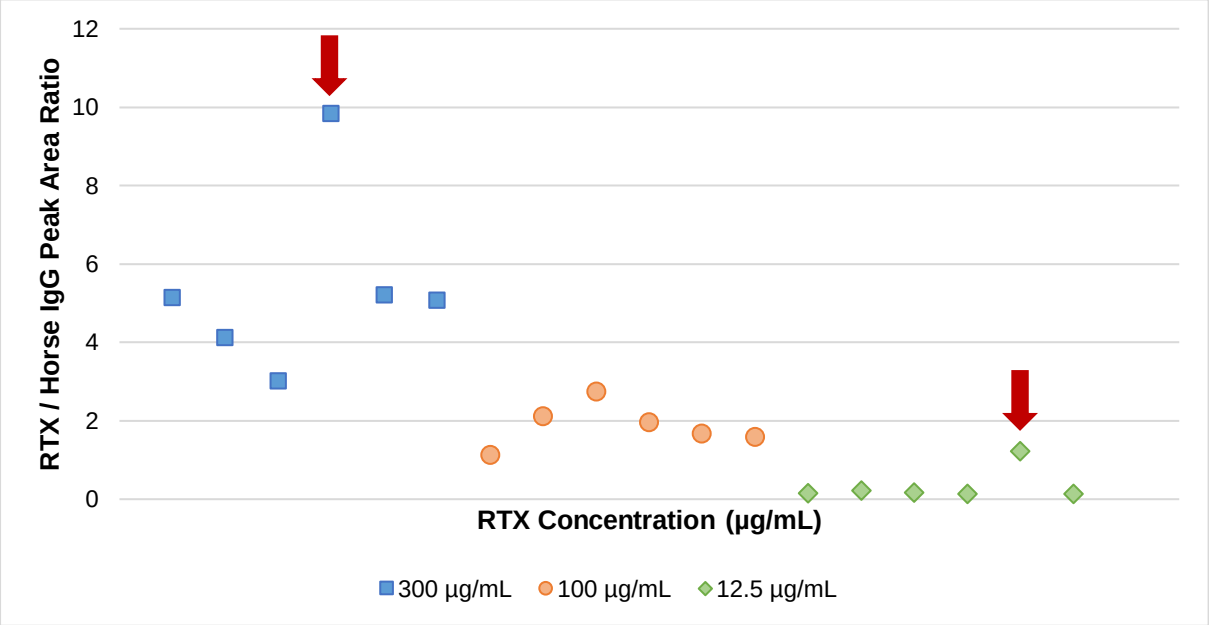

Figure 8.5. Peak area ratio plot (RTX / horse IgG) for the three calibration standards investigated (N=6). *Arrows indicate significant outliers, as per the Grubbs outlier test.*

Table 8.1. *Summary of the results of the Grubbs outlier test and the calculated coefficient of variation for the three RTX calibration standards when the ISTD horse IgG was employed (when significant outliers are present and excluded, a new coefficient of variation is calculated for comparison)*

RTX concentration	**300 µg/mL**		**100 µg/mL**	**12.5 µg/mL**	
Significant outliers present	Yes		No	Yes	
	Including outliers	Excluding outliers		Including outliers	Excluding outliers
Number of samples	N=6	N=5	N=6	N=6	N=5
Average peak area ratio	5.39	4.51	1.86	0.342	0.165
Standard deviation	2.33	0.944	0.550	0.435	0.0386
CV(%)	43.2%	20.9%	29.6%	127.1%	23.4%
Pass (<20%) Fail (>20%)	Fail	Fail	Fail	Fail	Fail

The threshold for acceptance of imprecision was 20% CV. The average CV(%) of the peak area ratio for the s-Pep in the presence of horse IgG as the ISTD was found to be 24.6% (±4.5%), excluding the

outliers. It was therefore concluded that the surrogate ISTD did not compensate sufficiently for extraction variability when quantifying RTX.

A possible reason for this inefficiency may be that the affinity binding of the two IgG molecules is not the same for protein A. Protein G is an alternative protein expressed in *Streptococcal* bacteria that has a high affinity for the Fc region of IgG. Each antibody-binding protein varies in its ability to bind to antibodies of different subtypes and species. Table 8.2 compares the relative binding strengths of protein A, protein G, and a combination of protein A and G (protein A/G) to different immunoglobulins. This information has been compiled from various publications (115,143,144). Binding strengths can be used as guidelines to predict the binding behaviour of different antibodies to protein A and protein G.

Table 8.2. *Antibody binding properties of protein A, protein G, and protein A/G by antibody species and subtype*

Species	Subclass	Protein A binding	Protein G binding	Protein A/G binding
Human	Total IgG	+++	+++	+++
	IgA1	+	-	+
	IgA2	+	-	+
	IgD	-	-	-
	IgG1	+++	+++	+++
	IgG2	+++	+++	+++
	IgG3	+	+++	+++
	IgG4	+++	+++	+++
	IgM	+	-	+
	Fab	+	+	+
Horse	Total IgG	+	+++	+++

Key: +++ = strong binding, ++ = medium binding, + = weak binding, - = no binding

While the binding affinity of human IgG is classified as “strong binding” for protein A, protein G, and protein A/G, horse IgG is reported to have a “weak binding” affinity to protein A and a “strong binding” affinity to protein G and protein A/G. Therefore, one may consider using protein G or protein A/G when using horse IgG as an ISTD for future work on the extraction of RTX.

A bioanalytical method should not, however, be altered to accommodate an ISTD, especially if the assay is sensitive and reproducible without the addition of an ISTD. No additional work on the use of horse IgG as an ISTD was therefore performed, and the use of the other two ISTDs was investigated.

8.1.2 Experiment 2: Stable Isotope Labelled Protein ISTD (SIL-RTX)

Introduction

A more representative ISTD is the original protein containing stable isotope-labelled (SIL) amino acids (27,124–126). The commercially available SIL derivative of RTX (SIL-RTX) should effectively correct for variations from the beginning of sample processing to ionisation in the mass spectrometer (124,125). SIL-RTX is a recombinant SIL monoclonal antibody that incorporates [$^{13}C_6{}^{15}N_2$]-Arginine and [$^{13}C_6{}^{15}N_2$]-Lysine. The unique signature peptide QVQQPGAELVK($^{13}C_6{}^{15}N_2$)PGASVK($^{13}C_6{}^{15}N_2$) (p-QVQ) selected to represent the SIL-RTX as an ISTD (Figure 8.6) (145).

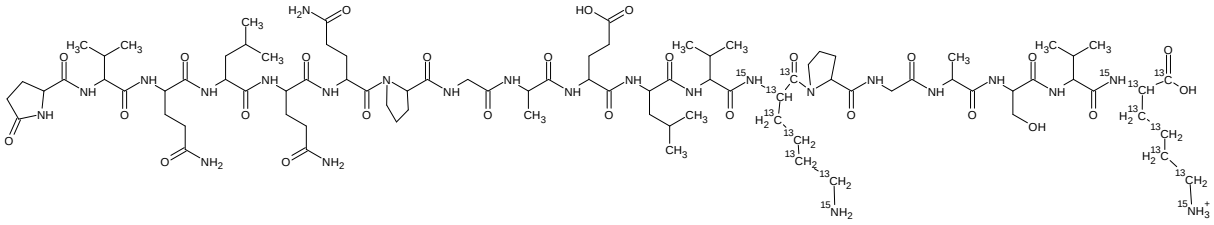

Figure 8.6. Structure of the signature peptide for SIL-RTX (p-QVQ). *Monoisotopic mass: 1976.1 Da.*

Methodology

The doubly charged protonated ion $[M+2H]^{2+}$ of p-QVQ (m/z = 988.5) produced a product ion at m/z = 1043.5 during collision-induced dissociation and this transition was used to detect the ISTD during LC-MS/MS analysis using the Shimadzu 8050. The signal was optimised in terms of gas settings, capillary voltage, declustering potential, and collision energy.

The s-Pep representing RTX was analysed using the same detection method and parameters that were used for Experiment 1.

The pure reference standard of SIL-RTX (100 µg lyophilised solid) was reconstituted with 500 µL of 0.1% formic acid to a final 50 µg/mL concentration. A volume of 35 µL of this reconstituted preparation was added during the affinity binding purification procedure with the different concentrations of RTX standards, similar to Experiment 1 (see Figure 8.1).

Following affinity binding purification, digestion, and SPE, the final extract was analysed and the resultant chromatogram indicating the analyte and the ISTD is depicted in Figure 8.7. The RTX s-Pep and p-QVQ coelute at 2.2 minutes, and therefore it can be expected that the ISTD will compensate for the s-Pep.

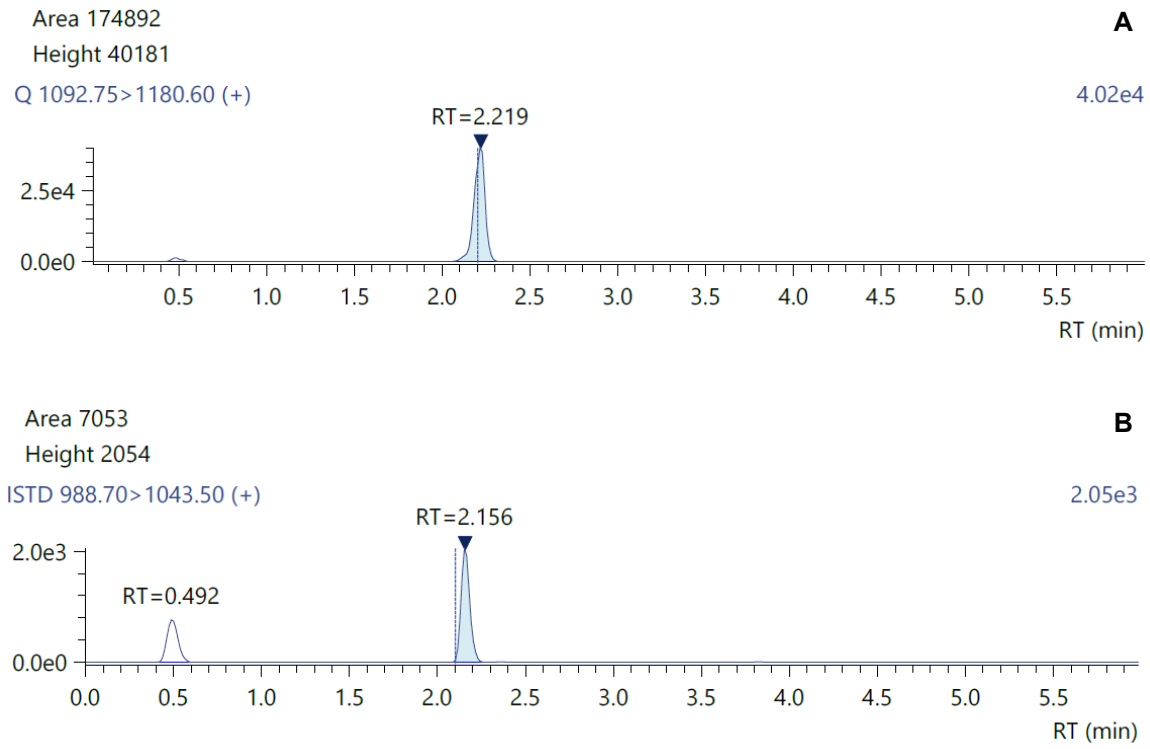

Figure 8.7. RTX Calibration standard sample (300 µg/mL). A: *analyte channel 1092.75/1180.6, RT 2.2 min, Area 174892.* ***B:*** *SIL-RTX ISTD channel 988.70/1043.50, RT 2.2 min, Area 7053.*

Results and Discussion

No outliers were indicated by applying the Grubbs test for any of the samples analysed. The analytical results expressed as peak area ratios and the repeatability (%CVs) are indicated in Table 8.3.

Table 8.3. *Summary of the results from the Grubbs outlier test and the calculated coefficient of variation for the three RTX calibration standards when the ISTD SIL-RTX was employed*

RTX concentration	**300 µg/mL**	**100 µg/mL**	**12.5 µg/mL**
Significant outliers present	No	No	No
Number of samples	6	6	6
Average peak area ratio	1.31	0.805	0.151
Standard deviation	0.212	0.113	0.0200
CV(%)	16.2%	14.0%	13.2%
Pass (<20%) Fail (>20%)	Pass	Pass	Pass

The average CV(%) of the peak area ratios across the three RTX concentrations tested was found to be 14.5% (±1.6%). Since the threshold for acceptance of repeatability is 20% CV, it was therefore concluded that the ISTD adequately compensated for any extraction variability when quantifying RTX. This substantiated the further use of SIL-RTX as an ISTD (see Investigation 2, Section 8.2).

8.1.3 Experiment 3: Stable Isotope Labelled Peptide ISTD (SIL-s-Pep)

Introduction

An alternative to SIL-proteins would be the use of an SIL version of the s-Pep as an ISTD to compensate for post-digestion sample preparation and analysis. For this workflow, the SIL-peptide (SIL-s-Pep) should therefore act as an ISTD to correct for variability during the SPE procedure and during chromatography and ionisation. Such an ISTD may suffice if the optimisation of affinity binding purification and digestion steps ensures adequate reproducibility.

For SIL-peptides, any one or a number of amino acids in the sequence can be replaced with the corresponding SIL amino acid. The SIL-peptide used in this investigation contained a labelled [$^{13}C_6{}^{15}N_2$]-Lysine, as indicated in Figure 8.8.

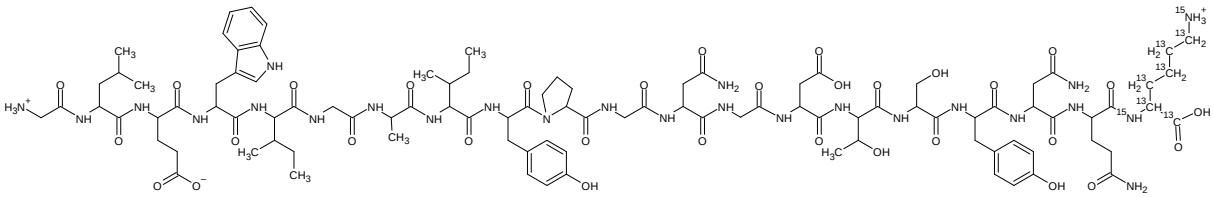

Figure 8.8. Signature peptide structure for SIL-s-Pep, GLEWIGAIYPGNGDTSYNQK($^{13}C_6{}^{15}N_2$). *Monoisotopic mass: 2191.055 Da.*

Methodology

The doubly charged protonated ion $[M+2H]^{2+}$ of SIL-s-Pep (m/z = 1096.4) produced a product ion at m/z = 727.4 during collision-induced dissociation, and this transition was used to detect the ISTD during LC-MS/MS analysis using the Shimadzu 8050. The signal was optimised in terms of gas settings, capillary voltage, declustering potential, and collision energy.

The s-Pep representing RTX was analysed using the same detection method and parameters used for Experiments 1 and 2 (Sections 8.1.1 and 8.1.2).

The ISTD stock solution is provided as 40 x 1 nM aliquots (200 µL of 5 pmol/µL in <5% acetonitrile/water). The ISTD was introduced into the sample preparation procedure at the point of termination of trypsinization (Section 7.4) (see Figure 8.1). Therefore, 20 µL of the SIL-s-Pep stock solution was directly spiked into the digestion mixture after quenching the trypsinization reaction.

Following affinity binding purification, digestion, and SPE, the final extract (with the ISTD now introduced prior to SPE) was analysed and the resultant chromatogram indicating the analyte and the ISTD is depicted in Figure 8.9. The RTX s-Pep and SIL-s-Pep coelute at 2.2 minutes.

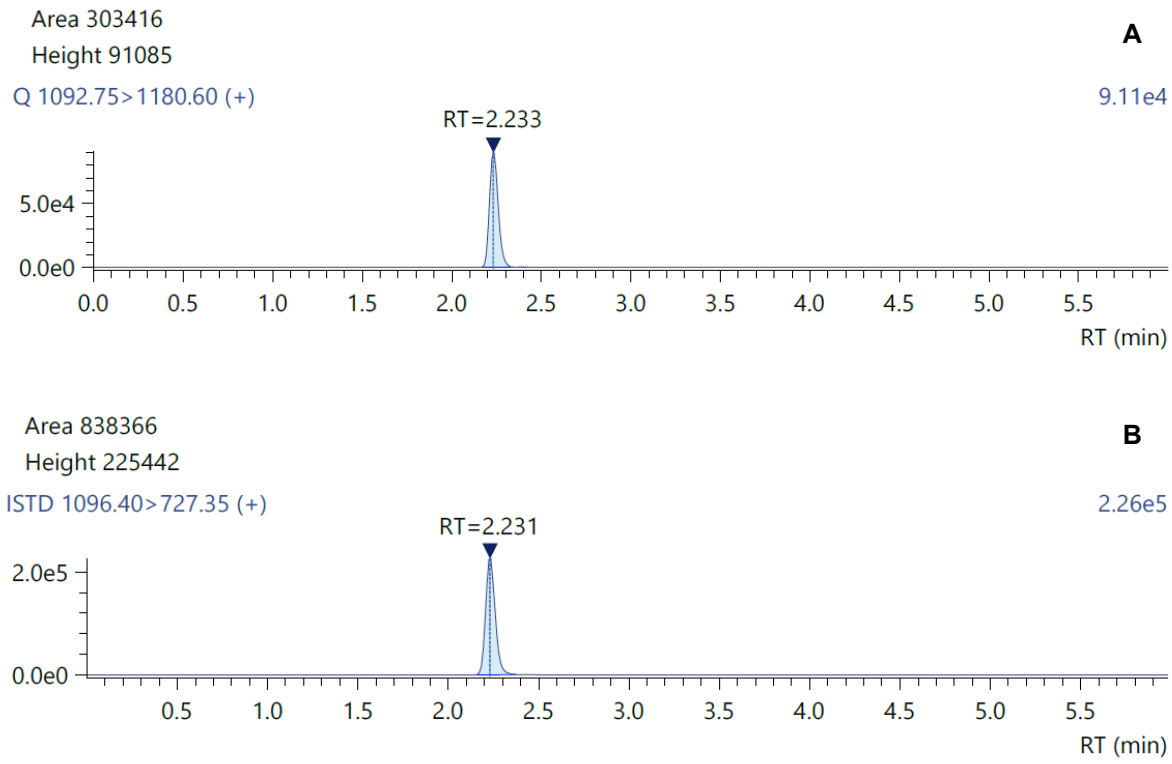

Figure 8.9. RTX calibration standard sample (300 µg/mL). A: *analyte channel 1092.75/1180.6, RT 2.2 min, Area 303416.* ***B:*** *SIL-s-Pep ISTD channel 1096.40/727.35, RT 2.2 min, Area 838366.*

Results and Discussion

No outliers were indicated by applying the Grubbs test for any of the samples analysed. The analytical results expressed as peak area ratios and the repeatability (%CVs) are indicated in Table 8.4.

Table 8.4. *Summary of the results from the Grubbs outlier test and the calculated coefficient of variation for the three RTX calibration standards when the ISTD SIL-s-Pep was employed*

RTX concentration	**300 µg/mL**	**100 µg/mL**	**12.5 µg/mL**
Significant outliers present	No	No	No
Number of samples	6	6	6
Average peak area ratio	0.397	0.181	0.0433
Standard deviation	0.0382	0.0113	0.00325
CV(%)	9.6%	6.2%	7.5%
Pass (<20%) Fail (>20%)	Pass	Pass	Pass

The average CV(%) of the peak area ratios across the three RTX concentrations tested was found to be 7.8% (±1.7%). Since the threshold for acceptance of repeatability is 20% CV, it was concluded that the SIL-s-Pep adequately compensated for any extraction variability when quantifying RTX. This substantiated the further use of SIL-s-Pep as an ISTD (see Investigation 2, Section 8.2).

Summary

The horse IgG, implemented as an ISTD, was found to inadequately compensate for variability in the extraction procedure while quantifying RTX. This is most probably because of a different binding affinity to protein A than to RTX. It was therefore discarded as a useful ISTD for the purpose of this project.

The SIL-RTX as an ISTD was found to adequately compensate for variability. Since SIL-RTX is processed similarly to RTX (affinity binding purification, digestion, and SPE), its compensation through the concentration range used in this investigation will be further explored using a relevant RTX calibration range.

When compared to SIL-RTX as an ISTD, the repeatability of the RTX analysis was better when using the SIL-s-Pep as the ISTD. Even though the SIL-s-Pep compensates only for variability during SPE, it is still considered to be a viable ISTD and will therefore also be included in further investigations using the relevant RTX calibration range.

8.2 INVESTIGATION 2: EXPLORING THE SUITABILITY OF DIFFERENT INTERNAL STANDARDS BASED ON ACCURACY

Introduction

In Investigation 1 (Section 8.1), three ISTDs were evaluated based on the measurement of the repeatability of the sample preparation procedure. Only three RTX concentrations across the expected analytical range were used for that purpose, and the assessments were based on peak area ratios. During this process, the horse IgG as an ISTD was eliminated because it was unable to compensate sufficiently for the measured RTX standards at all levels tested in order to pass the variability expectations. In Investigation 2, the compensation of the two remaining ISTDs, SIL-RTX and SIL-s-Pep, were tested by assessing the accuracy of RTX measurement over the analytical range. For this purpose, peak area ratios of RTX calibration standards and quality controls were converted to concentration of RTX and compared to nominal concentrations thereof. This was done in batches in which calibration standards and quality control samples were analysed with and without the ISTDs. The influence of the ISTDs on the accuracy measurement was therefore an indication of the efficacy of the ISTD by applying known acceptance criteria for accuracy. According to the criteria, a decision could be made on whether the ISTD was acceptable for future use.

A concentration value within 15% of the nominal concentration was considered as a guide for acceptable accuracy, except for the LLOQ, for which 20% of the nominal value will be acceptable. If at least 75% of the total calibration standards and quality controls were within 15% of the nominal concentration, the ISTD was considered to be acceptable for use. Duplicate standards were analysed at each calibration point. These standards were used to define the calibration equation. If one of the duplicate points were found to be outside of 15% of the nominal concentration, the data point would be excluded, allowing a single standard to be used.

Methodology

Solution preparation

1. *Analyte stock solution*

Calibration standards and quality control samples were prepared directly from the 10 mg/mL RTX stock solution by performing serial dilutions in human plasma (See Tables 8.5 and 8.6).

2. *Preparation of RTX calibration standards*

The 10 mg/mL RTX stock solution was used to prepare the highest calibration standard (S1) in blank plasma at room temperature. S1 was then used to prepare S2 to S6 by serial dilution with blank plasma to obtain desired concentrations of RTX as shown in Table 8.5. Calibration standards were prepared fresh on the day of extraction to allow for duplicate extractions during sample analysis.

Table 8.5. *Preparation of RTX calibration standards*

Calibration standard	Volume of blank plasma (µL)	Volume of RTX spiked (µL)	Dilution source	Dilution source volume (µL)	Total volume of dilution (µL)	RTX concentration in plasma (µg/mL)
S1 – ULOQ	485	15.0			500	300
S2	100		*S1*	200	300	200
S3	150		*S2*	150	300	100
S4	150		*S3*	150	300	50.0
S5	150		*S4*	150	300	25.0
S6 – LLOQ	150		*S5*	150	300	12.5

3. *Preparation of RTX quality controls*

The 10 mg/mL RTX stock solution was used to prepare the highest quality control sample (QCH) in blank plasma at room temperature. QCH was then used to prepare QCM, system suitability (SYS) samples, QCL, and QCLLOQ by serial dilution with blank plasma to obtain the desired concentrations of RTX – as shown in Table 8.6. QC and SYS samples were prepared fresh on the day of extraction to allow for six-fold extractions during sample analysis.

SYS samples were prepared and extracted similar to the calibration standards and QCs. They were then analysed at the beginning of the analytical batch and the resultant peak area ratios were observed. Once the peak area ratios were consistent, as indicated in Tables 8.7 and 8.14, the rest of the analytical batch was submitted for analysis.

Table 8.6. *Preparation of RTX quality controls*

Quality control sample	Volume of blank plasma (µL)	Volume of RTX spiked (µL)	Dilution source	Dilution source volume (µL)	Total volume of dilution (µL)	RTX concentration in plasma (µg/mL)
QCH	1220	30.0			1250	240
QCM	450		*QCH*	450	900	120
SYS	450		*QCM*	450	900	60.0
QCL	450		*SYS*	450	900	30.0
QCLLOQ	420		*QCL*	300	720	12.5

4. Preparation of ISTDs

The preparation of the 50 µg/mL SIL-RTX ISTD is described in Investigation 1. The reconstituted SIL-RTX is spiked with the calibration standards and quality controls during the affinity binding purification step, as described in Investigation 1 (Section 8.1) and illustrated in Figure 8.1.

The 5 pmol/µL RTX-s-Pep ISTD is spiked directly from the stock solution at the end of the digestion step, as described in Investigation 1 (Section 8.1) and illustrated in Figure 8.1.

Analysis

The final LC-MS/MS extraction method is presented in Chapter 7. Chromatographic separation is achieved with gradient elution, using a Poroshell C18 (2.1 mm x 50 mm 2.7-Micron) analytical column and a mobile phase that consists of 0.1% formic acid in water with 2% dimethyl sulfoxide (DMSO) (mobile phase A) and 0.1% formic acid in acetonitrile with 2% DMSO (mobile phase B). A Shimadzu-8050 mass spectrometer equipped with an electrospray ionisation source operating in the positive mode was used for mass detection. Multiple reaction monitoring acquisition at unit resolution was applied to monitor the transition of the protonated ions to their respective product ions, as described in Chapter 7 and Section 8.1. The s-Pep was the analyte of interest, and p-QVQ representing SIL-RTX or SIL-s-Pep was the ISTD.

The following construct was used to set up an analytical batch: A single extraction procedure was applied to all samples, including the SYS samples, the calibration standards analysed in duplicate, the four concentration levels of QCs analysed in six-fold, a blank, and a double blank sample. Calibration standards were spread in duplicate throughout the run and the QC samples were spread in two sets of triplicates throughout the run. Double blanks and blanks are run after the highest calibration standard to visually assess the level of carryover.

For this investigation, there were two analytical batches. The first contained the RTX analyte and the SIL-s-Pep ISTD. The second contained the RTX analyte and the SIL-RTX ISTD. The data from each

batch was analysed with and without the ISTD to assess how well the ISTD compensated for variability in the analytical process based on accuracy. The method is summarised in Figure 8.10 (below).

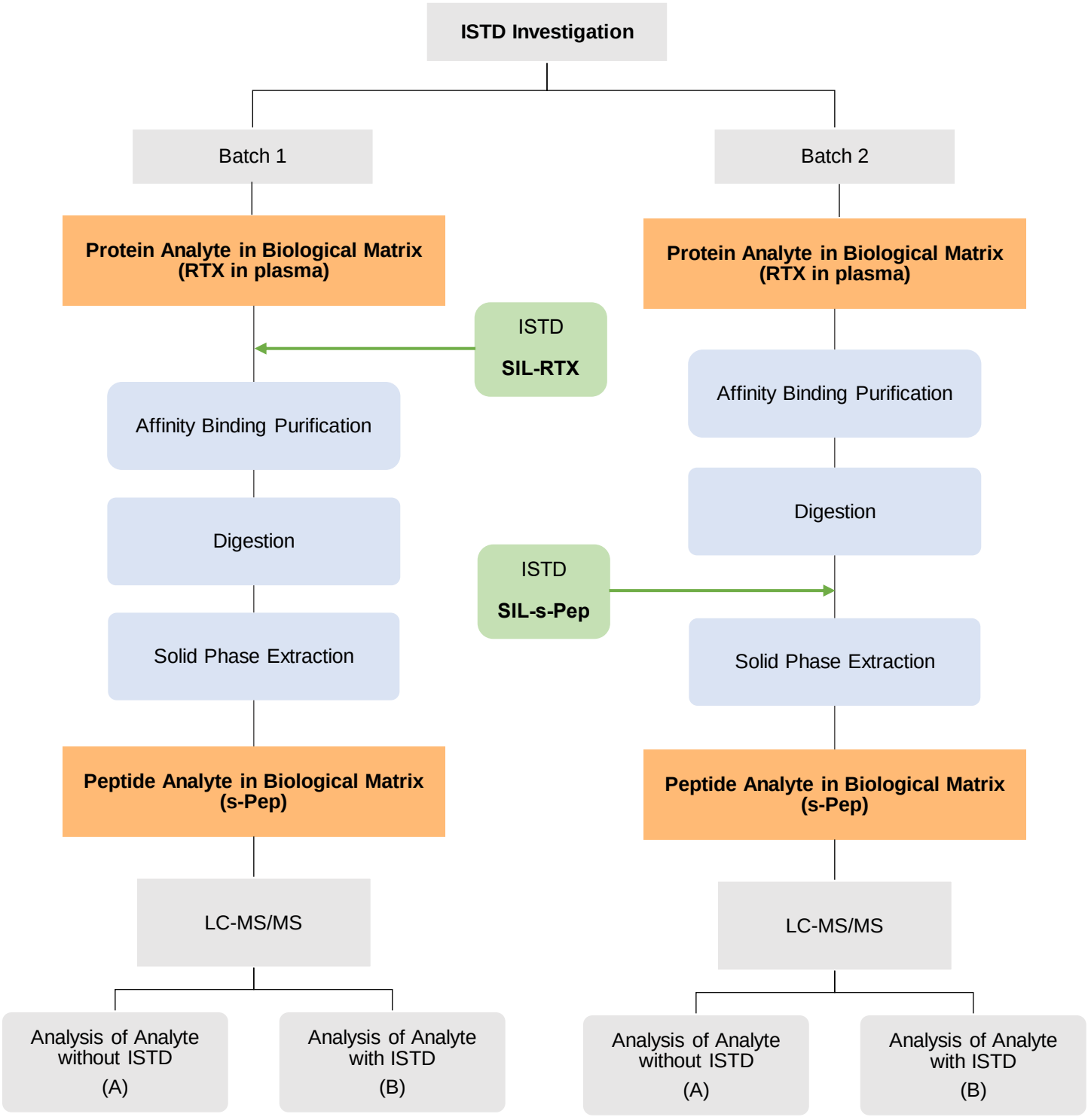

Figure 8.10. Method workflow illustrating where in the analytical procedure the ISTDs, RTX-SIL (Batch1) and SIL-s-Pep (Batch 2) are added. *Each batch involves analyses of the RTX analyte on its own (without ISTD) (A) and then analyses of the RTX analyte with the ISTD (B).*

Results

To ensure that the repeatability of the analytical process is acceptable, a series of SYS samples was injected at the beginning of each analytical batch. Tables 8.7 and 8 .14 summarise the analytical data of the SYS samples, indicating that the repeatability of the batches was acceptable.

The repeatability in terms of peak areas of the ISTDs was plotted in Figures 8.11 and 8.17.

The combined summary of the calibration standards and quality controls results over the entire calibration range (12.5–300 µg/mL), for the two batches, is represented in Tables 8.8–8.13 and Tables 8.15–8.20 below, and the representative calibration curves are shown in Figures 8.12 and 8.13 and in Figures 8.18 and 8.19. The accuracy was assessed by calculating the regression equation and constructing the calibration curve based on the peak area ratios of the analyte to the internal standard. The regression equation used was linear, f(x) = mx + c.

Representative chromatograms are indicated in Figures 8.14–8.16 and Figures 8.20–8.22.

Analytical Results of Batch 1: Assessment of SIL-RTX as ISTD

Table 8.7. *Summary of the SYS samples in terms of peak area ratios and CV(%)*

Sample number	Sample name	RTX peak area	SIL-RTX peak area	Peak area ratio (Analyte/ISTD)
		Analyte	ISTD	
1	SYS	22535	5604	4.02
2	SYS	24251	5185	4.68
3	SYS	23821	5676	4.20
4	SYS	23287	5232	4.45
5	SYS	20309	5150	3.94
6	SYS	25752	5710	4.51
			Average	4.30
			Standard deviation	0.292
			CV(%)	6.8%

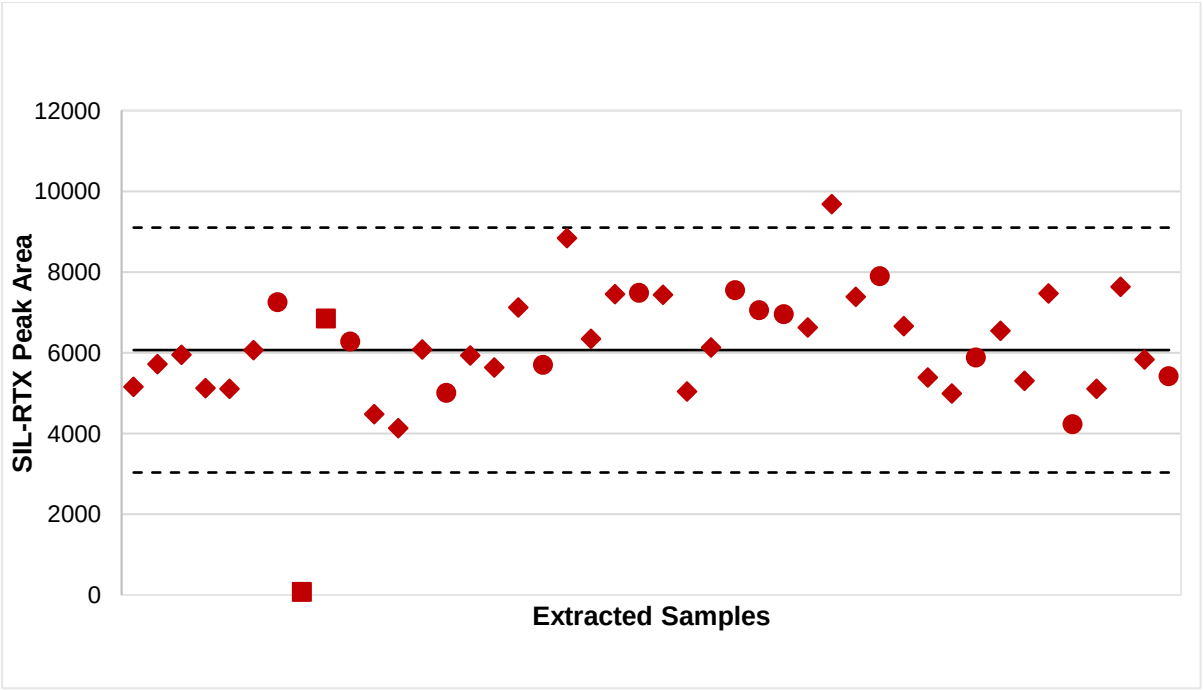

Figure 8.11. ISTD peak area plot for SIL-RTX. *Peak areas of the ISTD illustrated for the double blank (no ISTD or analyte), blank (ISTD only, no analyte), calibration standards, and quality control samples including mean peak area (±50%).*

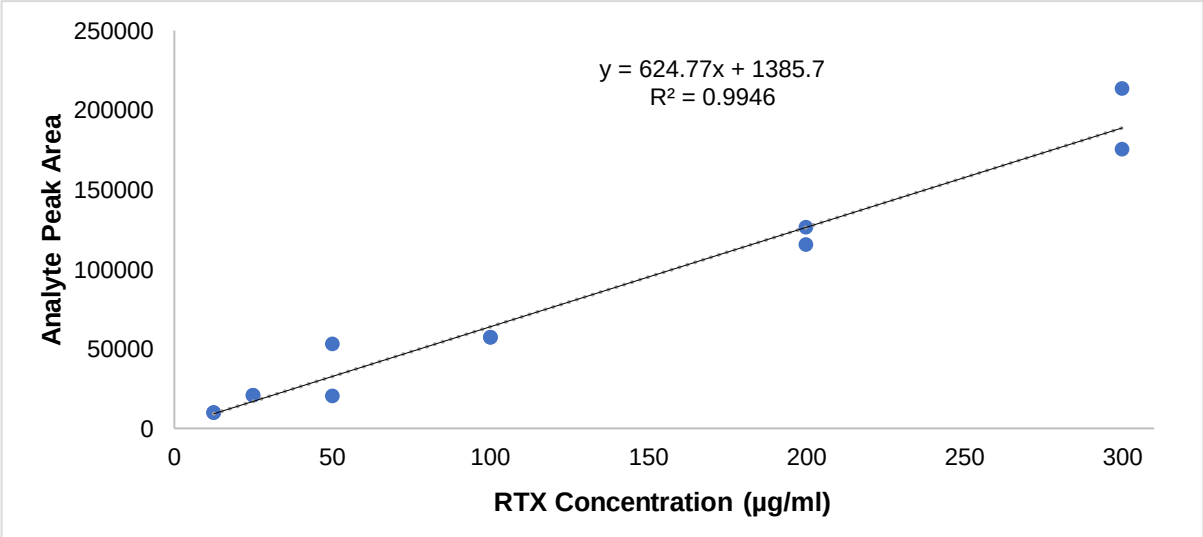

Figure 8.12. Representative calibration curve for s-Pep. *Analyte peak areas for the six calibration standards in duplicate (three data values excluded), equation y = 625.8x + 1385.7, R^2 = 0.995.*

Table 8.8. *Summary of the analyte peak areas and percentage accuracy from observed RTX concentrations for the six calibration standards (observed RTX concentrations calculated from the equation y = 624.8x + 1385.7; bold values indicate failed calibration standards)*

Calibration standard	Nominal concentration (µg/mL)	Analyte peak area	Number of repeats	Observed concentration (µg/mL)	Standard deviation	Percentage accuracy (%)
S1	300	194059	2	308	41.2	102.8
S2	200	120571	2	191	10.0	95.4
S3	100	56872	1	88.8	N/A	88.8
S4	50	36380	2	56.0	34.7	112.0
S5	25	20604	1	30.8	N/A	**123.0**
S6	12.5	9356	1	12.8	N/A	102.1
						104.0

Table 8.9. *Summary of the analyte peak areas and percentage accuracy from observed RTX concentrations for the four quality control samples without exclusions (observed RTX concentrations calculated from the equation y = 624.8x + 1385.7; bold values indicate failed quality controls)*

Quality control	Nominal concentration (µg/mL)	Analyte peak area	Number of repeats	Observed concentration (µg/mL)	Standard deviation	Percentage accuracy (%)
QCH	240	188171	6	299	50.0	**124.6**
QCM	120	87958	6	139	44.1	**115.5**
QCL	30	15936	6	23.3	10.4	**77.6**
QCLLOQ	12.5	8925	6	12.1	6.26	96.5
						103.6

Table 8.10. *Summary of the analyte peak areas and percentage accuracy from observed RTX concentrations for the four quality control samples with exclusions (observed RTX concentrations calculated from the equation y = 624.8x + 1385.7)*

Quality control	Nominal concentration (µg/mL)	Analyte peak area	Number of repeats	Observed concentration (µg/mL)	Standard deviation	Percentage accuracy (%)
QCH	240	170124	4	270	28.7	112.5
QCM	120	72712	4	114	28.8	95.1
QCL	30	17814	5	26.3	8.15	87.6
QCLLOQ	12.5	8925	6	12.1	6.26	96.5
						96.5

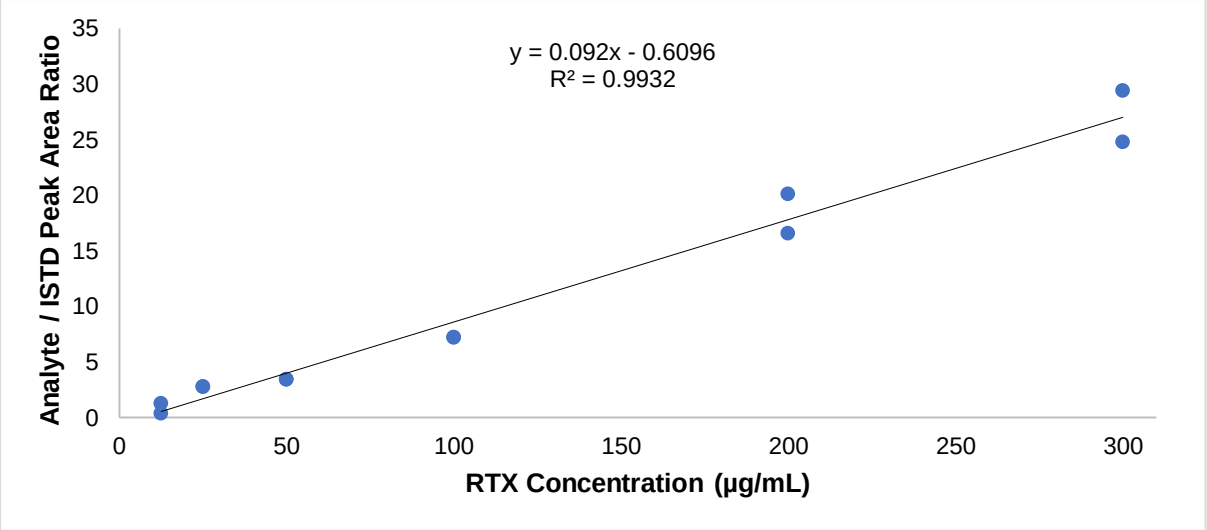

Figure 8.13. Representative calibration curve for s-Pep. *Analyte/ISTD (RTX/SIL-RTX) peak area ratios for six calibration standards in duplicate (three data values excluded), equation y = 0.092x - 0.610, R^2 = 0.993.*

Table 8.11. *Summary of the RTX/SIL-RTX peak area ratios and percentage accuracy from observed RTX concentrations for the six calibration standards (observed RTX concentrations calculated from the equation y = 0.092x - 0.610; bold values indicate failed calibration standards)*

Calibration standard	Nominal concentration (µg/mL)	Peak area ratio (Analyte/ISTD)	Number of repeats	Observed concentration (µg/mL)	Standard deviation	Percentage accuracy (%)
S1	300	27.1	2	301	28.9	100.4
S2	200	18.3	2	206	20.5	102.9
S3	100	7.20	1	84.9	N/A	**84.9**
S4	50	3.42	1	43.7	N/A	87.5
S5	25	2.75	1	36.6	N/A	**146.2**
S6	12.5	0.809	2	15.4	0.611	**123.4**
						107.6

Table 8.12. *Summary of the RTX/SIL-RTX peak area ratios and percentage accuracy from observed RTX concentrations for the four quality control samples without exclusions (observed RTX concentrations calculated from the equation y = 0.092x - 0.610; bold values indicate failed quality control)*

Quality control	Nominal concentration (µg/mL)	Peak area ratio (Analyte/ISTD)	Number of repeats	Observed concentration (µg/mL)	Standard deviation	Percentage accuracy (%)
QCH	240	32.6	6	360	143	**150.2**
QCM	120	15.1	6	171	58.3	**142.3**
QCL	30	2.21	6	30.6	6.81	102.1
QCLLOQ	12.5	1.54	6	23.4	9.65	**187.2**
						145.5

Table 8.13. *Summary of the RTX/SIL-RTX peak area ratios and percentage accuracy from observed RTX concentrations for the four quality control samples with exclusions (observed RTX concentrations calculated from the equation y = 0.092x - 0.610; bold values indicate failed quality controls)*

Quality control	Nominal concentration (µg/mL)	Peak area ratio (Analyte/ISTD)	Number of repeats	Observed concentration (µg/mL)	Standard deviation	Percentage accuracy (%)
QCH	240	26.0	4	289	89.0	**120.4**
QCM	120	12.4	4	141	47.0	**117.9**
QCL	30	2.21	6	30.6	6.81	102.1
QCLLOQ	12.5	1.08	4	18.3	4.95	**146.7**
						121.8

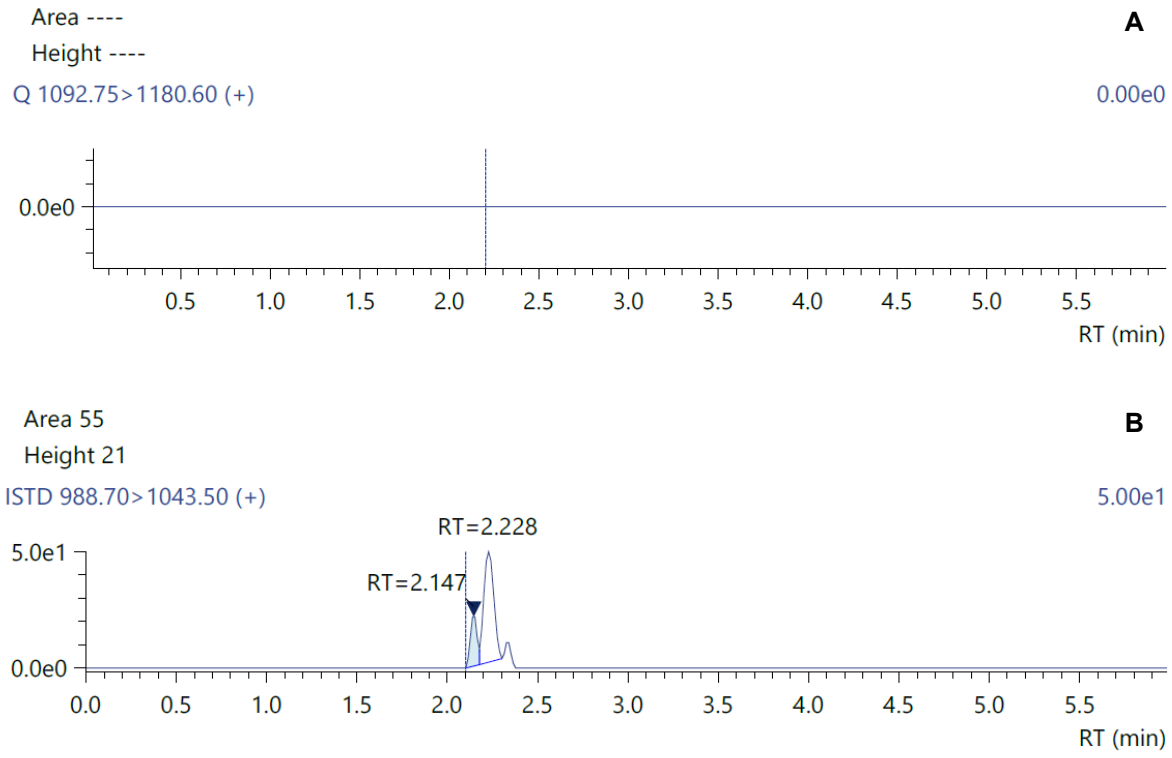

Figure 8.14. Representative double blank chromatogram (no RTX, no ISTD). A: *analyte channel 1092.75/1180.6, RT 2.2 min, peak area 0.* ***B:*** *ISTD channel 988.70/1043.50, RT 2.2 min, peak area 55.*

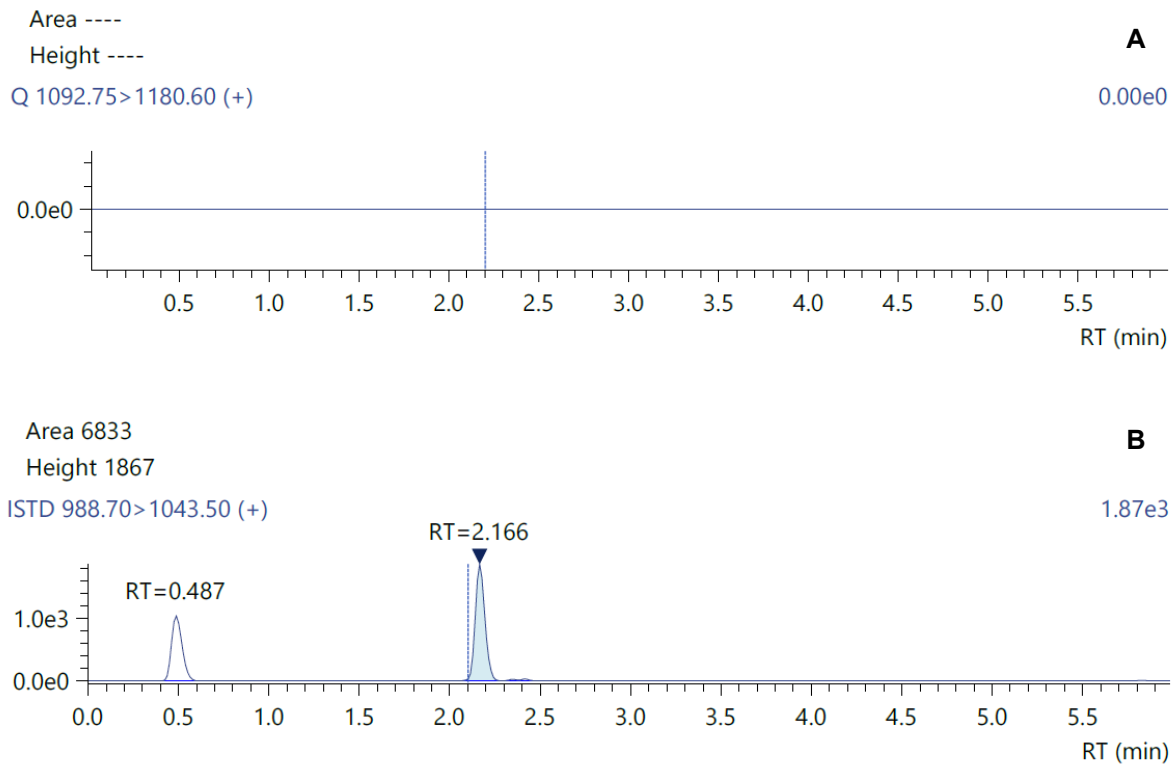

Figure 8.15. Representative blank chromatogram (ISTD only, no RTX). A: *analyte channel 1092.75/1180.6, RT 2.2 min, peak area 0.* ***B:*** *ISTD channel 988.70/1043.50, RT 2.2 min, peak area 6833.*

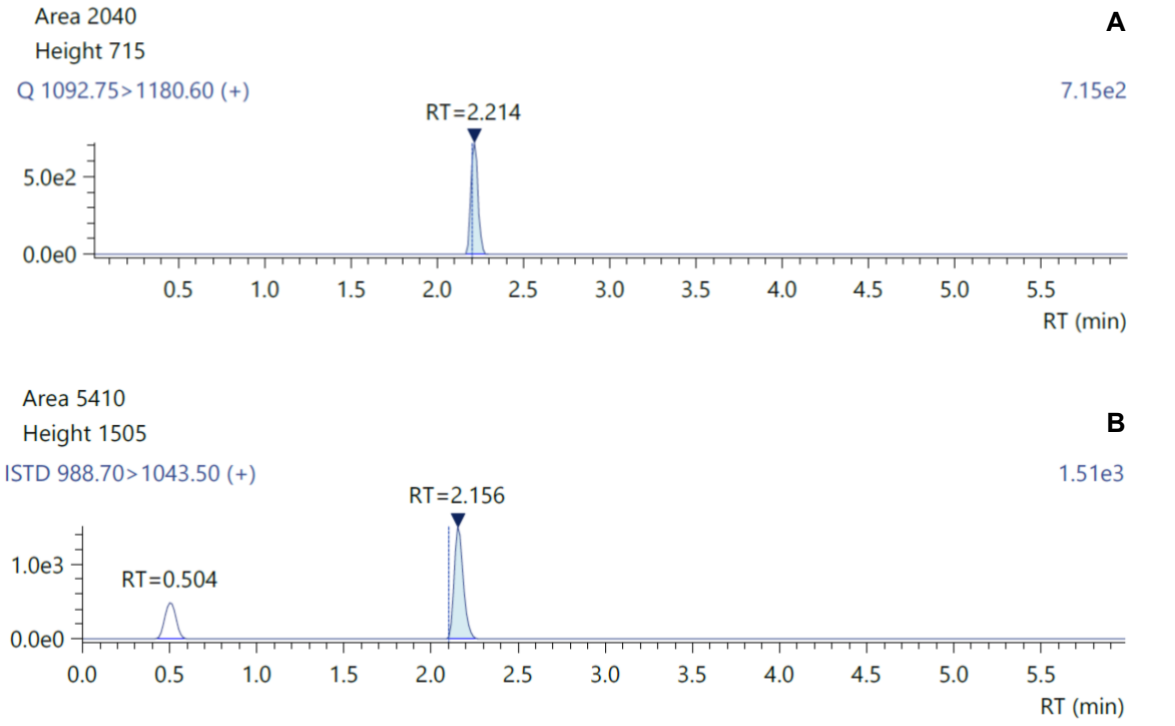

Figure 8.16. Representative LLOQ chromatogram of RTX (12.5 µg/mL RTX). A: *analyte channel 1092.75/1180.6, RT 2.2 min, peak area 2040.* ***B****: ISTD channel 988.70/1043.50, RT 2.2 min, peak area 5410.*

Analytical Results of Batch 2: Assessment of SIL-s-Pep as ISTD

Table 8.14. *Summary of the SYS samples in terms of peak area ratios and CV(%)*

Sample number	Sample name	RTX peak area	SIL-s-Pep peak area	Peak area ratio (Analyte/ISTD)
		Analyte	ISTD	
1	SYS	68897	776358	0.0890
2	SYS	63801	737678	0.0860
3	SYS	68107	802198	0.0850
4	SYS	70281	743323	0.0950
5	SYS	70285	795885	0.0880
6	SYS	67506	759514	0.0890
			Average	0.0890
			Standard deviation	0.00400
			CV(%)	4.0%

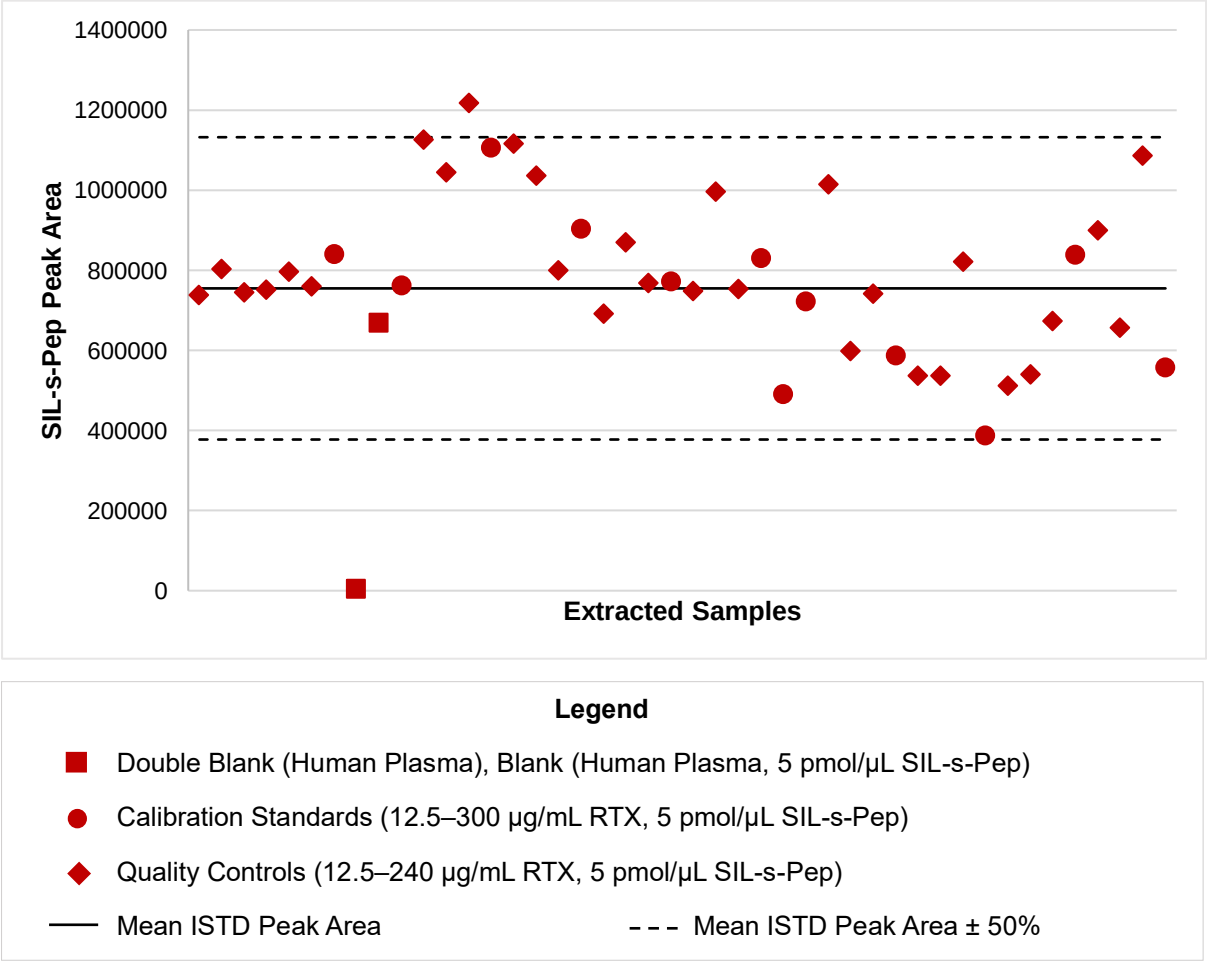

Figure 8.17. ISTD peak area plot for SIL-s-Pep. *Peak areas of the ISTD illustrated for the double blank (no ISTD or analyte), blank (ISTD only, no analyte), calibration standards, and quality control samples including mean peak area (±50%).*

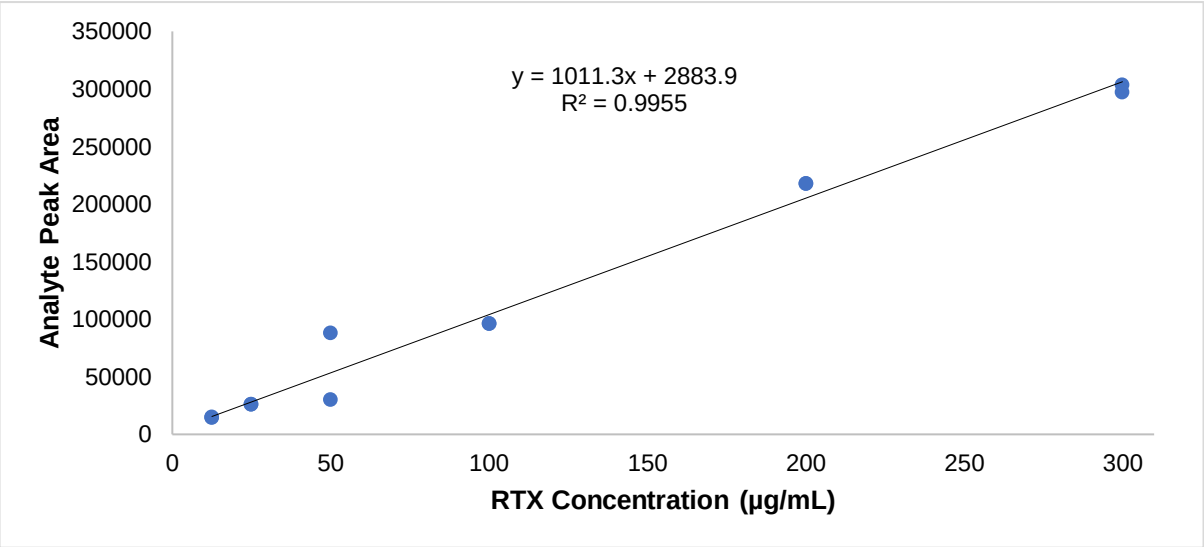

Figure 8.18. Representative calibration curve for s-Pep. *Analyte peak areas for the six calibration standards in duplicate (three data values excluded), equation y = 1011.3x + 2883.9, R^2 = 0.996.*

Table 8.15. *Summary of the analyte peak areas and percentage accuracy from observed RTX concentrations for the six calibration standards (observed RTX concentrations calculated from the equation y = 1011.3x + 2883.9)*

Calibration standard	Nominal concentration (µg/mL)	Analyte peak area	Number of repeats	Observed concentration (µg/mL)	Standard deviation	Percentage accuracy (%)
S1	300	300080	2	294	2.80	98.0
S2	200	217547	1	212	N/A	106.1
S3	100	95770	1	91.8	N/A	91.8
S4	50	58854	2	55.3	37.6	110.7
S5	25	25825	1	22.7	N/A	90.7
S6	12.5	14481	2	11.5	2.53	91.7
						98.2

Table 8.16. *Summary of the analyte peak areas and percentage accuracy from observed RTX concentrations for the four quality controls without exclusions (observed RTX concentrations calculated from the equation y = 1011.3x + 2883.9; bold values indicate failed quality controls)*

Quality control	Nominal concentration (µg/mL)	Analyte peak area	Number of repeats	Observed concentration (µg/mL)	Standard deviation	Percentage accuracy (%)
QCH	240	348568	6	342	121	**142.4**
QCM	120	173684	6	169	62.1	**140.7**
QCL	30	36890	6	33.6	12.9	112.1
QCLLOQ	12.5	16611	6	13.6	6.79	108.6
						126.0

Table 8.17. *Summary of the analyte peak areas and percentage accuracy from observed RTX concentrations for the four quality controls with exclusions (observed RTX concentrations calculated from the equation y = 1011.3x + 2883.9)*

Quality control	Nominal concentration (µg/mL)	Analyte peak area	Number of repeats	Observed concentration (µg/mL)	Standard deviation	Percentage accuracy (%)
QCH	240	270678	3	265	116	110.3
QCM	120	139066	4	135	42	112.2
QCL	30	36890	6	33.6	12.9	112.1
QCLLOQ	12.5	16611	6	13.6	6.79	108.6
						110.8

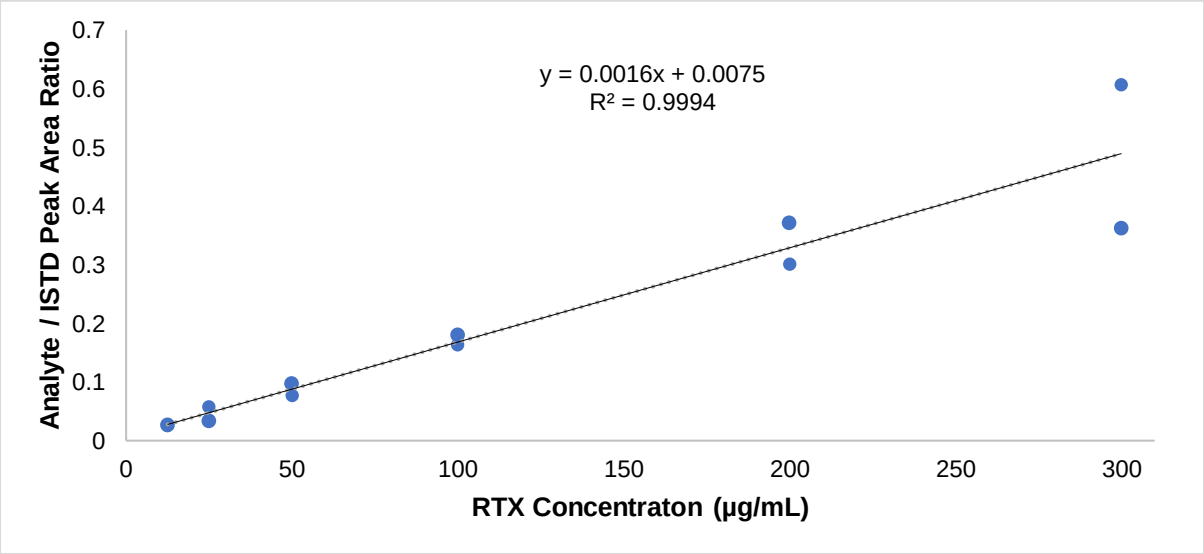

Figure 8.19. Representative calibration curve for s-Pep. *Analyte/ISTD (RTX/SIL-s-Pep) peak area ratios for the six calibration standards in duplicate (one data value excluded), equation y = 0.0016x + 0.0075, R^2 = 0.999.*

Table 8.18. *Summary of the RTX/SIL-s-Pep peak area ratios and percentage accuracy from observed RTX concentrations for the six calibration standards (observed RTX concentrations calculated from the equation y = 0.0016x + 0.0075)*

Calibration standard	Nominal concentration (µg/mL)	Peak area ratio (Analyte/ISTD)	Number of repeats	Observed concentration (µg/mL)	Standard deviation	Percentage accuracy (%)
S1	300	0.484	2	298	103	99.3
S2	200	0.336	2	205	26.3	102.7
S3	100	0.172	2	103	2.81	102.5
S4	50	0.0870	2	49.7	4.13	99.4
S5	25	0.0450	2	23.4	5.94	93.8
S6	12.5	0.0260	1	11.6	N/A	92.5
						98.3

Table 8.19. *Summary of the RTX/SIL-s-Pep peak area ratios and percentage accuracy from observed RTX concentrations for the four quality controls without exclusions (observed RTX concentrations calculated from the equation y = 0.0016x + 0.0075; bold values indicate failed quality controls)*

Quality control	Nominal concentration (µg/mL)	Peak area ratio (Analyte/ISTD)	Number of repeats	Observed concentration (µg/mL)	Standard deviation	Percentage accuracy (%)
QCH	240	0.358	6	219	54.0	91.4
QCM	120	0.214	6	129	28.2	107.6
QCL	30	0.0538	6	29.0	7.53	96.5
QCLLOQ	12.5	0.0200	6	7.81	4.91	**62.5**
						89.5

Table 8.20. *Summary of the RTX/SIL-s-Pep peak area ratios and percentage accuracy from observed RTX concentrations for the four quality controls with exclusions (observed RTX concentrations calculated from the equation y = 0.0016x + 0.0075)*

Quality control	Nominal concentration (µg/mL)	Peak area ratio (Analyte/ISTD)	Number of repeats	Observed concentration (µg/mL)	Standard deviation	Percentage accuracy (%)
QCH	240	0.358	6	219	54.0	91.4
QCM	120	0.214	6	129	28.2	107.6
QCL	30	0.0538	6	29.0	7.53	96.5
QCLLOQ	12.5	0.0248	4	10.8	1.80	86.3
						95.5

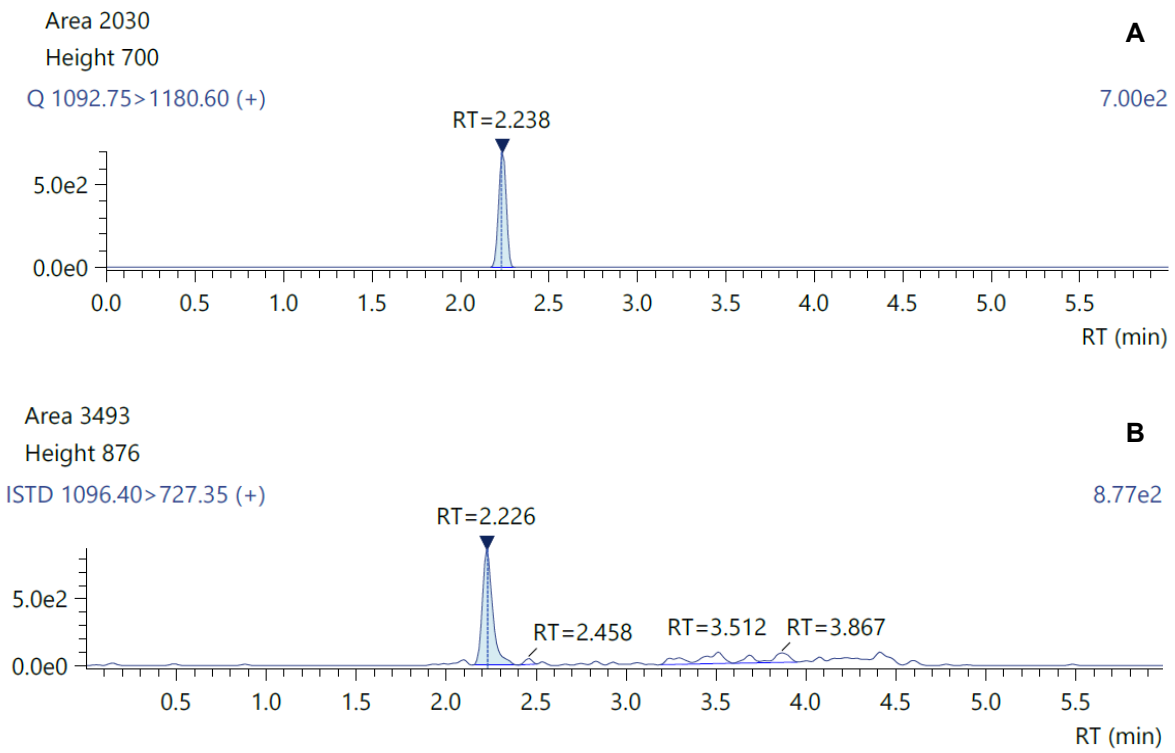

Figure 8.20. Representative double blank chromatogram (no RTX, no ISTD). A: *analyte channel 1092.75/1180.6, RT 2.2 min, peak area 2030 (13.8% of LLOQ).* ***B:*** *ISTD channel 1096.40/727.35, RT 2.2 min, peak area 3493 (0.4% of ISTD peak present in LLOQ).*

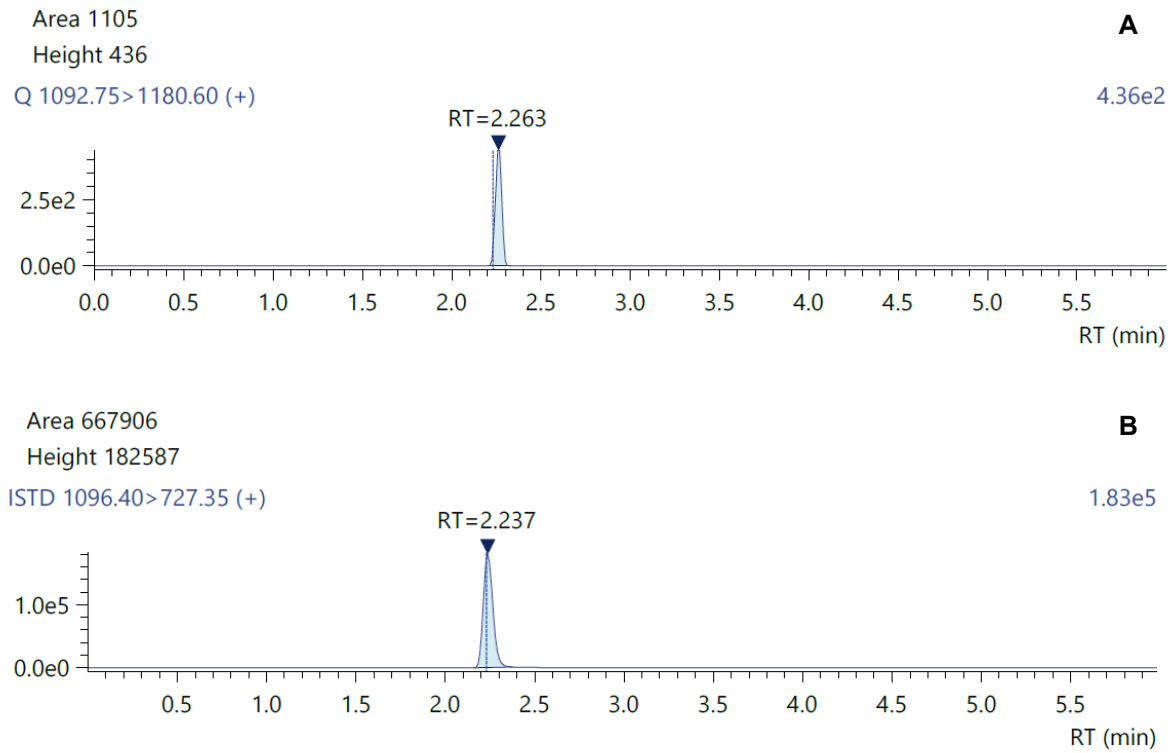

Figure 8.21. Representative blank chromatogram (ISTD only, no RTX). A: *analyte channel 1092.75/1180.6, RT 2.3 min, peak area 1105 (7.8% of LLOQ).* ***B:*** *ISTD channel 988.70/1043.50, RT 2.2 min, peak area 667906.*

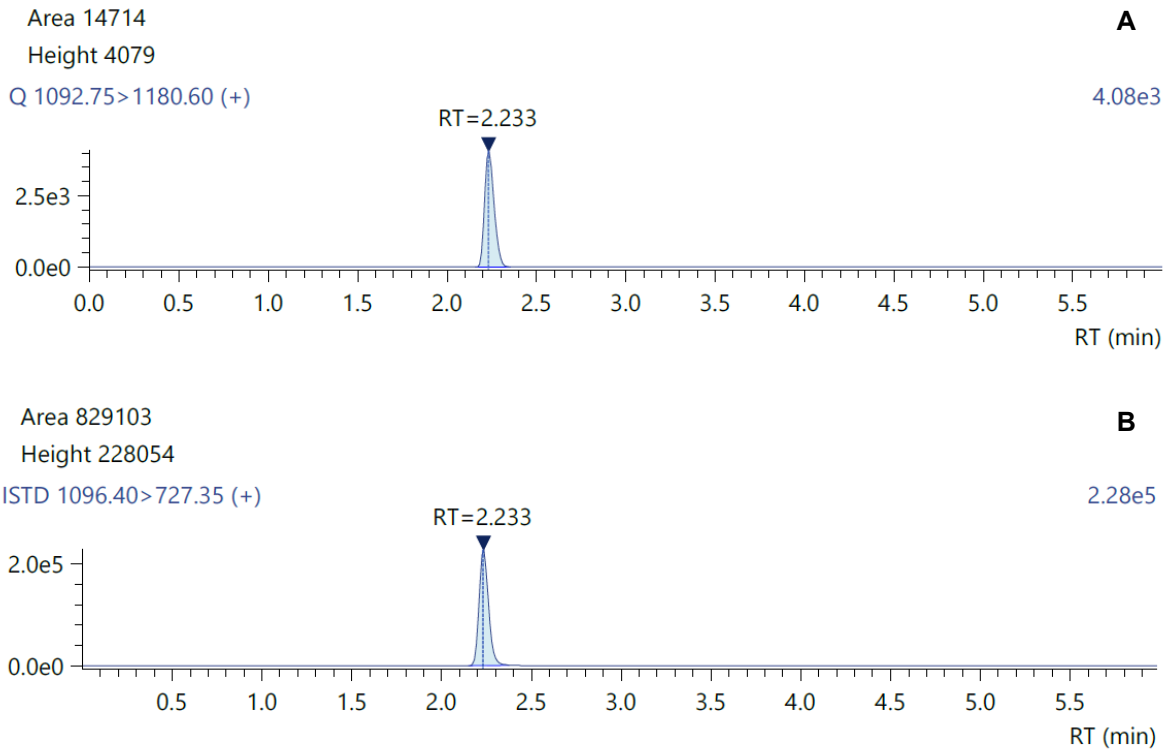

Figure 8.22. Representative LLOQ chromatogram of RTX (12.5 µg/mL RTX). A: *analyte channel 1092.75/1180.6, RT 2.2 min, peak area 14714.* ***B:*** *ISTD channel 1096.40/727.35, RT 2.2 min, peak area 829103.*

Summary

Table 8.21. *Summary of results*

Batch	Group	Sample	Pass / Fail
1 SIL-RTX	**A** Analyte only	Calibration standard	Pass (104%)
		Quality control samples (no exclusions)	Pass (103.6%)
		Quality controls (with exclusions)	Pass (96.5%)
1 SIL-RTX	**B** Analyte + ISTD	Calibration standard	Pass (107.6%)
		Quality control samples (no exclusions)	Fail (145.5%)
		Quality controls (with exclusions)	Fail (121.8%)
2 SIL-s-Pep	**A** Analyte only	Calibration standard	Pass (98.2%)
		Quality control samples (no exclusions)	Fail (126%)
		Quality controls (with exclusions)	Pass (110.8%)
2 SIL-s-Pep	**B** Analyte + ISTD	Calibration standard	Pass (98.3%)
		Quality control samples (no exclusions)	Pass (89.5%)
		Quality controls (with exclusions)	Pass (95.5%)

Group 1A: Calibration standards passed when the samples were analysed *without* ISTD. Quality controls passed (with and without exclusions) when the samples were analysed *without* ISTD.

Group 1B: Calibration standards passed when the samples were analysed *with* ISTD. Quality controls failed when the samples were analysed *with* ISTD.

Group 2A: Calibration standards passed when the samples were analysed *without* ISTD. Quality controls failed (without exclusions) when the samples were analysed *without* ISTD. Quality controls passed (with exclusions) when the samples were analysed *without* ISTD.

Group 2B: Calibration standards passed when the samples were analysed *with* ISTD. Quality controls passed (with and without exclusions) when the samples were analysed *without* ISTD.

Discussion

SIL-RTX ISTD

Figure 8.11 confirms the peak areas of p-QVQ, representing RTX-SIL, fall within the variability window of 50% of the average for all standards, QCs, and blanks. There is only one nominal outlier, which is QCH. This is considered to be an acceptable variation for the ISTD.

The average accuracy for the calculated RTX concentrations of the calibration standards and the QC samples analysed without the ISTD was 104% and 96.5%, respectively (see Tables 8.8 and 8.10). For those analysed with SIL-RTX as the ISTD, the average accuracy of the calculated RTX concentrations was 107.6% and 121.8% respectively (see Tables 8.11 and 8.13).

In terms of the analyte concentration, the presence of SIL-RTX as an ISTD caused a decrease in the measure of accuracy. From this, it can therefore be concluded that the SIL-RTX should not be used as an ISTD under the conditions of this analytical method.

It is clear that acceptable repeatability of the ISTD peak area in the samples does not imply adequate compensation for the accuracy of analyte quantification. The cause of this increased inaccuracy may be coupled with the fact that the signal peptide of the ISTD (p-QVQ) was different from that of the analyte (s-Pep). The choice of p-QVQ was because the s-Pep sequence could not be detected for SIL-RTX. Therefore, a substitute signal peptide in the form of p-QVQ was selected. This p-QVQ was used as a signal peptide by Millet *et al*., but the same sequence was also selected as a signal peptide for RTX. Millet *et al*. also detected s-Pep but did not proceed with using it as the signal peptide for RTX. It can also be argued that the concentration of SIL-RTX included in the method was too low; however, an alternative concentration was not investigated. The concentration decided upon was based on the calculated concentration of QCM but, obviously, the peak area of the p-QVQ sequence under the ionisation conditions used in the method, was not comparable to that of the s-Pep and therefore the peak intensity at that concentration may have been too low.

SIL-s-Pep ISTD

The repeatability of SIL-s-Pep was similar to that of SIL-RTX, as indicated by Figure 8.17. The one nominal outlier (QCH) similarly does not significantly influence the repeatability in all samples containing SIL-s-Pep.

The accuracy of RTX concentration measurement in calibration standards and QCs analysed without an ISTD was 98.2% and 110.8%, respectively (see Tables 8.15 and 8.17). When compared to the same samples analysed with SIL-s-Pep as an ISTD the accuracy measurement for both calibration standards and QCs improved to 98.3% and 95.5%, respectively (see Tables 8.18 and 8.20).

The use of SIL-s-Pep as an ISTD should therefore be considered when this method is tested under the conditions usually applied to the validation of quantitative procedures.

In the previous investigation, repeatability was used as a measure of ISTD acceptability. The findings showed that both the affinity binding purification and trypsin digestion procedures were sufficiently repeatable when adding only the ISTD (SIL-s-Pep) for the SPE procedure. Thus, the inclusion of solely the SIL-s-Pep is justified since the accuracy and repeatability of the affinity binding purification and trypsin digestion procedures have been proven without ISTD.

CHAPTER 9

DISCUSSION

This project was performed in order to develop an analytical method, and the process was as far as possible developed in the sequence of the analytical method. Throughout this process, the instrumental analytical methods were used as measuring tools to facilitate the appropriate refinement of the method. In this discussion, the same sequence regarding the interpretation of investigational results is followed. In summary, the chromatographic and detection method developed on the Sciex API-3200 was used to investigate and optimise most of the sample preparation procedures, which included affinity binding purification, trypsinization, and solid phase extraction (SPE). To optimise the method for the target RTX concentration range it was soon apparent that a more sensitive instrument was required. For that reason, a second analytical method on the Shimadzu 8050 was introduced, while still using the sample preparation previously optimised on the Sciex API-3200. This allowed the investigation to be completed by assessing the usability of different internal standards (ISTDs).

The RTX signal peptide (s-Pep) was used to optimise the chromatographic and detection parameters on the Sciex API-3200 LC-MS/MS system. Following infusion of the s-Pep, the expected precursor ion ($[M+2H]^{2+}$ = 1092.2) was identified and fragmented by collision-induced dissociation to produce a product mass spectrum. Interpretation of this spectrum confirmed the identity of s-Pep by displaying the expected peptide fragments for the related amino acid sequence. The most abundant fragment produced on the Sciex API-3200 was that at a m/z = 86.2, and therefore, the transition for the detection of s-Pep was a combination of the precursor ion and this most abundant fragment (1092.2/86.2). This transition used on the Sciex API-3200 was different from that found on the Shimadzu 8050, which was used for the final analytical method. The reason for this may be the high collision energy necessary in the fragmentation cell of the Sciex API-3200 to produce product ions of sufficient intensity. The optimised collision energy was 127 eV whereas in the Shimadzu 8050 the required intensity of the transition 1092.8/1180.6 was reached at - 35 eV. In addition, as indicated by the product ion mass spectrum in Figure 4.4, the intensities of fragment ions at m/z > 159.2 produced by the Sciex API-3200 were not sufficient to be used as transitions adequate for detection. This is probably a function of the particular collision cell in the Sciex API-3200 and may be one of the reasons the instrument was, in the end, not sensitive enough. The sensitivity was, however, sufficient to explore and optimise the sample preparation procedure when, at times, working above the expected therapeutic range of 12.5–300 µg/mL. For investigation at the lower concentrations of the range, the more sensitive instrument was used.

The therapeutic dosage of RTX is an infusion of 375 mg/m^2 which, from an analytical viewpoint, is an extremely high concentration. It was therefore considered feasible that total plasma protein precipitation as a primary sample cleanup before digestion should be investigated. A precipitation procedure designed for big batch analysis can however not be specific enough to selectively precipitate different classes of plasma proteins such as IgGs. Therefore, the only feasible precipitation procedure included indiscriminate precipitation of all plasma proteins. This non-specificity produced too high a

concentration of proteins to accurately and selectively produce s-Pep by trypsin digestion. Protein precipitation was therefore not further pursued.

IgG enrichment through proteins A and G is widely used for pre-digestion purification. This very specific association of IgG with a binding moiety which can be immobilised on agarose beads constitutes a powerful mechanism whereby purification can be achieved by a simple process such as on bench centrifugation and washing procedures. This resulted in a concentrated slurry, containing RTX, for better enzyme presentation during trypsinization. This was experimentally proven to result in higher production of the s-Pep than would have been the case if RTX were eluted from the bound protein A before trypsinization. This confirmed similar findings in the literature (140).

Using affinity binding purification with agarose protein A beads as the only mechanism to purify RTX from plasma is advantageous since an additional anti-IgG antibody is not used. This eliminates one more purification step during which analyte recovery can be compromised and also minimises the amount of protein to be digested.

During the assessment of different proteins for the use of ISTD, one of the candidates was horse IgG. This was chosen given its availability and species-specific target peptide (28,124). However, one of the disadvantages of using only protein A as an affinity binding mechanism for the purification of RTX is that the binding specificity of horse IgG to protein A is considerably lower than that of human IgG. According to the literature, a better choice is protein G or a mixture of protein G and protein A. Although protein G would also be an acceptable binding affinity moiety for RTX, it was considered unacceptable to change the extraction method to suit the ISTD.

During this project, the aspects of trypsinization investigated were the ratio of RTX/trypsin, time incubation, the presence of an organic solvent, and the addition of fresh trypsin (second incubation). Although trypsinization is well known and widely used to acquire signal peptides, it was considered necessary to perform investigative experiments into the optimisation of these fundamental digestion steps. The results of our experiments confirmed published findings (119).

Not all published trypsinization methods include a second incubation with the addition of fresh trypsin towards the end of the incubation period. Instead of this extra incubation step some methods would perform the incubation at 37°C to optimise trypsin activity. For this method, it was found to be necessary to mildly agitate the digestion mixture by rotating the reaction tubes. This had to be done on-bench at room temperature. Therefore, the method benefited from the addition of a second aliquot of trypsin instead of performing the incubation at 37°C.

After trypsinization there is no need for further protein level clean-up because the analyte is now in the form of s-Pep and the matrix following trypsinization is no longer plasma but a much less complex mixture of Tris buffer and residual protein fragments. Solid phase extraction is as an established extraction technique for signal peptides from such mixtures, essentially serving as a means of purification at the peptide level (peptide level clean-up).

As is usually done during method development, the SPE method was initially developed using the s-Pep in a buffer. These conditions resulted in the complete elution of s-Pep with 100 µL 70% acetonitrile containing 1% formic acid, and further elution with equal volumes of the same solvent did not elute any more s-Pep. When this was repeated during the full extraction procedure where trypsinization preceded SPE, only insignificant traces of s-Pep were detectable in the second and third elution steps. This can be expected because the peptide mixture applied to SPE contains non-specific peptides which may contribute to a low level of background interference in the measurement of s-Pep. This did not significantly impact the accurate detection and measurement of s-Pep – even at the lowest RTX concentration investigated. The results therefore confirmed that the SPE procedure, including elution, was optimised.

An additional indication of the specificity of the full sample preparation procedure is the fact that a consistent percentage recovery for the extraction method was found in PBS and in plasma. This indicates that the high protein concentration in plasma did not deleteriously influence any of the preparation steps including affinity binding purification, trypsinization and SPE. The percentage recovery over a range of RTX concentrations in plasma further confirms the repeatability of the analytical method. With the combination of affinity binding on protein A beads and the trypsinization, as developed using the Sciex API-3200, the recovery of the s-Pep as representative of RTX from plasma was thus proven. The sample preparation procedure was adequately robust enough to transfer it to the more sensitive Shimadzu 8050, without any adaptation.

The auto-selection by the Shimadzu 8050 of a different transition than that used by the Sciex API-3200 was regarded to be optimal for this instrument. This reiterates that the detection by ESI MS can vastly differ from one instrument design to another and therefore detection optimisation must be performed for each instrument and/or instrument type. This does not only include the ionisation process but also the parameters of, inter alia, the ion lenses, collision cell, and detectors.

The improved sensitivity of the analytical method incorporating the Shimadzu 8050 allowed for further optimisation of the sample preparation method in which the lowest concentration needed to be investigated. This was illustrated by the experiment for the optimisation of the sample loading volume which showed that 50 µL sample volume was adequate. The use of a sample volume as low as possible is advantageous. An additional advantage of using this instrument was the possibility of now investigating the choice of an ISTD by comparing both the repeatability and accuracy of the measurement of the analyte.

Although the use of an ISTD during quantitative analysis is regarded as standard practice, this work indicated that there are certain essential aspects that should be considered. The failure of horse IgG as an ISTD emphasised the necessity of similar binding affinities during the purification step. The SIL-RTX can well be considered the best ISTD to use since it is identical to the unlabelled RTX protein. However, the representative signal peptides of the analyte and the ISTD should probably also be identical since, in this case, where different signal peptides were used, proper compensation could not be demonstrated. The most successful ISTD was then the SIL-s-Pep, which comprised the same sequence

for both the ISTD and the analyte. One should remember that the SIL-s-Pep only accompanied the analyte through one of the sample preparation steps, namely SPE. An ideal ISTD should go through all the preparative steps along with the analyte. However, the use of only a SIL signature peptide as ISTD is common practice – as evident in the literature (27,123).

The measured repeatability and accuracy without an ISTD attest to the robustness of the method. Furthermore, although the measured recovery of the s-Pep in terms of applied RTX was low, the repeatability of this recovery as measured between different matrices (PBS and plasma) and across a full concentration range of RTX is further proof that the method was optimally developed and can be validated as is (123,146). Of note is that there are considerable differences between the quantification of macromolecules and small molecules. Not only are proteins much more complex in structure and chemical characteristics, but the acquisition of a measurable representative moiety from the protein, such as the signal peptide, is a much more complex process than the extraction of a small molecule from a complex biological matrix. There are significantly more steps involved in the sample preparation procedure and, at every step, variability, accuracy, and precision are compromised. Therefore, the application of the validation criteria for small molecules cannot per se be applied to the validation of an analytical method for a protein. As noted in the comprehensive review by Jenkins *et al*., small molecules and macromolecules require different analytical criteria for validation (123). Macromolecules cannot be validated using the same strict criteria that are applied to small molecules, as indicated by the review (123).

CHAPTER 10

CONCLUSION AND FUTURE WORK

A robust and reproducible quantification method was developed and optimised for the analysis of RTX in human plasma. To accurately detect total RTX concentrations, this research project provided an overview of various bottom-up sample preparation strategies that used a representative signal peptide chosen based on specificity and LC-MS/MS behaviour. All the steps of this comprehensive process have been described and discussed in terms of pre-digestion purification, digestion, and post-digestion purification. Regarding the use of ISTDs, this project proved that SIL-peptides, widely used in quantitative proteomics, are good alternatives to correct for variation in LC-MS/MS detection of the signature peptide. One should, however, bear in mind that the SIL-peptides cannot correct for variation in sample preparation steps, including affinity binding purification and digestion. Taking all the above into consideration, the robustness of this method allowed for this assay to be performed on two triple quadrupole LC-MS instruments with no adaptation in the sample preparation steps and only minor adaptations in the detection method.

The completeness of the method development described in this project will allow for the validation of this method with the selected ISTD, so that it can be applied to the analysis of samples from test subjects. It is well known that the use of mAbs for the treatment of various serious diseases is increasingly being applied. It has been shown that therapeutic antibody levels in circulation can also be regarded as biomarkers for therapeutic efficacy and more antibody therapeutics are in clinical trials and in the pipeline (147). Lower dosing of mAbs is also being explored, necessitating the need for higher assay sensitivity for the quantification at expected lower concentrations in plasma (65). Once this method has been validated and proven by application to subject samples, it could also be adjusted for the application to lower concentrations of RTX in order to better understand the pharmacokinetics thereof. In general, this could lead to regulatory changes that provide clearer guidelines for drug development and approval of new drugs.

As evident in this project, the unique exploitation of affinity binding purification and the highly selective and specific detection capabilities of LC-MS/MS are a powerful tool to investigate the therapeutic application of macromolecules. In most bioanalytical laboratories, the emphasis is still largely on the analysis of small molecules. In our laboratory, this project may be regarded as the nucleus of new development strategies for the bioanalysis of macromolecules. Although the emphasis was on RTX, the method is regarded as versatile enough to be adapted, with few modifications, to the analysis of a variety of proteins and peptides from patient samples. The techniques presented here apply not only to the analysis of proteins in plasma but are also adaptable to other biological matrices. Therefore, the investigated sample preparation techniques enable reproducible quantification of mAbs using LC-MS and should be widely adopted in the clinical laboratory.

Given the broad field of mAb research, there is a high demand for quantification methods. LC-MS/MS is gaining popularity over conventional ELISA assays. The detection of intact antibodies requires a multiplex assay. In conclusion, a platform has been developed that should provide a desperately needed

bridging technology between development-intensive biomarker discovery and clinical application. The field of drug development faces unique challenges in dealing with these new molecules, particularly in developing bioanalytical methods. However, these challenges also present opportunities for creating new bioanalytical techniques and tools that can assist in quantifying drug molecules. These advancements could lead to regulatory changes that provide clearer guidelines for drug development and approval of new drugs.

CHAPTER 11

REFERENCES

1. Zugazagoitia J, Guedes C, Ponce S, Ferrer I, Molina-Pinelo S, Paz-Ares L. Current Challenges in Cancer Treatment. Vol. 38, Clinical Therapeutics. Excerpta Medica Inc.; 2016. p. 1551–66.
2. Maloney DG, Smith B, Rose A. Rituximab: Mechanism of action and resistance. In: Seminars in Oncology. W.B. Saunders; 2002. p. 2–9.
3. Urruticoechea A, Alemany R, Balart J, Villanueva A, Viñals F, Capellá G. Recent Advances in Cancer Therapy: An Overview. Vol. 16, Current Pharmaceutical Design. 2010.
4. Kaur K, Khatik GL. Cancer Immunotherapy: An Effective Tool in Cancer Control and Treatment. Curr Cancer Ther Rev. 2019 Sep 13;16(1):62–9.
5. Karlitepe A, Ozalp O, Avci CB. New approaches for cancer immunotherapy. Tumor Biology. 2015 Jun 11;36(6):4075–8.
6. Yeh JC, Knight LS, Kane J, Doberman DJ, Gupta A, Smith TJ. Has There Been a Shift in Use of Subacute Rehabilitation Instead of Hospice Referral Since Immunotherapy Has Become Available? [Internet]. 2023. Available from: https://doi.org/10.
7. Hafeez U, Gan HK, Scott AM. Monoclonal antibodies as immunomodulatory therapy against cancer and autoimmune diseases. Vol. 41, Current Opinion in Pharmacology. Elsevier Ltd; 2018. p. 114–21.
8. Weiner GJ. Rituximab: Mechanism of action. Semin Hematol. 2010 Apr;47(2):115–23.
9. Ryman JT, Meibohm B. Pharmacokinetics of monoclonal antibodies. CPT: Pharmacometrics & Systems Pharmacology. 2017 Sep 1;6(9):576–88.
10. Mcmahon HE, Schwartz JW, Ray S. Monoclonal Antibody Production and Purification [Internet]. Available from: https://repository.upenn.edu/cbe_sdrhttps://repository.upenn.edu/cbe_sdr/104
11. Scott AM, Wolchok JD, Old LJ. Antibody therapy of cancer. Vol. 12, Nature Reviews Cancer. 2012. p. 278–87.
12. Whiteaker JR, Zhao L, Zhang HY, Feng LC, Piening BD, Anderson L, Paulovich AG. Antibody-based enrichment of peptides on magnetic beads for mass-spectrometry-based quantification of serum biomarkers. Analytical Biochemistry. 2007 Mar 1;362(1):44-54. doi: 10.1016/j.ab.2006.12.023. Epub 2006 Dec 20. PMID: 17241609; PMCID: PMC1852426.
13. Sen JW, Bergen HR, Heegaard NHH. On-line immunoaffinity-liquid chromatography-mass spectrometry for identification of amyloid disease markers in biological fluids. Anal Chem. 2003 Mar 1;75(5):1196–202.
14. Berna M, Ott L, Engle S, Watson D, Solter P, Ackermann B. Quantification of NTproBNP in rat serum using immunoprecipitation and LC/MS/MS: A biomarker of drug-induced cardiac hypertrophy. Anal Chem. 2008 Feb 1;80(3):561–6.
15. Becher F, Pruvost A, Clement G, Tabet JC, Ezan E. Quantification of small therapeutic proteins in plasma by liquid chromatography-tandem mass spectrometry: Application to an elastase inhibitor EPI-hNE4. Anal Chem. 2006 Apr 1;78(7):2306–13.

16. Irie K, Okada A, Yamasaki Y, Kokan C, Hata A, Kaji R, Fukushima K, Sugioka N, Okada Y, Katakami N, Fukushima S. An LC-MS/MS Method for Absolute Quantification of Nivolumab in Human Plasma: Application to Clinical Therapeutic Drug Monitoring. 2018 Dec;40(6):716-724. doi: 10.1097/FTD.0000000000000558. PMID: 30048380.
17. Eter P, Elves JD, Oitt VMR. The Immune System: First of Two Parts [Internet]. Vol. 343. 2000. Available from: www.nejm.org
18. Storey M, Jordan S. An overview of the immune system. Vol. 23, Nursing standard (Royal College of Nursing (Great Britain): 1987). 2008.
19. Kessler M, Goldsmith D, Schellekens H. Immunogenicity of biopharmaceuticals. Nephrology Dialysis Transplantation. 2006 Oct 15;21(SUPPL. 5).
20. Zhou Y, Penny HL, Kroenke MA, Bautista B, Hainline K, Chea LS, et al. Immunogenicity assessment of bispecific antibody-based immunotherapy in oncology. Vol. 10, Journal for ImmunoTherapy of Cancer. BMJ Publishing Group; 2022.
21. Kumar S. An Introduction to Bioanalysis of Biopharmaceuticals. Springer; 2022.
22. Pineda C, Castañeda Hernández G, Jacobs IA, Alvarez DF, Carini C. Assessing the Immunogenicity of Biopharmaceuticals. Vol. 30, BioDrugs. Springer International Publishing; 2016. p. 195–206.
23. Forthal DN. Functions of Antibodies. 2014; Available from: https://journals.asm.org/journal/spectrum
24. Nelson PN, Reynolds GM, Waldron EE, Ward E, Giannopoulos K, Murray PG. Demystified. Monoclonal antibodies. Vol. 53, J Clin Pathol: Mol Pathol. 2000.
25. Chemistry RHC, 1987 undefined. Human IgG subclass measurements in the clinical laboratory. academic.oup.com [Internet]. 1987 [cited 2022 Jul 28];33(10):1707. Available from: https://academic.oup.com/clinchem/article-abstract/33/10/1707/5653747
26. Moser AC, Hage DS. Immunoaffinity chromatography: An introduction to applications and recent developments. Vol. 2, Bioanalysis. 2010. p. 769–90.
27. De Jong KAM, Van Breugel SJ, Hillebrand MJX, Rosing H, Huitema ADR, Beijnen JH. Bottom-up sample preparation for the LC-MS/MS quantification of anti-cancer monoclonal antibodies in bio matrices. Vol. 12, Bioanalysis. Future Medicine Ltd.; 2020. p. 1405–25.
28. Willrich MAV. Analysis of tryptic peptides from therapeutic monoclonal antibodies using LC-MS/MS. In: Methods in Molecular Biology. Humana Press Inc.; 2019. p. 85–99.
29. Hoffman W, Lakkis FG, Chalasani G. B cells, antibodies, and more. Clinical Journal of the American Society of Nephrology. 2016 Jan 7;11(1):137–54.
30. Shimada T, Umino Y, Aoki C, Aoki Y, Sato TA, Hamada A, et al. Selective detection of complementarity-determining regions of monoclonal antibody by limiting protease access to the substrate: Nano-surface and molecular-orientation limited proteolysis. Analyst. 2014 Dec 23;139(3):576–80.
31. Iwamoto N, Takanashi M, Hamada A, Shimada T. Validated LC/MS Bioanalysis of Rituximab CDR Peptides Using Nano-surface and Molecular-Orientation Limited (nSMOL) Proteolysis. Vol. 39, Biol. Pharm. Bull. 1187.

32. Alberts B, Johnson A, Lewis J, Raff M, Roberts K, Walter P. Molecular Biology of the Cell. 4th ed. New York: Garland Science; 2002.
33. Vos Q, Lees A, Wu ZQ, Snapper CM, Mond JJ. B-cell activation by T-cell-independent type 2 antigens as an integral part of the humoral immune response to pathogenic microorganisms. Immunol Rev. 2000 Aug;176:154-70. doi: 10.1034/j.1600-065x.2000.00607.x. PMID: 11043775.
34. Lipman NS, Jackson LR, Trudel LJ, Weis-Garcia F. Monoclonal Versus Polyclonal Antibodies: Distinguishing Characteristics, Applications, and Information Resources [Internet]. Available from: https://academic.oup.com/ilarjournal/article/46/3/258/738903
35. Boye J, Elter T, Engert A. An overview of the current clinical use of the anti-CD20 monoclonal antibody rituximab. Vol. 14, Annals of Oncology. 2003. p. 520–35.
36. Wiseman AC. Induction therapy in renal transplantation: Why? What agent? What dose? We may never know. Vol. 10, Clinical Journal of the American Society of Nephrology; 2015. p. 923–5.
37. Breedveld FC. Therapeutic monoclonal antibodies. Lancet. 2000 Feb 26;355(9205):735-40. doi: 10.1016/s0140-6736(00)01034-5. PMID: 10703815.
38. Castelli MS, McGonigle P, Hornby PJ. The pharmacology and therapeutic applications of monoclonal antibodies. Vol. 7, Pharmacology Research & Perspectives. NLM (Medline); 2019. p. e00535.
39. Guidance on the establishment of new INN stems Programme on International Nonproprietary Names (INN) Quality Assurance and Safety: Medicines (QSM) Medicines Policy and Standards (PSM) World Health Organization Geneva [Internet]. 2007. Available from: http://www.who.int/medicines/services/inn/publication/en/index.html
40. Voge NV, Alvarez E. Monoclonal antibodies in multiple sclerosis: Present and future. Vol. 7, Biomedicines. MDPI AG; 2019.
41. Yao S, Zhu Y, Chen L. Advances in targeting cell surface signalling molecules for immune modulation. Vol. 12, Nature Reviews Drug Discovery. 2013. p. 130–46.
42. Salles G, Barrett M, Foà R, Maurer J, O'Brien S, Valente N, et al. Rituximab in B-Cell Hematologic Malignancies: A Review of 20 Years of Clinical Experience. Vol. 34, Advances in Therapy. Springer Healthcare; 2017. p. 2232–73.
43. Presta LG. Antibody engineering. Curr Opin Struct Biol. 1992 Aug 1;2(4):593–6.
44. Gao SH, Huang K, Tu H, Adler AS. Monoclonal antibody humanness score and its applications. BMC Biotechnol. 2013 Jul 5;13.
45. Berger M, Shankar V, Vafai A. Therapeutic Applications of Monoclonal Antibodies. The American Journal of the Medical Sciences. 2002 Jul;324(1):14-30. doi: 10.1097/00000441-200207000-00004. PMID: 12120821; PMCID: PMC7093874.
46. McMichael AJ, Bastin JM. Clinical applications of monoclonal antibodies. Immunology Today. 1980 Sep 1;1(3):56-61.
47. Kuhn E, Wu J, Karl J, Liao H, Zolg W, Guild B. Quantification of C-reactive protein in the serum of patients with rheumatoid arthritis using multiple reaction monitoring mass spectrometry and 13C-labeled peptide standards. Proteomics. 2004 Apr;4(4):1175–86.

48. Gaudinski MR, Coates EE, Houser KV, Chen GL, Yamshchikov G, Saunders JG, et al. Safety and pharmacokinetics of the Fc-modified HIV-1 human monoclonal antibody VRC01LS: A Phase 1 open-label clinical trial in healthy adults. PLoS Med. 2018 Jan 1;15(1).
49. Beccari MV, Mogle BT, Sidman EF, Mastro KA, Asiago-Reddy E, Kufel WD. Ibalizumab, a Novel Monoclonal Antibody for the Management of Multidrug-Resistant HIV-1 Infection. 2019; Available from: https://doi.org/10.1128/AAC
50. Bruno CJ, Jacobson JM. Ibalizumab: An anti-CD4 monoclonal antibody for the treatment of HIV-1 infection. Journal of Antimicrobial Chemotherapy. 2010 Jul 17;65(9):1839–41.
51. Saylor C, Dadachova E, Casadevall A. Monoclonal antibody-based therapies for microbial diseases. Vol. 27, Vaccine. 2009.
52. Pestronk A, Florence J, Miller T, Choksi R, Al-Lozi MT, Levine TD. Treatment of IgM antibody associated polyneuropathies using rituximab. J Neurol Neurosurg Psychiatry. 2003 Apr 1;74(4):485–9.
53. Molina A. Clinical Status and Optimal Use of Rituximab for B-Cell Lymphomas Published on Diagnostic Imaging (Clinical Status and Optimal Use of Rituximab for B-Cell Lymphomas) [Internet]. 1998. Available from: http://www.diagnosticimaging.com
54. Keating GM. Rituximab: a review of its use in chronic lymphocytic leukaemia, low-grade or follicular lymphoma and diffuse large B-cell lymphoma. Drugs. 2010 Jul 30;70(11):1445-76. doi: 10.2165/11201110-000000000-00000. PMID: 20614951.
55. Johnson PWM, Glennie MJ. Rituximab: Mechanisms and applications. Vol. 85, British Journal of Cancer. 2001. p. 1619–23.
56. Boye J, Elter T, Engert A. An overview of the current clinical use of the anti-CD20 monoclonal antibody rituximab. Vol. 14, Annals of Oncology. 2003. p. 520–35.
57. Smith MR. Rituximab (monoclonal anti-CD20 antibody): Mechanisms of action and resistance. Oncogene. 2003 Oct 20;22(47):7359–68.
58. Johnson PWM, Glennie MJ. Rituximab: Mechanisms and applications. Vol. 85, British Journal of Cancer. 2001. p. 1619–23.
59. Eisenbeis C, Caligiuri M, Research JBCC, 2003 undefined. Rituximab: converging mechanisms of action in non-Hodgkin's lymphoma? AACR [Internet]. 2003 [cited 2022 Jul 26]; Available from: https://aacrjournals.org/clincancerres/article-abstract/9/16/5810/202189
60. Scott AM, Wolchok JD, Old LJ. Antibody therapy of cancer. Vol. 12, Nature Reviews Cancer. 2012. p. 278–87.
61. Salles G, Barrett M, Foà R, Maurer J, O'Brien S, Valente N, et al. Rituximab in B-Cell Hematologic Malignancies: A Review of 20 Years of Clinical Experience. Vol. 34, Advances in Therapy. Springer Healthcare; 2017. p. 2232–73.
62. Adams GP, Weiner LM. Monoclonal antibody therapy of cancer. Vol. 23, Nature Biotechnology. 2005. p. 1147–57.
63. Selewski DT, Shah GV, Mody RJ, Rajdev PA, Mukherji SK. Rituximab (Rituxan). Vol. 31, American Journal of Neuroradiology. 2010. p. 1178–80.

64. Ruiz-Garcia A, Bermejo M, Moss A, Casabo VG. Pharmacokinetics in drug discovery. Vol. 97, Journal of Pharmaceutical Sciences. John Wiley and Sons Inc.; 2008. p. 654–90.
65. Cartron G, Blasco H, Paintaud G, Watier H, Le Guellec C. Pharmacokinetics of rituximab and its clinical use: Thought for the best use? Vol. 62, Critical Reviews in Oncology/Hematology. 2007. p. 43–52.
66. Golay J, Semenzato G, Rambaldi A, Foà R, Gaidano G, Gamba E, et al. Lessons for the clinic from rituximab pharmacokinetics and pharmacodynamics. Vol. 5, mAbs. Landes Bioscience; 2013. p. 826–37.
67. Müller C, Murawski N, Wiesen MHJ, Held G, Poeschel V, Zeynalova S, et al. The role of sex and weight on rituximab clearance and serum elimination half-life in elderly patients with DLBCL. 2012; Available from: www.bloodjournal.org
68. Plosker GL, Figgitt DP. Rituximab: a review of its use in non-Hodgkin's lymphoma and chronic lymphocytic leukaemia. Drugs. 2003;63(8):803-43. doi: 10.2165/00003495-200363080-00005. PMID: 12662126.
69. Cartron G, Blasco H, Paintaud G, Watier H, Le Guellec C. Pharmacokinetics of rituximab and its clinical use: Thought for the best use? Vol. 62, Critical Reviews in Oncology/Hematology. 2007. p. 43–52.
70. Looney RJ, Srinivasan R, Calabrese LH. Review: The effects of rituximab on immunocompetency in patients with autoimmune disease. Vol. 58, Arthritis and Rheumatism. 2008. p. 5–14.
71. Nelson RL, Dyke RW, Root MA. Comparative pharmacokinetics of vindesine, vincristine and vinblastine in patients with cancer. Cancer Treatment Reviews. 1980;7:17–24. doi:10.1016/s0305-7372(80)80003-x
72. Rahman A, Carmichael D, Harris M, Roh JK. Comparative pharmacokinetics of free doxorubicin and doxorubicin entrapped in cardiolipin liposomes. Cancer Res. 1986 May;46(5):2295–9.
73. Pestronk A, Florence J, Miller T, Choksi R, Al-Lozi MT, Levine TD. Treatment of IgM antibody associated polyneuropathies using rituximab. J Neurol Neurosurg Psychiatry. 2003 Apr 1;74(4):485–9.
74. Kaegi C, Wuest B, Schreiner J, Steiner UC, Vultaggio A, Matucci A, et al. Systematic Review of Safety and Efficacy of Rituximab in Treating Immune-Mediated Disorders. Front Immunol. 2019 Sep 6;10.
75. Maloney DG, Grillo-López AJ, White CA, Bodkin D, Schilder RJ, Neidhart JA, Janakiraman N, Foon KA, Liles TM, Dallaire BK, Wey K, Royston I, Davis T, Levy R. IDEC-C2B8 (Rituximab) anti-CD20 monoclonal antibody therapy in patients with relapsed low-grade non-Hodgkin's lymphoma. Blood. 1997 Sep 15;90(6):2188-95. PMID: 9310469.
76. Cartron G, Watier H, Golay J, Solal-Celigny P. From the bench to the bedside: ways to improve rituximab efficacy. Blood. 2004 Nov 1;104(9):2635-42. doi: 10.1182/blood-2004-03-1110. Epub 2004 Jun 29. PMID: 15226177.
77. Li H, Ortiz R, Tran LTB, Salimi-Moosavi H, Malella J, James CA, et al. Simultaneous analysis of multiple monoclonal antibody biotherapeutics by LC-MS/MS method in rat plasma following cassette-dosing. AAPS Journal. 2013 Apr;15(2):337–46.

78. Peng X, Liu B, Li Y, Wang H, Chen X, Guo H, et al. Development and Validation of LC–MS/MS Method for the Quantitation of Infliximab in Human Serum. Chromatographia. 2015 Mar 21;78(7–8):521–31.
79. Pham PA, Flexner C. Emerging antiretroviral drug interactions. Journal of Antimicrobial Chemotherapy. 2011 Feb;66(2):235–9.
80. Iwamoto N, Takanashi M, Hamada A, Shimada T. Validated LC/MS Bioanalysis of Rituximab CDR Peptides Using Nano-surface and Molecular-Orientation Limited (nSMOL) Proteolysis. Vol. 39, Biol. Pharm. Bull. 1187.
81. Shankland KR, Armitage JO, Hancock BW. Non-Hodgkin lymphoma. Vol. 380, The Lancet. Elsevier B.V.; 2012. p. 848–57.
82. Ansell SM, Armitage J. Non-Hodgkin lymphoma: Diagnosis and treatment. In: Mayo Clinic Proceedings. Elsevier Ltd; 2005. p. 1087–97.
83. Nikita B, Jasmin J. A Case of B-Cell Non-Hodgkin's Lymphoma of Inguinal Lymph Node: On True Cut Biopsy [Internet]. International Journal of Advance Research and Development. 2017. Available from: www.ijarnd.com
84. Bowzyk Al-Naeeb A, Ajithkumar T, Behan S, Hodson DJ. Non-Hodgkin lymphoma. BMJ (Online). 2018;362.
85. Mok CC. Rituximab for the treatment of rheumatoid arthritis: An update. Vol. 8, Drug Design, Development and Therapy. 2013. p. 87–100.
86. Tavakolpour S, Alesaeidi S, Darvishi M, GhasemiAdl M, Darabi-Monadi S, Akhlaghdoust M, et al. A comprehensive review of rituximab therapy in rheumatoid arthritis patients. Vol. 38, Clinical Rheumatology. Springer London; 2019. p. 2977–94.
87. Roskar R, Trdan T. Analytical Methods for Quantification of Drug Metabolites in Biological Samples. In: Chromatography - The Most Versatile Method of Chemical Analysis. InTech; 2012.
88. Pitt JJ. Principles and applications of liquid chromatography-mass spectrometry in clinical biochemistry. Clinical Biochemistry Reviews. 2009 Feb;30(1):19-34. PMID: 19224008; PMCID: PMC2643089.
89. Becker JO, Hoofnagle AN. Replacing immunoassays with tryptic digestion-peptide immunoaffinity enrichment and LC-MS/MS. Vol. 4, Bioanalysis. 2012. p. 281–90.
90. Moein MM, El Beqqali A, Abdel-Rehim M. Bioanalytical method development and validation: Critical concepts and strategies. J Chromatogr B Analyt Technol Biomed Life Sci. 2017 Feb 1;1043:3–11.
91. Ji QC, Gage EM, Rodila R, Chang MS, El-Shourbagy TA. Method development for the concentration determination of a protein in human plasma utilizing 96-well solid-phase extraction and liquid chromatography/tandem mass spectrometric detection. Rapid Communications in Mass Spectrometry. 2003;17(8):794–9.
92. Parasuraman S, Anish R, Balamurugan S, Muralidharan S, Kumar KJ, Vijayan V. An overview of liquid chromatography-mass spectroscopy instrumentation. Pharmaceutical methods. 2014 Jul 1;5(2):47-55.

93. Knauer. https://www.knauer.net/en/Systems-Solutions/Analytical-HPLC-UHPLC/HPLC-Basics---principles-and-parameters. HPLC basics – Principles and parameters.
94. Mittal RD. Tandem Mass Spectroscopy in Diagnosis and Clinical Research. Vol. 30, Indian Journal of Clinical Biochemistry. Springer India; 2015. p. 121–3.
95. Smith JS, Thakur RA. Mass Spectrometry. 2017;165–81. Available from: https://link.springer.com/10.1007/978-3-319-45776-5_11
96. Kebarle P, Tang L. From ions in solution to ions in the gas phase - the mechanism of electrospray mass spectrometry. Anal Chem. 1993;65(22):972–86.
97. Fenn JB, Mann M, Meng CK, Wong SF, Whitehouse CM. Electrospray Ionization for Mass Spectrometry of Large Biomolecules [Internet]. Available from: www.sciencemag.org
98. Van den Broek I, Sparidans RW, Schellens JHM, Beijnen JH. Quantitative bioanalysis of peptides by liquid chromatography coupled to (tandem) mass spectrometry. Vol. 872, Journal of Chromatography B: Analytical Technologies in the Biomedical and Life Sciences. 2008. p. 1–22.
99. Iwamoto N, Shimada T. Regulated LC-MS/MS bioanalysis technology for therapeutic antibodies and Fc-fusion proteins using structure-indicated approach. Vol. 34, Drug Metabolism and Pharmacokinetics. Japanese Society for the Study of Xenobiotics; 2019. p. 19–24.
100. Prabu SL, Suriyaprakash TNK. Extraction of Drug from the Biological Matrix: A Review [Internet]. Available from: www.intechopen.com
101. Gundry RL, White MY, Murray CI, Kane LA, Fu Q, Stanley BA, et al. Preparation of proteins and peptides for mass spectrometry analysis in a bottom-up proteomics workflow. Curr Protoc Mol Biol. 2009;(SUPPL. 88).
102. Dee KC, Puleo DA, Bizios R. An Introduction to Tissue-Biomaterial Interactions. John Wiley & Sons; 2003.
103. Khalid Khan. Waters Corporation. 2017. Introduction to Peptides and Proteins for Bioanalysis Using LC-MS.
104. ABSciex. Peptide Quant Series - 3. Introduction to Sample Preparation Techniques for Peptides. 2016.
105. Miller RM, Smith LM. Overview and considerations in bottom-up proteomics. Vol. 148, Analyst. Royal Society of Chemistry; 2022. p. 475–86.
106. Zhang Y, Fonslow BR, Shan B, Baek MC, Yates JR. Protein analysis by shotgun/bottom-up proteomics. Vol. 113, Chemical Reviews. 2013. p. 2343–94.
107. Dupree EJ, Jayathirtha M, Yorkey H, Mihasan M, Petre BA, Darie CC. A critical review of bottom-up proteomics: The good, the bad, and the future of this field. Vol. 8, Proteomes. MDPI AG; 2020. p. 1–26.
108. Cristobal A, Marino F, Post H, Van Den Toorn HWP, Mohammed S, Heck AJR. Toward an Optimized Workflow for Middle-Down Proteomics. Anal Chem. 2017 Mar 21;89(6):3318–25.
109. Arsene CG, Ohlendorf R, Burkitt W, Pritchard C, Henrion A, O'Connor G, et al. Protein quantification by isotope dilution mass spectrometry of proteolytic fragments: Cleavage rate and accuracy. Anal Chem. 2008 Jun 1;80(11):4154–60.

110. Qiu XI, Ruterbories KJ, Ji QC, Jenkins GJ. Signature peptide selection workflow for biomarker quantification using LC-MS-based targeted proteomics. Bioanalysis. 2023 Mar 1;15(5):295–300.
111. Lange V, Picotti P, Domon B, Aebersold R. Selected reaction monitoring for quantitative proteomics: A tutorial. Vol. 4, Molecular Systems Biology. 2008.
112. Burgess RR. Chapter 20 Protein Precipitation Techniques. In: Methods in Enzymology. Academic Press Inc.; 2009. p. 331–42.
113. Jiang L, He L, Fountoulakis M. Comparison of protein precipitation methods for sample preparation prior to proteomic analysis. J Chromatogr A. 2004 Jan 16;1023(2):317–20.
114. Hober S, Nord K, Linhult M. Protein A chromatography for antibody purification. Vol. 848, Journal of Chromatography B: Analytical Technologies in the Biomedical and Life Sciences. 2007. p. 40–7.
115. TECH TIP # 64 [Internet]. Available from: www.thermo.com/pierce
116. Schimadzu Excellence in Science. Bioanalysis of Antibody Drugs: using Fab-selective Proteolysis 'nSMOL' method and LC-MS/MS. Spinco Biotech. 2017;58–60.
117. Gillet LC, Leitner A, Aebersold R. Mass Spectrometry Applied to Bottom-Up Proteomics: Entering the High-Throughput Era for Hypothesis Testing. Vol. 9, Annual Review of Analytical Chemistry. Annual Reviews Inc.; 2016. p. 449–72.
118. Trypsin Gold, Mass Spectrometry Grade Instructions for Use of Product V5280 [Internet]. Available from: www.promega.com
119. Norrgran J, Williams TL, Woolfitt AR, Solano MI, Pirkle JL, Barr JR. Optimization of digestion parameters for protein quantification. Anal Biochem. 2009 Oct 1;393(1):48–55.
120. Li C, Rossomando A, Wu SL, Karger BL. Comparability analysis of anti-CD20 commercial (rituximab) and RNAi-mediated fucosylated antibodies by two LC-MS approaches. MAbs. 2013 Jul;5(4):565–75.
121. Shen CH. Diagnostic Molecular Biology. Academic Press; 2019. 187–214 p.
122. Biziuk M. Solid phase extraction technique - trends, opportunities and applications [Internet]. 2015. Available from: https://www.researchgate.net/publication/279597851
123. Jenkins R, Duggan JX, Aubry AF, Zeng J, Lee JW, Cojocaru L, et al. Recommendations for Validation of LC-MS/MS Bioanalytical Methods for Protein Biotherapeutics. AAPS Journal. 2015 Jan 6;17(1):1–16.
124. Faria M, Halquist MS. Internal Standards for Absolute Quantification of Large Molecules (Proteins) from Biological Matrices by LC-MS/MS. In: Calibration and Validation of Analytical Methods - a Sampling of Current Approaches. InTech; 2018.
125. Brun V, Dupuis A, Adrait A, Marcellin M, Thomas D, Court M, et al. Isotope-labeled protein standards: Toward absolute quantitative proteomics. Molecular and Cellular Proteomics. 2007;6(12):2139–49.
126. Ezan E, Dubois M, Becher F. Bioanalysis of recombinant proteins and antibodies by mass spectrometry. Vol. 134, Analyst. Royal Society of Chemistry; 2009. p. 825–34.
127. Hahne H, Pachl F, Ruprecht B, Maier SK, Klaeger S, Helm D, et al. DMSO enhances electrospray response, boosting sensitivity of proteomic experiments. Nat Methods. 2013 Oct;10(10):989–91.

128. Chen H, Horwith C. High-speed high-performance liquid chromatography of peptides and proteins. Vol. 705, Journal of Chromatography A. 1995.
129. Camel V. Solid phase extraction of trace elements. Spectrochimica Acta Part B. 2003;58:1177–233.
130. Zeng W, Fisher AL, Musson DG, Wang AQ. High-throughput liquid chromatography for drug analysis in biological fluids: Investigation of extraction column life. J Chromatogr B Analyt Technol Biomed Life Sci. 2004 Jul 5;806(2):177–83.
131. Haynes K. Waters Corporation. 2020. Peptide Bioanalysis Sample Preparation Challenges.
132. Trinh A, Marlatt L, Bell DS. Controlling SPE Selectivity Through pH and Organic Modifier Manipulation. Reporter EU. 2006 Jan;21.
133. Maranata GJ, Surya NO, Hasanah AN. Optimising factors affecting solid phase extraction performances of molecular imprinted polymer as recent sample preparation technique. Vol. 7, Heliyon. Elsevier Ltd; 2021.
134. Agilent Technologies. www.agilent.com. SPE Method Development Tips and Tricks.
135. Björk I, Petersson B, Sjöquist J. Some Physicochemical Properties of Protein A from Staphylococcus aureus. Eur J Biochem. 1972;29(3):579–84.
136. Hjelm H, Sjödahl J, Sjöquist J. Immunologically Active and Structurally Similar Fragments of Protein A from Staphylococcus aureus. European Journal of Biochemistry. 1975;57(2):395–403.
137. Pierce Protein A Agarose. ThermoScientific. [Internet]. Available from: https://www.thermofisher.com/order/catalog/product/20333
138. Otieno BA, Krause CE, Rusling JF. Bioconjugation of Antibodies and Enzyme Labels onto Magnetic Beads. In: Methods in Enzymology. Academic Press Inc.; 2016. p. 135–50.
139. Iwamoto N, Yokoyama K, Takanashi M, Yonezawa A, Matsubara K, Shimada T. Application of nSMOL coupled with LC-MS bioanalysis for monitoring the Fc-fusion biopharmaceuticals Etanercept and Abatacept in human serum. Pharmacol Res Perspect. 2018 Jul 1;6(4).
140. Levernæs MCS, Broughton MN, Reubsaet L, Halvorsen TG. To elute or not to elute in immunocapture bottom-up LC–MS. J Chromatogr B Analyt Technol Biomed Life Sci. 2017 Jun 15;1055–1056:51–60.
141. https://www.graphpad.com/quickcalcs/Grubbs1.cfm [Internet]. GraphPad Outlier Calculator.
142. http://db.systemsbiology.net:8080/proteomicsToolkit/FragIonServlet.html [Internet]. Fragment Ion Calculator.
143. Kronvall G, Williams RC. Differences in Anti-Protein A Activity among IgG Subgroups. The Journal of Immunology. 1969 Oct 1;103(4):828–33.
144. Surolia A, Pain D, Khan MI. Protein A: nature's universal anti-antibody. Trends in Biochemical Sciences. 1982 Feb 1;7(2):74-6.
145. Millet A, Khoudour N, Lebert D, Machon C, Terrier B, Blanchet B, et al. Development, validation, and comparison of two mass spectrometry methods (LC-MS/HRMS and LC-MS/MS) for the quantification of rituximab in human plasma. Molecules. 2021 Mar 1;26(5).

146. Yuan L, Aubry AF, Arnold ME, Ji QC. Systematic investigation of orthogonal SPE sample preparation for the LC-MS/MS bioanalysis of a monoclonal antibody after pellet digestion. Bioanalysis. 2013 Oct;5(19):2379–91.
147. Iwamoto N, Koguchi Y, Yokoyama K, Hamada A, Yonezawa A, Piening BD, et al. A rapid and universal liquid chromatograph-mass spectrometry-based platform, refmAb-Q nSMOL, for monitoring monoclonal antibody therapeutics. Analyst. 2022 Aug 18;147(19):4275–84.
148. Protein Purification. AB. Amersham Pharmacia Biotech; 1999.